

CBX2011-003
May 11, 2013

Absolute Determination of Branching Fractions for Hadronic D Decays and Measurements of the Cross Sections for $e^+e^- \rightarrow D^0\bar{D}^0$ and $e^+e^- \rightarrow D^+D^-$

X. Shi, P. Onyisi, J. Alexander, D. Cassel, D. Kreinick, and A. Ryd
Cornell University

Revision

Abstract

This note describes measurement of absolute branching fractions for several hadronic D decays using a double tag technique. The analysis described here uses about 818 pb^{-1} of data recorded at the $\psi(3770)$ resonance. This sample is contained in data sets 31, 32, 33, 35, 36, 37, 43, 44, 45, and 46. Using the measured luminosity we also calculate the $D\bar{D}$ cross sections $\sigma_{D^0\bar{D}^0}$ and $\sigma_{D^+D^-}$.

Contents

List of Figures

List of Tables

1 Introduction

This analysis aims at measuring the absolute branching fractions for charged and neutral D meson decays listed in Table ???. In addition to the absolute branching fractions we also measure the cross-sections for $e^+e^- \rightarrow D^0\bar{D}^0$ and $e^+e^- \rightarrow D^+D^-$ at a center-of-mass energy of 3.77 GeV corresponding to the $\psi(3770)$.

Table 1: Modes considered in this analysis.

Mode
$D^0 \rightarrow K^-\pi^+$
$D^0 \rightarrow K^-\pi^+\pi^0$
$D^0 \rightarrow K^-\pi^+\pi^-\pi^+$
$D^+ \rightarrow K^-\pi^+\pi^+$
$D^+ \rightarrow K^-\pi^+\pi^+\pi^0$
$D^+ \rightarrow K_S^0\pi^+, K_S \rightarrow \pi^+\pi^-$
$D^+ \rightarrow K_S^0\pi^+\pi^0, K_S \rightarrow \pi^+\pi^-$
$D^+ \rightarrow K_S^0\pi^+\pi^+\pi^-, K_S \rightarrow \pi^+\pi^-$
$D^+ \rightarrow K^+K^-\pi^+$

The analysis technique is similar to that used by Mark III [?, ?] where the modes are reconstructed both as single tags and double tags. Given the produced number of $D\bar{D}$ pairs, $N_{D\bar{D}}$, the number of reconstructed single tags is given by

$$N_i = \epsilon_i \mathcal{B}_i N_{D\bar{D}}$$

and

$$\bar{N}_j = \bar{\epsilon}_j \mathcal{B}_j N_{D\bar{D}}$$

for reconstructing a D and a \bar{D} respectively and ϵ_i and $\bar{\epsilon}_j$ are the efficiencies and \mathcal{B}_i is the branching fraction for the mode that is reconstructed. The double tag yield can be expressed as

$$N_{ij} = \epsilon_{ij} \mathcal{B}_i \mathcal{B}_j N_{D\bar{D}}$$

where ϵ_{ij} is the efficiency for reconstructing a double tag in the mode i for the D and mode j for the \bar{D} . Taking the product of two single tag yields for a D and \bar{D} yield and dividing by the corresponding double tag yield one arrive at

$$N_{D\bar{D}} = \frac{N_i \bar{N}_j}{N_{ij}} \frac{\epsilon_{ij}}{\epsilon_i \bar{\epsilon}_j}.$$

Given the number of produced $D\bar{D}$ pairs the cross section is easily calculated using the luminosity. Also the hadronic branching fractions are easily measured using the single tag

yields. Note that to first order systematics, such as tracking efficiencies, cancel out in the calculation of the number of $D\bar{D}$ pairs as the double tag efficiency is approximately equal to the single tag efficiency squared.

However, to correctly treat the correlations between single and double tag modes, as well as handling backgrounds, a combined χ^2 fit is used to extract the produced number of $D\bar{D}$ pairs and branching fractions. This fit is described in detail in Ref. [?].

This document is structured as follows. In Section ?? we describe the data and Monte Carlo samples used in this analysis. In the following section we describe how this data is processed. Section ?? document our selection criteria. The selection criteria are based on the DTag production. Section ?? describes the extraction of single and double tag yields. The (small) peaking backgrounds that we have in this analysis are discussed in Section ?? and in the next Section, ??, we discuss the systematics that affects this analysis. Section ?? gives the final result for the cross sections and branching fractions.

We describe in detail the analysis as performed on a sample of generic Monte Carlo events. This provides a very important check that the analysis technique is working.

The work reported in this note is an update of a previous analysis [?, ?] based on 281 pb⁻¹. This note is self contained but adds more detailed discussion about systematic effects that are even more important in the 818 pb⁻¹ analysis as the statistical error is reduced by a factor of 1.7.

2 What's new

In this analysis, besides we're having more data – from 281 pb⁻¹ to 818 pb⁻¹ – our software has also been updated in the last two years. So, before we move on to analyze the new data, we want to run the same analysis with the original 281/pb data and look for possible difference in the new software environment.

We traced several places in order to find the source of the MC difference. The whole process of this procedure can be viewed as in Fig.?? where the places which have difference has been indicated in yellow color in the diagram. We figured that to fit the new signal MC, one has to use new lineshape function along with a few new parameters and tweaking a factor in the fitting code. For detailes can be seen in Table ??.. If we compare the χ^2 from the previous table by re-arranging the label based on the new elements added, we'll see a patter in Table ?? there, we knew that the biggest resource of this difference comes from the updated DECAY.DEC file.

Comparing the DECAY.DEC file between the ‘Original’ (2005) and the ‘Defult’ (2008), we can see that for D^+ , there were 59 modes unchanged (common modes), but all of their decay ratios have been changed, 14 modes were removed, and 30 new modes were added. For D^0 , there were 72 modes unchanged 7 modes added and 56 new modes added.

Certain particles related with the D-Hadronic decay are also changed in the evt.pdl file, selected in Table ??.

Table 2: Comparison of the signal yields between the new release and original release. The new release used the same line shape as data to fit signal MC. Also changed the width of ψ 3770 from 0.0286 GeV to 0.0252 GeV, the mass of ψ 3770 from 3.7718 GeV to 3.7724 GeV, the Blatt-Weisskopf radius from 12.3 GeV^{-1} to 12.7 GeV^{-1} . In addition, the factor of “ $1/(1.0 + (\text{mr} * \text{p}) * (\text{mr} * \text{p}))$ ” had been removed in the fitting code. The differences are in percentage with respect to the original one, and the labels defined as: **Default**: start from the original user decay file. Then we use the CLEOG, MCPass2 with new release. Once we get the pass2 pds file, then use the HadronicDNtupleProc compiled in the new release to make the ntuple. We select DDBar with the same python script and then do the fit with RooFit compiled under new release. Used the modified lineshape and the fitting code as described above. **EvtGen**: use all of the original CLEOG constants, evt.pdl and DECAY.DEC file, only new EvtGen code. **PdlDec**: use the original Particle Data listing evt.pdl and DECAY.DEC file, **EBeam**: use the original CLEOG constants, which has different Beam energy, **Decay**: use the original generic DECAY.DEC file.

Mode	Default	EvtGen	PdlDec	EBeam	Decay
$D^0 \rightarrow K^- \pi^+$	+0.1(+0.3 σ)	+0.2(+0.4 σ)	-0.1(-0.1 σ)	+0.2(+0.4 σ)	+0.4(+0.9 σ)
$\bar{D}^0 \rightarrow K^+ \pi^-$	+0.3(+0.7 σ)	+0.3(+0.6 σ)	+0.1(+0.3 σ)	-0.1(-0.2 σ)	+0.1(+0.1 σ)
$D^0 \rightarrow K^- \pi^+ \pi^0$	+0.5(+1.2 σ)	-0.6(-1.6 σ)	-0.4(-1.0 σ)	+0.3(+0.8 σ)	+0.4(+1.0 σ)
$\bar{D}^0 \rightarrow K^+ \pi^- \pi^0$	+0.6(+1.4 σ)	0.0(+0.1 σ)	-0.2(-0.5 σ)	+0.3(+0.7 σ)	+0.7(+1.7 σ)
$D^0 \rightarrow K^- \pi^+ \pi^+ \pi^-$	+0.8(+1.7 σ)	+1.0(+2.1 σ)	+0.7(+1.5 σ)	+0.6(+1.3 σ)	+1.2(+2.6 σ)
$\bar{D}^0 \rightarrow K^+ \pi^- \pi^- \pi^+$	+0.2(+0.4 σ)	-0.3(-0.6 σ)	+0.1(+0.3 σ)	0.0(0.0 σ)	+1.2(+2.5 σ)
$D^+ \rightarrow K^- \pi^+ \pi^+$	-0.8(-1.6 σ)	-1.2(-2.5 σ)	-0.3(-0.6 σ)	-0.2(-0.4 σ)	-0.3(-0.7 σ)
$D^- \rightarrow K^+ \pi^- \pi^-$	+0.6(+1.3 σ)	+0.3(+0.6 σ)	-0.0(-0.1 σ)	-0.3(-0.7 σ)	+0.5(+1.0 σ)
$D^+ \rightarrow K^- \pi^+ \pi^+ \pi^0$	+1.8(+2.4 σ)	+0.7(+0.9 σ)	+1.1(+1.4 σ)	+1.9(+2.6 σ)	+1.0(+1.4 σ)
$D^- \rightarrow K^+ \pi^- \pi^- \pi^0$	-0.4(-0.5 σ)	-0.3(-0.5 σ)	+0.4(+0.5 σ)	+2.3(+3.1 σ)	+0.4(+0.6 σ)
$D^+ \rightarrow K_S^0 \pi^+$	0.0(0.0 σ)	+0.3(+0.5 σ)	-0.2(-0.4 σ)	-0.8(-1.5 σ)	-0.5(-0.9 σ)
$D^- \rightarrow K_S^0 \pi^-$	-1.0(-1.9 σ)	+0.1(+0.3 σ)	-1.2(-2.2 σ)	-0.7(-1.4 σ)	-0.7(-1.3 σ)
$D^+ \rightarrow K_S^0 \pi^+ \pi^0$	+1.0(+1.1 σ)	-1.2(-1.3 σ)	+0.5(+0.6 σ)	+1.2(+1.4 σ)	-0.8(-0.9 σ)
$D^- \rightarrow K_S^0 \pi^- \pi^0$	+2.7(+2.9 σ)	+0.3(+0.3 σ)	+1.2(+1.3 σ)	+2.6(+2.8 σ)	-0.5(-0.5 σ)
$D^+ \rightarrow K_S^0 \pi^+ \pi^+ \pi^-$	+2.2(+2.4 σ)	+1.7(+1.8 σ)	+3.0(+3.2 σ)	+1.4(+1.5 σ)	+1.3(+1.4 σ)
$D^- \rightarrow K_S^0 \pi^- \pi^- \pi^+$	+1.9(+2.0 σ)	+0.9(+0.9 σ)	+1.1(+1.2 σ)	+2.6(+2.8 σ)	+1.6(+1.7 σ)
$D^+ \rightarrow K^+ K^- \pi^+$	+0.3(+0.2 σ)	+0.2(+0.2 σ)	-1.4(-1.4 σ)	-0.5(-0.4 σ)	-0.2(-0.2 σ)
$D^- \rightarrow K^- K^+ \pi^-$	+0.6(+0.6 σ)	+2.3(+2.2 σ)	-0.5(-0.5 σ)	+0.9(+0.9 σ)	+0.9(+0.9 σ)
χ^2	40.68	26.58	27.21	45.11	30.79
Mean	0.80 ± 0.30	0.26 ± 0.29	0.19 ± 0.29	0.76 ± 0.33	0.62 ± 0.27
Sigma	1.26 ± 0.21	1.21 ± 0.20	1.22 ± 0.20	1.39 ± 0.24	1.16 ± 0.19

Table 3: Comparison of the χ^2 . We can see that by adding new EBeam, and new `evt.pdl`, the difference is still quite small. However, once we use the new `DECAY.DEC`, we can't reproduce the original result. This indicate that the biggest problem lies in the change of the `DECAY.DEC` file.

Label	New Elements	χ^2
EvtGen	—	26.6
PdlDec	EBeam	27.2
Decay	EBeam PDL	30.8
Default	EBeam PDL DEC	40.7

Table 4: Difference in the `evt.pdl`.

Name	Mass(Original)	Mass(Default)	Mass diff(%)	Width(Original)	Width(Default)	Width diff(%)
$\psi(2S)$	3.686111	3.68609	-0.00	0.00028	0.000327	16.79
$\psi(3770)$	3.7699	3.7724	0.07	0.0236	0.0252	6.78
J/ψ	3.09687	3.096916	0.00	0.000087	0.0000934	7.36
K_1^-	1.273	1.272	-0.08	0.09	0.09	0.00
\bar{D}^0	1.8645	1.86484	0.02	0	0	0
\bar{K}^{*0}	0.8961	0.89600	-0.01	0.0505	0.0503	-0.40
ρ^0	0.7685	0.77549	0.91	0.151	0.1494	-1.06
ρ^+	0.7685	0.77549	0.91	0.151	0.1494	-1.06
ρ^-	0.7685	0.77549	0.91	0.151	0.1494	-1.06
D^-	1.8693	1.86962	0.02	0	0	0
K^+	0.49368	0.493677	-0.00	0	0	0
K^-	0.49368	0.493677	-0.00	0	0	0
K^0	0.49767	0.497648	-0.00	0	0	0
f_0	1.000	0.980	-2.00	0.05	0.05	0.00
f_2	1.275	1.2751	0.01	0.185	0.185	0.00
D^+	1.8693	1.86962	0.02	0	0	0
K_1^+	1.273	1.272	-0.08	0.09	0.09	0.00
η	0.54784	0.547785	-0.01	0	0	0
ϕ	1.01941	1.019455	0.00	0.00443	0.00426	-3.84
\bar{K}^0	0.49767	0.497648	-0.00	0	0	0
π^0	0.134976	0.134977	0.00	0	0	0
$\eta(2S)$	1.297	1.294	-0.23	0.053	0.055	3.77
ω	0.78257	0.78265	0.01	0.00844	0.00849	0.59
D^0	1.8645	1.86484	0.02	0	0	0

Table 5: Comparison of 281 pb^{-1} and Subsequent 537 pb^{-1} Single Tag Yields, Luminosity Scale Factor = 1.91.

Mode	ST(281 pb^{-1})	Scaled ST (281 pb^{-1})	ST(537 pb^{-1})	χ^2
$D^0 \rightarrow K^- \pi^+$	25760 ± 165	49202 ± 314	49477 ± 228	0.5
$\bar{D}^0 \rightarrow K^+ \pi^-$	26258 ± 166	50153 ± 317	49404 ± 228	3.7
$D^0 \rightarrow K^- \pi^+ \pi^0$	50276 ± 258	96027 ± 493	94524 ± 354	6.1
$\bar{D}^0 \rightarrow K^+ \pi^- \pi^0$	50537 ± 259	96525 ± 495	95325 ± 356	3.9
$D^0 \rightarrow K^- \pi^+ \pi^+ \pi^-$	39709 ± 216	75844 ± 413	74710 ± 296	5.0
$\bar{D}^0 \rightarrow K^+ \pi^- \pi^- \pi^+$	39606 ± 216	75648 ± 413	75360 ± 298	0.3
$D^+ \rightarrow K^- \pi^+ \pi^+$	40248 ± 208	76874 ± 396	76426 ± 286	0.8
$D^- \rightarrow K^+ \pi^- \pi^-$	40734 ± 209	77801 ± 399	77254 ± 288	1.2
$D^+ \rightarrow K^- \pi^+ \pi^+ \pi^0$	12844 ± 153	24532 ± 292	23974 ± 209	2.4
$D^- \rightarrow K^+ \pi^- \pi^- \pi^0$	12756 ± 153	24365 ± 291	24398 ± 211	0.0
$D^+ \rightarrow K_S^0 \pi^+$	5789 ± 82	11058 ± 156	11085 ± 111	0.0
$D^- \rightarrow K_S^0 \pi^-$	5868 ± 82	11208 ± 156	11246 ± 112	0.0
$D^+ \rightarrow K_S^0 \pi^+ \pi^0$	13275 ± 157	25355 ± 299	25006 ± 213	0.9
$D^- \rightarrow K_S^0 \pi^- \pi^0$	13126 ± 155	25070 ± 296	25459 ± 215	1.1
$D^+ \rightarrow K_S^0 \pi^+ \pi^+ \pi^-$	8275 ± 134	15805 ± 256	15484 ± 183	1.0
$D^- \rightarrow K_S^0 \pi^- \pi^- \pi^+$	8285 ± 134	15824 ± 255	15690 ± 184	0.2
$D^+ \rightarrow K^+ K^- \pi^+$	3519 ± 73	6721 ± 140	6627 ± 99	0.3
$D^- \rightarrow K^- K^+ \pi^-$	3501 ± 73	6686 ± 139	6588 ± 99	0.3
Total χ^2				27.7
$p(\chi^2)$				6.7%

Table 6: Comparison of 281 pb^{-1} and Subsequent 537 pb^{-1} Double Tag Yields, Luminosity Scale Factor = 1.91.

Mode	DT(281 pb^{-1})	Scaled DT (281 pb^{-1})	DT(537 pb^{-1})	χ^2
$D^0 \rightarrow K^-\pi^+ \bar{D}^0 \rightarrow K^+\pi^-$	630 ± 25	1203 ± 48	1189 ± 35	0.1
$D^0 \rightarrow K^-\pi^+ \bar{D}^0 \rightarrow K^+\pi^-\pi^0$	1378 ± 38	2631 ± 73	2487 ± 51	2.6
$D^0 \rightarrow K^-\pi^+ \bar{D}^0 \rightarrow K^+\pi^-\pi^-\pi^+$	1002 ± 32	1914 ± 61	1983 ± 45	0.8
$D^0 \rightarrow K^-\pi^+\pi^0 \bar{D}^0 \rightarrow K^+\pi^-$	1383 ± 38	2642 ± 72	2563 ± 52	0.8
$D^0 \rightarrow K^-\pi^+\pi^0 \bar{D}^0 \rightarrow K^+\pi^-\pi^0$	2679 ± 53	5117 ± 102	4863 ± 72	4.1
$D^0 \rightarrow K^-\pi^+\pi^0 \bar{D}^0 \rightarrow K^+\pi^-\pi^+\pi^+$	1964 ± 46	3752 ± 87	3774 ± 63	0.0
$D^0 \rightarrow K^-\pi^+\pi^+\pi^- \bar{D}^0 \rightarrow K^+\pi^-$	955 ± 31	1824 ± 60	1940 ± 44	2.4
$D^0 \rightarrow K^-\pi^+\pi^+\pi^- \bar{D}^0 \rightarrow K^+\pi^-\pi^0$	1999 ± 46	3818 ± 88	3696 ± 63	1.3
$D^0 \rightarrow K^-\pi^+\pi^+\pi^- \bar{D}^0 \rightarrow K^+\pi^-\pi^-\pi^+$	1601 ± 41	3057 ± 78	2964 ± 56	0.9
$D^+ \rightarrow K^-\pi^+\pi^+ D^- \rightarrow K^+\pi^-\pi^-$	2002 ± 45	3823 ± 86	3948 ± 63	1.4
$D^+ \rightarrow K^-\pi^+\pi^+ D^- \rightarrow K^+\pi^-\pi^-\pi^0$	685 ± 27	1308 ± 52	1226 ± 36	1.7
$D^+ \rightarrow K^-\pi^+\pi^+ D^- \rightarrow K_S^0 \pi^-$	272 ± 17	520 ± 32	587 ± 24	2.8
$D^+ \rightarrow K^-\pi^+\pi^+ D^- \rightarrow K_S^0 \pi^-\pi^0$	747 ± 28	1426 ± 53	1301 ± 37	3.7
$D^+ \rightarrow K^-\pi^+\pi^+ D^- \rightarrow K_S^0 \pi^-\pi^-\pi^+$	404 ± 20	771 ± 39	692 ± 27	2.8
$D^+ \rightarrow K^-\pi^+\pi^+ D^- \rightarrow K^-K^+\pi^-$	167 ± 13	318 ± 25	315 ± 18	0.0
$D^+ \rightarrow K^-\pi^+\pi^0 D^- \rightarrow K^+\pi^-\pi^-$	653 ± 26	1248 ± 50	1188 ± 36	0.9
$D^+ \rightarrow K^-\pi^+\pi^0 D^- \rightarrow K^+\pi^-\pi^-\pi^0$	213 ± 17	407 ± 32	426 ± 24	0.2
$D^+ \rightarrow K^-\pi^+\pi^+\pi^0 D^- \rightarrow K_S^0 \pi^-$	102 ± 10	195 ± 20	194 ± 14	0.0
$D^+ \rightarrow K^-\pi^+\pi^+\pi^0 D^- \rightarrow K_S^0 \pi^-\pi^0$	210 ± 16	402 ± 30	394 ± 21	0.0
$D^+ \rightarrow K^-\pi^+\pi^+\pi^0 D^- \rightarrow K_S^0 \pi^-\pi^-\pi^+$	125 ± 12	239 ± 23	248 ± 17	0.1
$D^+ \rightarrow K^-\pi^+\pi^+\pi^0 D^- \rightarrow K^-K^+\pi^-$	54 ± 8	103 ± 15	105 ± 11	0.0
$D^+ \rightarrow K_S^0 \pi^+ D^- \rightarrow K^+\pi^-\pi^-$	273 ± 17	521 ± 32	553 ± 24	0.6
$D^+ \rightarrow K_S^0 \pi^+ D^- \rightarrow K^+\pi^-\pi^-\pi^0$	102 ± 10	196 ± 20	192 ± 14	0.0
$D^+ \rightarrow K_S^0 \pi^+ D^- \rightarrow K_S^0 \pi^-$	36 ± 6	70 ± 12	71 ± 9	0.0
$D^+ \rightarrow K_S^0 \pi^+ D^- \rightarrow K_S^0 \pi^-\pi^0$	92 ± 10	177 ± 19	171 ± 13	0.1
$D^+ \rightarrow K_S^0 \pi^+ D^- \rightarrow K_S^0 \pi^-\pi^-\pi^+$	66 ± 8	126 ± 16	84 ± 9	5.2
$D^+ \rightarrow K_S^0 \pi^+ D^- \rightarrow K^-K^+\pi^-$	23 ± 5	44 ± 10	49 ± 7	0.2
$D^+ \rightarrow K_S^0 \pi^+\pi^0 D^- \rightarrow K^+\pi^-\pi^-$	660 ± 26	1260 ± 50	1202 ± 35	0.9
$D^+ \rightarrow K_S^0 \pi^+\pi^0 D^- \rightarrow K^+\pi^-\pi^-\pi^0$	236 ± 16	451 ± 31	404 ± 21	1.6
$D^+ \rightarrow K_S^0 \pi^+\pi^0 D^- \rightarrow K_S^0 \pi^-$	94 ± 10	179 ± 19	162 ± 13	0.5
$D^+ \rightarrow K_S^0 \pi^+\pi^0 D^- \rightarrow K_S^0 \pi^-\pi^0$	233 ± 16	446 ± 30	421 ± 22	0.5
$D^+ \rightarrow K_S^0 \pi^+\pi^0 D^- \rightarrow K_S^0 \pi^-\pi^-\pi^+$	138 ± 13	264 ± 24	233 ± 16	1.2
$D^+ \rightarrow K_S^0 \pi^+\pi^0 D^- \rightarrow K^-K^+\pi^-$	48 ± 7	92 ± 14	96 ± 10	0.1
$D^+ \rightarrow K_S^0 \pi^+\pi^+\pi^- D^- \rightarrow K^+\pi^-\pi^-$	415 ± 21	792 ± 40	754 ± 28	0.6
$D^+ \rightarrow K_S^0 \pi^+\pi^+\pi^- D^- \rightarrow K^+\pi^-\pi^-\pi^0$	122 ± 12	234 ± 24	226 ± 17	0.1
$D^+ \rightarrow K_S^0 \pi^+\pi^+\pi^- D^- \rightarrow K_S^0 \pi^-$	61 ± 8	117 ± 15	99 ± 10	1.0
$D^+ \rightarrow K_S^0 \pi^+\pi^+\pi^- D^- \rightarrow K_S^0 \pi^-\pi^0$	136 ± 12	260 ± 24	226 ± 16	1.4
$D^+ \rightarrow K_S^0 \pi^+\pi^+\pi^- D^- \rightarrow K_S^0 \pi^-\pi^-\pi^+$	87 ± 10	167 ± 20	138 ± 13	1.5
$D^+ \rightarrow K_S^0 \pi^+\pi^+\pi^- D^- \rightarrow K^-K^+\pi^-$	33 ± 6	62 ± 12	59 ± 8	0.0
$D^+ \rightarrow K^+K^-\pi^+ D^- \rightarrow K^+\pi^-\pi^-$	169 ± 13	322 ± 25	316 ± 18	0.0
$D^+ \rightarrow K^+K^-\pi^+ D^- \rightarrow K^+\pi^-\pi^-\pi^0$	64 ± 8	122 ± 15	103 ± 11	1.0
$D^+ \rightarrow K^+K^-\pi^+ D^- \rightarrow K_S^0 \pi^-$	20 ± 5	38 ± 9	43 ± 7	0.2
$D^+ \rightarrow K^+K^-\pi^+ D^- \rightarrow K_S^0 \pi^-\pi^0$	76 ± 9	145 ± 18	105 ± 11	3.6
$D^+ \rightarrow K^+K^-\pi^+ D^- \rightarrow K_S^0 \pi^-\pi^-\pi^+$	39 ± 7	75 ± 13	59 ± 9	1.0
$D^+ \rightarrow K^+K^-\pi^+ D^- \rightarrow K^-K^+\pi^-$	13 ± 4	24 ± 8	29 ± 6	0.3
		Total χ^2	48.2	
		$p(\chi^2)$	34.5%	

Table 7: Comparison of 281 pb^{-1} and Subsequent 537 pb^{-1} Single Tag Yields, Luminosity Scale Factor = 1.91. Using 281 momentum resolution parameters. Apparently, this only make things worse.

Mode	ST(281 pb^{-1})	Scaled ST (281 pb^{-1})	ST(537 pb^{-1})	χ^2
$D^0 \rightarrow K^- \pi^+$	25760 ± 165	49202 ± 314	49419 ± 228	0.3
$\bar{D}^0 \rightarrow K^+ \pi^-$	26258 ± 166	50153 ± 317	49348 ± 228	4.3
$D^0 \rightarrow K^- \pi^+ \pi^0$	50276 ± 258	96027 ± 493	93950 ± 352	11.8
$\bar{D}^0 \rightarrow K^+ \pi^- \pi^0$	50537 ± 259	96525 ± 495	94750 ± 354	8.5
$D^0 \rightarrow K^- \pi^+ \pi^+ \pi^-$	39709 ± 216	75844 ± 413	74755 ± 297	4.6
$\bar{D}^0 \rightarrow K^+ \pi^- \pi^- \pi^+$	39606 ± 216	75648 ± 413	75405 ± 298	0.2
$D^+ \rightarrow K^- \pi^+ \pi^+$	40248 ± 208	76874 ± 396	76392 ± 286	1.0
$D^- \rightarrow K^+ \pi^- \pi^-$	40734 ± 209	77801 ± 399	77218 ± 288	1.4
$D^+ \rightarrow K^- \pi^+ \pi^+ \pi^0$	12844 ± 153	24532 ± 292	23809 ± 208	4.1
$D^- \rightarrow K^+ \pi^- \pi^- \pi^0$	12756 ± 153	24365 ± 291	24231 ± 210	0.1
$D^+ \rightarrow K_S^0 \pi^+$	5789 ± 82	11058 ± 156	11118 ± 113	0.1
$D^- \rightarrow K_S^0 \pi^-$	5868 ± 82	11208 ± 156	11283 ± 113	0.2
$D^+ \rightarrow K_S^0 \pi^+ \pi^0$	13275 ± 157	25355 ± 299	24899 ± 215	1.5
$D^- \rightarrow K_S^0 \pi^- \pi^0$	13126 ± 155	25070 ± 296	25359 ± 217	0.6
$D^+ \rightarrow K_S^0 \pi^+ \pi^+ \pi^-$	8275 ± 134	15805 ± 256	15422 ± 184	1.5
$D^- \rightarrow K_S^0 \pi^- \pi^- \pi^+$	8285 ± 134	15824 ± 255	15628 ± 185	0.4
$D^+ \rightarrow K^+ K^- \pi^+$	3519 ± 73	6721 ± 140	6634 ± 100	0.3
$D^- \rightarrow K^- K^+ \pi^-$	3501 ± 73	6686 ± 139	6595 ± 100	0.3
Total χ^2				41.2
$p(\chi^2)$				0.1%

3 Code

3.1 MC Generation

Signal Monte Carlo was generated with the following prescription:

- CLEOG was run using release 20080624_MCGEN.
- MCPass2 was run using release 20041104_MCP2_A_1 for data31–33, data35–37 and release 20071023_MCP2_A for data43–46.
- DSkim was run using release 20060224_FULL_A_3.

3.2 Ntuples

The creation of ntuples was done in the 20080228_FULL release, with the following additional package tags (with minor tweaks in order to compile in the new release and run on the new datasample) :

```
HadronicDNtupleProc          ponyisi060929
```

4 Event samples

4.1 Data

CLEO-c data samples used consists of data31–33, data35–37, and data43–46 runs taken at energies above 3.7 GeV. The data are obtained from the Eventstore dskim grade. For sideband studies of the K_S^0 a separate skim is made from the physics grade.

Run 208087 in data37 has, we think, an incorrect beam energy. It is reported as 1.87679 GeV, while it is surrounded by runs at 1.88679 GeV. Checking the logbook, it appears that the beam energy was manually input for this run, and it's probably more likely that a digit was entered wrong than that CESR dropped 10 MeV for one run.

While running the data43–46, we encountered several events which had a lot of DDBar candidates and cause the CPUs to run exceedingly long and finally kicked off by the que system. By looking at those events in EventDispaly, we found they were all junks. So, we skipped them using module SkipBadEventsProc.

The events are listed in:

```
/home/xs32/work/CLE0/analysis/DHad/src/10.1.10/proc/
HadronicDNtupleProc/Test/EventsToSkip.txt
```

4.2 MC

Signal MC samples were generated with the versions of code indicated above for both single and double tag measurements. For single tags, either the D or \bar{D} was forced to decay into the target mode with the relative weighting of different intermediate states equal to that set in `DECAY.DEC`, and the other side was left to decay generically. For double tags, each D was decayed in the same manner as the corresponding single tags. The number of events generated in each signal MC sample was set to provide extra events in the high-statistics modes in the fit. The number of events generated for each mode is given in Tables ?? and ??.

Generic Monte Carlo, produced on the Minnesota farm, was produced for $20 \times$ data, using the release 20080215_MCGEN for `cleog`. The releases used for `mcpass2` are: 20041104_MCP2_A_1 (data31–33, 35–37), 20060802_MCP2_A_1 (data43–44), 20070912_MCP2_A (data45), and 20071023_MCP2_A (data46). In our analysis we used the DSkimmed generic sample, which was produced with release 20060224_FULL_A_3.

We used MC samples generated by Minnesota for continuum, tau-pair production, and ψ' radiative-return events. We used these releases to establish the lack of peaking background from these sources. The details of the releases can be found in [?].

5 Event selection

5.1 DSkim selection

This analysis reconstructs charged and neutral D mesons in the modes listed in Table ???. It uses the selection criteria used in the ‘DSkim’ production, more specifically the ‘version 2’, which are documented in the DTag note [?, ?].

In order to be consistent with previous analysis, we added additional cuts after the DSkimmed sample to reproduce the same DSkim Version 1. See details in the next section.

5.2 Event selection criteria

In addition to the DTag criteria we use the following requirements

- We require the K_S^0 mass cut window ± 12 MeV
- We apply E9/E25 cut on the diphoton decay candidates (*i.e.* π^0 , η , and $\eta' \rightarrow \gamma\gamma$)
- We apply the mode dependent $\Delta E \equiv E_{\text{reco}} - E_{\text{beam}}$ cuts as listed in Table ??
- In the $D^0 \rightarrow K^-\pi^+$ mode in events with exactly 2 reconstructed tracks we also require that the tracks pass the ‘lepton veto’ which rejects Bhabha and μ -pairs, Ref.[?]. Note that this cut is only applied to events that have exactly two tracks. In particular, it only effects single tags.

- In the $D^+ \rightarrow K_S^0 \pi^+ \pi^+ \pi^-$ mode we have backgrounds from Cabibbo suppressed modes with two K_S^0 . Hence, in this mode we have a veto against candidates where the invariant masses of a pair of oppositely charged tracks fall in the mass range $491 < m_{\pi^+ \pi^-} < 504$ MeV.
- In addition, we also select one candidate per mode per event for the single tags. We keep the candidate that has the smallest $|\Delta E|$.
- For double tags we also select one candidate per event per $D\bar{D}$ combination. We apply the ΔE cuts and then select the best combination based on the average M_{BC} value.
- We select on-resonance events by requiring $E_{CM} > 3.7$ GeV.

Table 8: The mode dependent cuts on ΔE .

Mode	ΔE cut (GeV)
$D^0 \rightarrow K^- \pi^+$	$ \Delta E < 0.0294$
$D^0 \rightarrow K^- \pi^+ \pi^0$	$-0.0583 < \Delta E < 0.0350$
$D^0 \rightarrow K^- \pi^+ \pi^- \pi^+$	$ \Delta E < 0.0200$
$D^+ \rightarrow K^- \pi^+ \pi^+$	$ \Delta E < 0.0218$
$D^+ \rightarrow K^- \pi^+ \pi^+ \pi^0$	$-0.0518 < \Delta E < 0.0401$
$D^+ \rightarrow K_S^0 \pi^+$	$ \Delta E < 0.0265$
$D^+ \rightarrow K_S^0 \pi^+ \pi^0$	$-0.0455 < \Delta E < 0.0423$
$D^+ \rightarrow K_S^0 \pi^+ \pi^+ \pi^-$	$-0.0455 < \Delta E < 0.0423$
$D^+ \rightarrow K^+ K^- \pi^+$	$-0.0455 < \Delta E < 0.0423$

6 Yield extraction

Yields in this analysis are extracted using an unbinned maximum likelihood fit. We extract yields in the signal MC to determine the efficiency and also in the generic MC or data for the branching fraction measurement. This section describes how the various samples are fit. The single tag yields are obtained from a fit to the M_{BC} distribution, whereas the double tag yields are obtained from a two-dimensional fit to the M_{BC} distributions of the two D candidates.

The parameterization of the signal shape, and the implementations as a RooFit object is described in Ref.[?]. In short, this lineshape includes the effects of beam energy spread, initial state radiation from the beam particles, the $\psi(3770)$ line shape, and momentum resolution. We fixed the beam energy spread to 2.1 MeV by fitting the generic MC in Fig.???. The background is described by an ‘ARGUS’ function:

$$\text{ARGUS}(m; m_0, \xi, p) = N m (1 - m^2/m_0^2)^p \exp(\xi(1 - m^2/m_0^2))$$

where N is a normalization. m_0 is the endpoint given by the beam energy. The form above is a slight generalization of the ARGUS function in that we allow the ‘power’ parameter, p , to be different from 1/2.

We first fit the ‘diagonal’ double tag samples – those in which D and \bar{D} decay to charge conjugate final states – to determine the parameters of the signal shape. There are two reasons for doing this:

- In most modes the signal to background ratio is significantly better in the double tag modes.
- But more importantly, the double tag fits allow us to separate the effects of beam energy smearing and detector resolution.

For the single tag fits the effects of detector resolution and beam energy smearing are very similar; they both broaden the M_{BC} resolution. However, for double tag fits the effect of beam energy smearing moves the events diagonally on the M_{BC1} vs. M_{BC2} plot in a fully correlated way while the effects of detector resolution smears the events off this diagonal. Hence the two dimensional fits allow us the separate the effect of detector resolution and beam energy smearing.

6.1 Fits for double tag yields

As discussed above, the double tag yields are fit using a two-dimensional fit to M_{BC1} vs. M_{BC2} . The first mass corresponds to the D decay and the second mass corresponds to the \bar{D} decay. We first fit the modes where the D and \bar{D} decays to the same final state. We use these modes to determine the signal shape parameters in signal Monte Carlo. This includes the D mass and the beam energy spread, and a set of parameters describing the detector resolution. We have used a set of three Gaussians to describe the detector resolution. More specifically we have 5 parameters:

- A core Gaussian, with width σ_p .
- A second wider Gaussian that in the fit is allowed to have a width that is 1.5 to 4 times as wide as the core Gaussian, s_a .
- The fraction of events that are smeared according to this second Gaussian, f_a .
- A third, yet wider, Gaussian that is required to be 1.5 to 4 times as wide as the second Gaussian, s_b .
- The fraction of events that are smeared according to the third Gaussian, f_b .

This gives a resolution function of the form

$$G(\mathbf{p}; \mathbf{p}', \sigma_p, f_a, s_a, f_b, s_b) = \frac{1}{(2\pi)^{3/2}\sigma_p^3} \left[(1 - f_a - f_b)e^{-|\mathbf{p}-\mathbf{p}'|^2/2\sigma_p^2} + \frac{f_a}{s_a^3}e^{-|\mathbf{p}-\mathbf{p}'|^2/2(s_a\sigma_p)^2} + \frac{f_b}{(s_a s_b)^3}e^{-|\mathbf{p}-\mathbf{p}'|^2/2(s_a s_b \sigma_p)^2} \right]$$

In addition to the signal shape we also include four different background terms in the fit:

- First we have two background terms where one of the D mesons are correctly reconstructed and the second is incorrectly reconstructed. We model this as a product of an ARGUS function for the incorrectly reconstructed D and the signal shape for the correctly reconstructed D .
- We also have a background shape for the “mispartition” background, in which final-state particles are swapped between the D and \bar{D} . This is modeled as an ARGUS function in the average mass of M_{BC1} and M_{BC2} multiplied by a Gaussian in the mass difference. These events are distributed along the diagonal as they will have, within detector resolution, the same beam constrained mass for the two D candidates.
- We also introduce a background which is taken as a product of two ARGUS functions.

The fits for the diagonal double tag modes can be found in Figs??, ??, ??, ??, ??, ??, ??, ??, ?? and the shape parameters are summarized in Table ??.

Table 9: σ_p is the width of the ‘core’ resolution function. f_a and f_b is the fraction in the two secondary gaussians in the resolution function. The width of the second gaussian is $s_a\sigma$, and the width of the third gaussian is $s_a s_b \sigma$.

Mode	σ (MeV)	f_a	f_b	s_a	s_b
$D^0 \rightarrow K^- \pi^+$	3.94 ± 0.10	0.195 ± 0.026	0.0059 ± 0.0017	2.33 ± 0.07	3.43 ± 0.41
$D^0 \rightarrow K^- \pi^+ \pi^0$	6.71 ± 0.21	0.212 ± 0.027	0.0260 ± 0.0049	2.53 ± 0.12	3.02 ± 0.31
$D^0 \rightarrow K^- \pi^+ \pi^+ \pi^-$	4.37 ± 0.20	0.168 ± 0.061	0.0115 ± 0.0040	2.08 ± 0.19	3.27 ± 0.43
$D^+ \rightarrow K^- \pi^+ \pi^+$	4.25 ± 0.12	0.121 ± 0.030	0.0060 ± 0.0012	2.30 ± 0.14	4.00 ± 0.16
$D^+ \rightarrow K^- \pi^+ \pi^+ \pi^0$	6.03 ± 0.46	0.277 ± 0.083	0.0501 ± 0.0099	2.18 ± 0.18	3.32 ± 0.34
$D^+ \rightarrow K_S^0 \pi^+$	3.98 ± 0.12	0.158 ± 0.028	0.0046 ± 0.0011	2.48 ± 0.11	4.00 ± 0.47
$D^+ \rightarrow K_S^0 \pi^+ \pi^0$	7.22 ± 0.67	0.169 ± 0.098	0.0396 ± 0.0498	2.20 ± 0.76	2.17 ± 0.41
$D^+ \rightarrow K_S^0 \pi^+ \pi^+ \pi^-$	4.39 ± 0.17	0.148 ± 0.034	0.0161 ± 0.0028	2.52 ± 0.18	4.00 ± 0.17
$D^+ \rightarrow K^+ K^- \pi^+$	4.68 ± 0.16	0.143 ± 0.046	0.0092 ± 0.0021	2.05 ± 0.15	3.59 ± 0.39

Using the shape parameters determined from the fit to the diagonal modes we fit the rest of the double tag modes. All fits can be seen in Figs.??–???. These fits contains the fits to signal Monte Carlo, generic $D\bar{D}$ Monte Carlo, and data.

6.1.1 Double tag efficiencies

The results of these fits to the signal Monte Carlo are summarized in Table ??.

6.1.2 Double tag yields in generic MC

The double tag yields in the generic $D\bar{D}$ MC are summarized in Table ?? and the fits are shown in Figs.??–??.

6.1.3 Double tag yields in data

We are using the same line shape as BES [?] when fitting data. The default values for the line shape parameters are:

For the fit of the data we need to determine the value of $\Gamma_{\psi(3770)}$ to use. The PDG reports 3 measurements by MARK I, MARK II, and DELCO, of 28 ± 5 MeV, 24 ± 5 MeV, and 24 ± 5 MeV respectively. In addition there is a recent measurement from BES [?] that gives the width of $28.6 \pm 1.2 \pm 0.2$. In our fits we use $\Gamma_{\psi(3770)} = 25.2$ MeV.

In addition to the width we need to use a value for the mass of the $\psi(3770)$ resonance in the line shape. We use $m_{\psi(3770)} = 3.7724$ GeV. This parameter is highly correlated with the width in our fits. This is discussed further in Section ???. This mass is somewhat higher e.g. that the recent BES measurement[?].

There is also a factor $-'R'$ – in the line shape called ‘Blatt-Weiskopf’ factor which corresponds to an interaction radius. We use the default value of $R = 12.7$ GeV^{-1} which corresponds to 2.5 fm.

As discussed more in the section on systematic uncertainties, we allow $\Gamma_{\psi(3770)}$ to vary by ± 2.5 MeV, and $m_{\psi(3770)}$ by ± 0.5 MeV and R by ± 4 GeV^{-1} in the systematic studies.

The double tag yields in the data are summarized in Table ???. The fits are shown in Figs. ??–??.

6.2 Fits for single tag yields

We fit for both the D and \bar{D} yields in a simultaneous fit. In this fit we use the same mass and momentum resolution for the D and \bar{D} . All signal shape parameters are fixed from the fit to the double tag samples. D and \bar{D} yields are allowed to vary independently.

6.2.1 Single tag efficiencies

We describe the background shape in the single tag fits with an ARGUS function where we allow the “power” parameter to float. See Table ?? and Figs. ??, ??, and ??.

6.2.2 Single tag yields for generic MC

The generic Monte Carlo is fit in the same way as the signal MC – to a signal shape plus an ARGUS background. The results of these fits are shown in Figs.??, ??, and ?? and are

Table 10: Efficiency for double tag from signal Monte Carlo. The errors on the efficiency are calculated by $\sigma_{yield}\sqrt{1 - \epsilon}$, which has the binomial uncertainty information [?].

Mode	Generated	Signal yield	Efficiency(%)	Efficiency no FSR(%)
$D^0 \rightarrow K^-\pi^+ \bar{D}^0 \rightarrow K^+\pi^-$	60000	25791 ± 161	42.99 ± 0.20	45.42 ± 0.25
$D^0 \rightarrow K^-\pi^+ \bar{D}^0 \rightarrow K^+\pi^-\pi^0$	60000	14835 ± 122	24.73 ± 0.18	25.68 ± 0.21
$D^0 \rightarrow K^-\pi^+ \bar{D}^0 \rightarrow K^+\pi^-\pi^-\pi^+$	60000	18943 ± 138	31.57 ± 0.19	33.27 ± 0.24
$D^0 \rightarrow K^-\pi^+\pi^0 \bar{D}^0 \rightarrow K^+\pi^-$	60000	14642 ± 121	24.40 ± 0.18	25.18 ± 0.21
$D^0 \rightarrow K^-\pi^+\pi^0 \bar{D}^0 \rightarrow K^+\pi^-\pi^0$	60000	8171 ± 91	13.62 ± 0.14	13.72 ± 0.16
$D^0 \rightarrow K^-\pi^+\pi^0 \bar{D}^0 \rightarrow K^+\pi^-\pi^-\pi^+$	60000	10441 ± 103	17.40 ± 0.16	18.27 ± 0.19
$D^0 \rightarrow K^-\pi^+\pi^+\pi^- \bar{D}^0 \rightarrow K^+\pi^-$	60000	18947 ± 138	31.58 ± 0.19	33.49 ± 0.24
$D^0 \rightarrow K^-\pi^+\pi^+\pi^- \bar{D}^0 \rightarrow K^+\pi^-\pi^0$	60000	10389 ± 103	17.32 ± 0.16	17.97 ± 0.19
$D^0 \rightarrow K^-\pi^+\pi^+\pi^- \bar{D}^0 \rightarrow K^+\pi^-\pi^-\pi^+$	60000	13730 ± 117	22.88 ± 0.17	24.16 ± 0.22
$D^+ \rightarrow K^-\pi^+\pi^+ D^- \rightarrow K^+\pi^-\pi^-$	60000	18123 ± 135	30.21 ± 0.19	31.53 ± 0.22
$D^+ \rightarrow K^-\pi^+\pi^+ D^- \rightarrow K^+\pi^-\pi^-\pi^0$	60000	9400 ± 97	15.67 ± 0.15	16.01 ± 0.18
$D^+ \rightarrow K^-\pi^+\pi^+ D^- \rightarrow K_S^0 \pi^-$	60000	15014 ± 123	25.02 ± 0.18	26.07 ± 0.21
$D^+ \rightarrow K^-\pi^+\pi^+ D^- \rightarrow K_S^0 \pi^0\pi^-$	60000	7977 ± 90	13.30 ± 0.14	13.53 ± 0.16
$D^+ \rightarrow K^-\pi^+\pi^+ D^- \rightarrow K_S^0 \pi^-\pi^-\pi^+$	60000	10148 ± 101	16.91 ± 0.15	17.77 ± 0.19
$D^+ \rightarrow K^-\pi^+\pi^+ D^- \rightarrow K^-K^+\pi^-$	60000	14129 ± 119	23.55 ± 0.17	24.32 ± 0.20
$D^+ \rightarrow K^-\pi^+\pi^+\pi^0 D^- \rightarrow K^+\pi^-\pi^-$	60000	9490 ± 98	15.82 ± 0.15	16.24 ± 0.18
$D^+ \rightarrow K^-\pi^+\pi^+\pi^0 D^- \rightarrow K^+\pi^-\pi^-\pi^0$	60000	4954 ± 71	8.26 ± 0.11	8.22 ± 0.13
$D^+ \rightarrow K^-\pi^+\pi^+\pi^0 D^- \rightarrow K_S^0 \pi^-$	60000	7815 ± 89	13.03 ± 0.14	13.33 ± 0.16
$D^+ \rightarrow K^-\pi^+\pi^+\pi^0 D^- \rightarrow K_S^0 \pi^0\pi^-$	60000	4126 ± 65	6.88 ± 0.10	6.96 ± 0.11
$D^+ \rightarrow K^-\pi^+\pi^+\pi^0 D^- \rightarrow K_S^0 \pi^-\pi^-\pi^+$	60000	5101 ± 72	8.50 ± 0.11	8.62 ± 0.13
$D^+ \rightarrow K^-\pi^+\pi^+\pi^0 D^- \rightarrow K^-K^+\pi^-$	60000	7248 ± 86	12.08 ± 0.13	12.41 ± 0.15
$D^+ \rightarrow K_S^0 \pi^+ D^- \rightarrow K^+\pi^-\pi^-$	60000	15090 ± 123	25.15 ± 0.18	25.78 ± 0.20
$D^+ \rightarrow K_S^0 \pi^+ D^- \rightarrow K^+\pi^-\pi^-\pi^0$	60000	7883 ± 89	13.14 ± 0.14	13.56 ± 0.16
$D^+ \rightarrow K_S^0 \pi^+ D^- \rightarrow K_S^0 \pi^-$	60000	12456 ± 112	20.76 ± 0.17	21.36 ± 0.19
$D^+ \rightarrow K_S^0 \pi^+ D^- \rightarrow K_S^0 \pi^0\pi^-$	60000	6524 ± 81	10.87 ± 0.13	11.24 ± 0.14
$D^+ \rightarrow K_S^0 \pi^+ D^- \rightarrow K_S^0 \pi^-\pi^-\pi^+$	60000	8546 ± 93	14.24 ± 0.14	14.68 ± 0.17
$D^+ \rightarrow K_S^0 \pi^+ D^- \rightarrow K^-K^+\pi^-$	60000	11670 ± 108	19.45 ± 0.16	20.05 ± 0.18
$D^+ \rightarrow K_S^0 \pi^+\pi^0 D^- \rightarrow K^+\pi^-\pi^-$	60000	8094 ± 90	13.49 ± 0.14	13.88 ± 0.16
$D^+ \rightarrow K_S^0 \pi^+\pi^0 D^- \rightarrow K^+\pi^-\pi^-\pi^0$	60000	4008 ± 64	6.68 ± 0.10	6.79 ± 0.11
$D^+ \rightarrow K_S^0 \pi^+\pi^0 D^- \rightarrow K_S^0 \pi^-$	60000	6621 ± 82	11.04 ± 0.13	11.28 ± 0.14
$D^+ \rightarrow K_S^0 \pi^+\pi^0 D^- \rightarrow K_S^0 \pi^0\pi^-$	60000	3471 ± 59	5.79 ± 0.10	5.86 ± 0.10
$D^+ \rightarrow K_S^0 \pi^+\pi^0 D^- \rightarrow K_S^0 \pi^-\pi^-\pi^+$	60000	4302 ± 66	7.17 ± 0.11	7.42 ± 0.12
$D^+ \rightarrow K_S^0 \pi^+\pi^0 D^- \rightarrow K^-K^+\pi^-$	60000	6207 ± 79	10.35 ± 0.12	10.52 ± 0.14
$D^+ \rightarrow K_S^0 \pi^+\pi^+\pi^- D^- \rightarrow K^+\pi^-\pi^-$	60000	10383 ± 102	17.31 ± 0.15	17.89 ± 0.19
$D^+ \rightarrow K_S^0 \pi^+\pi^+\pi^- D^- \rightarrow K^+\pi^-\pi^-\pi^0$	60000	5314 ± 74	8.86 ± 0.12	9.09 ± 0.14
$D^+ \rightarrow K_S^0 \pi^+\pi^+\pi^- D^- \rightarrow K_S^0 \pi^-$	60000	8583 ± 93	14.31 ± 0.14	14.71 ± 0.17
$D^+ \rightarrow K_S^0 \pi^+\pi^+\pi^- D^- \rightarrow K_S^0 \pi^0\pi^-$	60000	4326 ± 66	7.21 ± 0.11	7.29 ± 0.12
$D^+ \rightarrow K_S^0 \pi^+\pi^+\pi^- D^- \rightarrow K_S^0 \pi^-\pi^-\pi^+$	60000	5774 ± 77	9.62 ± 0.12	9.96 ± 0.15
$D^+ \rightarrow K_S^0 \pi^+\pi^+\pi^- D^- \rightarrow K^-K^+\pi^-$	60000	7922 ± 89	13.20 ± 0.14	13.73 ± 0.16
$D^+ \rightarrow K^+K^-\pi^+ D^- \rightarrow K^+\pi^-\pi^-$	60000	14232 ± 119	23.72 ± 0.17	24.52 ± 0.20
$D^+ \rightarrow K^+K^-\pi^+ D^- \rightarrow K^+\pi^-\pi^-\pi^0$	60000	7395 ± 87	12.33 ± 0.14	12.63 ± 0.15
$D^+ \rightarrow K^+K^-\pi^+ D^- \rightarrow K_S^0 \pi^-$	60000	11631 ± 108	19.39 ± 0.16	19.99 ± 0.18
$D^+ \rightarrow K^+K^-\pi^+ D^- \rightarrow K_S^0 \pi^0\pi^-$	60000	6113 ± 79	10.19 ± 0.12	10.38 ± 0.14
$D^+ \rightarrow K^+K^-\pi^+ D^- \rightarrow K_S^0 \pi^-\pi^-\pi^+$	60000	8015 ± 90	13.36 ± 0.14	13.73 ± 0.16
$D^+ \rightarrow K^+K^-\pi^+ D^- \rightarrow K^-K^+\pi^-$	60000	11068 ± 105	18.45 ± 0.16	19.10 ± 0.18

Table 11: Double tag yields in generic Monte Carlo. The table also includes the number of events that were generated, a background estimate, and the efficiency from the generic Monte Carlo, and the ratio from the efficiency determined in the signal Monte Carlo. And $\sigma = x/\Delta x$ for $x \pm \Delta x$.

Mode	Generated	Yield	Bkgd	Efficiency(%)	$\epsilon_{\text{sig}}/\epsilon_{\text{gen}} - 1$ (%)
$D^0 \rightarrow K^-\pi^+ \bar{D}^0 \rightarrow K^+\pi^-$	14644	6436 ± 80	0.1	43.95 ± 0.41	+1.25%(+1.01 σ)
$D^0 \rightarrow K^-\pi^+ \bar{D}^0 \rightarrow K^+\pi^-\pi^0$	52229	13229 ± 116	0.2	25.33 ± 0.19	-2.25%(-1.57 σ)
$D^0 \rightarrow K^-\pi^+ \bar{D}^0 \rightarrow K^+\pi^-\pi^+\pi^-$	29230	9524 ± 98	45.4	32.43 ± 0.28	-2.65%(-2.01 σ)
$D^0 \rightarrow K^-\pi^+\pi^0 \bar{D}^0 \rightarrow K^+\pi^-$	52518	13061 ± 115	0.2	24.87 ± 0.19	+1.05%(+0.71 σ)
$D^0 \rightarrow K^-\pi^+\pi^0 \bar{D}^0 \rightarrow K^+\pi^-\pi^0$	189598	26524 ± 165	0.3	13.99 ± 0.08	+0.14%(+0.10 σ)
$D^0 \rightarrow K^-\pi^+\pi^0 \bar{D}^0 \rightarrow K^+\pi^-\pi^+\pi^-$	106433	19062 ± 140	88.5	17.83 ± 0.12	-2.30%(-1.39 σ)
$D^0 \rightarrow K^-\pi^+\pi^-\pi^+ \bar{D}^0 \rightarrow K^+\pi^-$	29374	9410 ± 97	45.4	31.88 ± 0.27	-1.32%(-0.99 σ)
$D^0 \rightarrow K^-\pi^+\pi^-\pi^+ \bar{D}^0 \rightarrow K^+\pi^-\pi^0$	107277	18756 ± 139	88.5	17.40 ± 0.12	+0.80%(+0.47 σ)
$D^0 \rightarrow K^-\pi^+\pi^-\pi^+ \bar{D}^0 \rightarrow K^+\pi^-\pi^+\pi^-$	60669	13784 ± 118	131.8	22.50 ± 0.17	+1.38%(+0.90 σ)
$D^+ \rightarrow K^-\pi^+\pi^+ D^- \rightarrow K^+\pi^-\pi^-$	59284	17941 ± 134	0	30.26 ± 0.19	+0.30%(+0.24 σ)
$D^+ \rightarrow K^-\pi^+\pi^+ D^- \rightarrow K^+\pi^-\pi^-\pi^0$	44810	7207 ± 87	0	16.08 ± 0.18	+2.30%(+1.13 σ)
$D^+ \rightarrow K^-\pi^+\pi^+ D^- \rightarrow K_S^0\pi^-$	9419	2375 ± 49	23.7	24.96 ± 0.45	-0.16%(-0.07 σ)
$D^+ \rightarrow K^-\pi^+\pi^+ D^- \rightarrow K_S^0\pi^-\pi^0$	36165	5062 ± 72	168.0	13.53 ± 0.19	+2.59%(+1.11 σ)
$D^+ \rightarrow K^-\pi^+\pi^+ D^- \rightarrow K_S^0\pi^-\pi^-\pi^+$	23480	4297 ± 66	110.7	17.83 ± 0.25	-0.79%(-0.38 σ)
$D^+ \rightarrow K^-\pi^+\pi^+ D^- \rightarrow K^-K^+\pi^-$	10085	2552 ± 51	0	25.30 ± 0.44	+2.77%(+1.28 σ)
$D^+ \rightarrow K^-\pi^+\pi^+\pi^0 D^- \rightarrow K^+\pi^-\pi^-$	44905	7166 ± 86	0	15.96 ± 0.18	+0.81%(+0.41 σ)
$D^+ \rightarrow K^-\pi^+\pi^+\pi^0 D^- \rightarrow K^+\pi^-\pi^-\pi^0$	34006	2846 ± 59	0	8.37 ± 0.17	-4.18%(-1.36 σ)
$D^+ \rightarrow K^-\pi^+\pi^+\pi^0 D^- \rightarrow K_S^0\pi^-$	7048	935 ± 31	9.2	13.14 ± 0.41	-4.03%(-1.16 σ)
$D^+ \rightarrow K^-\pi^+\pi^+\pi^0 D^- \rightarrow K_S^0\pi^-\pi^0$	27549	1998 ± 47	65.2	7.02 ± 0.16	+3.13%(+0.90 σ)
$D^+ \rightarrow K^-\pi^+\pi^+\pi^0 D^- \rightarrow K_S^0\pi^-\pi^-\pi^+$	17886	1634 ± 43	43.0	8.90 ± 0.23	+6.97%(+1.92 σ)
$D^+ \rightarrow K^-\pi^+\pi^+\pi^0 D^- \rightarrow K^-K^+\pi^-$	7438	1038 ± 33	0	13.96 ± 0.41	-1.86%(-0.55 σ)
$D^+ \rightarrow K_S^0\pi^+ D^- \rightarrow K^+\pi^-\pi^-$	9626	2493 ± 50	23.7	25.65 ± 0.45	-1.36%(-0.64 σ)
$D^+ \rightarrow K_S^0\pi^+ D^- \rightarrow K^+\pi^-\pi^-\pi^0$	7408	980 ± 32	9.2	13.10 ± 0.40	+0.69%(+0.19 σ)
$D^+ \rightarrow K_S^0\pi^+ D^- \rightarrow K_S^0\pi^-$	1441	280 ± 17	6.3	18.99 ± 1.06	+8.43%(+1.35 σ)
$D^+ \rightarrow K_S^0\pi^+ D^- \rightarrow K_S^0\pi^-\pi^0$	5770	676 ± 26	28.2	11.23 ± 0.42	-2.32%(-0.56 σ)
$D^+ \rightarrow K_S^0\pi^+ D^- \rightarrow K_S^0\pi^-\pi^-\pi^+$	3773	526 ± 23	20.0	13.41 ± 0.57	+8.05%(+1.62 σ)
$D^+ \rightarrow K_S^0\pi^+ D^- \rightarrow K^-K^+\pi^-$	1572	337 ± 19	3.3	21.23 ± 1.07	+1.18%(+0.22 σ)
$D^+ \rightarrow K_S^0\pi^+ \pi^0 D^- \rightarrow K^+\pi^-\pi^-$	36171	5180 ± 73	168.0	13.86 ± 0.19	-0.87%(-0.38 σ)
$D^+ \rightarrow K_S^0\pi^+ \pi^0 D^- \rightarrow K^+\pi^-\pi^-\pi^0$	27363	2035 ± 47	65.2	7.20 ± 0.17	+0.42%(+0.12 σ)
$D^+ \rightarrow K_S^0\pi^+ \pi^0 D^- \rightarrow K_S^0\pi^-$	5799	610 ± 25	28.2	10.03 ± 0.41	+16.35%(+3.10 σ)
$D^+ \rightarrow K_S^0\pi^+ \pi^0 D^- \rightarrow K_S^0\pi^-\pi^0$	21371	1316 ± 37	85.1	5.76 ± 0.17	+1.74%(+0.43 σ)
$D^+ \rightarrow K_S^0\pi^+ \pi^0 D^- \rightarrow K_S^0\pi^-\pi^-\pi^+$	14414	1161 ± 35	66.6	7.59 ± 0.23	+3.29%(+0.82 σ)
$D^+ \rightarrow K_S^0\pi^+ \pi^0 D^- \rightarrow K^-K^+\pi^-$	6026	677 ± 27	23.7	10.84 ± 0.42	+4.98%(+1.08 σ)
$D^+ \rightarrow K_S^0\pi^+ \pi^+ \pi^- D^- \rightarrow K^+\pi^-\pi^-$	23876	4438 ± 67	110.7	18.12 ± 0.25	-1.38%(-0.68 σ)
$D^+ \rightarrow K_S^0\pi^+ \pi^+ \pi^- D^- \rightarrow K^+\pi^-\pi^-\pi^0$	17953	1619 ± 43	43.0	8.78 ± 0.23	+6.26%(+1.71 σ)
$D^+ \rightarrow K_S^0\pi^+ \pi^+ \pi^- D^- \rightarrow K_S^0\pi^-$	3920	643 ± 26	20.0	15.89 ± 0.61	-7.68%(-1.98 σ)
$D^+ \rightarrow K_S^0\pi^+ \pi^+ \pi^- D^- \rightarrow K_S^0\pi^-\pi^0$	14210	1100 ± 34	66.6	7.27 ± 0.23	+6.33%(+1.49 σ)
$D^+ \rightarrow K_S^0\pi^+ \pi^+ \pi^- D^- \rightarrow K_S^0\pi^-\pi^-\pi^+$	9496	1088 ± 34	50.8	10.92 ± 0.34	-2.47%(-0.68 σ)
$D^+ \rightarrow K_S^0\pi^+ \pi^+ \pi^- D^- \rightarrow K^-K^+\pi^-$	3894	629 ± 26	15.6	15.75 ± 0.61	-0.32%(-0.08 σ)
$D^+ \rightarrow K^+K^-\pi^+ D^- \rightarrow K^+\pi^-\pi^-$	9953	2604 ± 51	0	26.16 ± 0.44	+2.03%(+0.97 σ)
$D^+ \rightarrow K^+K^-\pi^+ D^- \rightarrow K^+\pi^-\pi^-\pi^0$	7337	1003 ± 32	0	13.67 ± 0.41	-0.44%(-0.13 σ)
$D^+ \rightarrow K^+K^-\pi^+ D^- \rightarrow K_S^0\pi^-$	1597	371 ± 19	3.3	23.02 ± 1.04	-7.30%(-1.67 σ)
$D^+ \rightarrow K^+K^-\pi^+ D^- \rightarrow K_S^0\pi^-\pi^0$	6045	733 ± 28	23.7	11.73 ± 0.44	-1.11%(-0.26 σ)
$D^+ \rightarrow K^+K^-\pi^+ D^- \rightarrow K_S^0\pi^-\pi^-\pi^+$	3890	616 ± 26	15.6	15.43 ± 0.61	-1.36%(-0.32 σ)
$D^+ \rightarrow K^+K^-\pi^+ D^- \rightarrow K^-K^+\pi^-$	1607	361 ± 19	0	22.46 ± 1.04	-0.62%(-0.13 σ)

Table 12: Double tag yields in data. Backgrounds are estimated as described in Section ??.

Mode	Yield			Background
	$\Gamma = 22.7 \text{ MeV}$	$\Gamma = 25.2 \text{ MeV}$	$\Gamma = 27.7 \text{ MeV}$	
$D^0 \rightarrow K^-\pi^+ \bar{D}^0 \rightarrow K^+\pi^-$	1823 ± 43	1825 ± 43	1827 ± 43	< 0.1
$D^0 \rightarrow K^-\pi^+ \bar{D}^0 \rightarrow K^+\pi^-\pi^0$	3879 ± 64	3886 ± 64	3892 ± 64	< 0.1
$D^0 \rightarrow K^-\pi^+ \bar{D}^0 \rightarrow K^+\pi^-\pi^-\pi^+$	2984 ± 55	2987 ± 55	2990 ± 55	32.7 ± 4.7
$D^0 \rightarrow K^-\pi^+\pi^0 \bar{D}^0 \rightarrow K^+\pi^-$	3958 ± 64	3964 ± 64	3969 ± 64	< 0.1
$D^0 \rightarrow K^-\pi^+\pi^0 \bar{D}^0 \rightarrow K^+\pi^-\pi^0$	7584 ± 90	7600 ± 90	7613 ± 90	< 0.1
$D^0 \rightarrow K^-\pi^+\pi^0 \bar{D}^0 \rightarrow K^+\pi^-\pi^-\pi^+$	5748 ± 78	5760 ± 78	5769 ± 78	59.4 ± 8.5
$D^0 \rightarrow K^-\pi^+\pi^+\pi^- \bar{D}^0 \rightarrow K^+\pi^-$	2890 ± 54	2895 ± 54	2898 ± 54	32.7 ± 4.7
$D^0 \rightarrow K^-\pi^+\pi^+\pi^- \bar{D}^0 \rightarrow K^+\pi^-\pi^0$	5712 ± 78	5723 ± 78	5733 ± 78	59.4 ± 8.5
$D^0 \rightarrow K^-\pi^+\pi^+\pi^- \bar{D}^0 \rightarrow K^+\pi^-\pi^-\pi^+$	4549 ± 69	4559 ± 69	4568 ± 69	96.9 ± 9.7
$D^+ \rightarrow K^-\pi^+\pi^+ D^- \rightarrow K^+\pi^-\pi^-$	5947 ± 78	5951 ± 78	5954 ± 78	< 0.1
$D^+ \rightarrow K^-\pi^+\pi^+ D^- \rightarrow K^+\pi^-\pi^-\pi^0$	1904 ± 45	1908 ± 45	1911 ± 45	< 0.1
$D^+ \rightarrow K^-\pi^+\pi^+ D^- \rightarrow K_S^0 \pi^-$	862 ± 30	862 ± 30	863 ± 30	10.0 ± 2.2
$D^+ \rightarrow K^-\pi^+\pi^+ D^- \rightarrow K_S^0 \pi^-\pi^0$	2030 ± 46	2032 ± 46	2034 ± 46	21.9 ± 10.1
$D^+ \rightarrow K^-\pi^+\pi^+ D^- \rightarrow K_S^0 \pi^-\pi^-\pi^+$	1066 ± 33	1067 ± 33	1068 ± 33	37.2 ± 15.4
$D^+ \rightarrow K^-\pi^+\pi^+ D^- \rightarrow K^-K^+\pi^-$	483 ± 22	483 ± 22	483 ± 22	< 0.1
$D^+ \rightarrow K^-\pi^+\pi^+\pi^0 D^- \rightarrow K^+\pi^-\pi^-$	1835 ± 44	1839 ± 44	1842 ± 44	< 0.1
$D^+ \rightarrow K^-\pi^+\pi^+\pi^0 D^- \rightarrow K^+\pi^-\pi^-\pi^0$	641 ± 29	644 ± 29	648 ± 30	< 0.1
$D^+ \rightarrow K^-\pi^+\pi^+\pi^0 D^- \rightarrow K_S^0 \pi^-$	294 ± 18	295 ± 18	295 ± 18	3.1 ± 0.7
$D^+ \rightarrow K^-\pi^+\pi^+\pi^0 D^- \rightarrow K_S^0 \pi^-\pi^0$	599 ± 26	601 ± 26	602 ± 26	6.8 ± 3.2
$D^+ \rightarrow K^-\pi^+\pi^+\pi^0 D^- \rightarrow K_S^0 \pi^-\pi^-\pi^+$	367 ± 21	369 ± 21	370 ± 21	11.6 ± 4.8
$D^+ \rightarrow K^-\pi^+\pi^+\pi^0 D^- \rightarrow K^-K^+\pi^-$	160 ± 14	160 ± 14	160 ± 14	< 0.1
$D^+ \rightarrow K_S^0 \pi^+ D^- \rightarrow K^+\pi^-\pi^-$	827 ± 29	828 ± 29	828 ± 29	10.0 ± 2.2
$D^+ \rightarrow K_S^0 \pi^+ D^- \rightarrow K^+\pi^-\pi^-\pi^0$	294 ± 17	294 ± 17	295 ± 17	3.1 ± 0.7
$D^+ \rightarrow K_S^0 \pi^+ D^- \rightarrow K_S^0 \pi^-$	109 ± 11	109 ± 11	109 ± 11	2.7 ± 0.6
$D^+ \rightarrow K_S^0 \pi^+ D^- \rightarrow K_S^0 \pi^-\pi^0$	260 ± 17	260 ± 17	260 ± 17	6.0 ± 1.5
$D^+ \rightarrow K_S^0 \pi^+ D^- \rightarrow K_S^0 \pi^-\pi^-\pi^+$	147 ± 12	147 ± 12	147 ± 12	6.9 ± 2.1
$D^+ \rightarrow K_S^0 \pi^+ D^- \rightarrow K^-K^+\pi^-$	72 ± 9	72 ± 9	72 ± 9	0.8 ± 0.2
$D^+ \rightarrow K_S^0 \pi^+\pi^0 D^- \rightarrow K^+\pi^-\pi^-$	1849 ± 44	1851 ± 44	1852 ± 44	21.9 ± 10.1
$D^+ \rightarrow K_S^0 \pi^+\pi^0 D^- \rightarrow K^+\pi^-\pi^-\pi^0$	630 ± 26	632 ± 26	633 ± 26	6.8 ± 3.2
$D^+ \rightarrow K_S^0 \pi^+\pi^0 D^- \rightarrow K_S^0 \pi^-$	257 ± 16	257 ± 16	257 ± 16	6.0 ± 1.5
$D^+ \rightarrow K_S^0 \pi^+\pi^0 D^- \rightarrow K_S^0 \pi^-\pi^0$	644 ± 27	645 ± 27	647 ± 27	13.4 ± 6.2
$D^+ \rightarrow K_S^0 \pi^+\pi^0 D^- \rightarrow K_S^0 \pi^-\pi^-\pi^+$	359 ± 20	361 ± 20	362 ± 20	15.6 ± 5.1
$D^+ \rightarrow K_S^0 \pi^+\pi^0 D^- \rightarrow K^-K^+\pi^-$	144 ± 13	144 ± 13	144 ± 13	1.8 ± 0.8
$D^+ \rightarrow K_S^0 \pi^+\pi^+\pi^- D^- \rightarrow K^+\pi^-\pi^-$	1143 ± 34	1145 ± 34	1146 ± 34	37.2 ± 15.4
$D^+ \rightarrow K_S^0 \pi^+\pi^+\pi^- D^- \rightarrow K^+\pi^-\pi^-\pi^0$	337 ± 20	339 ± 20	341 ± 20	11.6 ± 4.8
$D^+ \rightarrow K_S^0 \pi^+\pi^+\pi^- D^- \rightarrow K_S^0 \pi^-$	160 ± 13	160 ± 13	160 ± 13	6.9 ± 2.1
$D^+ \rightarrow K_S^0 \pi^+\pi^+\pi^- D^- \rightarrow K_S^0 \pi^-\pi^0$	357 ± 20	359 ± 20	360 ± 20	15.6 ± 5.1
$D^+ \rightarrow K_S^0 \pi^+\pi^+\pi^- D^- \rightarrow K_S^0 \pi^-\pi^-\pi^+$	204 ± 16	205 ± 16	206 ± 16	14.5 ± 5.2
$D^+ \rightarrow K_S^0 \pi^+\pi^+\pi^- D^- \rightarrow K^-K^+\pi^-$	91 ± 10	91 ± 10	92 ± 10	3.0 ± 1.2
$D^+ \rightarrow K^+K^-\pi^+ D^- \rightarrow K^+\pi^-\pi^-$	485 ± 22	485 ± 22	485 ± 22	< 0.1
$D^+ \rightarrow K^+K^-\pi^+ D^- \rightarrow K^+\pi^-\pi^-\pi^0$	166 ± 13	166 ± 13	166 ± 13	< 0.1
$D^+ \rightarrow K^+K^-\pi^+ D^- \rightarrow K_S^0 \pi^-$	62 ± 8	62 ± 8	63 ± 8	0.8 ± 0.2
$D^+ \rightarrow K^+K^-\pi^+ D^- \rightarrow K_S^0 \pi^-\pi^0$	180 ± 14	180 ± 14	180 ± 14	1.8 ± 0.8
$D^+ \rightarrow K^+K^-\pi^+ D^- \rightarrow K_S^0 \pi^-\pi^-\pi^+$	95 ± 11	96 ± 11	97 ± 11	3.0 ± 1.2
$D^+ \rightarrow K^+K^-\pi^+ D^- \rightarrow K^-K^+\pi^-$	41 ± 8	42 ± 8	42 ± 8	< 0.1

Table 13: Single tag efficiencies in our signal Monte Carlo.

Mode	Generated	Yield	mass	ξ	p	Efficiency(%)
$D^0 \rightarrow K^-\pi^+$	188220	122658 ± 350	1864.879 ± 0.003	-4.7 ± 5.7	0.50 ± 0.00	65.17 ± 0.11
$\bar{D}^0 \rightarrow K^+\pi^-$	188220	124000 ± 352	1864.879 ± 0.003	-4.7 ± 5.7	0.50 ± 0.00	65.88 ± 0.11
$D^0 \rightarrow K^-\pi^+\pi^0$	592050	208889 ± 487	1864.928 ± 0.003	-38.5 ± 1.0	0.76 ± 0.02	35.28 ± 0.07
$\bar{D}^0 \rightarrow K^+\pi^-\pi^0$	592050	210915 ± 489	1864.928 ± 0.003	-38.5 ± 1.0	0.76 ± 0.02	35.62 ± 0.07
$D^0 \rightarrow K^-\pi^+\pi^+\pi^-$	298440	139725 ± 379	1864.870 ± 0.003	-9.6 ± 1.9	0.44 ± 0.04	46.82 ± 0.09
$\bar{D}^0 \rightarrow K^+\pi^-\pi^-\pi^+$	298440	140839 ± 381	1864.870 ± 0.003	-9.6 ± 1.9	0.44 ± 0.04	47.19 ± 0.09
$D^+ \rightarrow K^-\pi^+\pi^+$	239940	131766 ± 364	1869.676 ± 0.003	-7.5 ± 3.2	0.50 ± 0.00	54.92 ± 0.10
$D^- \rightarrow K^+\pi^-\pi^-$	239940	132373 ± 365	1869.676 ± 0.003	-7.5 ± 3.2	0.50 ± 0.00	55.17 ± 0.10
$D^+ \rightarrow K^-\pi^+\pi^+\pi^0$	220140	61918 ± 261	1869.708 ± 0.005	-21.4 ± 1.9	0.56 ± 0.03	28.13 ± 0.10
$D^- \rightarrow K^+\pi^-\pi^-\pi^0$	220140	62095 ± 261	1869.708 ± 0.005	-21.4 ± 1.9	0.56 ± 0.03	28.21 ± 0.10
$D^+ \rightarrow K_S^0 \pi^+$	240000	109514 ± 332	1869.675 ± 0.003	-14.9 ± 4.5	0.50 ± 0.00	45.63 ± 0.10
$D^- \rightarrow K_S^0 \pi^-$	240000	108794 ± 331	1869.675 ± 0.003	-14.9 ± 4.5	0.50 ± 0.00	45.33 ± 0.10
$D^+ \rightarrow K_S^0 \pi^+\pi^0$	171480	41078 ± 213	1869.721 ± 0.007	-28.8 ± 2.4	0.57 ± 0.04	23.95 ± 0.11
$D^- \rightarrow K_S^0 \pi^-\pi^0$	171480	41323 ± 213	1869.721 ± 0.007	-28.8 ± 2.4	0.57 ± 0.04	24.10 ± 0.11
$D^+ \rightarrow K_S^0 \pi^+\pi^+\pi^-$	117930	38075 ± 200	1869.674 ± 0.006	-12.6 ± 2.2	0.52 ± 0.05	32.29 ± 0.14
$D^- \rightarrow K_S^0 \pi^-\pi^-\pi^+$	117930	38449 ± 201	1869.674 ± 0.006	-12.6 ± 2.2	0.52 ± 0.05	32.60 ± 0.14
$D^+ \rightarrow K^+K^-\pi^+$	60000	25636 ± 166	1869.688 ± 0.006	-45.7 ± 38.9	1.50 ± 1.11	42.73 ± 0.21
$D^- \rightarrow K^-K^+\pi^-$	60000	25482 ± 159	1869.688 ± 0.006	-45.7 ± 38.9	1.50 ± 1.11	42.47 ± 0.20

summarized in Table ??.

6.2.3 Single tag yields for data

Using the same fit as for the Monte Carlo, we extract the single tag yields from data. The yields are summarized in Table ?? and the fits are shown in Figs. ??-??.

6.2.4 Single tag yields comparison between D and \bar{D}

We compared the yields difference between D and \bar{D} in Table ??.

7 Backgrounds

7.1 Single Tag Backgrounds

Non-peaking backgrounds in the Monte Carlo are well described by our background function models, so we need to explicitly determine only the peaking backgrounds *a priori*. These can be categorized as crossfeeds, where D 's that actually decay into one signal mode are reconstructed as candidates from a different signal mode, and “external” backgrounds, where decays we do not measure for the fit contaminate modes we are measuring. We separate these so that for crossfeeds the branching fractions from the fit can be used to update the background subtractions between iterations. To measure backgrounds, we find the major

Table 14: Single tag yields for generic MC. Backgrounds are estimated as described in Section ???. And $\sigma = x/\Delta x$ for $x \pm \Delta x$.

Mode	Generated	Yield	Background	Efficiency	$\epsilon_{\text{sig}}/\epsilon_{\text{gen}} - 1$
$D^0 \rightarrow K^- \pi^+$	374853	247417 ± 499	970	65.74 ± 0.08	$+0.03(+0.07\sigma)$
$\bar{D}^0 \rightarrow K^+ \pi^-$	376072	251921 ± 503	970	66.73 ± 0.08	$+0.14(+0.33\sigma)$
$D^0 \rightarrow K^- \pi^+ \pi^0$	1360131	485360 ± 763	1736	35.56 ± 0.05	$-0.53(-1.43\sigma)$
$\bar{D}^0 \rightarrow K^+ \pi^- \pi^0$	1362706	490786 ± 767	1736	35.89 ± 0.05	$+0.08(+0.22\sigma)$
$D^0 \rightarrow K^- \pi^+ \pi^- \pi^+$	769682	363676 ± 633	2701	46.90 ± 0.06	$+0.02(+0.06\sigma)$
$\bar{D}^0 \rightarrow K^+ \pi^- \pi^+ \pi^-$	767957	366636 ± 635	2701	47.39 ± 0.06	$-0.78(-2.17\sigma)$
$D^+ \rightarrow K^- \pi^+ \pi^+$	662059	363948 ± 620	0	54.97 ± 0.06	$+0.11(+0.31\sigma)$
$D^- \rightarrow K^+ \pi^- \pi^-$	662616	367075 ± 623	0	55.40 ± 0.06	$+0.14(+0.41\sigma)$
$D^+ \rightarrow K^- \pi^+ \pi^+ \pi^0$	500235	142708 ± 469	0	28.53 ± 0.08	$-0.81(-1.17\sigma)$
$D^- \rightarrow K^+ \pi^- \pi^- \pi^0$	500338	143892 ± 471	0	28.76 ± 0.08	$-1.39(-2.04\sigma)$
$D^+ \rightarrow K_S^0 \pi^+$	106522	48908 ± 227	477	45.47 ± 0.16	$+0.57(+1.08\sigma)$
$D^- \rightarrow K_S^0 \pi^-$	105329	48467 ± 226	477	45.56 ± 0.16	$-0.62(-1.17\sigma)$
$D^+ \rightarrow K_S^0 \pi^+ \pi^0$	399417	97467 ± 388	3381	23.56 ± 0.08	$+3.91(+4.44\sigma)$
$D^- \rightarrow K_S^0 \pi^- \pi^0$	398275	97039 ± 387	3381	23.52 ± 0.08	$+4.08(+4.64\sigma)$
$D^+ \rightarrow K_S^0 \pi^+ \pi^+ \pi^-$	263198	87459 ± 349	2229	32.38 ± 0.11	$-0.93(-1.15\sigma)$
$D^- \rightarrow K_S^0 \pi^- \pi^- \pi^+$	263091	87040 ± 348	2229	32.24 ± 0.11	$-1.64(-2.00\sigma)$
$D^+ \rightarrow K^+ K^- \pi^+$	109611	51633 ± 250	0	47.11 ± 0.17	$-0.21(-0.25\sigma)$
$D^- \rightarrow K^- K^+ \pi^-$	109917	51955 ± 251	0	47.27 ± 0.17	$-0.44(-0.52\sigma)$

Table 15: Single tag yields for data with different fixed values of Γ . The default value is 25.2 MeV. Backgrounds are estimated as described in Section ??.

Mode	Yield			D mass (MeV)	Bkg
	$\Gamma = 22.7$ MeV	$\Gamma = 25.2$ MeV	$\Gamma = 27.7$ MeV		
$D^0 \rightarrow K^- \pi^+$	74908 ± 282	75177 ± 281	75412 ± 282	1864.297 ± 0.004	289 ± 14
$\bar{D}^0 \rightarrow K^+ \pi^-$	75314 ± 282	75584 ± 282	75819 ± 283	1864.297 ± 0.004	289 ± 14
$D^0 \rightarrow K^- \pi^+ \pi^0$	144073 ± 438	144710 ± 439	145339 ± 441	1864.308 ± 0.004	300 ± 17
$\bar{D}^0 \rightarrow K^+ \pi^- \pi^0$	145146 ± 440	145798 ± 441	146440 ± 443	1864.308 ± 0.004	300 ± 17
$D^0 \rightarrow K^- \pi^+ \pi^+ \pi^-$	113697 ± 366	114222 ± 366	114726 ± 367	1864.294 ± 0.004	2633 ± 265
$\bar{D}^0 \rightarrow K^+ \pi^- \pi^- \pi^+$	114233 ± 367	114759 ± 368	115264 ± 368	1864.294 ± 0.004	2633 ± 265
$D^+ \rightarrow K^- \pi^+ \pi^+$	116212 ± 353	116545 ± 354	116852 ± 354	1869.106 ± 0.003	< 1
$D^- \rightarrow K^+ \pi^- \pi^-$	117497 ± 355	117831 ± 356	118140 ± 356	1869.106 ± 0.003	< 1
$D^+ \rightarrow K^- \pi^+ \pi^+ \pi^0$	36669 ± 259	36813 ± 260	36956 ± 261	1869.109 ± 0.009	< 1
$D^- \rightarrow K^+ \pi^- \pi^- \pi^0$	36993 ± 261	37143 ± 261	37292 ± 262	1869.109 ± 0.009	< 1
$D^+ \rightarrow K_S^0 \pi^+$	16788 ± 137	16844 ± 137	16896 ± 138	1869.107 ± 0.009	197 ± 43
$D^- \rightarrow K_S^0 \pi^-$	17034 ± 138	17087 ± 138	17137 ± 138	1869.107 ± 0.009	197 ± 43
$D^+ \rightarrow K_S^0 \pi^+ \pi^0$	38171 ± 264	38329 ± 262	38482 ± 266	1869.106 ± 0.009	433 ± 201
$D^- \rightarrow K_S^0 \pi^- \pi^0$	38471 ± 265	38626 ± 263	38777 ± 266	1869.106 ± 0.009	433 ± 201
$D^+ \rightarrow K_S^0 \pi^+ \pi^+ \pi^-$	23597 ± 224	23706 ± 224	23814 ± 226	1869.087 ± 0.010	735 ± 305
$D^- \rightarrow K_S^0 \pi^- \pi^- \pi^+$	23798 ± 225	23909 ± 225	24018 ± 227	1869.087 ± 0.010	735 ± 305
$D^+ \rightarrow K^+ K^- \pi^+$	10069 ± 124	10115 ± 123	10160 ± 124	1869.118 ± 0.013	< 1
$D^- \rightarrow K^- K^+ \pi^-$	10020 ± 123	10066 ± 123	10109 ± 124	1869.118 ± 0.013	< 1

sources of external background in generic $D\bar{D}$ Monte Carlo samples, then look at crossfeed rates in single-tag signal samples with the external background sources removed. Efficiencies for backgrounds are measured from signal Monte Carlo samples.

In the fitter input crossfeed backgrounds are characterized simply by an efficiency (in this case, the probability that the real decay will be reconstructed and accepted as another mode), with the branching fractions and $N_{D\bar{D}}$ being supplied by the fitter. External backgrounds are specified by an efficiency for detection and an effective branching fraction, which is constant between iterations, or by an absolute subtraction.

Crossfeed backgrounds are summarized in Table ?? and external backgrounds in Table ???. The background sources accounted for are:

Doubly-Cabibbo-suppressed modes (external) In Monte Carlo, the channels $\bar{D}^0 \rightarrow K^- \pi^+$ and $\bar{D}^0 \rightarrow K^- \pi^+ \pi^0$ are the largest peaking backgrounds for the decays $D^0 \rightarrow K^- \pi^+$ and $D^0 \rightarrow K^- \pi^+ \pi^0$, respectively. In addition, in data the decay $\bar{D}^0 \rightarrow K^- \pi^+ \pi^+ \pi^-$ is expected to contribute to the channel $D^0 \rightarrow K^- \pi^+ \pi^+ \pi^-$, although it is not generated in the Monte Carlo. DCSD should not be a background for D^+ decays because the decay products will have the wrong charge.

The DCSD modes form external backgrounds dependent on $N_{D^0 \bar{D}^0}$. The efficiency for these modes is only weakly dependent on the resonant substructure. The efficiency for $D^0 \rightarrow K^+ \pi^-$ is the same as for $\bar{D}^0 \rightarrow K^+ \pi^-$, but those for $D^0 \rightarrow K^+ \pi^- \pi^0$

Table 16: Ratios of single tag data yields and efficiencies with the standard ΔE cuts (Yield1 and eff1) to those with $2 \times \Delta E$ cuts (Yield2 and eff2). The last column (eff1'/eff2') is the ratio of the efficiencies without FSR cuts to the efficiencies with the wide ΔE cuts and without FSR cuts.

Mode	Yield1/Yield2	eff1/eff2	Ratio	eff1'/eff2'
$D^0 \rightarrow K^- \pi^+$	0.9850 ± 0.0005	0.9848 ± 0.0003	1.000 ± 0.001	0.993 ± 0.000
$\bar{D}^0 \rightarrow K^+ \pi^-$	0.9850 ± 0.0004	0.9842 ± 0.0004	1.001 ± 0.001	0.993 ± 0.000
$D^0 \rightarrow K^- \pi^+ \pi^0$	0.9879 ± 0.0003	0.9910 ± 0.0002	0.997 ± 0.000	0.992 ± 0.000
$\bar{D}^0 \rightarrow K^+ \pi^- \pi^0$	0.9896 ± 0.0003	0.9914 ± 0.0002	0.998 ± 0.000	0.992 ± 0.000
$D^0 \rightarrow K^- \pi^+ \pi^+ \pi^-$	0.9759 ± 0.0005	0.9790 ± 0.0004	0.997 ± 0.001	0.986 ± 0.000
$\bar{D}^0 \rightarrow K^+ \pi^- \pi^- \pi^+$	0.9766 ± 0.0005	0.9781 ± 0.0004	0.998 ± 0.001	0.985 ± 0.000
$D^+ \rightarrow K^- \pi^+ \pi^+$	0.9783 ± 0.0004	0.9801 ± 0.0004	0.998 ± 0.001	0.988 ± 0.000
$D^- \rightarrow K^+ \pi^- \pi^-$	0.9815 ± 0.0004	0.9801 ± 0.0004	1.001 ± 0.001	0.987 ± 0.000
$D^+ \rightarrow K^- \pi^+ \pi^+ \pi^0$	0.9914 ± 0.0006	0.9892 ± 0.0004	1.002 ± 0.001	0.991 ± 0.000
$D^- \rightarrow K^+ \pi^- \pi^- \pi^0$	0.9885 ± 0.0007	0.9896 ± 0.0004	0.999 ± 0.001	0.991 ± 0.000
$D^+ \rightarrow K_S^0 \pi^+$	0.9833 ± 0.0010	0.9833 ± 0.0004	1.000 ± 0.001	0.988 ± 0.000
$D^- \rightarrow K_S^0 \pi^-$	0.9782 ± 0.0012	0.9832 ± 0.0004	0.995 ± 0.001	0.988 ± 0.000
$D^+ \rightarrow K_S^0 \pi^+ \pi^0$	0.9877 ± 0.0007	0.9841 ± 0.0006	1.004 ± 0.001	0.986 ± 0.001
$D^- \rightarrow K_S^0 \pi^- \pi^0$	0.9830 ± 0.0009	0.9839 ± 0.0006	0.999 ± 0.001	0.986 ± 0.001
$D^+ \rightarrow K_S^0 \pi^+ \pi^+ \pi^-$	0.9822 ± 0.0012	0.9824 ± 0.0007	1.000 ± 0.001	0.988 ± 0.001
$D^- \rightarrow K_S^0 \pi^- \pi^- \pi^+$	0.9911 ± 0.0009	0.9795 ± 0.0007	1.012 ± 0.001	0.985 ± 0.001
$D^+ \rightarrow K^+ K^- \pi^+$	0.9848 ± 0.0015	0.9868 ± 0.0007	0.998 ± 0.002	0.991 ± 0.000
$D^- \rightarrow K^- K^+ \pi^-$	0.9849 ± 0.0015	0.9871 ± 0.0007	0.998 ± 0.002	0.991 ± 0.000

Table 17: Systematic of ΔE cuts. The Ratios are taken from the max of the value in Table ??, and the systematics are the difference between the Ratios and 1.

Mode	Ratio	Syst (%)
$\bar{D}^0 \rightarrow K^+ \pi^-$	1.001 ± 0.001	0.1
$\bar{D}^0 \rightarrow K^+ \pi^- \pi^0$	0.998 ± 0.000	0.2
$\bar{D}^0 \rightarrow K^+ \pi^- \pi^- \pi^+$	0.998 ± 0.001	0.2
$D^- \rightarrow K^+ \pi^- \pi^-$	1.001 ± 0.001	0.1
$D^+ \rightarrow K^- \pi^+ \pi^+ \pi^0$	1.002 ± 0.001	0.2
$D^+ \rightarrow K_S^0 \pi^+$	1.000 ± 0.001	0.0
$D^+ \rightarrow K_S^0 \pi^+ \pi^0$	1.004 ± 0.001	0.4
$D^- \rightarrow K_S^0 \pi^- \pi^- \pi^+$	1.012 ± 0.001	1.2
$D^+ \rightarrow K^+ K^- \pi^+$	0.998 ± 0.002	0.2

Table 18: Ratios of double tags data yields and efficiencies ΔE cuts (Yield1 and eff1) to those with $2 \times \Delta E$ cuts (Yield2 and eff2). The last column (eff1'/eff2') is the ratio of the efficiencies without FSR cuts to the efficiencies with the wide ΔE and without FSR cuts.

Mode	Yield1/Yield2	eff1/eff2	Ratio	eff1'/eff2'
$D^0 \rightarrow K^- \pi^+ \bar{D}^0 \rightarrow K^+ \pi^-$	—	0.9705 ± 0.0010	—	—
$D^0 \rightarrow K^- \pi^+ \bar{D}^0 \rightarrow K^+ \pi^- \pi^0$	—	0.9663 ± 0.0015	—	—
$D^0 \rightarrow K^- \pi^+ \bar{D}^0 \rightarrow K^+ \pi^- \pi^- \pi^+$	—	0.9590 ± 0.0014	—	—
$D^0 \rightarrow K^- \pi^+ \pi^0 \bar{D}^0 \rightarrow K^+ \pi^-$	0.9666 ± 0.0029	0.9686 ± 0.0014	0.998 ± 0.003	—
$D^0 \rightarrow K^- \pi^+ \pi^0 \bar{D}^0 \rightarrow K^+ \pi^- \pi^0$	0.9506 ± 0.0025	0.9613 ± 0.0021	0.989 ± 0.003	—
$D^0 \rightarrow K^- \pi^+ \pi^0 \bar{D}^0 \rightarrow K^+ \pi^- \pi^- \pi^+$	0.9532 ± 0.0028	0.9585 ± 0.0019	0.994 ± 0.004	—
$D^0 \rightarrow K^- \pi^+ \pi^+ \pi^- \bar{D}^0 \rightarrow K^+ \pi^-$	0.9532 ± 0.0038	0.9586 ± 0.0014	0.994 ± 0.004	—
$D^0 \rightarrow K^- \pi^+ \pi^+ \pi^- \bar{D}^0 \rightarrow K^+ \pi^- \pi^0$	0.9548 ± 0.0028	0.9609 ± 0.0019	0.994 ± 0.004	—
$D^0 \rightarrow K^- \pi^+ \pi^+ \pi^- \bar{D}^0 \rightarrow K^+ \pi^- \pi^- \pi^+$	0.9427 ± 0.0034	0.9494 ± 0.0018	0.993 ± 0.004	—
$D^+ \rightarrow K^- \pi^+ \pi^+ D^- \rightarrow K^+ \pi^- \pi^-$	0.9620 ± 0.0025	0.9611 ± 0.0014	1.001 ± 0.003	—
$D^+ \rightarrow K^- \pi^+ \pi^+ D^- \rightarrow K^+ \pi^- \pi^- \pi^0$	0.9550 ± 0.0048	0.9572 ± 0.0020	0.998 ± 0.005	—
$D^+ \rightarrow K^- \pi^+ \pi^+ D^- \rightarrow K_S^0 \pi^-$	0.9493 ± 0.0074	0.9631 ± 0.0015	0.986 ± 0.008	—
$D^+ \rightarrow K^- \pi^+ \pi^+ D^- \rightarrow K_S^0 \pi^- \pi^0$	0.9513 ± 0.0048	0.9487 ± 0.0024	1.003 ± 0.006	—
$D^+ \rightarrow K^- \pi^+ \pi^+ D^- \rightarrow K_S^0 \pi^- \pi^- \pi^+$	0.9510 ± 0.0065	0.9532 ± 0.0021	0.998 ± 0.007	—
$D^+ \rightarrow K^- \pi^+ \pi^+ D^- \rightarrow K^- K^+ \pi^-$	0.9837 ± 0.0057	0.9668 ± 0.0015	1.017 ± 0.006	—
$D^+ \rightarrow K^- \pi^+ \pi^+ \pi^0 D^- \rightarrow K^+ \pi^- \pi^-$	0.9494 ± 0.0051	0.9595 ± 0.0020	0.989 ± 0.006	—
$D^+ \rightarrow K^- \pi^+ \pi^+ \pi^0 D^- \rightarrow K^+ \pi^- \pi^- \pi^0$	0.9499 ± 0.0096	0.9496 ± 0.0031	1.000 ± 0.011	—
$D^+ \rightarrow K^- \pi^+ \pi^+ \pi^0 D^- \rightarrow K_S^0 \pi^-$	0.9486 ± 0.0131	0.9627 ± 0.0021	0.985 ± 0.014	—
$D^+ \rightarrow K^- \pi^+ \pi^+ \pi^0 D^- \rightarrow K_S^0 \pi^- \pi^0$	0.9450 ± 0.0096	0.9564 ± 0.0031	0.988 ± 0.011	—
$D^+ \rightarrow K^- \pi^+ \pi^+ \pi^0 D^- \rightarrow K_S^0 \pi^- \pi^- \pi^+$	0.9318 ± 0.0138	0.9487 ± 0.0030	0.982 ± 0.015	—
$D^+ \rightarrow K^- \pi^+ \pi^+ \pi^0 D^- \rightarrow K^- K^+ \pi^-$	0.9816 ± 0.0117	0.9652 ± 0.0021	1.017 ± 0.012	—
$D^+ \rightarrow K_S^0 \pi^+ D^- \rightarrow K^+ \pi^- \pi^-$	0.9594 ± 0.0068	0.9622 ± 0.0015	0.997 ± 0.007	—
$D^+ \rightarrow K_S^0 \pi^+ D^- \rightarrow K^+ \pi^- \pi^- \pi^0$	0.9515 ± 0.0121	0.9560 ± 0.0023	0.995 ± 0.013	—
$D^+ \rightarrow K_S^0 \pi^+ D^- \rightarrow K_S^0 \pi^-$	0.9732 ± 0.0161	0.9654 ± 0.0016	1.008 ± 0.017	—
$D^+ \rightarrow K_S^0 \pi^+ D^- \rightarrow K_S^0 \pi^- \pi^- \pi^0$	0.9155 ± 0.0174	0.9525 ± 0.0026	0.961 ± 0.018	—
$D^+ \rightarrow K_S^0 \pi^+ D^- \rightarrow K_S^0 \pi^- \pi^- \pi^-$	0.9423 ± 0.0185	0.9568 ± 0.0022	0.985 ± 0.019	—
$D^+ \rightarrow K_S^0 \pi^+ D^- \rightarrow K^- K^+ \pi^-$	1.0000 ± 0.0000	0.9698 ± 0.0016	1.031 ± 0.002	—
$D^+ \rightarrow K_S^0 \pi^+ \pi^0 D^- \rightarrow K^+ \pi^- \pi^-$	0.9561 ± 0.0048	0.9508 ± 0.0023	1.006 ± 0.006	—
$D^+ \rightarrow K_S^0 \pi^+ \pi^0 D^- \rightarrow K^+ \pi^- \pi^- \pi^0$	0.9475 ± 0.0089	0.9460 ± 0.0035	1.002 ± 0.010	—
$D^+ \rightarrow K_S^0 \pi^+ \pi^0 D^- \rightarrow K_S^0 \pi^-$	0.9698 ± 0.0105	0.9569 ± 0.0025	1.013 ± 0.011	—
$D^+ \rightarrow K_S^0 \pi^+ \pi^0 D^- \rightarrow K_S^0 \pi^- \pi^0$	0.9294 ± 0.0103	0.9447 ± 0.0038	0.984 ± 0.012	—
$D^+ \rightarrow K_S^0 \pi^+ \pi^0 D^- \rightarrow K_S^0 \pi^- \pi^- \pi^+$	0.9550 ± 0.0112	0.9424 ± 0.0035	1.013 ± 0.012	—
$D^+ \rightarrow K_S^0 \pi^+ \pi^0 D^- \rightarrow K^- K^+ \pi^-$	0.9412 ± 0.0206	0.9549 ± 0.0026	0.986 ± 0.022	—
$D^+ \rightarrow K_S^0 \pi^+ \pi^+ \pi^- D^- \rightarrow K^+ \pi^- \pi^-$	0.9558 ± 0.0060	0.9591 ± 0.0019	0.997 ± 0.007	—
$D^+ \rightarrow K_S^0 \pi^+ \pi^+ \pi^- D^- \rightarrow K^+ \pi^- \pi^- \pi^0$	0.9417 ± 0.0134	0.9535 ± 0.0029	0.988 ± 0.014	—
$D^+ \rightarrow K_S^0 \pi^+ \pi^+ \pi^- D^- \rightarrow K_S^0 \pi^-$	0.9357 ± 0.0193	0.9584 ± 0.0021	0.976 ± 0.020	—
$D^+ \rightarrow K_S^0 \pi^+ \pi^+ \pi^- D^- \rightarrow K_S^0 \pi^- \pi^0$	0.9205 ± 0.0145	0.9454 ± 0.0034	0.974 ± 0.016	—
$D^+ \rightarrow K_S^0 \pi^+ \pi^+ \pi^- D^- \rightarrow K_S^0 \pi^- \pi^- \pi^+$	0.8836 ± 0.0235	0.9304 ± 0.0033	0.950 ± 0.025	—
$D^+ \rightarrow K_S^0 \pi^+ \pi^+ \pi^- D^- \rightarrow K^- K^+ \pi^-$	0.9479 ± 0.0238	0.9585 ± 0.0022	0.989 ± 0.025	—
$D^+ \rightarrow K^+ K^- \pi^+ D^- \rightarrow K^+ \pi^- \pi^-$	0.9700 ± 0.0076	0.9671 ± 0.0015	1.003 ± 0.008	—
$D^+ \rightarrow K^+ K^- \pi^+ D^- \rightarrow K^+ \pi^- \pi^- \pi^0$	0.9222 ± 0.0201	0.9640 ± 0.0022	0.957 ± 0.021	—
$D^+ \rightarrow K^+ K^- \pi^+ D^- \rightarrow K_S^0 \pi^-$	1.0164 ± 0.0168	0.9703 ± 0.0016	1.048 ± 0.017	—
$D^+ \rightarrow K^+ K^- \pi^+ D^- \rightarrow K_S^0 \pi^- \pi^0$	0.9326 ± 0.0188	0.9628 ± 0.0024	0.969 ± 0.020	—
$D^+ \rightarrow K^+ K^- \pi^+ D^- \rightarrow K_S^0 \pi^- \pi^- \pi^+$	0.9505 ± 0.0242	0.9614 ± 0.0021	0.989 ± 0.025	—
$D^+ \rightarrow K^+ K^- \pi^+ D^- \rightarrow K^- K^+ \pi^-$	0.9545 ± 0.0388	0.9742 ± 0.0015	0.980 ± 0.040	—

Table 19: Systematic of ΔE cuts for double tags. The Ratios are taken from the Table ??, and the systematics are the difference between the Ratios and 1.

Mode	Ratio	Syst (%)
$D^0 \rightarrow K^-\pi^+ \bar{D}^0 \rightarrow K^+\pi^-$	–	–
$D^0 \rightarrow K^-\pi^+ \bar{D}^0 \rightarrow K^+\pi^-\pi^0$	–	–
$D^0 \rightarrow K^-\pi^+ \bar{D}^0 \rightarrow K^+\pi^-\pi^-\pi^+$	–	–
$D^0 \rightarrow K^-\pi^+\pi^0 \bar{D}^0 \rightarrow K^+\pi^-$	0.998 ± 0.003	0.2
$D^0 \rightarrow K^-\pi^+\pi^0 \bar{D}^0 \rightarrow K^+\pi^-\pi^0$	0.989 ± 0.003	1.1
$D^0 \rightarrow K^-\pi^+\pi^0 \bar{D}^0 \rightarrow K^+\pi^-\pi^-\pi^+$	0.994 ± 0.004	0.6
$D^0 \rightarrow K^-\pi^+\pi^+\pi^- \bar{D}^0 \rightarrow K^+\pi^-$	0.994 ± 0.004	0.6
$D^0 \rightarrow K^-\pi^+\pi^+\pi^- \bar{D}^0 \rightarrow K^+\pi^-\pi^0$	0.994 ± 0.004	0.6
$D^0 \rightarrow K^-\pi^+\pi^+\pi^- \bar{D}^0 \rightarrow K^+\pi^-\pi^-\pi^+$	0.993 ± 0.004	0.7
$D^+ \rightarrow K^-\pi^+\pi^+ D^- \rightarrow K^+\pi^-\pi^-$	1.001 ± 0.003	0.1
$D^+ \rightarrow K^-\pi^+\pi^+ D^- \rightarrow K^+\pi^-\pi^-\pi^0$	0.998 ± 0.005	0.2
$D^+ \rightarrow K^-\pi^+\pi^+ D^- \rightarrow K_S^0 \pi^-$	0.986 ± 0.008	1.4
$D^+ \rightarrow K^-\pi^+\pi^+ D^- \rightarrow K_S^0 \pi^-\pi^0$	1.003 ± 0.006	0.3
$D^+ \rightarrow K^-\pi^+\pi^+ D^- \rightarrow K_S^0 \pi^-\pi^-\pi^+$	0.998 ± 0.007	0.2
$D^+ \rightarrow K^-\pi^+\pi^+ D^- \rightarrow K^-K^+\pi^-$	1.017 ± 0.006	1.7
$D^+ \rightarrow K^-\pi^+\pi^+\pi^0 D^- \rightarrow K^+\pi^-\pi^-$	0.989 ± 0.006	1.1
$D^+ \rightarrow K^-\pi^+\pi^+\pi^0 D^- \rightarrow K^+\pi^-\pi^-\pi^0$	1.000 ± 0.011	0.0
$D^+ \rightarrow K^-\pi^+\pi^+\pi^0 D^- \rightarrow K_S^0 \pi^-$	0.985 ± 0.014	1.5
$D^+ \rightarrow K^-\pi^+\pi^+\pi^0 D^- \rightarrow K_S^0 \pi^-\pi^0$	0.988 ± 0.011	1.2
$D^+ \rightarrow K^-\pi^+\pi^+\pi^0 D^- \rightarrow K_S^0 \pi^-\pi^-\pi^+$	0.982 ± 0.015	1.8
$D^+ \rightarrow K^-\pi^+\pi^+\pi^0 D^- \rightarrow K^-K^+\pi^-$	1.017 ± 0.012	1.7
$D^+ \rightarrow K_S^0 \pi^+ D^- \rightarrow K^+\pi^-\pi^-$	0.997 ± 0.007	0.3
$D^+ \rightarrow K_S^0 \pi^+ D^- \rightarrow K^+\pi^-\pi^-\pi^0$	0.995 ± 0.013	0.5
$D^+ \rightarrow K_S^0 \pi^+ D^- \rightarrow K_S^0 \pi^-$	1.008 ± 0.017	0.8
$D^+ \rightarrow K_S^0 \pi^+ D^- \rightarrow K_S^0 \pi^-\pi^0$	0.961 ± 0.018	3.9
$D^+ \rightarrow K_S^0 \pi^+ D^- \rightarrow K_S^0 \pi^-\pi^-\pi^+$	0.985 ± 0.019	1.5
$D^+ \rightarrow K_S^0 \pi^+ D^- \rightarrow K^-K^+\pi^-$	1.031 ± 0.002	3.1
$D^+ \rightarrow K_S^0 \pi^+\pi^0 D^- \rightarrow K^+\pi^-\pi^-$	1.006 ± 0.006	0.6
$D^+ \rightarrow K_S^0 \pi^+\pi^0 D^- \rightarrow K^+\pi^-\pi^-\pi^0$	1.002 ± 0.010	0.2
$D^+ \rightarrow K_S^0 \pi^+\pi^0 D^- \rightarrow K_S^0 \pi^-$	1.013 ± 0.011	1.3
$D^+ \rightarrow K_S^0 \pi^+\pi^0 D^- \rightarrow K_S^0 \pi^-\pi^0$	0.984 ± 0.012	1.6
$D^+ \rightarrow K_S^0 \pi^+\pi^0 D^- \rightarrow K_S^0 \pi^-\pi^-\pi^+$	1.013 ± 0.012	1.3
$D^+ \rightarrow K_S^0 \pi^+\pi^0 D^- \rightarrow K^-K^+\pi^-$	0.986 ± 0.022	1.4
$D^+ \rightarrow K_S^0 \pi^+\pi^+\pi^- D^- \rightarrow K^+\pi^-\pi^-$	0.997 ± 0.007	0.3
$D^+ \rightarrow K_S^0 \pi^+\pi^+\pi^- D^- \rightarrow K^+\pi^-\pi^-\pi^0$	0.988 ± 0.014	1.2
$D^+ \rightarrow K_S^0 \pi^+\pi^+\pi^- D^- \rightarrow K_S^0 \pi^-$	0.976 ± 0.020	2.4
$D^+ \rightarrow K_S^0 \pi^+\pi^+\pi^- D^- \rightarrow K_S^0 \pi^-\pi^0$	0.974 ± 0.016	2.6
$D^+ \rightarrow K_S^0 \pi^+\pi^+\pi^- D^- \rightarrow K_S^0 \pi^-\pi^-\pi^+$	0.950 ± 0.025	5.0
$D^+ \rightarrow K_S^0 \pi^+\pi^+\pi^- D^- \rightarrow K^-K^+\pi^-$	0.989 ± 0.025	1.1
$D^+ \rightarrow K^+K^-\pi^+ D^- \rightarrow K^+\pi^-\pi^-$	1.003 ± 0.008	0.3
$D^+ \rightarrow K^+K^-\pi^+ D^- \rightarrow K^+\pi^-\pi^-\pi^0$	0.957 ± 0.021	4.3
$D^+ \rightarrow K^+K^-\pi^+ D^- \rightarrow K_S^0 \pi^-$	1.048 ± 0.017	4.8
$D^+ \rightarrow K^+K^-\pi^+ D^- \rightarrow K_S^0 \pi^-\pi^0$	0.969 ± 0.020	3.1
$D^+ \rightarrow K^+K^-\pi^+ D^- \rightarrow K_S^0 \pi^-\pi^-\pi^+$	0.989 ± 0.025	1.1
$D^+ \rightarrow K^+K^-\pi^+ D^- \rightarrow K^-K^+\pi^-$	0.980 ± 0.040	2.0

Table 20: Ratios of single tag data yields and efficiencies with a power parameter fixed to 0.5 (Yield2 and eff2) to those with a power parameter floating (Yield1 and eff1).

Mode	Yield1/Yield2	eff1/eff2	Ratio
$D^0 \rightarrow K^-\pi^+$	1.0027 ± 0.0002	1.0000 ± 0.0000	1.0027 ± 0.0002
$\bar{D}^0 \rightarrow K^+\pi^-$	1.0027 ± 0.0002	1.0000 ± 0.0000	1.0027 ± 0.0002
$D^0 \rightarrow K^-\pi^+\pi^0$	0.9962 ± 0.0002	0.9944 ± 0.0002	1.0018 ± 0.0003
$\bar{D}^0 \rightarrow K^+\pi^-\pi^0$	0.9962 ± 0.0002	0.9946 ± 0.0002	1.0016 ± 0.0003
$D^0 \rightarrow K^-\pi^+\pi^+\pi^-$	0.9994 ± 0.0001	1.0002 ± 0.0000	0.9992 ± 0.0001
$\bar{D}^0 \rightarrow K^+\pi^-\pi^-\pi^+$	0.9994 ± 0.0001	1.0003 ± 0.0000	0.9991 ± 0.0001
$D^+ \rightarrow K^-\pi^+\pi^+$	0.9998 ± 0.0000	1.0000 ± 0.0000	0.9998 ± 0.0000
$D^- \rightarrow K^+\pi^-\pi^-$	0.9998 ± 0.0000	1.0000 ± 0.0000	0.9998 ± 0.0000
$D^+ \rightarrow K^-\pi^+\pi^+\pi^0$	1.0003 ± 0.0001	0.9992 ± 0.0001	1.0011 ± 0.0001
$D^- \rightarrow K^+\pi^-\pi^-\pi^0$	1.0003 ± 0.0001	0.9993 ± 0.0001	1.0010 ± 0.0001
$D^+ \rightarrow K_S^0\pi^+$	0.9996 ± 0.0002	1.0000 ± 0.0000	0.9996 ± 0.0002
$D^- \rightarrow K_S^0\pi^-$	0.9995 ± 0.0002	1.0000 ± 0.0000	0.9995 ± 0.0002
$D^+ \rightarrow K_S^0\pi^+\pi^0$	0.9980 ± 0.0003	0.9989 ± 0.0002	0.9991 ± 0.0004
$D^- \rightarrow K_S^0\pi^-\pi^0$	0.9980 ± 0.0003	0.9989 ± 0.0002	0.9991 ± 0.0004
$D^+ \rightarrow K_S^0\pi^+\pi^+\pi^-$	0.9992 ± 0.0003	0.9998 ± 0.0001	0.9994 ± 0.0003
$D^- \rightarrow K_S^0\pi^-\pi^-\pi^+$	0.9993 ± 0.0003	0.9998 ± 0.0001	0.9995 ± 0.0003
$D^+ \rightarrow K^+K^-\pi^+$	0.9997 ± 0.0002	1.0009 ± 0.0002	0.9988 ± 0.0003
$D^- \rightarrow K^-K^+\pi^-$	0.9997 ± 0.0002	1.0005 ± 0.0001	0.9992 ± 0.0002

Table 21: Single tag yields comparison between D and \bar{D}

Mode	data diff(%)	signal diff(%)
$D^0 \rightarrow K^-\pi^+$	0.54 ± 0.53	1.09 ± 0.40
$D^0 \rightarrow K^-\pi^+\pi^0$	0.75 ± 0.43	0.97 ± 0.33
$D^0 \rightarrow K^-\pi^+\pi^+\pi^-$	0.47 ± 0.45	0.80 ± 0.38
$D^+ \rightarrow K^-\pi^+\pi^+$	1.10 ± 0.43	0.46 ± 0.39
$D^+ \rightarrow K^-\pi^+\pi^+\pi^0$	0.90 ± 1.00	0.29 ± 0.60
$D^+ \rightarrow K_S^0\pi^+$	1.44 ± 1.15	-0.66 ± 0.43
$D^+ \rightarrow K_S^0\pi^+\pi^0$	0.77 ± 0.97	0.60 ± 0.73
$D^+ \rightarrow K_S^0\pi^+\pi^+\pi^-$	0.86 ± 1.34	0.98 ± 0.74
$D^+ \rightarrow K^+K^-\pi^+$	-0.48 ± 1.72	-0.60 ± 0.90

Table 22: Single tag crossfeed efficiencies. All uncertainties statistical.

From	To	Efficiency ($\times 10^{-4} \%$)
$D^0 \rightarrow K^+ \pi^-$	$D^0 \rightarrow K^- \pi^+$	8.0 ± 0.7
$D^0 \rightarrow K^- \pi^+$	$D^0 \rightarrow K^+ \pi^-$	9.0 ± 0.7

Table 23: External backgrounds. Efficiency uncertainties include systematics. Data branching fractions are taken from the 2010 PDG. < Charge conjugate modes are taken to have the same efficiencies and branching fractions.

From	To	Type	Data efficiency	Nominal data \mathcal{B}
$D^0 \rightarrow K^+ \pi^-$	$\bar{D}^0 \rightarrow K^+ \pi^-$	DCSD	0.663 ± 0.005	$(1.48 \pm 0.07) \times 10^{-4}$
$D^0 \rightarrow K^+ \pi^- \pi^0$	$\bar{D}^0 \rightarrow K^+ \pi^- \pi^0$	DCSD	0.356 ± 0.012	$(3.05 \pm 0.17) \times 10^{-4}$
$D^0 \rightarrow K^+ \pi^- \pi^- \pi^+$	$\bar{D}^0 \rightarrow K^+ \pi^- \pi^- \pi^+$	DCSD	0.470 ± 0.010	$(2.62 \pm 0.21) \times 10^{-4}$
$D^0 \rightarrow K^- K_S^0 \pi^+$	$D^0 \rightarrow K^- \pi^+ \pi^- \pi^+$	SCSD	0.128 ± 0.004	$(3.5 \pm 0.5) \times 10^{-3}$
$D^0 \rightarrow K^+ K_S^0 \pi^-$	$\bar{D}^0 \rightarrow K^+ \pi^- \pi^+ \pi^-$	SCSD	0.128 ± 0.004	$(2.6 \pm 0.5) \times 10^{-3}$
$D^+ \rightarrow K_S^0 K_S^0 \pi^+$	$D^+ \rightarrow K_S^0 \pi^+ \pi^+ \pi^-$	SCSD	0.013 ± 0.001	$(1.6 \pm 0.7) \times 10^{-2}$

Table 24: External backgrounds measured as absolute subtractions to data yields. Raw yield uncertainty is statistical only; corrected background uncertainties are statistical, efficiency uncertainty, and generic MC agreement.

From	To	Raw sideband yield	Corrected background	Final
$D^+ \rightarrow \pi^+ \pi^- \pi^+$	$D^+ \rightarrow K_S^0 \pi^+$	482 ± 33	$198 \pm 34 \pm 21 \pm 18$	197.9 ± 43.7
$D^+ \rightarrow \pi^+ \pi^- \pi^+ \pi^0$	$D^+ \rightarrow K_S^0 \pi^+ \pi^0$	1965 ± 108	$463 \pm 113 \pm 69 \pm 169$	463.4 ± 214.7
$D^+ \rightarrow 3\pi^+ 2\pi^-$	$D^+ \rightarrow K_S^0 \pi^+ \pi^+ \pi^-$	2647 ± 153	$250 \pm 172 \pm 57 \pm 125$	249.5 ± 220.2

and $D^0 \rightarrow K^+ \pi^- \pi^+ \pi^-$ could differ from those for the Cabibbo-allowed decays. We simulated these decays with kinematic distributions flat in phase space and compared the efficiencies in these samples with the nominal Cabibbo-allowed efficiencies as a gauge of the size of these effects. There is no statistically significant difference in either the $K\pi\pi^0$ or $K\pi\pi\pi$ modes. We use the efficiencies for the flat distribution when making the background estimates.

The PDG branching fractions for these modes are well-established.

$D^0 \rightarrow K^- K_S^0 \pi^+$, $D^0 \rightarrow K^+ K_S^0 \pi^-$ (**external**) These singly-Cabibbo-suppressed modes can fake the decays $D^0 \rightarrow K^- \pi^+ \pi^+ \pi^-$ and $\bar{D}^0 \rightarrow K^+ \pi^- \pi^+ \pi^-$, respectively, if the K_S^0 decays to $\pi^+ \pi^-$. The efficiencies for these backgrounds are suppressed by the d_0 cut on the pion tracks. We do not use an explicit K_S^0 veto to further reduce the contribution.

Because of the d_0 cut on the pion tracks, the K_S^0 momentum spectrum can affect the efficiency. EvtGen models resonant ($K^{*\pm} K^\mp$) and non-resonant contributions to this mode. Signal MC samples were generated with two different mixtures of resonant and non-resonant contributions. In both cases the final state of the EvtGen decay tree is $KK_S\pi$, and the probability of decay to $K\pi\pi\pi$ is 68.8%, a factor which is included in the efficiencies.

The following two mixtures were generated to measure efficiencies. For $D^0 \rightarrow K^+ K_S^0 \pi^-$, the D^0 decayed 52% into $K^{*+} K^-$ and 48% into phase space-distributed $K^- K^0 \pi^+$. The K^{*+} was forced to decay to $K^0 \pi^+$, and the K^0 to K_S . For $D^0 \rightarrow K^- K_S^0 \pi^+$, the D^0 decayed 25.5% into $K^{*-} K^+$ and 74.5% into $K^+ \bar{K}^0 \pi^-$; again the K^{*-} was forced to $\bar{K}^0 \pi^-$ and the \bar{K}^0 to K_S . The two efficiencies show no significant difference.

$D^+ \rightarrow$ **multipions (external)** Singly Cabibbo-suppressed decays can fake D^+ decays to final states with K_S^0 mesons when a $\pi^+ \pi^-$ invariant mass falls within the K_S^0 window. We estimate the size of this background by using K_S^0 mass sidebands. We require that the reconstructed K_S^0 candidate have a mass in the ranges $0.470 \text{ GeV} < m < 0.482 \text{ GeV}$ or $0.5134 \text{ GeV} < m < 0.5254 \text{ GeV}$, and that the D^+ candidate using this K_S^0 otherwise satisfies all standard requirements. The M_{BC} spectra of these candidates are then fit with the standard lineshapes for the mode being faked. The narrow Gaussian widths are set to the values obtained from the diagonal double tag fits for those modes.

The yields obtained have a significant contribution from the tails of the K_S^0 mass resolution; some signal is counted in our “sidebands.” To disentangle this effect, we use Monte Carlo to obtain efficiencies for events with real K_S^0 mesons to be reconstructed in our sideband region, shown in Table ???. The efficiency to be reconstructed in the signal region is just the signal efficiency in Table ???. The sidebands are assumed to have the same number of background events as the signal region. We write an efficiency matrix E , with entries giving the efficiencies for real and background events to be found in

Table 25: Efficiency for signal events to be reconstructed in K_S^0 sidebands, taken from signal MC. Uncertainties are statistical only.

Mode	$E_{sig \rightarrow sb} (10^{-3})$
$D^+ \rightarrow K_S^0 \pi^+$	7.8 ± 0.2
$D^+ \rightarrow K_S^0 \pi^+ \pi^0$	9.5 ± 0.3
$D^+ \rightarrow K_S^0 \pi^+ \pi^+ \pi^-$	33.0 ± 0.6

signal and sideband regions, and invert it to obtain the number of real and background events:

$$\begin{pmatrix} N_{sig} \\ N_{bkg} \end{pmatrix} = \begin{pmatrix} E_{sig \rightarrow sig} & E_{bkg \rightarrow sig} \\ E_{sig \rightarrow sb} & E_{bkg \rightarrow sb} \end{pmatrix}^{-1} \begin{pmatrix} Y_{sig} \\ Y_{sb} \end{pmatrix}$$

We use the prescription of Ref. [?] to propagate the systematic and statistical errors (the former are the efficiency statistical errors). In addition we test this procedure on generic MC by reconstructing events with the signal K_S^0 mass region that arose from multipion events and using the fractional difference between the sideband prediction and the observed yield to set a fractional systematic error.

$D^+ \rightarrow K_S^0 K_S^0 \pi^+$ (**external**) This singly-Cabibbo-suppressed decay can be reconstructed as $Dp \rightarrow K_S^0 \pi^+ \pi^+ \pi^-$. The contribution is limited by two factors: first, we veto $K_S^0 \pi^+ \pi^+ \pi^-$ events where a $\pi^+ \pi^-$ combination satisfies $0.491 \text{ GeV} < m_{\pi^+ \pi^-} < 0.504 \text{ GeV}$; second, there is the additional inefficiency due to the d_0 cut for K_S^0 faking $\pi\pi$ mentioned above.

This final state is dominated by the intermediate state $K^{*+} K_S^0$, and so can be modeled straightforwardly with EvtGen. The branching fraction is known to within a factor of three or so. (The 2006 PDG fit value is based on a single E687 measurement [?] which is much larger than CLEO-c data indicates [?] but which has large errors.)

Particle swap (crossfeed) Reconstructing a K^+ as a π^+ and a π^- as a K^- can result in a \bar{D}^0 decay being reconstructed as a D^0 decay. This is suppressed relative to correct reconstruction by a factor $\approx 10^3$ for $D^0 \rightarrow K^- \pi^+$, and is not observable in any of the other modes, where the particles have lower momentum and better dE/dx discrimination.

We obtain the efficiency for this process by using the signal MC for $D^0 \rightarrow K^- \pi^+$. Events with genuine $\bar{D}^0 \rightarrow K^+ \pi^-$ on the other side are rejected, and the yield of candidates reconstructed in the remaining events as having $\bar{D}^0 \rightarrow K^+ \pi^-$ is measured. The yield is the numerator for the efficiency and the number of events without $\bar{D}^0 \rightarrow K^+ \pi^-$ is the denominator. The yield fits to signal MC are shown in Fig. ??.

Once these backgrounds are accounted for, there is no indication in the generic $D\bar{D}$ MC sample for other backgrounds exceeding a part per 10^4 (Fig. ??).

7.1.1 Continuum, radiative return, and τ -pairs

We have looked at continuum, radiative return, and τ -pair MC samples, and find no evidence for peaking background to any of the D decay modes. The M_{BC} spectra for background from continuum, radiative return, and τ -pair events are shown in Figs. ??, ??, and ??.

7.2 Double Tag Backgrounds

The fitter uses separate backgrounds for single and double tags, and does not attempt to automatically correlate single tag backgrounds with double tag backgrounds. For example, including a rate for $D^0 \rightarrow K^- K_S^0 \pi^+$ to fake $D^0 \rightarrow K^- \pi^+ \pi^- \pi^+$ does not automatically give a rate for $D^0 \rightarrow K^- K_S^0 \pi^+$ to create fake double tags. We calculate effective efficiencies for the single tag backgrounds to fake double tags in most cases using the following:

$$\epsilon_{eff} = \epsilon_{single\ tag} \mathcal{B}_{other\ side} \epsilon_{other\ side, single\ tag}$$

where $\mathcal{B}_{other\ side}$ is the nominal branching fraction for the non-faked decay on the other side. The probability of having a (peaking) fake on both sides is so small that we ignore it, except as noted below.

The exceptions to the procedure above are the neutral DCSD modes and the “wrong-sign” mode $D^0 \rightarrow K^+ K_S^0 \pi^-$. If one side produces such a decay, it is impossible to produce a double tag unless the other side undergoes a wrong-sign decay too. This severely suppresses these backgrounds in the double tags, so for example the background due to DCSD decays for $K\pi\pi^0/K\pi\pi^0$ is expected to be less than 10^{-2} event for our data sample. We include them in the efficiency matrix anyway, with the effective efficiency

$$\epsilon_{eff} = \sum_{wrong-sign\ decays} \epsilon_{single\ tag} \mathcal{B}_{other\ side} \epsilon_{other\ side, single\ tag}$$

8 Systematics

Systematic uncertainties are accounted for in the branching fraction fit, by including them directly in the χ^2 minimization. When fitting generic MC, the simulation-related uncertainties are not applicable, and the only uncertainties applied are statistical uncertainties on yields, efficiencies, and background branching fractions. For the data, we include the uncertainties listed in Table ???. Not included in these tables but present in the fits are uncertainties associated with the branching fractions of the background D decay processes listed in Table ??.

Yield excursions under variations of the fit function are probed by fixing the ARGUS power parameter to 0.5, as shown in Tables ?? and ???. Most yields move by less than

0.5%, and we assign an uncorrelated uncertainty of this size to all yields, which is especially conservative for the double tag yields.

The nine double tags formed from the three D^0 modes have final states that can be represented by the notation $f_1\bar{f}_2$. Each final state results from the coherent sum of two transition amplitudes [?]: Cabibbo-favored ($D^0 \rightarrow f_1$, $\bar{D}^0 \rightarrow \bar{f}_2$) and doubly-Cabibbo-suppressed ($D^0 \rightarrow \bar{f}_2$, $\bar{D}^0 \rightarrow f_1$). The interference between these two processes is governed by the amplitude ratios $\langle f_1 | \bar{D}^0 \rangle / \langle f_1 | D^0 \rangle \equiv -r_1 e^{-i\delta_1}$ and $\langle f_2 | \bar{D}^0 \rangle / \langle f_2 | D^0 \rangle \equiv -r_2 e^{-i\delta_2}$, where the r_i are magnitudes and therefore strictly positive, and the δ_i are mode-dependent strong phases. This interference modifies the double tag rate by a factor of $1 - 2r_1 r_2 \cos(\delta_1 + \delta_2) + r_1^2 r_2^2$. For decay $D^0 \rightarrow K^- \pi^+$, we take the r and δ from [?]. For $D^0 \rightarrow K^- \pi^+ \pi^0$ and $D^0 \rightarrow K^- \pi^+ \pi^+ \pi^-$ decays, we take the r from [?] and take δ from [?]. To apply the values from [?] to the equation factor, we have to rotate the δ for 180° due to a difference in the phase convention, also substitute $\cos\delta$ as $R \cos \delta$, where R is the coherence factor, also measured in this paper. The correction factors, $1/(1 - 2r_1 r_2 \cos(\delta_1 + \delta_2) + r_1^2 r_2^2)$, for the yields are shown in Table ??.

Table 26: DCSD interference corrections

Mode	Yield correction factor
$D^0 \rightarrow K^- \pi^+ \bar{D}^0 \rightarrow K^+ \pi^-$	1.005 ± 0.002
$D^0 \rightarrow K^- \pi^+ \bar{D}^0 \rightarrow K^+ \pi^- \pi^0$	1.002 ± 0.002
$D^0 \rightarrow K^- \pi^+ \bar{D}^0 \rightarrow K^+ \pi^- \pi^- \pi^+$	1.005 ± 0.003
$D^0 \rightarrow K^- \pi^+ \pi^0 \bar{D}^0 \rightarrow K^+ \pi^-$	1.002 ± 0.002
$D^0 \rightarrow K^- \pi^+ \pi^0 \bar{D}^0 \rightarrow K^+ \pi^- \pi^0$	1.000 ± 0.002
$D^0 \rightarrow K^- \pi^+ \pi^0 \bar{D}^0 \rightarrow K^+ \pi^- \pi^- \pi^+$	1.005 ± 0.002
$D^0 \rightarrow K^- \pi^+ \pi^+ \pi^- \bar{D}^0 \rightarrow K^+ \pi^-$	1.005 ± 0.003
$D^0 \rightarrow K^- \pi^+ \pi^+ \pi^- \bar{D}^0 \rightarrow K^+ \pi^- \pi^0$	1.005 ± 0.002
$D^0 \rightarrow K^- \pi^+ \pi^+ \pi^- \bar{D}^0 \rightarrow K^+ \pi^- \pi^- \pi^+$	0.996 ± 0.004

Efficiency uncertainties in the data fit tend to be correlated across modes. Those for tracks, PID, and K^0_S s are assigned according to the particle content of the tag modes. Based on the studies in Ref. [?], we correct the efficiencies in Tables ?? and ?? by multiplying by

$$0.995^l \cdot 0.990^m, \quad (1)$$

where l and m are the numbers of PID-identified π^\pm and PID-identified K^\pm in each final state.

From the study of π^0 efficiency in Ref. [?], we first get the average π^0 momentum in data for modes: $D^0 \rightarrow K^- \pi^+ \pi^0$, $D^+ \rightarrow K^- \pi^+ \pi^+ \pi^0$, and $D^+ \rightarrow K^0_S \pi^+ \pi^0$, as shown in Fig. ???. Next we take the parameters from Table 11 in [?], for “Standard Cuts”, the fitting parameters of First Order Polynomial are: $a_0 = 0.939 \pm 0.022$, $a_1 = 0.001 \pm 0.021$, $\rho_{01} = -0.947$. Then we plug the π^0 momentum into the efficiency correction equation ?? and ?? (Corresponds to

equation 8 and 9 from [?], Note: there is a typo in equation 9 in the paper, where the σ in the left hand side should be squared.), we get the correction for the three modes in Table ???. We correct the efficiencies in Tables ?? and ?? by a factor of 0.939 for these three modes, and take systematic uncertainties for 1.3%, 1.5%, and 1.3% for each mode respectively.

$$\epsilon_{data}/\epsilon_{MC} = a_1 \bar{p}_{\pi^0} + a_0 \quad (2)$$

$$\sigma_{\epsilon_{data}/\epsilon_{MC}}^2 = \sigma_{a_1}^2 \bar{p}_{\pi^0}^2 + \sigma_{a_0}^2 + 2\rho_{01}\sigma_{a_0}\sigma_{a_1}\bar{p}_{\pi^0} \quad (3)$$

Table 27: π^0 efficiency correction

Mode	Average π^0 momentum	$\epsilon_{data}/\epsilon_{MC}$
$D^0 \rightarrow K^-\pi^+\pi^0$	0.478	0.939 ± 0.013
$D^+ \rightarrow K^-\pi^+\pi^+\pi^0$	0.339	0.939 ± 0.015
$D^+ \rightarrow K_S^0\pi^+\pi^0$	0.498	0.939 ± 0.013

We use events that are accepted by any trigger line. In practice most of our events are flagged by the two-track trigger, which has some inefficiency for soft tracks. Based on the Monte Carlo trigger simulation, there is no significant deviations from 100% efficiency for all modes (see Table ??). So, we do not assign systematic uncertainty on trigger.

Table 28: Trigger efficiencies derived from signal MC (correspond to data 818pb^{-1}); uncertainties statistical

Mode	Trigger efficiency (%)
$D^0 \rightarrow K^-\pi^+$	99.983 ± 0.004
$D^0 \rightarrow K^-\pi^+\pi^0$	99.981 ± 0.004
$D^0 \rightarrow K^-\pi^+\pi^+\pi^-$	99.974 ± 0.004
$D^+ \rightarrow K^-\pi^+\pi^+$	99.969 ± 0.004
$D^+ \rightarrow K^-\pi^+\pi^+\pi^0$	$100^{+0}_{-0.000}$
$D^+ \rightarrow K_S^0\pi^+$	$100^{+0}_{-0.000}$
$D^+ \rightarrow K_S^0\pi^+\pi^0$	$100^{+0}_{-0.002}$
$D^+ \rightarrow K_S^0\pi^+\pi^+\pi^-$	99.996 ± 0.002
$D^+ \rightarrow K^+K^-\pi^+$	99.998 ± 0.002

We estimate the uncertainty in ST yields due to the background shape by repeating the ST fits with alternative background shape parameters. These alternative parameters are determined from the M_{BC} distributions of events in high and low ΔE sidebands. For each mode, we fit each sideband with an ARGUS function to determine shape parameters and then repeat the ST yield fits with the ARGUS parameters fixed to these values. The

resulting shifts in the ST yields are used to set the value of the systematic for each mode. (see Table ??). To investigate the differences, we also performed the same calculation for generic $D\bar{D}$ MC, see Table ??.

Table 29: Single tag yields with fixed ARGUS parameters of $\psi(3770)$.

Mode	Yield		diff(low)	diff(high)	max-diff	
	ARGUS Low	Std	ARGUS High	(%)	(%)	
$D^0 \rightarrow K^-\pi^+$	75463 ± 280	75177 ± 281	75453 ± 280	0.38	0.37	0.38
$\bar{D}^0 \rightarrow K^+\pi^-$	75870 ± 280	75584 ± 282	75860 ± 280	0.38	0.36	0.38
$D^0 \rightarrow K^-\pi^+\pi^0$	143119 ± 423	144710 ± 439	144169 ± 424	-1.10	-0.37	-1.10
$\bar{D}^0 \rightarrow K^+\pi^-\pi^0$	144180 ± 425	145798 ± 441	145246 ± 426	-1.11	-0.38	-1.11
$D^0 \rightarrow K^-\pi^+\pi^+\pi^-$	115079 ± 361	114222 ± 366	114252 ± 361	0.75	0.03	0.75
$\bar{D}^0 \rightarrow K^+\pi^-\pi^-\pi^+$	115626 ± 362	114759 ± 368	114790 ± 362	0.76	0.03	0.76
$D^+ \rightarrow K^-\pi^+\pi^+$	116580 ± 350	116545 ± 354	117010 ± 350	0.03	0.40	0.40
$D^- \rightarrow K^+\pi^-\pi^-$	117867 ± 352	117831 ± 356	118306 ± 352	0.03	0.40	0.40
$D^+ \rightarrow K^-\pi^+\pi^+\pi^0$	35833 ± 242	36813 ± 260	35692 ± 242	-2.66	-3.05	-3.05
$D^- \rightarrow K^+\pi^-\pi^-\pi^0$	36152 ± 243	37143 ± 261	36010 ± 243	-2.67	-3.05	-3.05
$D^+ \rightarrow K_S^0 \pi^+$	16973 ± 136	16844 ± 137	16862 ± 136	0.77	0.11	0.77
$D^- \rightarrow K_S^0 \pi^-$	17212 ± 136	17087 ± 138	17105 ± 136	0.73	0.10	0.73
$D^+ \rightarrow K_S^0 \pi^+\pi^0$	37807 ± 249	38329 ± 262	37737 ± 248	-1.36	-1.54	-1.54
$D^- \rightarrow K_S^0 \pi^-\pi^0$	38105 ± 249	38626 ± 263	38035 ± 249	-1.35	-1.53	-1.53
$D^+ \rightarrow K_S^0 \pi^+\pi^+\pi^-$	23439 ± 213	23706 ± 224	23415 ± 213	-1.13	-1.23	-1.23
$D^- \rightarrow K_S^0 \pi^-\pi^-\pi^+$	23641 ± 214	23909 ± 225	23617 ± 214	-1.12	-1.22	-1.22
$D^+ \rightarrow K^+K^-\pi^+$	10198 ± 120	10115 ± 123	10145 ± 120	0.82	0.29	0.82
$D^- \rightarrow K^-K^+\pi^-$	10148 ± 120	10066 ± 123	10095 ± 120	0.81	0.29	0.81

FSR is simulated by PHOTOS in both the signal MC and the generic MC, so it is not assigned an uncertainty in the generic MC fit. The presence of FSR reduces signal efficiencies in all modes. In principle, the size of the reduction varies by mode, but we find it to be approximately 1.5% for single tags and 2.9% for double tags. The accuracy of the FSR simulation has been verified to 8% of itself using $J/\psi \rightarrow \mu^+\mu^-$ decays [?].

We assign conservative uncertainties of $\pm 25\%$ [?] of the FSR correction to the efficiency difference in Table ?? as the uncertainty in each mode. This uncertainty is correlated across all modes. See Table ??.

The efficiency of the ΔE cuts can be incorrectly estimated if the resolutions in data and MC disagree. Table ?? shows the ratios of single tag data yields and efficiencies measured with standard ΔE and with $2 \times \Delta E$ cut. In Section ??, in addition to the standard data fit, we also perform a fit using yields and efficiencies measured with the $2 \times \Delta E$ cut. The shifts in branching fractions compared to the standard fit agree with the ratios in Table ??, ???. To account for these shifts, for single tags, we choose the max value of the ratios and use the difference between these values and 1 as the systematics for the ΔE cuts (Table ??). For double tags, a similar procedure gives Table ???. In the BF fitter, we assign the uncertainty 1.0% for the diagonal double tags, and $\sqrt{2} \cdot 0.5\%$ for all other double tags.

The fractional changes in yield under variation of $\Gamma(3770)$, shown in Tables ?? and ??,

Table 30: Single tag yields with fixed ARGUS parameters of $\psi(3770)$ for Generic MC

Mode	Yield			diff(low) (%)	diff(high) (%)	max-diff (%)
	ARGUS Low	Std	ARGUS High			
$D^0 \rightarrow K^-\pi^+$	1454743 \pm 1208	1454801 \pm 1209	1454401 \pm 1207	-0.00	-0.03	-0.03
$\bar{D}^0 \rightarrow K^+\pi^-$	1478028 \pm 1217	1478121 \pm 1218	1477722 \pm 1217	-0.01	-0.03	-0.03
$D^0 \rightarrow K^-\pi^+\pi^0$	2780776 \pm 1788	2806397 \pm 1829	2788292 \pm 1788	-0.91	-0.65	-0.91
$\bar{D}^0 \rightarrow K^+\pi^-\pi^0$	2807836 \pm 1796	2833573 \pm 1837	2815389 \pm 1796	-0.91	-0.64	-0.91
$D^0 \rightarrow K^-\pi^+\pi^+\pi^-$	2158719 \pm 1522	2165187 \pm 1540	2162328 \pm 1521	-0.30	-0.13	-0.30
$\bar{D}^0 \rightarrow K^+\pi^-\pi^-\pi^+$	2180038 \pm 1529	2186402 \pm 1547	2183668 \pm 1529	-0.29	-0.13	-0.29
$D^+ \rightarrow K^-\pi^+\pi^+$	2421553 \pm 1581	2422093 \pm 1588	2420055 \pm 1580	-0.02	-0.08	-0.08
$D^- \rightarrow K^+\pi^-\pi^-$	2445500 \pm 1590	2445719 \pm 1595	2444027 \pm 1587	-0.01	-0.07	-0.07
$D^+ \rightarrow K^-\pi^+\pi^+\pi^0$	778204 \pm 1032	793897 \pm 1078	781739 \pm 1033	-1.98	-1.53	-1.98
$D^- \rightarrow K^+\pi^-\pi^-\pi^0$	785509 \pm 1037	801319 \pm 1083	789067 \pm 1038	-1.97	-1.53	-1.97
$D^+ \rightarrow K_S^0\pi^+$	315063 \pm 568	314283 \pm 571	313091 \pm 569	0.25	-0.38	-0.38
$D^- \rightarrow K_S^0\pi^-$	313878 \pm 567	313099 \pm 570	311911 \pm 568	0.25	-0.38	-0.38
$D^+ \rightarrow K_S^0\pi^+\pi^0$	798831 \pm 1012	796700 \pm 1048	791236 \pm 1011	0.27	-0.69	-0.69
$D^- \rightarrow K_S^0\pi^-\pi^0$	799337 \pm 1012	797207 \pm 1047	791788 \pm 1010	0.27	-0.68	-0.68
$D^+ \rightarrow K_S^0\pi^+\pi^+\pi^-$	485678 \pm 811	486617 \pm 831	487610 \pm 811	-0.19	0.20	0.20
$D^- \rightarrow K_S^0\pi^-\pi^-\pi^+$	485819 \pm 811	486745 \pm 831	487753 \pm 811	-0.19	0.21	0.21
$D^+ \rightarrow K^+K^-\pi^+$	199306 \pm 489	198420 \pm 496	197781 \pm 489	0.45	-0.32	0.45
$D^- \rightarrow K^-K^+\pi^-$	199770 \pm 490	198895 \pm 497	198248 \pm 489	0.44	-0.33	0.44

 Table 31: Contributions, in percent, to the uncertainty on each single tag efficiency-corrected yield, enumerated by source. Uncorrelated uncertainties (bkg shape) applied to individual yields or efficiencies propagate to all branching fractions of the same charge via their dependence on $N_{D^0\bar{D}^0}$ or $N_{D^+D^-}$. Correlated uncertainties are given in the last section and, except for those marked by asterisks, are coherent across all modes.

Source	$K\pi$	$K\pi\pi^0$	$K\pi\pi\pi$	$K\pi\pi$	$K\pi\pi\pi^0$	$K_S^0\pi$	$K_S^0\pi\pi^0$	$K_S^0\pi\pi\pi$	$KK\pi$
Bkgd shape	0.38	1.10	0.76	0.40	3.05	0.77	1.53	1.22	0.82
Tracking	0.9	0.9	1.5	1.2	1.2	0.3	0.3	0.9	1.5
KS0	-	-	-	-	-	0.8	0.8	0.8	-
pi0	-	1.3	-	-	1.5	-	1.3	-	-
pi PID	0.25	0.25	0.75	0.5	0.5	0.25	0.25	0.75	0.25
K PID	0.3	0.3	0.3	0.3	0.3	-	-	-	0.6
Lepton veto	0.1	-	-	-	-	-	-	-	-
FSR	0.8	0.4	0.7	0.5	0.2	0.4	0.2	0.5	0.3
Delta E (*)	0.1	0.2	0.2	0.1	0.2	0.0	0.4	1.2	0.2
Signal shape	0.40	0.50	0.51	0.34	0.48	0.39	0.48	0.55	0.54
Substructure (*)	-	0.58	1.3	0.53	0.94	-	0.42	0.62	0.99
Mult. cand. (*)	0	0.7	0	0	0.2	0.2	0	0	0

are roughly the same for single and double tags. Therefore, we assign a common correlated fractional uncertainty to all yields of 0.6%. In practice, this multiplicative yield uncertainty is implemented as an efficiency uncertainty, and it affects only the measurements of $N_{D^0\bar{D}^0}$ and $N_{D^+D^-}$, not the branching fractions.

A possible source of background bias is the single candidate selection procedure for double tags, which may introduce peaking in the continuum background. However, this possible effect is studied with continuum MC and is found to be negligible. We do not assign an associated systematic uncertainty.

Finally, we have considered the effect of the quantum correlation between D^0 and \bar{D}^0 on the observed branching fractions and $N_{D^0\bar{D}^0}$ [?]. Based on D^0 lifetime measurements in decays to CP eigenstates, this effect has been found to be negligible.

For the $e^+e^- \rightarrow D\bar{D}$ peak cross section measurements, we include uncertainties on the luminosity measurement and on the center-of-mass energy relative to the peak. The luminosity reported in **suez** jobs is corrected by a dataset-dependent factor, with an overall systematic uncertainty of 1% [?]. The center-of-mass energy at which the $\psi(3770)$ runs were taken has been found to vary by about 4 MeV (which is comparable to the beam energy spread), with three distinct regions of concentration (see Figure ??). Using single tag yields in the runs clustered around 3771 MeV and 3774 MeV, we determine the cross section ratio $\sigma(3771)/\sigma(3774) = 0.965 \pm 0.017$. Figure ?? shows the predicted value of this ratio as a function of $M(\psi(3770))$ for various assumptions of $\Gamma(\psi(3770))$. If we take $\Gamma(\psi(3770))$ to be 30 MeV with a generous uncertainty of 5 MeV, these curves suggest that $M(\psi(3770))$ is 3776.5 ± 1.4 MeV. Table ?? shows, for each given $M(\psi(3770))$, the value of E_{cm} where the peak cross section occurs and the difference between the peak cross section and the cross section at $E_{\text{cm}} = 3773.0$ MeV (assuming $\Gamma(\psi(3770)) = 30$ MeV). This cross section difference represents the amount by which we have potentially underestimated the peak cross section, and based on the largest excursions observed in this Table, we assign systematic uncertainties of 1.6% to $\sigma_{D^0\bar{D}^0}$ and 3.2% to $\sigma_{D^+D^-}$. These uncertainties are one-sided because variations in E_{cm} can only cause the peak cross section to be underestimated, not overestimated. We take these uncertainties to be correlated between $D^0\bar{D}^0$ and D^+D^- .

Table 32: Locations of the $D^0\bar{D}^0$ and D^+D^- peak cross sections as a function of $M(\psi(3770))$, for $\Gamma(\psi(3770)) = 30$ MeV. Also given are the relative differences between the peak cross section and the cross section at $E_{\text{cm}} = 3773.0$ MeV, $\Delta\sigma/\sigma \equiv [\sigma(E_{\text{cm}}^{\text{peak}}) - \sigma(3773.0 \text{ MeV})]/\sigma(3773.0 \text{ MeV})$

$M(\psi(3770))$	$E_{\text{cm}}^{\text{peak}}(D^0\bar{D}^0)$	$\Delta\sigma/\sigma(D^0\bar{D}^0)$	$E_{\text{cm}}^{\text{peak}}(D^+D^-)$	$\Delta\sigma/\sigma(D^+D^-)$
3775.1 MeV	3771.5 MeV	1.6%	3772.2 MeV	0.4%
3776.5 MeV	3773.0 MeV	0.0%	3773.6 MeV	0.3%
3777.9 MeV	3774.4 MeV	1.5%	3775.1 MeV	3.2%

8.1 Event topology-dependent systematics

It is possible for the efficiency derived from the Monte Carlo to differ from the real efficiency, even if the Monte Carlo models track- and π^0 -level efficiency correctly, because it does not correctly deal with global features of an event. Here we evaluate and check three sources of such error:

- Incorrect generated momentum distribution of the decay products of the tag side
- Incorrect modelling of the effect of the decay of the other side on the efficiency of the tag side
- Incorrect modelling of combinatoric fakes producing real signal

If the generator includes an incorrect resonant substructure for ≥ 3 -body decays, the momentum distribution of the final state particles will be distorted and, due to the momentum dependence of the particle detection efficiency, this can have an effect on the average efficiency for the D reconstruction. The three-body modes, except for $KK\pi$, are tuned to previous measurements of the Dalitz distributions. We expect, and find, larger uncertainties in the modes which are not tuned. To extract a systematic uncertainty on the efficiencies due to these effects, we obtain the effective efficiency as a function of momentum for each of the daughter particles in a given mode from Monte Carlo, then unweight the observed momentum distribution in generic MC and data for each daughter. This gives an effective overall efficiency for that data sample. The largest difference between the MC and data effective efficiencies among all the daughters is taken as the systematic uncertainty. In all cases the daughters all give consistent values for the difference between MC and data. A sideband subtraction was tried but found to have negligible effect and to introduce complications, so the uncertainties given are without sideband subtraction. The systematic uncertainties for each mode are shown in Table ??, the data/MC comparison plots used to determine this systematic uncertainty are shown in Figures ??–??.

For $D^+ \rightarrow K^+ K^- \pi^+$ mode, we used the method in Peter's thesis to determine the syst error. The Data/MC comparisons for mass distributions are shown in Figure ???. We divide the signal MC sample into three subsets: $\phi\pi$, K_0^* , and $K^*(1410)$ (this represents more than 95% for the total sample). Then calculate the efficiency for each subset. For the three submodes, if mode i has branching fraction b_i and efficiency ϵ_i it is natural to use

$$\epsilon \equiv \frac{\sum_i \epsilon_i b_i}{B} \quad \text{with} \quad B \equiv \sum_i b_i, \quad (4)$$

for the efficiency of the threebody mode. However, the efficiencies and branching fractions are not precise. Let σ_i be the error for branching fraction b_i and s_i be the error for ϵ_i . To propagate these errors to a systematic error for ϵ , we need the following derivatives:

$$\frac{\partial \epsilon}{\partial \epsilon_i} = \frac{b_i}{B} \quad (5)$$

Table 33: Resonant substructure systematic uncertainties.

Mode	dau1(%)	dau2(%)	dau3(%)	dau4(%)	max (%)
$D^0 \rightarrow K^- \pi^+$	–	–	–	–	–
$D^0 \rightarrow K^- \pi^+ \pi^0$	0.58	0.09	0.19	–	0.58
$D^0 \rightarrow K^- \pi^+ \pi^+ \pi^-$	1.3	0.12	0.58	0.16	1.3
$D^+ \rightarrow K^- \pi^+ \pi^+$	0.53	0.23	0.21	–	0.53
$D^+ \rightarrow K^- \pi^+ \pi^+ \pi^0$	0.94	0.43	0.19	0.12	0.94
$D^+ \rightarrow K_S^0 \pi^+$	–	–	–	–	–
$D^+ \rightarrow K_S^0 \pi^+ \pi^0$	0.42	0.23	0.39	–	0.42
$D^+ \rightarrow K_S^0 \pi^+ \pi^+ \pi^-$	0.62	0.22	0.41	0.13	0.62
$D^+ \rightarrow K^+ K^- \pi^+$	0.62	1.63	0.01	–	1.63

and

$$\frac{\partial \epsilon}{\partial b_i} = \frac{\epsilon_i}{B} - \frac{\sum_j \epsilon_j b_j}{B^2} = \frac{(\epsilon_i - \epsilon)}{B} \quad (6)$$

To get the error σ_ϵ for ϵ , we sum the errors in quadrature using the partial derivatives for the weights:

$$\sigma_\epsilon^2 = \sum_i \frac{(b_i s_i)^2}{B^2} + \sum_i \frac{(\epsilon_i - \epsilon)^2 \sigma_i^2}{B^2} \quad (7)$$

To be conservative, we use 30% of the branching fraction value as the uncertainties to calculate the weighted efficiency to be 0.4289 ± 0.0042 (0.99%). The efficiencies and the branching fractions for the three submodes are shown in Table ???. Therefore, we assign 0.99% as the systematic uncertainty for this mode.

 Table 34: Efficiencies and branching fractions for the three submodes for mode $D^+ \rightarrow K^+ K^- \pi^+$.

Sub Mode	Effs (%)	BFs ($\times 10^{-3}$)
$\phi \pi$	43.68 ± 0.38	3.20 ± 0.96
K_0^*	45.21 ± 0.37	3.02 ± 0.91
$K^*(1410)$	40.30 ± 0.34	3.70 ± 1.11

For modes with π^0 's, we repeated the resonant substructure uncertainty check, explicitly fitting for the yields in each momentum bin rather than following the cut-and-count method used above. The results are consistent with the nominal method.

It is possible for the decay of one D in an event to affect the reconstruction of the other D . This can arise subtly, through changes in the tracking and π^0 -finding efficiency, or in a direct manner, by changing the fake rate with multiple candidates. We have investigated both possibilities.

Table 35: Reweighting ratios for other-side track and π^0 multiplicity study. The MC samples are reweighted so the data/MC ratio is changed from the second column to one of the “reweight” ratios. The “+” reweight increases the mean multiplicity and the “−” reweight decreases it. The π^0 data/MC ratio is assumed to be 1.

Multiplicity	Data/MC ratio	Reweighting “−” ratio	Reweighting “+” ratio
Tracks			
0	1.15	0.70	1.30
1	1.071	0.85	1.15
2	0.955	1.00	1.00
3	0.955	1.15	0.85
4	1.04	1.15	0.85
5	0.991	1.30	0.70
6	2.64	5.00	0.4
7	10.3	10.0	0.2
π^0 's			
0	1.0*	0.7	1.3
1	1.0*	0.85	1.15
2	1.0*	1.0	1.0
3	1.0*	1.15	0.85
4	1.0*	1.30	0.7
5	1.0*	5.0	0.4

First, the track and π^0 -level efficiencies may change as a function of the other side. The Monte Carlo shows, in fact, that there can be changes in reconstruction efficiencies of $K\pi$ of a few percent between the other side being all-neutral and being a 4-prong decay. However, the generic mixture of D decays generated by the default DECAY.DEC produces a multiplicity spectrum that is quite close to data. To obtain a feel for the size of the effect on the efficiency due to any difference between MC and data, we reweight events based on the generator-level number of tracks and the number of π^0 's on the other side, with weight variations on the level of “ 3σ ” (Table ??) based on Qing He's study [?] of MC-data discrepancy. The results are shown in Table ???. The largest change due to the track reweighting is 0.26% in the $D^+ \rightarrow K_S^0 \pi^+ \pi^+ \pi^-$ efficiency, and all modes show reduced efficiency when the mean track multiplicity increases and increased efficiency when the mean decreases. Under a π^0 multiplicity shift, the only modes to show significant change are π^0 modes (which is to be expected). The largest such change is 0.48% for $D^0 \rightarrow K^- \pi^+ \pi^0$. The sizes of the multiplicity shifts are designed to be about three times larger than the observed discrepancies, so these translate to relative shifts of $\mathcal{O}(0.2\%)$, which we choose not to include as a systematic uncertainty.

Second, we consider the effect of the multiple candidate rate. If there is more than one acceptable candidate for a particular D single tag decay, we choose the one with the smallest

Table 36: Effects on efficiency of reweighting the multiplicity distribution of the other side. Values are $\delta\epsilon/\epsilon$.

Mode	Track +	Track -	$\pi^0 +$	$\pi^0 -$
$D^0 \rightarrow K^- \pi^+$	-0.0004	+0.0002	+0.0005	-0.0001
$D^0 \rightarrow K^- \pi^+ \pi^0$	+0.0014	-0.0013	-0.0048	+0.0041
$D^0 \rightarrow K^- \pi^+ \pi^+ \pi^-$	-0.0011	+0.0003	+0.0002	+0.0000
$D^+ \rightarrow K^- \pi^+ \pi^+$	-0.0012	-0.0002	+0.0002	-0.0001
$D^+ \rightarrow K^- \pi^+ \pi^+ \pi^0$	+0.0016	-0.0012	-0.0029	+0.0027
$D^+ \rightarrow K_S^0 \pi^+$	+0.0006	-0.0004	-0.0001	+0.0001
$D^+ \rightarrow K_S^0 \pi^+ \pi^0$	+0.0003	-0.0006	-0.0018	+0.0019
$D^+ \rightarrow K_S^0 \pi^+ \pi^+ \pi^-$	-0.0026	+0.0026	+0.0004	-0.0004
$D^+ \rightarrow K^+ K^- \pi^+$	+0.0025	+0.0000	+0.0000	-0.0001

$|\Delta E|$ for the M_{BC} fit. This choice is not 100% accurate, and wrong choices will in general have the effect of moving signal into the background shape, *i.e.*, reducing the average efficiency. If, for example, the right choice is made 80% of the time, this has the effect of reducing the efficiency in multiple candidate events by 20%. This reduces the overall efficiency by the product of the error rate and the fraction of events with multiple candidates, so if either of these two rates are simulated wrong it will result in an error.

The two reweighting studies mentioned earlier in this section probe the variation of this product within the constraints of the Monte Carlo. However, because the multiple candidate rate is dependent on the fake rate for tracks and π^0 's, it is possible that a systematic difference in the fake rates between MC and data would result in an error that cannot be modelled within the constraints of the MC. We therefore compare the multiple candidate rate in MC and data to gauge the possible size of this effect.

We restrict our study of the multiple candidate rate to single tags, and we define F to be the fraction of the reconstructed single tag yield that comes from multiple-candidate events. We also introduce ϵ_s and ϵ_m , which are the signal efficiencies in single- and multiple-candidate events, respectively. The denominators of ϵ_s and ϵ_m are not well-defined, as it is impossible to know whether a signal MC event that failed to be reconstructed *would have* been a single- or multiple-candidate event. Nonetheless, these efficiencies are conceptually useful for estimating systematic uncertainties.

The total single tag efficiency can be expressed in terms of ϵ_s , ϵ_m , and F :

$$\frac{1}{\epsilon} = \frac{1-F}{\epsilon_s} + \frac{F}{\epsilon_m} \quad (8)$$

$$\epsilon = \frac{\epsilon_s \epsilon_m}{(1-F)\epsilon_m + F\epsilon_s} \quad (9)$$

We then assume that there are no data/MC discrepancies for ϵ_s and ϵ_m , and we derive the shift between data and MC efficiency that arises from a data/MC discrepancy in F :

$$\Delta\epsilon = \epsilon_{\text{MC}} - \epsilon_{\text{data}} = (F_{\text{data}} - F_{\text{MC}})(\epsilon_s - \epsilon_m) \cdot \frac{\epsilon_{\text{MC}}\epsilon_{\text{data}}}{\epsilon_s\epsilon_m}. \quad (10)$$

For small F , $\epsilon \approx \epsilon_s$, so the fractional efficiency bias is

$$\frac{\Delta\epsilon}{\epsilon_{\text{MC}}} \approx (F_{\text{data}} - F_{\text{MC}}) \left(\frac{\epsilon_s}{\epsilon_m} - 1 \right) = \left(\frac{F_{\text{data}}}{F_{\text{MC}}} - 1 \right) \left(\frac{\epsilon_s}{\epsilon_{\text{MC}}} - 1 \right), \quad (11)$$

where we have used

$$\epsilon_m = \frac{F_{\text{MC}}\epsilon_{\text{MC}}\epsilon_s}{\epsilon_s - (1 - F_{\text{MC}})\epsilon_{\text{MC}}}. \quad (12)$$

Thus, a bias in efficiency appears only if both $F_{\text{MC}} \neq F_{\text{data}}$ and $\epsilon_s \neq \epsilon_m$.

To evaluate this bias, we measure F_{MC} and F_{data} directly in MC and data, and we take ϵ_{MC} from signal MC (Table ??). We also find ϵ_{DT} , the single tag efficiency measured in a clean double tag signal MC sample (versus $D^0 \rightarrow K^-\pi^+$ for D^0 modes and versus $D^+ \rightarrow K^-\pi^+\pi^+$ for D^+ modes) where F is much smaller than in a generic single tag sample. Knowing F_{MC} and F_{DT} , we can then solve for ϵ_s

Where the multiple candidate rate is appreciable, we find $\epsilon_m < \epsilon_s$ because multiple candidates do not always resolve to the correct candidate. For instance, for $D^0 \rightarrow K^-\pi^+\pi^0$, ϵ_m is roughly 30% smaller than ϵ_s , which implies that the correct candidate is chosen only 70% of the time.

The size of any effect is limited by the value of $|F_{\text{MC}} - F_{\text{data}}|$; even if events with multiple candidates have zero efficiency of correct reconstruction, the total efficiency will change by only this amount. Therefore, to set the final systematic that we will use, we take the smaller of the central values of $|F_{\text{MC}} - F_{\text{data}}|$ and $|\Delta\epsilon/\epsilon_{\text{MC}}|$. If this is less than 0.2% we assign no systematic.

Some of the difference between the data and MC multiple candidate fraction may arise from differences in track and π^0 multiplicity on the other side. To check this possibility, we look at the multiple candidate fraction in MC, reweighting the other side to the ratios in Table ??, and measuring the change. The results are shown in Table ??.

8.2 Signal shape parameterization

With the increase in statistics from the 56 pb⁻¹ to the 281 pb⁻¹ analysis we have become more sensitive to the lineshape parameters used in this analysis. In particular, we have spent a fair amount of time exploring the sensitivity to the $\psi(3770)$ mass and width. As described in Section ?? we have used as default values 3.7718 GeV for the mass and 28.6 MeV for the width of the $\psi(3770)$. We also used $R = 12.3$ as the default value. In this section we explore the sensitivity to these parameters.

First we note that the mass of the produced $\psi(3770)$ in the e^+e^- interaction is not controlled by the natural width of the $\psi(3770)$, rather it is shaped by the beam energy

Table 37: The fraction of the total yield in multiple candidate events in data and Monte Carlo, the estimated efficiency change due to this effect, and the final systematic uncertainty used for this mode. The Error is taken from the smaller of the central values of $|F_{\text{MC}} - F_{\text{data}}|$ and $|\Delta\epsilon/\epsilon_{\text{MC}}|$, if it is less than 0.2% we assign no systematic error.

Mode	$F_{\text{data}} (\%)$	$F_{\text{MC}} (\%)$	$F_{\text{MC}} - F_{\text{data}} (\%)$	$\Delta\epsilon/\epsilon_{\text{MC}} (\%)$	Error (%)
$D^0 \rightarrow K^-\pi^+$	0.05 ± 0.01	0.05 ± 0.00	-0.00 ± 0.01	0.01 ± 0.03	0
$D^0 \rightarrow K^-\pi^+\pi^0$	13.97 ± 0.08	15.52 ± 0.02	1.55 ± 0.08	-0.74 ± 0.09	0.7
$D^0 \rightarrow K^-\pi^+\pi^+\pi^-$	7.25 ± 0.06	7.22 ± 0.01	-0.03 ± 0.06	0.01 ± 0.03	0
$D^+ \rightarrow K^-\pi^+\pi^+$	0.87 ± 0.02	0.76 ± 0.00	-0.10 ± 0.02	-0.04 ± 0.06	0
$D^+ \rightarrow K^-\pi^+\pi^+\pi^0$	15.05 ± 0.20	14.35 ± 0.04	-0.70 ± 0.20	0.24 ± 0.09	0.2
$D^+ \rightarrow K_S^0\pi^+$	0.99 ± 0.06	0.75 ± 0.01	-0.24 ± 0.06	-0.65 ± 2.28	0.2
$D^+ \rightarrow K_S^0\pi^+\pi^0$	12.34 ± 0.17	12.72 ± 0.03	0.38 ± 0.18	-0.09 ± 0.06	0
$D^+ \rightarrow K_S^0\pi^+\pi^+\pi^-$	17.75 ± 0.27	17.63 ± 0.05	-0.12 ± 0.27	0.06 ± 0.15	0
$D^+ \rightarrow K^+K^-\pi^+$	1.51 ± 0.11	1.50 ± 0.02	-0.01 ± 0.11	0.03 ± 0.22	0

spread of CESR. The spread in the center of mass energy is about 2.1 MeV, which is much smaller than the $\psi(3770)$ width. However, due to ISR the effective e^+e^- energy has a tail to lower center of mass energy for the produced $\psi(3770)$. This tail is observed as the high side tail in the m_{BC} distribution. The number of events in this tail is controlled by the amount of ISR radiation and the cross-section at this lower center of mass energy. The cross-section is simply given by the line shape of the $\psi(3770)$. There are two ways that the line shape can be changed to increase the event rate in the ISR tail. First you can make the $\psi(3770)$ wider; this increases the cross-section in the tails of the Breit-Wigner. The second thing you can do is to reduce the mass of the $\psi(3770)$. In our data these two parameters are strongly correlated and we can not really separate them. What we can do is to fix one parameter, *e.g.*, the mass, and fit for the width. To illustrate the very strong correlation, and to justify our choice of the $\psi(3770)$ mass, we performed fits for the width for two choices of the $\psi(3770)$ mass as shown in Table ???. It is clear that the PDG mass of 3.770 GeV for the $\psi(3770)$ gives widths that are not consistent with direct measurements of the width from scans of the $\psi(3770)$. (CLEO/CESR has not done a scan that allow us to measure the lineshape parameters.) However, for the choice of $m_{\psi(3770)} = 3.7718$ GeV we find that the determined width is much more consistent with the existing measurements.

8.2.1 Variation of Mass, width, and R

We are using the same line shape as BES [?] when fitting data. The default values for the line shape parameters are:

Mass of $\psi(3770) = 3771.8$ MeV (This is the number we use, since our energy scale has been shifted by 0.6 MeV). Width of $\psi(3770) = 28.6$ MeV, ‘Blatt-Weiskopf’ factor $R = 12.3\text{GeV}^{-1}$. We fit data by using the above default values and get yields which are referred to as ‘regular’ yields.

Then, we vary the mass by ± 0.5 MeV (*i.e.* 3772.3 MeV and 3771.3 MeV) and fit data.

Table 38: Effect on multiple candidate fraction in Monte Carlo of reweighting of the track and π^0 multiplicity of the other side. Note that Fr_{MC} differs from other tables due to slightly different MC samples and simplified fitting functions.

Mode	Fr_{MC}	Track “+”	Track “-”	π^0 “+”	π^0 “-”
$D^0 \rightarrow K^- \pi^+$	0.06%	-0.01%	+0.00%	-0.01%	+0.01%
$D^0 \rightarrow K^- \pi^+ \pi^0$	15.6%	+0.3%	+0.1%	+1.3%	-1.3%
$D^0 \rightarrow K^- \pi^+ \pi^- \pi^+$	7.1%	+1.2%	-0.5%	-0.1%	+0.0%
$D^+ \rightarrow K^- \pi^+ \pi^+$	0.82%	+0.09%	-0.12%	-0.02%	+0.01%
$D^+ \rightarrow K^- \pi^+ \pi^+ \pi^0$	16.3%	+0.04%	-0.02%	+1.2%	-1.1%
$D^+ \rightarrow K_S^0 \pi^+$	0.79%	+0.02%	-0.06%	-0.04%	+0.04%
$D^+ \rightarrow K_S^0 \pi^+ \pi^0$	13.5%	+0.3%	-0.4%	+0.6%	-0.7%
$D^+ \rightarrow K_S^0 \pi^+ \pi^+ \pi^-$	17.8%	+0.7%	-1.2%	+0.0%	+0.0%
$D^+ \rightarrow K^+ K^- \pi^+$	1.5%	+0.1%	-0.2%	+0.0%	+0.0%

Table 39: The fitted $\psi(3770)$ width for two choices of the $\psi(3770)$ mass.

Mode	Γ ($M = 3.774$ GeV)	Γ ($M = 3.770$ GeV)
$D^0 \rightarrow K^- \pi^+$	32.8 ± 0.6	22.4 ± 0.5
$D^0 \rightarrow K^- \pi^+ \pi^0$	37.1 ± 0.7	24.4 ± 0.8
$D^0 \rightarrow K^- \pi^+ \pi^- \pi^+$	31.5 ± 0.8	20.7 ± 0.6
$D^+ \rightarrow K^- \pi^+ \pi^+$	28.5 ± 0.6	19.2 ± 0.5
$D^+ \rightarrow K^- \pi^+ \pi^+ \pi^0$	28.9 ± 1.8	20.1 ± 2.0
$D^+ \rightarrow K_S^0 \pi^+$	26.5 ± 1.3	18.1 ± 1.2
$D^+ \rightarrow K_S^0 \pi^+ \pi^0$	20.4 ± 2.1	15.5 ± 1.4
$D^+ \rightarrow K_S^0 \pi^+ \pi^+ \pi^-$	25.9 ± 3.6	22.3 ± 1.9
$D^+ \rightarrow K^+ K^- \pi^+$	29.1 ± 2.8	20.9 ± 2.1

We compare the yields with the regular fits and choose the larger one from the two groups (either 3772.3 MeV or 3771.3 MeV) as systematic errors of the Mass part in the line shape parameters. (See Table ?? and Table ???. for double tags and single tags respectively).

Similarly, we vary the width of $\psi(3770)$ by ± 2.5 MeV (Table ?? for double tags and Table ?? for single tags) and R by ± 4 GeV^{-1} (Table ?? for double tags and Table ?? for single tags).

As the differences in the double tags are negligible compared with single tags, we only consider the single tags (Table ??, ??, ??). Among two charge conjugate decays in each mode, we choose the larger difference for that mode and then add quadrature the three differences (mass, width, and R) to get the systematic uncertainties for the line shape parameters as shown in Table ??.

Table 40: Single tag efficiencies without FSR in our signal Monte Carlo.

Mode	Efficiency without FSR(%)	Efficiency with FSR(%)	Ratio
$D^0 \rightarrow K^-\pi^+$	67.00 ± 0.12	65.17 ± 0.11	1.028 ± 0.002
$\bar{D}^0 \rightarrow K^+\pi^-$	67.89 ± 0.12	65.88 ± 0.11	1.031 ± 0.002
$D^0 \rightarrow K^-\pi^+\pi^0$	35.78 ± 0.07	35.28 ± 0.07	1.014 ± 0.001
$\bar{D}^0 \rightarrow K^+\pi^-\pi^0$	36.11 ± 0.07	35.62 ± 0.07	1.014 ± 0.001
$D^0 \rightarrow K^-\pi^+\pi^+\pi^-$	48.05 ± 0.10	46.82 ± 0.09	1.026 ± 0.001
$\bar{D}^0 \rightarrow K^+\pi^-\pi^+\pi^+$	48.39 ± 0.10	47.19 ± 0.09	1.025 ± 0.002
$D^+ \rightarrow K^-\pi^+\pi^+$	56.04 ± 0.11	54.92 ± 0.10	1.020 ± 0.001
$D^- \rightarrow K^+\pi^-\pi^-$	56.28 ± 0.11	55.17 ± 0.10	1.020 ± 0.001
$D^+ \rightarrow K^-\pi^+\pi^+\pi^0$	28.32 ± 0.11	28.13 ± 0.10	1.007 ± 0.002
$D^- \rightarrow K^+\pi^-\pi^-\pi^0$	28.46 ± 0.11	28.21 ± 0.10	1.009 ± 0.002
$D^+ \rightarrow K_S^0\pi^+$	46.39 ± 0.11	45.63 ± 0.10	1.017 ± 0.001
$D^- \rightarrow K_S^0\pi^-$	46.11 ± 0.11	45.33 ± 0.10	1.017 ± 0.001
$D^+ \rightarrow K_S^0\pi^+\pi^0$	24.07 ± 0.11	23.95 ± 0.11	1.005 ± 0.001
$D^- \rightarrow K_S^0\pi^-\pi^0$	24.25 ± 0.11	24.10 ± 0.11	1.006 ± 0.001
$D^+ \rightarrow K_S^0\pi^+\pi^+\pi^-$	32.84 ± 0.15	32.29 ± 0.14	1.017 ± 0.003
$D^- \rightarrow K_S^0\pi^-\pi^-\pi^+$	33.22 ± 0.15	32.60 ± 0.14	1.019 ± 0.003
$D^+ \rightarrow K^+K^-\pi^+$	43.25 ± 0.14	42.73 ± 0.21	1.012 ± 0.002
$D^- \rightarrow K^-K^+\pi^-$	43.03 ± 0.14	42.47 ± 0.20	1.013 ± 0.002

8.3 π^0 momentum

To study the effect of the discrepancy in π^0 momentum between the data and Monte Carlo on the ΔE distribution, we rescale the π^0 momentum by a factor of 0.997 (decrease of 0.3%). The corresponding effect on M_{BC} is less than 0.03%. The yield changes are less than 0.05%, which are shown in Table ???. This effect is negligible.

8.4 Reconstruction of $D^0 \rightarrow K^-\pi^+\gamma$ as cross-check of FSR

To cross-check the simulation of final state radiation, we attempt to reconstruct $D^0 \rightarrow K^-\pi^+\gamma$ in data and Monte Carlo. This is very difficult because the signal is dominated by backgrounds, especially from $D^0 \rightarrow K^-\pi^+\pi^0$. As a result, we are only able to make a measurement for photons with energy below the π^0 mass. This measurement shows no sign of a difference between data and Monte Carlo, but the precision is poor.

With a tag \bar{D}^0 , we can hope to distinguish $D^0 \rightarrow K^-\pi^+\gamma$ from $D^0 \rightarrow K^-\pi^+\pi^0$ with the missing momentum of the γ or π^0 . At high missing energy, the missing mass squared peaks for γ and π^0 smear into each other, but at low energy they are better separated. Still, because the $D^0 \rightarrow K^-\pi^+\pi^0$ background is so much larger than the $D^0 \rightarrow K^-\pi^+\gamma$ signal, even a small amount of background leakage will dominate the signal. Therefore, while we do cut on the missing mass squared, requiring consistency with zero, we cannot rely on only this cut.

A cleaner rejection of $D^0 \rightarrow K^-\pi^+\pi^0$ is accomplished by requiring that the missing energy is less than the π^0 mass. We actually cut at a lower energy, 120 MeV, to eliminate

Table 41: Double tag yields with different mass of $\psi(3770)$.

Mode	Yield			max-diff (%)
	$M = 3771.9 \text{ MeV}$	$M = 3772.4 \text{ MeV}$	$M = 3772.9 \text{ MeV}$	
$D^0 \rightarrow K^-\pi^+ \bar{D}^0 \rightarrow K^+\pi^-$	1826 ± 43	1825 ± 43	1825 ± 43	0.05
$D^0 \rightarrow K^-\pi^+ \bar{D}^0 \rightarrow K^+\pi^-\pi^0$	3889 ± 64	3886 ± 64	3884 ± 64	-0.06
$D^0 \rightarrow K^-\pi^+ \bar{D}^0 \rightarrow K^+\pi^-\pi^-\pi^+$	2989 ± 55	2987 ± 55	2986 ± 55	-0.04
$D^0 \rightarrow K^-\pi^+\pi^0 \bar{D}^0 \rightarrow K^+\pi^-$	3966 ± 64	3964 ± 64	3962 ± 64	-0.05
$D^0 \rightarrow K^-\pi^+\pi^0 \bar{D}^0 \rightarrow K^+\pi^-\pi^0$	7605 ± 90	7600 ± 90	7595 ± 90	-0.07
$D^0 \rightarrow K^-\pi^+\pi^0 \bar{D}^0 \rightarrow K^+\pi^-\pi^-\pi^+$	5764 ± 78	5760 ± 78	5755 ± 78	-0.09
$D^0 \rightarrow K^-\pi^+\pi^+\pi^- \bar{D}^0 \rightarrow K^+\pi^-$	2896 ± 54	2895 ± 54	2893 ± 54	-0.06
$D^0 \rightarrow K^-\pi^+\pi^+\pi^- \bar{D}^0 \rightarrow K^+\pi^-\pi^0$	5727 ± 78	5723 ± 78	5719 ± 78	-0.07
$D^0 \rightarrow K^-\pi^+\pi^+\pi^- \bar{D}^0 \rightarrow K^+\pi^-\pi^-\pi^+$	4562 ± 69	4559 ± 69	4555 ± 69	-0.08
$D^+ \rightarrow K^-\pi^+\pi^+ D^- \rightarrow K^+\pi^-\pi^-$	5953 ± 78	5951 ± 78	5950 ± 78	-0.02
$D^+ \rightarrow K^-\pi^+\pi^+ D^- \rightarrow K^+\pi^-\pi^-\pi^0$	1909 ± 45	1908 ± 45	1906 ± 45	-0.07
$D^+ \rightarrow K^-\pi^+\pi^+ D^- \rightarrow K_S^0\pi^-$	863 ± 30	862 ± 30	862 ± 30	-0.03
$D^+ \rightarrow K^-\pi^+\pi^+ D^- \rightarrow K_S^0\pi^-\pi^0$	2033 ± 46	2032 ± 46	2031 ± 46	-0.03
$D^+ \rightarrow K^-\pi^+\pi^+ D^- \rightarrow K_S^0\pi^-\pi^-\pi^+$	1068 ± 33	1067 ± 33	1067 ± 33	0.05
$D^+ \rightarrow K^-\pi^+\pi^+ D^- \rightarrow K^-K^+\pi^-$	483 ± 22	483 ± 22	483 ± 22	0.02
$D^+ \rightarrow K^-\pi^+\pi^+\pi^0 D^- \rightarrow K^+\pi^-\pi^-$	1840 ± 44	1839 ± 44	1838 ± 44	0.07
$D^+ \rightarrow K^-\pi^+\pi^+\pi^0 D^- \rightarrow K^+\pi^-\pi^-\pi^0$	646 ± 29	644 ± 29	643 ± 29	0.27
$D^+ \rightarrow K^-\pi^+\pi^+\pi^0 D^- \rightarrow K_S^0\pi^-$	295 ± 18	295 ± 18	294 ± 18	-0.07
$D^+ \rightarrow K^-\pi^+\pi^+\pi^0 D^- \rightarrow K_S^0\pi^-\pi^0$	601 ± 26	601 ± 26	600 ± 26	-0.09
$D^+ \rightarrow K^-\pi^+\pi^+\pi^0 D^- \rightarrow K_S^0\pi^-\pi^-\pi^+$	369 ± 21	369 ± 21	368 ± 21	0.16
$D^+ \rightarrow K^-\pi^+\pi^+\pi^0 D^- \rightarrow K^-K^+\pi^-$	160 ± 14	160 ± 14	160 ± 14	-0.04
$D^+ \rightarrow K_S^0\pi^+ D^- \rightarrow K^+\pi^-\pi^-$	828 ± 29	828 ± 29	828 ± 29	-0.02
$D^+ \rightarrow K_S^0\pi^+ D^- \rightarrow K^+\pi^-\pi^-\pi^0$	294 ± 17	294 ± 17	294 ± 17	0.04
$D^+ \rightarrow K_S^0\pi^+ D^- \rightarrow K_S^0\pi^-$	109 ± 11	109 ± 11	109 ± 11	-0.03
$D^+ \rightarrow K_S^0\pi^+ D^- \rightarrow K_S^0\pi^-\pi^0$	260 ± 17	260 ± 17	260 ± 17	-0.06
$D^+ \rightarrow K_S^0\pi^+ D^- \rightarrow K_S^0\pi^-\pi^-\pi^+$	147 ± 12	147 ± 12	147 ± 12	0.03
$D^+ \rightarrow K_S^0\pi^+ D^- \rightarrow K^-K^+\pi^-$	72 ± 9	72 ± 9	72 ± 9	-0.11
$D^+ \rightarrow K_S^0\pi^+\pi^0 D^- \rightarrow K^+\pi^-\pi^-$	1852 ± 44	1851 ± 44	1851 ± 44	-0.03
$D^+ \rightarrow K_S^0\pi^+\pi^0 D^- \rightarrow K^+\pi^-\pi^-\pi^0$	632 ± 26	632 ± 26	631 ± 26	-0.16
$D^+ \rightarrow K_S^0\pi^+\pi^0 D^- \rightarrow K_S^0\pi^-$	257 ± 16	257 ± 16	257 ± 16	-0.03
$D^+ \rightarrow K_S^0\pi^+\pi^0 D^- \rightarrow K_S^0\pi^-\pi^0$	646 ± 27	645 ± 27	645 ± 27	0.11
$D^+ \rightarrow K_S^0\pi^+\pi^0 D^- \rightarrow K_S^0\pi^-\pi^-\pi^+$	361 ± 20	361 ± 20	360 ± 20	-0.14
$D^+ \rightarrow K_S^0\pi^+\pi^0 D^- \rightarrow K^-K^+\pi^-$	144 ± 13	144 ± 13	144 ± 13	0.04
$D^+ \rightarrow K_S^0\pi^+\pi^+\pi^- D^- \rightarrow K^+\pi^-\pi^-$	1146 ± 34	1145 ± 34	1145 ± 34	-0.05
$D^+ \rightarrow K_S^0\pi^+\pi^+\pi^- D^- \rightarrow K^+\pi^-\pi^-\pi^0$	340 ± 20	339 ± 20	338 ± 20	0.23
$D^+ \rightarrow K_S^0\pi^+\pi^+\pi^- D^- \rightarrow K_S^0\pi^-$	160 ± 13	160 ± 13	160 ± 13	0.05
$D^+ \rightarrow K_S^0\pi^+\pi^+\pi^- D^- \rightarrow K_S^0\pi^-\pi^0$	359 ± 20	359 ± 20	358 ± 20	0.19
$D^+ \rightarrow K_S^0\pi^+\pi^+\pi^- D^- \rightarrow K_S^0\pi^-\pi^-\pi^+$	206 ± 16	205 ± 16	205 ± 16	0.22
$D^+ \rightarrow K_S^0\pi^+\pi^+\pi^- D^- \rightarrow K^-K^+\pi^-$	91 ± 10	91 ± 10	91 ± 10	0.16
$D^+ \rightarrow K^+K^-\pi^+ D^- \rightarrow K^+\pi^-\pi^-$	485 ± 22	485 ± 22	485 ± 22	-0.03
$D^+ \rightarrow K^+K^-\pi^+ D^- \rightarrow K^+\pi^-\pi^-\pi^0$	166 ± 13	166 ± 13	166 ± 13	-0.00
$D^+ \rightarrow K^+K^-\pi^+ D^- \rightarrow K_S^0\pi^-$	62 ± 8	62 ± 8	62 ± 8	-0.13
$D^+ \rightarrow K^+K^-\pi^+ D^- \rightarrow K_S^0\pi^-\pi^0$	180 ± 14	180 ± 14	180 ± 14	-0.11
$D^+ \rightarrow K^+K^-\pi^+ D^- \rightarrow K_S^0\pi^-\pi^-\pi^+$	96 ± 11	96 ± 11	96 ± 11	0.22
$D^+ \rightarrow K^+K^-\pi^+ D^- \rightarrow K^-K^+\pi^-$	42 ± 8	42 ± 8	42 ± 8	0.49

Table 42: Single tag yields with different mass of $\psi(3770)$.

Mode	Yield			max-diff (%)
	$M = 3771.9$ MeV	$M = 3772.4$ MeV	$M = 3772.9$ MeV	
$D^0 \rightarrow K^-\pi^+$	75284 ± 282	75177 ± 281	75079 ± 282	0.14
$\bar{D}^0 \rightarrow K^+\pi^-$	75691 ± 283	75584 ± 282	75487 ± 282	0.14
$D^0 \rightarrow K^-\pi^+\pi^0$	144968 ± 438	144710 ± 439	144467 ± 438	0.18
$\bar{D}^0 \rightarrow K^+\pi^-\pi^0$	146064 ± 441	145798 ± 441	145548 ± 440	0.18
$D^0 \rightarrow K^-\pi^+\pi^+\pi^-$	114450 ± 366	114222 ± 366	114005 ± 366	0.20
$\bar{D}^0 \rightarrow K^+\pi^-\pi^-\pi^+$	114988 ± 367	114759 ± 368	114540 ± 367	0.20
$D^+ \rightarrow K^-\pi^+\pi^+$	116690 ± 353	116545 ± 354	116405 ± 353	-0.12
$D^- \rightarrow K^+\pi^-\pi^-$	117978 ± 355	117831 ± 356	117690 ± 356	-0.12
$D^+ \rightarrow K^-\pi^+\pi^+\pi^0$	36887 ± 258	36813 ± 260	36745 ± 260	0.20
$D^- \rightarrow K^+\pi^-\pi^-\pi^0$	37220 ± 260	37143 ± 261	37073 ± 262	0.21
$D^+ \rightarrow K_S^0\pi^+$	16870 ± 137	16844 ± 137	16820 ± 137	0.15
$D^- \rightarrow K_S^0\pi^-$	17112 ± 138	17087 ± 138	17065 ± 138	0.14
$D^+ \rightarrow K_S^0\pi^+\pi^0$	38407 ± 263	38329 ± 262	38257 ± 262	0.20
$D^- \rightarrow K_S^0\pi^-\pi^0$	38702 ± 263	38626 ± 263	38555 ± 262	0.20
$D^+ \rightarrow K_S^0\pi^+\pi^+\pi^-$	23769 ± 226	23706 ± 224	23649 ± 225	0.26
$D^- \rightarrow K_S^0\pi^-\pi^-\pi^+$	23972 ± 227	23909 ± 225	23851 ± 225	0.26
$D^+ \rightarrow K^+K^-\pi^+$	10140 ± 124	10115 ± 123	10091 ± 123	-0.24
$D^- \rightarrow K^-K^+\pi^-$	10090 ± 124	10066 ± 123	10042 ± 122	-0.24

Table 43: Double tag yields with different width of $\psi(3770)$.

Mode	Yield			max-diff (%)
	$\Gamma = 22.7 \text{ MeV}$	$\Gamma = 25.2 \text{ MeV}$	$\Gamma = 27.2 \text{ MeV}$	
$D^0 \rightarrow K^- \pi^+ \bar{D}^0 \rightarrow K^+ \pi^-$	1823 ± 43	1825 ± 43	1827 ± 43	-0.13
$D^0 \rightarrow K^- \pi^+ \bar{D}^0 \rightarrow K^+ \pi^- \pi^0$	3879 ± 64	3886 ± 64	3892 ± 64	-0.18
$D^0 \rightarrow K^- \pi^+ \bar{D}^0 \rightarrow K^+ \pi^- \pi^- \pi^+$	2984 ± 55	2987 ± 55	2990 ± 55	-0.12
$D^0 \rightarrow K^- \pi^+ \pi^0 \bar{D}^0 \rightarrow K^+ \pi^-$	3958 ± 64	3964 ± 64	3969 ± 64	-0.15
$D^0 \rightarrow K^- \pi^+ \pi^0 \bar{D}^0 \rightarrow K^+ \pi^- \pi^0$	7584 ± 90	7600 ± 90	7613 ± 90	-0.21
$D^0 \rightarrow K^- \pi^+ \pi^0 \bar{D}^0 \rightarrow K^+ \pi^- \pi^- \pi^+$	5748 ± 78	5760 ± 78	5769 ± 78	-0.21
$D^0 \rightarrow K^- \pi^+ \pi^+ \pi^- \bar{D}^0 \rightarrow K^+ \pi^-$	2890 ± 54	2895 ± 54	2898 ± 54	-0.16
$D^0 \rightarrow K^- \pi^+ \pi^+ \pi^- \bar{D}^0 \rightarrow K^+ \pi^- \pi^0$	5712 ± 78	5723 ± 78	5733 ± 78	-0.20
$D^0 \rightarrow K^- \pi^+ \pi^+ \pi^- \bar{D}^0 \rightarrow K^+ \pi^- \pi^- \pi^+$	4549 ± 69	4559 ± 69	4568 ± 69	-0.23
$D^+ \rightarrow K^- \pi^+ \pi^+ D^- \rightarrow K^+ \pi^- \pi^-$	5947 ± 78	5951 ± 78	5954 ± 78	-0.07
$D^+ \rightarrow K^- \pi^+ \pi^+ D^- \rightarrow K^+ \pi^- \pi^- \pi^0$	1904 ± 45	1908 ± 45	1911 ± 45	-0.21
$D^+ \rightarrow K^- \pi^+ \pi^+ D^- \rightarrow K_S^0 \pi^-$	862 ± 30	862 ± 30	863 ± 30	-0.08
$D^+ \rightarrow K^- \pi^+ \pi^+ D^- \rightarrow K_S^0 \pi^- \pi^0$	2030 ± 46	2032 ± 46	2034 ± 46	-0.10
$D^+ \rightarrow K^- \pi^+ \pi^+ D^- \rightarrow K_S^0 \pi^- \pi^- \pi^+$	1066 ± 33	1067 ± 33	1068 ± 33	-0.11
$D^+ \rightarrow K^- \pi^+ \pi^+ D^- \rightarrow K^- K^+ \pi^-$	483 ± 22	483 ± 22	483 ± 22	-0.05
$D^+ \rightarrow K^- \pi^+ \pi^+ \pi^0 D^- \rightarrow K^+ \pi^- \pi^-$	1835 ± 44	1839 ± 44	1842 ± 44	-0.20
$D^+ \rightarrow K^- \pi^+ \pi^+ \pi^0 D^- \rightarrow K^+ \pi^- \pi^- \pi^0$	641 ± 29	644 ± 29	648 ± 30	0.53
$D^+ \rightarrow K^- \pi^+ \pi^+ \pi^0 D^- \rightarrow K_S^0 \pi^-$	294 ± 18	295 ± 18	295 ± 18	-0.18
$D^+ \rightarrow K^- \pi^+ \pi^+ \pi^0 D^- \rightarrow K_S^0 \pi^- \pi^-$	599 ± 26	601 ± 26	602 ± 26	-0.30
$D^+ \rightarrow K^- \pi^+ \pi^+ \pi^0 D^- \rightarrow K_S^0 \pi^- \pi^- \pi^+$	367 ± 21	369 ± 21	370 ± 21	0.33
$D^+ \rightarrow K^- \pi^+ \pi^+ \pi^0 D^- \rightarrow K^- K^+ \pi^-$	160 ± 14	160 ± 14	160 ± 14	-0.11
$D^+ \rightarrow K_S^0 \pi^+ D^- \rightarrow K^+ \pi^- \pi^-$	827 ± 29	828 ± 29	828 ± 29	-0.06
$D^+ \rightarrow K_S^0 \pi^+ D^- \rightarrow K^+ \pi^- \pi^- \pi^0$	294 ± 17	294 ± 17	295 ± 17	-0.10
$D^+ \rightarrow K_S^0 \pi^+ D^- \rightarrow K_S^0 \pi^-$	109 ± 11	109 ± 11	109 ± 11	-0.09
$D^+ \rightarrow K_S^0 \pi^+ D^- \rightarrow K_S^0 \pi^- \pi^0$	260 ± 17	260 ± 17	260 ± 17	-0.19
$D^+ \rightarrow K_S^0 \pi^+ D^- \rightarrow K_S^0 \pi^- \pi^- \pi^+$	147 ± 12	147 ± 12	147 ± 12	-0.12
$D^+ \rightarrow K_S^0 \pi^+ D^- \rightarrow K^- K^+ \pi^-$	72 ± 9	72 ± 9	72 ± 9	-0.33
$D^+ \rightarrow K_S^0 \pi^+ \pi^0 D^- \rightarrow K^+ \pi^- \pi^-$	1849 ± 44	1851 ± 44	1852 ± 44	-0.09
$D^+ \rightarrow K_S^0 \pi^+ \pi^0 D^- \rightarrow K^+ \pi^- \pi^- \pi^0$	630 ± 26	632 ± 26	633 ± 26	-0.31
$D^+ \rightarrow K_S^0 \pi^+ \pi^0 D^- \rightarrow K_S^0 \pi^-$	257 ± 16	257 ± 16	257 ± 16	-0.10
$D^+ \rightarrow K_S^0 \pi^+ \pi^0 D^- \rightarrow K_S^0 \pi^- \pi^0$	644 ± 27	645 ± 27	647 ± 27	0.21
$D^+ \rightarrow K_S^0 \pi^+ \pi^0 D^- \rightarrow K_S^0 \pi^- \pi^- \pi^+$	359 ± 20	361 ± 20	362 ± 20	-0.42
$D^+ \rightarrow K_S^0 \pi^+ \pi^0 D^- \rightarrow K^- K^+ \pi^-$	144 ± 13	144 ± 13	144 ± 13	0.15
$D^+ \rightarrow K_S^0 \pi^+ \pi^+ \pi^- D^- \rightarrow K^+ \pi^- \pi^-$	1143 ± 34	1145 ± 34	1146 ± 34	-0.14
$D^+ \rightarrow K_S^0 \pi^+ \pi^+ \pi^- D^- \rightarrow K^+ \pi^- \pi^- \pi^0$	337 ± 20	339 ± 20	341 ± 20	-0.55
$D^+ \rightarrow K_S^0 \pi^+ \pi^+ \pi^- D^- \rightarrow K_S^0 \pi^-$	160 ± 13	160 ± 13	160 ± 13	-0.11
$D^+ \rightarrow K_S^0 \pi^+ \pi^+ \pi^- D^- \rightarrow K_S^0 \pi^- \pi^0$	357 ± 20	359 ± 20	360 ± 20	-0.44
$D^+ \rightarrow K_S^0 \pi^+ \pi^+ \pi^- D^- \rightarrow K_S^0 \pi^- \pi^- \pi^+$	204 ± 16	205 ± 16	206 ± 16	-0.51
$D^+ \rightarrow K_S^0 \pi^+ \pi^+ \pi^- D^- \rightarrow K^- K^+ \pi^-$	91 ± 10	91 ± 10	92 ± 10	-0.51
$D^+ \rightarrow K^+ K^- \pi^+ D^- \rightarrow K^+ \pi^- \pi^-$	485 ± 22	485 ± 22	485 ± 22	-0.03
$D^+ \rightarrow K^+ K^- \pi^+ D^- \rightarrow K^+ \pi^- \pi^- \pi^0$	166 ± 13	166 ± 13	166 ± 13	-0.05
$D^+ \rightarrow K^+ K^- \pi^+ D^- \rightarrow K_S^0 \pi^-$	62 ± 8	62 ± 8	63 ± 8	-0.36
$D^+ \rightarrow K^+ K^- \pi^+ D^- \rightarrow K_S^0 \pi^- \pi^0$	180 ± 14	180 ± 14	180 ± 14	-0.30
$D^+ \rightarrow K^+ K^- \pi^+ D^- \rightarrow K_S^0 \pi^- \pi^- \pi^+$	95 ± 11	96 ± 11	97 ± 11	-0.68
$D^+ \rightarrow K^+ K^- \pi^+ D^- \rightarrow K^- K^+ \pi^-$	41 ± 8	42 ± 8	42 ± 8	-0.99

Table 44: Single tag yields with different width of $\psi(3770)$.

Mode	Yield			max-diff (%)
	$\Gamma = 22.7$ MeV	$\Gamma = 25.2$ MeV	$\Gamma = 27.2$ MeV	
$D^0 \rightarrow K^- \pi^+$	74908 ± 282	75177 ± 281	75412 ± 282	-0.36
$\bar{D}^0 \rightarrow K^+ \pi^-$	75314 ± 282	75584 ± 282	75819 ± 283	-0.36
$D^0 \rightarrow K^- \pi^+ \pi^0$	144073 ± 438	144710 ± 439	145339 ± 441	0.44
$\bar{D}^0 \rightarrow K^+ \pi^- \pi^0$	145146 ± 440	145798 ± 441	146440 ± 443	-0.45
$D^0 \rightarrow K^- \pi^+ \pi^+ \pi^-$	113697 ± 366	114222 ± 366	114726 ± 367	-0.46
$\bar{D}^0 \rightarrow K^+ \pi^- \pi^- \pi^+$	114233 ± 367	114759 ± 368	115264 ± 368	-0.46
$D^+ \rightarrow K^- \pi^+ \pi^+$	116212 ± 353	116545 ± 354	116852 ± 354	-0.29
$D^- \rightarrow K^+ \pi^- \pi^-$	117497 ± 355	117831 ± 356	118140 ± 356	-0.28
$D^+ \rightarrow K^- \pi^+ \pi^+ \pi^0$	36669 ± 259	36813 ± 260	36956 ± 261	0.39
$D^- \rightarrow K^+ \pi^- \pi^- \pi^0$	36993 ± 261	37143 ± 261	37292 ± 262	-0.41
$D^+ \rightarrow K_S^0 \pi^+$	16788 ± 137	16844 ± 137	16896 ± 138	-0.33
$D^- \rightarrow K_S^0 \pi^-$	17034 ± 138	17087 ± 138	17137 ± 138	-0.31
$D^+ \rightarrow K_S^0 \pi^+ \pi^0$	38171 ± 264	38329 ± 262	38482 ± 266	-0.41
$D^- \rightarrow K_S^0 \pi^- \pi^0$	38471 ± 265	38626 ± 263	38777 ± 266	-0.40
$D^+ \rightarrow K_S^0 \pi^+ \pi^+ \pi^-$	23597 ± 224	23706 ± 224	23814 ± 226	-0.46
$D^- \rightarrow K_S^0 \pi^- \pi^- \pi^+$	23798 ± 225	23909 ± 225	24018 ± 227	0.46
$D^+ \rightarrow K^+ K^- \pi^+$	10069 ± 124	10115 ± 123	10160 ± 124	-0.46
$D^- \rightarrow K^- K^+ \pi^-$	10020 ± 123	10066 ± 123	10109 ± 124	-0.46

Table 45: Double tag yields with different R.

Mode	Yield			max-diff (%)
	$R = 8.7 \text{ GeV}^{-1}$	$R = 12.7 \text{ GeV}^{-1}$	$R = 16.7 \text{ GeV}^{-1}$	
$D^0 \rightarrow K^-\pi^+ \bar{D}^0 \rightarrow K^+\pi^-$	1825 ± 43	1825 ± 43	1826 ± 43	-0.04
$D^0 \rightarrow K^-\pi^+ \bar{D}^0 \rightarrow K^+\pi^-\pi^0$	3884 ± 64	3886 ± 64	3888 ± 64	-0.06
$D^0 \rightarrow K^-\pi^+ \bar{D}^0 \rightarrow K^+\pi^-\pi^-\pi^+$	2987 ± 55	2987 ± 55	2988 ± 55	-0.03
$D^0 \rightarrow K^-\pi^+\pi^0 \bar{D}^0 \rightarrow K^+\pi^-$	3962 ± 64	3964 ± 64	3965 ± 64	-0.05
$D^0 \rightarrow K^-\pi^+\pi^0 \bar{D}^0 \rightarrow K^+\pi^-\pi^0$	7594 ± 90	7600 ± 90	7603 ± 90	-0.07
$D^0 \rightarrow K^-\pi^+\pi^0 \bar{D}^0 \rightarrow K^+\pi^-\pi^-\pi^+$	5757 ± 78	5760 ± 78	5761 ± 78	-0.05
$D^0 \rightarrow K^-\pi^+\pi^+\pi^- \bar{D}^0 \rightarrow K^+\pi^-$	2893 ± 54	2895 ± 54	2895 ± 54	-0.04
$D^0 \rightarrow K^-\pi^+\pi^+\pi^- \bar{D}^0 \rightarrow K^+\pi^-\pi^0$	5720 ± 78	5723 ± 78	5725 ± 78	-0.05
$D^0 \rightarrow K^-\pi^+\pi^+\pi^- \bar{D}^0 \rightarrow K^+\pi^-\pi^-\pi^+$	4556 ± 69	4559 ± 69	4560 ± 69	-0.06
$D^+ \rightarrow K^-\pi^+\pi^+ D^- \rightarrow K^+\pi^-\pi^-$	5950 ± 78	5951 ± 78	5952 ± 78	-0.03
$D^+ \rightarrow K^-\pi^+\pi^+ D^- \rightarrow K^+\pi^-\pi^-\pi^0$	1906 ± 45	1908 ± 45	1909 ± 45	-0.08
$D^+ \rightarrow K^-\pi^+\pi^+ D^- \rightarrow K_S^0 \pi^-$	862 ± 30	862 ± 30	862 ± 30	-0.03
$D^+ \rightarrow K^-\pi^+\pi^+ D^- \rightarrow K_S^0 \pi^-\pi^0$	2031 ± 46	2032 ± 46	2032 ± 46	-0.03
$D^+ \rightarrow K^-\pi^+\pi^+ D^- \rightarrow K_S^0 \pi^-\pi^-\pi^+$	1067 ± 33	1067 ± 33	1067 ± 33	0.02
$D^+ \rightarrow K^-\pi^+\pi^+ D^- \rightarrow K^-K^+\pi^-$	483 ± 22	483 ± 22	483 ± 22	-0.02
$D^+ \rightarrow K^-\pi^+\pi^+\pi^0 D^- \rightarrow K^+\pi^-\pi^-$	1838 ± 44	1839 ± 44	1839 ± 44	-0.05
$D^+ \rightarrow K^-\pi^+\pi^+\pi^0 D^- \rightarrow K^+\pi^-\pi^-\pi^0$	644 ± 29	644 ± 29	645 ± 29	-0.12
$D^+ \rightarrow K^-\pi^+\pi^+\pi^0 D^- \rightarrow K_S^0 \pi^-$	294 ± 18	295 ± 18	295 ± 18	-0.05
$D^+ \rightarrow K^-\pi^+\pi^+\pi^0 D^- \rightarrow K_S^0 \pi^-\pi^0$	600 ± 26	601 ± 26	601 ± 26	-0.10
$D^+ \rightarrow K^-\pi^+\pi^+\pi^0 D^- \rightarrow K_S^0 \pi^-\pi^-\pi^+$	368 ± 21	369 ± 21	369 ± 21	-0.12
$D^+ \rightarrow K^-\pi^+\pi^+\pi^0 D^- \rightarrow K^-K^+\pi^-$	160 ± 14	160 ± 14	160 ± 14	-0.02
$D^+ \rightarrow K_S^0 \pi^+ D^- \rightarrow K^+\pi^-\pi^-$	828 ± 29	828 ± 29	828 ± 29	-0.02
$D^+ \rightarrow K_S^0 \pi^+ D^- \rightarrow K^+\pi^-\pi^-\pi^0$	294 ± 17	294 ± 17	294 ± 17	-0.02
$D^+ \rightarrow K_S^0 \pi^+ D^- \rightarrow K_S^0 \pi^-$	109 ± 11	109 ± 11	109 ± 11	-0.04
$D^+ \rightarrow K_S^0 \pi^+ D^- \rightarrow K_S^0 \pi^-\pi^0$	260 ± 17	260 ± 17	260 ± 17	-0.07
$D^+ \rightarrow K_S^0 \pi^+ D^- \rightarrow K_S^0 \pi^-\pi^-\pi^+$	147 ± 12	147 ± 12	147 ± 12	-0.15
$D^+ \rightarrow K_S^0 \pi^+ D^- \rightarrow K^-K^+\pi^-$	72 ± 9	72 ± 9	72 ± 9	-0.16
$D^+ \rightarrow K_S^0 \pi^+\pi^0 D^- \rightarrow K^+\pi^-\pi^-$	1851 ± 44	1851 ± 44	1851 ± 44	-0.03
$D^+ \rightarrow K_S^0 \pi^+\pi^0 D^- \rightarrow K^+\pi^-\pi^-\pi^0$	631 ± 26	632 ± 26	632 ± 26	-0.14
$D^+ \rightarrow K_S^0 \pi^+\pi^0 D^- \rightarrow K_S^0 \pi^-$	257 ± 16	257 ± 16	257 ± 16	-0.02
$D^+ \rightarrow K_S^0 \pi^+\pi^0 D^- \rightarrow K_S^0 \pi^-\pi^0$	645 ± 27	645 ± 27	646 ± 27	0.03
$D^+ \rightarrow K_S^0 \pi^+\pi^0 D^- \rightarrow K_S^0 \pi^-\pi^-\pi^+$	360 ± 20	361 ± 20	361 ± 20	-0.14
$D^+ \rightarrow K_S^0 \pi^+\pi^0 D^- \rightarrow K^-K^+\pi^-$	144 ± 13	144 ± 13	144 ± 13	-0.11
$D^+ \rightarrow K_S^0 \pi^+\pi^+\pi^- D^- \rightarrow K^+\pi^-\pi^-$	1144 ± 34	1145 ± 34	1145 ± 34	-0.06
$D^+ \rightarrow K_S^0 \pi^+\pi^+\pi^- D^- \rightarrow K^+\pi^-\pi^-\pi^0$	338 ± 20	339 ± 20	340 ± 20	-0.20
$D^+ \rightarrow K_S^0 \pi^+\pi^+\pi^- D^- \rightarrow K_S^0 \pi^-$	160 ± 13	160 ± 13	160 ± 13	-0.02
$D^+ \rightarrow K_S^0 \pi^+\pi^+\pi^- D^- \rightarrow K_S^0 \pi^-\pi^0$	358 ± 20	359 ± 20	359 ± 20	-0.13
$D^+ \rightarrow K_S^0 \pi^+\pi^+\pi^- D^- \rightarrow K_S^0 \pi^-\pi^-\pi^+$	205 ± 16	205 ± 16	205 ± 16	-0.14
$D^+ \rightarrow K_S^0 \pi^+\pi^+\pi^- D^- \rightarrow K^-K^+\pi^-$	91 ± 10	91 ± 10	91 ± 10	-0.13
$D^+ \rightarrow K^+K^-\pi^+ D^- \rightarrow K^+\pi^-\pi^-$	485 ± 22	485 ± 22	485 ± 22	-0.03
$D^+ \rightarrow K^+K^-\pi^+ D^- \rightarrow K^+\pi^-\pi^-\pi^0$	166 ± 13	166 ± 13	166 ± 13	-0.01
$D^+ \rightarrow K^+K^-\pi^+ D^- \rightarrow K_S^0 \pi^-$	62 ± 8	62 ± 8	62 ± 8	-0.32
$D^+ \rightarrow K^+K^-\pi^+ D^- \rightarrow K_S^0 \pi^-\pi^0$	180 ± 14	180 ± 14	180 ± 14	-0.06
$D^+ \rightarrow K^+K^-\pi^+ D^- \rightarrow K_S^0 \pi^-\pi^-\pi^+$	96 ± 11	96 ± 11	96 ± 11	-0.14
$D^+ \rightarrow K^+K^-\pi^+ D^- \rightarrow K^-K^+\pi^-$	42 ± 8	42 ± 8	42 ± 8	-0.17

Table 46: Single tag yields with different R.

Mode	Yield			max-diff (%)
	$R = 8.7 \text{ GeV}^{-1}$	$R = 12.7 \text{ GeV}^{-1}$	$R = 16.7 \text{ GeV}^{-1}$	
$D^0 \rightarrow K^- \pi^+$	75090 ± 282	75177 ± 281	75211 ± 282	-0.12
$\bar{D}^0 \rightarrow K^+ \pi^-$	75497 ± 282	75584 ± 282	75618 ± 283	-0.12
$D^0 \rightarrow K^- \pi^+ \pi^0$	144534 ± 438	144710 ± 439	144790 ± 439	-0.12
$\bar{D}^0 \rightarrow K^+ \pi^- \pi^0$	145620 ± 440	145798 ± 441	145879 ± 441	-0.12
$D^0 \rightarrow K^- \pi^+ \pi^+ \pi^-$	114105 ± 366	114222 ± 366	114276 ± 366	-0.10
$\bar{D}^0 \rightarrow K^+ \pi^- \pi^- \pi^+$	114643 ± 367	114759 ± 368	114812 ± 367	-0.10
$D^+ \rightarrow K^- \pi^+ \pi^+$	116395 ± 353	116545 ± 354	116625 ± 354	-0.13
$D^- \rightarrow K^+ \pi^- \pi^-$	117681 ± 355	117831 ± 356	117912 ± 356	-0.13
$D^+ \rightarrow K^- \pi^+ \pi^+ \pi^0$	36758 ± 260	36813 ± 260	36840 ± 260	-0.15
$D^- \rightarrow K^+ \pi^- \pi^- \pi^0$	37086 ± 261	37143 ± 261	37172 ± 261	-0.15
$D^+ \rightarrow K_S^0 \pi^+$	16821 ± 137	16844 ± 137	16856 ± 138	-0.14
$D^- \rightarrow K_S^0 \pi^-$	17065 ± 138	17087 ± 138	17100 ± 138	-0.13
$D^+ \rightarrow K_S^0 \pi^+ \pi^0$	38271 ± 262	38329 ± 262	38358 ± 262	-0.15
$D^- \rightarrow K_S^0 \pi^- \pi^0$	38568 ± 262	38626 ± 263	38655 ± 263	-0.15
$D^+ \rightarrow K_S^0 \pi^+ \pi^+ \pi^-$	23671 ± 224	23706 ± 224	23723 ± 226	-0.15
$D^- \rightarrow K_S^0 \pi^- \pi^- \pi^+$	23874 ± 224	23909 ± 225	23925 ± 226	-0.15
$D^+ \rightarrow K^+ K^- \pi^+$	10100 ± 124	10115 ± 123	10122 ± 123	-0.15
$D^- \rightarrow K^- K^+ \pi^-$	10050 ± 123	10066 ± 123	10072 ± 123	-0.15

Table 47: Systematic of line shape parameters.

Mode	Difference(%)			Total (%)
	Mass(± 0.5) MeV	$\Gamma(\pm 2.5)$ MeV	$R(\pm 4 \text{ GeV}^{-1})$	
$D^0 \rightarrow K^- \pi^+$	0.14	-0.36	-0.12	0.40
$\bar{D}^0 \rightarrow K^+ \pi^- \pi^0$	0.18	-0.45	-0.12	0.50
$D^0 \rightarrow K^- \pi^+ \pi^+ \pi^-$	0.20	-0.46	-0.10	0.51
$D^+ \rightarrow K^- \pi^+ \pi^+$	-0.12	-0.29	-0.13	0.34
$D^- \rightarrow K^+ \pi^- \pi^- \pi^0$	0.21	-0.41	-0.15	0.48
$D^+ \rightarrow K_S^0 \pi^+$	0.15	-0.33	-0.14	0.39
$D^+ \rightarrow K_S^0 \pi^+ \pi^0$	0.20	-0.41	-0.15	0.48
$D^+ \rightarrow K_S^0 \pi^+ \pi^+ \pi^-$	0.26	-0.46	-0.15	0.55
$D^+ \rightarrow K^+ K^- \pi^+$	-0.24	-0.46	-0.15	0.54

Table 48: Comparison of the fit result between signal MC events with and without rescaled π^0 momentum.

Name	$\pi^0 - 0.997$	regular	diff(%)
N1	69769 ± 284	69799 ± 284	-0.04 ± 0.58
N2	70859 ± 286	70891 ± 286	-0.04 ± 0.57
Nbkgd1	9004 ± 142	8975 ± 141	0.33 ± 2.23
Nbkgd2	8903 ± 141	8877 ± 140	0.30 ± 2.23
md	1.86470 ± 0.00001	1.86466 ± 0.00001	0.00186 ± 0.00043
p	0.89 ± 0.03	0.87 ± 0.03	2.05 ± 5.45
sigmap1	0.00703 ± 0.00004	0.00694 ± 0.00004	1.39 ± 0.83
xi	-44.75 ± 1.72	-43.57 ± 1.71	2.72 ± 5.57
chisq1	139	126	10.39
chisq2	94	76	23.31

$D^0 \rightarrow K^-\pi^+\pi^0$ events in which imprecise reconstruction produces a missing energy just below the π^0 mass. While this cut does eliminate the dominant background, it also restricts the photon energy range that we may study.

The analysis is as follows. We reconstruct tag \bar{D}^0 candidates in the modes $\bar{D}^0 \rightarrow K^+\pi^-$, $\bar{D}^0 \rightarrow K^+\pi^-\pi^0$, and $\bar{D}^0 \rightarrow K^+\pi^-\pi^-\pi^+$, with cuts on M_{BC} and ΔE . We then find an additional K^- and π^+ and calculate the missing energy, momentum, and mass squared. We also look at the remaining photons and find the one which puts the $K^-\pi^+\gamma$ mass closest to the nominal D^0 mass – and if the $K^-\pi^+$ mass is closer than any $K^-\pi^+\gamma$ mass, the “best photon” is taken to be “no photon.”

For $D^0 \rightarrow K^-\pi^+\gamma$ candidates, we require that the $K^-\pi^+\gamma$ mass is consistent with the D^0 mass, that the missing mass squared is consistent with zero but not with the π^0 mass squared, and that the missing energy is less than 120 MeV. Photon candidates must have energy greater than 60 MeV; this eliminates events without FSR since 60 MeV is approximately three times the ΔE resolution of $D^0 \rightarrow K^-\pi^+$ events.

The $D^0 \rightarrow K^-\pi^+\gamma$ candidates are normalized relative to the number of reconstructed $D^0 \rightarrow K^-\pi^+$ events. In data and MC, we form the ratio of $D^0 \rightarrow K^-\pi^+\gamma$ (with $60 < E_\gamma < 120\text{MeV}$) to $D^0 \rightarrow K^-\pi^+$ (with less than 30 MeV of FSR).

In data, we find 43 $D^0 \rightarrow K^-\pi^+\gamma$ and 5648 $D^0 \rightarrow K^-\pi^+$ events, which gives a ratio of $0.76 \pm 0.12\%$. In a 10x generic Monte Carlo sample, we find 469 $D^0 \rightarrow K^-\pi^+\gamma$ and 55595 $D^0 \rightarrow K^-\pi^+$ events, which gives a ratio of $0.84 \pm 0.04\%$. The ratio of data over Monte Carlo is 0.90 ± 0.15 . There is no sign of a discrepancy.

It should be noted that the yields quoted above are not free of background. In fact, in Monte Carlo, 189 out of the 469 signal candidates were truth-tagged as something other than $D^0 \rightarrow K^-\pi^+\gamma$. Thus, approximately 40% of events in the signal region are not true $D^0 \rightarrow K^-\pi^+\gamma$ events, and the uncertainty on the ratio between data and Monte Carlo (0.90 ± 0.15) is larger than the quoted value of 0.15.

Figure ?? shows the energy spectrum of the photon in $D^0 \rightarrow K^-\pi^+\gamma$ candidates. Here, the cuts on photon energy and missing energy have been removed to show the entire spectrum (most of which is background). The signal region is relatively small in this plot – from 0.060 to about 0.120 GeV. Data and (scaled) Monte Carlo are compared. We also plot Monte Carlo events which are truth-tagged with the signal D decaying to $K\pi\gamma$. In this plot we see that data and Monte Carlo are consistent, but also that many background events contaminate the signal.

This analysis shows consistency between data and Monte Carlo, but it does not provide a precise cross-check of the simulation of final state radiation. The signal is contaminated by substantial background, even for photon energies below the π^0 mass. Even if the signal was clean at these low energies, this study would not allow us to cross-check the simulation of high-energy FSR.

9 Results

To extract estimates of $N_{D^0\bar{D}^0}$, $N_{D^+D^-}$, and the branching fractions for the nine modes listed in Table ??, we employ the χ^2 fitter implemented in the package `HadronicDBrFitter`. The procedure is described at length in Ref. [?]. This fitter forms a χ^2 statistic from the 18 single tag and 45 double tag yields and minimizes it while accounting for both the statistical and systematic uncertainties on these measurements. Using toy MC simulations, the fitter has been shown to be unbiased and to deliver correct error matrices.

9.1 Generic Monte Carlo

Table ?? gives the results of the fit to the $10\times$ generic MC sample, along with the values input to the MC. For this fit, the efficiencies are not corrected by the factor given in Equation ???. The χ^2 of the fit is 57.5 for 52 degrees of freedom, corresponding to a confidence level of 27.9%. The overall χ^2 of the difference between the fit results and the MC inputs, accounting for the correlations among the fit parameters, is 13.6 for 11 degrees of freedom, corresponding to a confidence level of 25.7%. Table ?? contains the correlation matrix for the 11 fit parameters. Because we have not included any correlated systematics in the generic MC fit, the charged and neutral fit parameters are independent, and the precision of all the fit parameters is dominated by the double tag yields, which accounts for the similarity in fractional uncertainty among the parameters for each charge. Also, for each parameter, we give the global correlation coefficient, defined by $\rho_i^{\text{global}} \equiv \sqrt{1 - \frac{1}{V_{ii}(V^{-1})_{ii}}}$, where V is the fit parameter variance matrix. The global correlation coefficient is a measure of the strongest correlation between parameter i and a linear combination of all other variables. The residuals for the single and double tag yields are listed in Tables ?? and ??, and it can be seen that no one measurement pulls the fit with undue weight.

Table 49: Results of the fit to generic MC. No systematic effects are included. Fractional uncertainties are given in parentheses. The agreement between the fitted and input values has an overall confidence level of 25.7%.

Parameters	Fitted Value	Generated Value	Difference
$N_{D^0\bar{D}^0}$	$(9.754 \pm 0.056) \times 10^6(0.6\%)$	9.797×10^6	-0.8σ
$\mathcal{B}(D^0 \rightarrow K^-\pi^+)$	$0.03845 \pm 0.00021(0.6\%)$	0.0383	$+0.7\sigma$
$\mathcal{B}(D^0 \rightarrow K^-\pi^+\pi^0)$	$0.13984 \pm 0.00078(0.6\%)$	0.139	$+1.1\sigma$
$\mathcal{B}(D^0 \rightarrow K^-\pi^+\pi^+\pi^-)$	$0.07908 \pm 0.00045(0.6\%)$	0.07867	$+0.9\sigma$
$N_{D^+D^-}$	$(7.410 \pm 0.043) \times 10^6(0.6\%)$	7.346×10^6	$+1.5\sigma$
$\mathcal{B}(D^+ \rightarrow K^-\pi^+\pi^+)$	$0.08931 \pm 0.00049(0.6\%)$	0.09	-1.4σ
$\mathcal{B}(D^+ \rightarrow K^-\pi^+\pi^+\pi^0)$	$0.06811 \pm 0.00044(0.6\%)$	0.06812	0.0σ
$\mathcal{B}(D^+ \rightarrow K_S^0\pi^+)$	$0.01430 \pm 0.00010(0.7\%)$	0.01445	-1.5σ
$\mathcal{B}(D^+ \rightarrow K_S^0\pi^+\pi^0)$	$0.05451 \pm 0.00039(0.7\%)$	0.05425	$+0.7\sigma$
$\mathcal{B}(D^+ \rightarrow K_S^0\pi^+\pi^+\pi^-)$	$0.03586 \pm 0.00025(0.7\%)$	0.03582	$+0.2\sigma$
$\mathcal{B}(D^+ \rightarrow K^+K^-\pi^+)$	$0.01486 \pm 0.00011(0.7\%)$	0.01493	-0.7σ

Table 50: Correlation matrix for the fitted parameters in generic MC. The parameter order matches that in Table ???. The last row contains the global correlation coefficients.

1.00	-0.86	-0.91	-0.89	-0.00	-0.00	-0.00	-0.00	-0.00	-0.00	-0.00
1.00	0.77	0.76	-0.00	-0.00	-0.00	-0.00	-0.00	-0.00	-0.00	-0.00
	1.00	0.81	-0.00	-0.00	-0.00	-0.00	-0.00	-0.00	-0.00	-0.00
		1.00	-0.00	-0.00	-0.00	-0.00	-0.00	-0.00	-0.00	-0.00
			1.00	-0.90	-0.72	-0.78	-0.61	-0.64	-0.62	
				1.00	0.64	0.71	0.55	0.57	0.55	
					1.00	0.56	0.43	0.44	0.43	
						1.00	0.48	0.50	0.49	
							1.00	0.38	0.37	
								1.00	0.39	
									1.00	
0.96	0.86	0.91	0.89	0.95	0.90	0.72	0.78	0.62	0.64	0.62

Table 51: Residuals on efficiency-corrected and background-subtracted single tag yields including systematics from the fit to generic MC.

Mode	Residual	χ^2
$D^0 \rightarrow K^- \pi^+$	-838 ± 1715	0.2
$\bar{D}^0 \rightarrow K^+ \pi^-$	-72 ± 1679	0.0
$D^0 \rightarrow K^- \pi^+ \pi^0$	3395 ± 4946	0.5
$\bar{D}^0 \rightarrow K^+ \pi^- \pi^0$	-2569 ± 4886	0.3
$D^0 \rightarrow K^- \pi^+ \pi^+ \pi^-$	-1786 ± 2963	0.4
$\bar{D}^0 \rightarrow K^+ \pi^- \pi^- \pi^+$	2683 ± 2966	0.8
$D^+ \rightarrow K^- \pi^+ \pi^+$	-424 ± 2413	0.0
$D^- \rightarrow K^+ \pi^- \pi^-$	-267 ± 2394	0.0
$D^+ \rightarrow K^- \pi^+ \pi^+ \pi^0$	-419 ± 3577	0.0
$D^- \rightarrow K^+ \pi^- \pi^- \pi^0$	2617 ± 3571	0.5
$D^+ \rightarrow K_S^0 \pi^+$	-28 ± 645	0.0
$D^- \rightarrow K_S^0 \pi^-$	75 ± 651	0.0
$D^+ \rightarrow K_S^0 \pi^+ \pi^0$	-458 ± 3717	0.0
$D^- \rightarrow K_S^0 \pi^- \pi^0$	-2293 ± 3693	0.4
$D^+ \rightarrow K_S^0 \pi^+ \pi^+ \pi^-$	-38 ± 2295	0.0
$D^- \rightarrow K_S^0 \pi^- \pi^- \pi^+$	1735 ± 2310	0.6
$D^+ \rightarrow K^+ K^- \pi^+$	-257 ± 991	0.1
$D^- \rightarrow K^- K^+ \pi^-$	309 ± 990	0.1

Table 52: Residuals on efficiency-corrected and background-subtracted double tag yields including systematics from the fit to generic MC.

Mode	Residual	χ^2
$D^0 \rightarrow K^- \pi^+ \bar{D}^0 \rightarrow K^+ \pi^-$	41 ± 213	0.0
$D^0 \rightarrow K^- \pi^+ \bar{D}^0 \rightarrow K^+ \pi^- \pi^0$	975 ± 803	1.5
$D^0 \rightarrow K^- \pi^+ \bar{D}^0 \rightarrow K^+ \pi^- \pi^- \pi^+$	363 ± 439	0.7
$D^0 \rightarrow K^- \pi^+ \pi^0 \bar{D}^0 \rightarrow K^+ \pi^-$	-484 ± 788	0.4
$D^0 \rightarrow K^- \pi^+ \pi^0 \bar{D}^0 \rightarrow K^+ \pi^- \pi^0$	-1469 ± 2740	0.3
$D^0 \rightarrow K^- \pi^+ \pi^0 \bar{D}^0 \rightarrow K^+ \pi^- \pi^- \pi^+$	1020 ± 1852	0.3
$D^0 \rightarrow K^- \pi^+ \pi^+ \pi^- \bar{D}^0 \rightarrow K^+ \pi^-$	106 ± 436	0.1
$D^0 \rightarrow K^- \pi^+ \pi^+ \pi^- \bar{D}^0 \rightarrow K^+ \pi^- \pi^0$	-1430 ± 1836	0.6
$D^0 \rightarrow K^- \pi^+ \pi^+ \pi^- \bar{D}^0 \rightarrow K^+ \pi^- \pi^- \pi^+$	-1133 ± 952	1.4
$D^+ \rightarrow K^- \pi^+ \pi^+ D^- \rightarrow K^+ \pi^- \pi^-$	28 ± 773	0.0
$D^+ \rightarrow K^- \pi^+ \pi^+ D^- \rightarrow K^+ \pi^- \pi^- \pi^0$	-1260 ± 899	2.0
$D^+ \rightarrow K^- \pi^+ \pi^+ D^- \rightarrow K_S^0 \pi^-$	-32 ± 229	0.0
$D^+ \rightarrow K^- \pi^+ \pi^+ D^- \rightarrow K_S^0 \pi^- \pi^0$	889 ± 852	1.1
$D^+ \rightarrow K^- \pi^+ \pi^+ D^- \rightarrow K_S^0 \pi^- \pi^- \pi^+$	-62 ± 522	0.0
$D^+ \rightarrow K^- \pi^+ \pi^+ D^- \rightarrow K^- K^+ \pi^-$	-16 ± 229	0.0
$D^+ \rightarrow K^- \pi^+ \pi^+ \pi^0 D^- \rightarrow K^+ \pi^- \pi^-$	-540 ± 906	0.4
$D^+ \rightarrow K^- \pi^+ \pi^+ \pi^0 D^- \rightarrow K^+ \pi^- \pi^- \pi^0$	1109 ± 1119	1.0
$D^+ \rightarrow K^- \pi^+ \pi^+ \pi^0 D^- \rightarrow K_S^0 \pi^-$	122 ± 280	0.2
$D^+ \rightarrow K^- \pi^+ \pi^+ \pi^0 D^- \rightarrow K_S^0 \pi^- \pi^- \pi^0$	401 ± 994	0.2
$D^+ \rightarrow K^- \pi^+ \pi^+ \pi^0 D^- \rightarrow K_S^0 \pi^- \pi^- \pi^- \pi^+$	-1387 ± 602	5.3
$D^+ \rightarrow K^- \pi^+ \pi^+ \pi^0 D^- \rightarrow K^- K^+ \pi^-$	81 ± 276	0.1
$D^+ \rightarrow K_S^0 \pi^+ D^- \rightarrow K^+ \pi^- \pi^-$	295 ± 229	1.7
$D^+ \rightarrow K_S^0 \pi^+ D^- \rightarrow K^+ \pi^- \pi^- \pi^0$	146 ± 277	0.3
$D^+ \rightarrow K_S^0 \pi^+ D^- \rightarrow K_S^0 \pi^-$	-185 ± 85	4.7
$D^+ \rightarrow K_S^0 \pi^+ D^- \rightarrow K_S^0 \pi^- \pi^0$	210 ± 267	0.6
$D^+ \rightarrow K_S^0 \pi^+ D^- \rightarrow K_S^0 \pi^- \pi^- \pi^+$	-307 ± 172	3.2
$D^+ \rightarrow K_S^0 \pi^+ D^- \rightarrow K^- K^+ \pi^-$	-21 ± 91	0.1
$D^+ \rightarrow K_S^0 \pi^+ \pi^0 D^- \rightarrow K^+ \pi^- \pi^-$	1680 ± 854	3.9
$D^+ \rightarrow K_S^0 \pi^+ \pi^0 D^- \rightarrow K^+ \pi^- \pi^- \pi^0$	1550 ± 1015	2.3
$D^+ \rightarrow K_S^0 \pi^+ \pi^0 D^- \rightarrow K_S^0 \pi^-$	-452 ± 256	3.1
$D^+ \rightarrow K_S^0 \pi^+ \pi^0 D^- \rightarrow K_S^0 \pi^- \pi^0$	-692 ± 896	0.6
$D^+ \rightarrow K_S^0 \pi^+ \pi^0 D^- \rightarrow K_S^0 \pi^- \pi^- \pi^+$	-46 ± 583	0.0
$D^+ \rightarrow K_S^0 \pi^+ \pi^0 D^- \rightarrow K^- K^+ \pi^-$	-198 ± 268	0.5
$D^+ \rightarrow K_S^0 \pi^+ \pi^+ \pi^- D^- \rightarrow K^+ \pi^- \pi^-$	489 ± 521	0.9
$D^+ \rightarrow K_S^0 \pi^+ \pi^+ \pi^- D^- \rightarrow K^+ \pi^- \pi^- \pi^0$	-1208 ± 614	3.9
$D^+ \rightarrow K_S^0 \pi^+ \pi^+ \pi^- D^- \rightarrow K_S^0 \pi^-$	447 ± 189	5.6
$D^+ \rightarrow K_S^0 \pi^+ \pi^+ \pi^- D^- \rightarrow K_S^0 \pi^- \pi^0$	-767 ± 586	1.7
$D^+ \rightarrow K_S^0 \pi^+ \pi^+ \pi^- D^- \rightarrow K_S^0 \pi^- \pi^- \pi^- \pi^+$	210 ± 376	0.3
$D^+ \rightarrow K_S^0 \pi^+ \pi^+ \pi^- D^- \rightarrow K^- K^+ \pi^-$	-41 ± 178	0.1
$D^+ \rightarrow K^+ K^- \pi^+ D^- \rightarrow K^+ \pi^- \pi^-$	-76 ± 223	0.1
$D^+ \rightarrow K^+ K^- \pi^+ D^- \rightarrow K^+ \pi^- \pi^- \pi^0$	-127 ± 272	0.2
$D^+ \rightarrow K^+ K^- \pi^+ D^- \rightarrow K_S^0 \pi^-$	149 ± 92	2.6
$D^+ \rightarrow K^+ K^- \pi^+ D^- \rightarrow K_S^0 \pi^- \pi^0$	290 ± 276	1.1
$D^+ \rightarrow K^+ K^- \pi^+ D^- \rightarrow K_S^0 \pi^- \pi^- \pi^+$	-2 ± 183	0.0
$D^+ \rightarrow K^+ K^- \pi^+ D^- \rightarrow K^- K^+ \pi^-$	-18 ± 88	0.0

9.2 Data

The results of the data fit are shown in Tables ??, ??, ??, and ???. The χ^2 of the fit is 49.1 for 52 degrees of freedom, corresponding to a confidence level of 58.8%.

In Table ??, we compute various ratios of branching fractions, which have higher precision than the constituent branching fractions. The correlation matrix for the data fit is very different from the one for generic MC because of the presence of correlated systematics. Without systematics, there would be no correlation between the charged and neutral D parameters. That these correlations are large indicates that the precision of our branching fraction measurements is limited by the systematic uncertainties.

The $e^+e^- \rightarrow D\bar{D}$ cross sections are obtained by dividing $N_{D^0\bar{D}^0}$ and $N_{D^+\bar{D}^-}$ by the luminosity for $\psi(3770)$ runs in data31–33, data35–37 and data43–46, which has been determined to be $(818.1 \pm 8.2) \text{ pb}^{-1}$. We find

$$\sigma(e^+e^- \rightarrow D^0\bar{D}^0) = (3.651 \pm 0.017 \pm 0.083) \text{ nb} \quad (13)$$

$$\sigma(e^+e^- \rightarrow D^+\bar{D}^-) = (2.920 \pm 0.018 \pm 0.062) \text{ nb} \quad (14)$$

$$\sigma(e^+e^- \rightarrow D\bar{D}) = (6.571 \pm 0.024 \pm 0.142) \text{ nb} \quad (15)$$

$$\sigma(e^+e^- \rightarrow D^+\bar{D}^-)/\sigma(e^+e^- \rightarrow D^0\bar{D}^0) = 0.800 \pm 0.006 \pm 0.008 \quad (16)$$

where the uncertainties are statistical and systematic, respectively. The charged and neutral cross sections have a correlation coefficient of 0.69 stemming from the systematics and from the luminosity measurement. For this reason, the uncertainty on $\sigma(e^+e^- \rightarrow D\bar{D})$ is larger than quadrature sums of the charged and neutral cross section uncertainties.

Table 53: Results of the fit to 818 pb^{-1} data. The uncertainties quoted are statistical and systematic, respectively. Fractional uncertainties are given in parentheses.

Parameters	Fitted Value	PDG 2004	Difference
$N_{D^0\bar{D}^0}$	$(2.987 \pm 0.014 \pm 0.061) \times 10^6 (2.1\%)$	–	–
$\mathcal{B}(D^0 \rightarrow K^-\pi^+)$	$0.03906 \pm 0.00021 \pm 0.00062 (1.7\%)$	0.0380 ± 0.0009	$+1.2\sigma$
$\mathcal{B}(D^0 \rightarrow K^-\pi^+\pi^0)$	$0.14858 \pm 0.00074 \pm 0.00334 (2.3\%)$	0.130 ± 0.008	$+2.3\sigma$
$\mathcal{B}(D^0 \rightarrow K^-\pi^+\pi^+\pi^-)$	$0.08241 \pm 0.00043 \pm 0.00164 (2.1\%)$	0.0746 ± 0.0031	$+2.5\sigma$
$N_{D^+\bar{D}^-}$	$(2.389 \pm 0.014 \pm 0.045) \times 10^6 (2.0\%)$	–	–
$\mathcal{B}(D^+ \rightarrow K^-\pi^+\pi^+)$	$0.09156 \pm 0.00059 \pm 0.00124 (1.5\%)$	0.092 ± 0.006	-0.1σ
$\mathcal{B}(D^+ \rightarrow K^-\pi^+\pi^+\pi^0)$	$0.06101 \pm 0.00045 \pm 0.00142 (2.4\%)$	0.065 ± 0.011	-0.4σ
$\mathcal{B}(D^+ \rightarrow K_S^0\pi^+)$	$0.01562 \pm 0.00013 \pm 0.00028 (2.0\%)$	0.014 ± 0.001	$+1.6\sigma$
$\mathcal{B}(D^+ \rightarrow K_S^0\pi^+\pi^0)$	$0.07184 \pm 0.00053 \pm 0.00168 (2.5\%)$	0.049 ± 0.015	$+1.5\sigma$
$\mathcal{B}(D^+ \rightarrow K_S^0\pi^+\pi^+\pi^-)$	$0.03028 \pm 0.00027 \pm 0.00071 (2.5\%)$	0.036 ± 0.005	-1.1σ
$\mathcal{B}(D^+ \rightarrow K^+K^-\pi^+)$	$0.01019 \pm 0.00011 \pm 0.00016 (1.9\%)$	0.0089 ± 0.0008	$+1.6\sigma$

Table 54: Branching fraction ratios from the fit to 818 pb^{-1} . The uncertainties quoted are statistical and systematic, respectively.

Parameters	Fitted Value	PDG 2004	Difference
$\mathcal{B}(D^0 \rightarrow K^-\pi^+\pi^0)/\mathcal{B}(K^-\pi^+)$	$3.804 \pm 0.022 \pm 0.074$	3.42 ± 0.22	$+1.7\sigma$
$\mathcal{B}(D^0 \rightarrow K^-\pi^+\pi^+\pi^-)/\mathcal{B}(K^-\pi^+)$	$2.110 \pm 0.013 \pm 0.031$	1.96 ± 0.08	$+1.9\sigma$
$\mathcal{B}(D^+ \rightarrow K^-\pi^+\pi^+\pi^0)/\mathcal{B}(K^-\pi^+\pi^+)$	$0.666 \pm 0.006 \pm 0.014$	0.70 ± 0.12	-0.3σ
$\mathcal{B}(D^+ \rightarrow K_S^0 \pi^+)/\mathcal{B}(K^-\pi^+\pi^+)$	$0.171 \pm 0.002 \pm 0.002$	0.153 ± 0.003	$+6.0\sigma$
$\mathcal{B}(D^+ \rightarrow K_S^0 \pi^+\pi^0)/\mathcal{B}(K^-\pi^+\pi^+)$	$0.785 \pm 0.007 \pm 0.016$	0.527 ± 0.167	$+1.5\sigma$
$\mathcal{B}(D^+ \rightarrow K_S^0 \pi^+\pi^+\pi^-)/\mathcal{B}(K^-\pi^+\pi^+)$	$0.331 \pm 0.004 \pm 0.006$	0.385 ± 0.050	-1.1σ
$\mathcal{B}(D^+ \rightarrow K^+K^-\pi^+)/\mathcal{B}(K^-\pi^+\pi^+)$	$0.111 \pm 0.002 \pm 0.001$	0.097 ± 0.006	$+2.3\sigma$

Table 55: Correlation matrix for the fitted parameters including systematic uncertainties in data. The parameter order matches that in Table ???. The last row contains the global correlation coefficients.

1.00	-0.80	-0.49	-0.48	0.81	-0.48	-0.32	-0.60	-0.41	-0.34	-0.26
1.00	0.52	0.65	-0.59	0.60	0.33	0.56	0.36	0.40	0.35	
1.00	0.35	-0.40	0.36	0.67	0.35	0.68	0.24	0.22		
1.00	-0.35	0.48	0.27	0.38	0.25	0.34	0.27			
	1.00	-0.71	-0.38	-0.78	-0.50	-0.46	-0.45			
		1.00	0.38	0.68	0.42	0.52	0.54			
			1.00	0.33	0.64	0.25	0.24			
				1.00	0.55	0.58	0.42			
					1.00	0.39	0.25			
						1.00	0.30			
							1.00			
0.95	0.91	0.81	0.68	0.95	0.87	0.73	0.85	0.81	0.62	0.58

Table 56: Residuals on efficiency-corrected and background-subtracted single tag yields including systematics from the fit to data.

Mode	Residual
$D^0 \rightarrow K^- \pi^+$	-136 ± 1696
$\bar{D}^0 \rightarrow K^+ \pi^-$	-788 ± 1694
$D^0 \rightarrow K^- \pi^+ \pi^0$	-1287 ± 11006
$\bar{D}^0 \rightarrow K^+ \pi^- \pi^0$	-2234 ± 11000
$D^0 \rightarrow K^- \pi^+ \pi^+ \pi^-$	-1734 ± 6209
$\bar{D}^0 \rightarrow K^+ \pi^- \pi^- \pi^+$	-2501 ± 6205
$D^+ \rightarrow K^- \pi^+ \pi^+$	-2192 ± 3610
$D^- \rightarrow K^+ \pi^- \pi^-$	-807 ± 3611
$D^+ \rightarrow K^- \pi^+ \pi^+ \pi^0$	-3520 ± 5654
$D^- \rightarrow K^+ \pi^- \pi^- \pi^0$	-2651 ± 5675
$D^+ \rightarrow K_S^0 \pi^+$	-400 ± 586
$D^- \rightarrow K_S^0 \pi^-$	385 ± 591
$D^+ \rightarrow K_S^0 \pi^+ \pi^0$	-844 ± 4548
$D^- \rightarrow K_S^0 \pi^- \pi^0$	-535 ± 4548
$D^+ \rightarrow K_S^0 \pi^+ \pi^+ \pi^-$	301 ± 2076
$D^- \rightarrow K_S^0 \pi^- \pi^- \pi^+$	224 ± 2071
$D^+ \rightarrow K^+ K^- \pi^+$	-63 ± 619
$D^- \rightarrow K^- K^+ \pi^-$	-36 ± 619

Table 57: Residuals on efficiency-corrected and background-subtracted double tag yields including systematics from the fit to data.

Mode	Residual
$D^0 \rightarrow K^-\pi^+ \bar{D}^0 \rightarrow K^+\pi^-$	-36 ± 619
$D^0 \rightarrow K^-\pi^+ \bar{D}^0 \rightarrow K^+\pi^-\pi^0$	-158 ± 134
$D^0 \rightarrow K^-\pi^+ \bar{D}^0 \rightarrow K^+\pi^-\pi^-\pi^+$	-47 ± 515
$D^0 \rightarrow K^-\pi^+\pi^0 \bar{D}^0 \rightarrow K^+\pi^-$	179 ± 298
$D^0 \rightarrow K^-\pi^+\pi^0 \bar{D}^0 \rightarrow K^+\pi^-\pi^0$	532 ± 519
$D^0 \rightarrow K^-\pi^+\pi^0 \bar{D}^0 \rightarrow K^+\pi^-\pi^-\pi^+$	-708 ± 2786
$D^0 \rightarrow K^-\pi^+\pi^+\pi^- \bar{D}^0 \rightarrow K^+\pi^-$	-71 ± 1202
$D^0 \rightarrow K^-\pi^+\pi^+\pi^- \bar{D}^0 \rightarrow K^+\pi^-\pi^0$	-131 ± 296
$D^0 \rightarrow K^-\pi^+\pi^+\pi^- \bar{D}^0 \rightarrow K^+\pi^-\pi^-\pi^+$	-125 ± 1202
$D^+ \rightarrow K^-\pi^+\pi^+ D^- \rightarrow K^+\pi^-\pi^-$	136 ± 787
$D^+ \rightarrow K^-\pi^+\pi^+ D^- \rightarrow K^+\pi^-\pi^-\pi^0$	485 ± 482
$D^+ \rightarrow K^-\pi^+\pi^+ D^- \rightarrow K_S^0 \pi^-$	158 ± 473
$D^+ \rightarrow K^-\pi^+\pi^+ D^- \rightarrow K_S^0 \pi^-\pi^0$	100 ± 135
$D^+ \rightarrow K^-\pi^+\pi^+ D^- \rightarrow K_S^0 \pi^-\pi^-\pi^+$	933 ± 547
$D^+ \rightarrow K^-\pi^+\pi^+ D^- \rightarrow K^-K^+\pi^-$	-275 ± 273
$D^+ \rightarrow K^-\pi^+\pi^+\pi^0 D^- \rightarrow K^+\pi^-\pi^-$	-83 ± 109
$D^+ \rightarrow K^-\pi^+\pi^+\pi^0 D^- \rightarrow K^+\pi^-\pi^-\pi^0$	-456 ± 467
$D^+ \rightarrow K^-\pi^+\pi^+\pi^0 D^- \rightarrow K_S^0 \pi^-$	325 ± 567
$D^+ \rightarrow K^-\pi^+\pi^+\pi^0 D^- \rightarrow K_S^0 \pi^-\pi^0$	182 ± 158
$D^+ \rightarrow K^-\pi^+\pi^+\pi^0 D^- \rightarrow K_S^0 \pi^-\pi^-\pi^+$	-340 ± 611
$D^+ \rightarrow K^-\pi^+\pi^+\pi^0 D^- \rightarrow K^-K^+\pi^-$	247 ± 309
$D^+ \rightarrow K_S^0 \pi^+ D^- \rightarrow K^+\pi^-\pi^-$	-9 ± 131
$D^+ \rightarrow K_S^0 \pi^+ D^- \rightarrow K^+\pi^-\pi^-\pi^0$	-58 ± 132
$D^+ \rightarrow K_S^0 \pi^+ D^- \rightarrow K_S^0 \pi^-$	158 ± 157
$D^+ \rightarrow K_S^0 \pi^+ D^- \rightarrow K_S^0 \pi^-\pi^0$	-58 ± 53
$D^+ \rightarrow K_S^0 \pi^+ D^- \rightarrow K_S^0 \pi^-\pi^-\pi^+$	-128 ± 180
$D^+ \rightarrow K_S^0 \pi^+ D^- \rightarrow K^-K^+\pi^-$	-113 ± 94
$D^+ \rightarrow K_S^0 \pi^+\pi^0 D^- \rightarrow K^+\pi^-\pi^-$	1 ± 47
$D^+ \rightarrow K_S^0 \pi^+\pi^0 D^- \rightarrow K^+\pi^-\pi^-\pi^0$	-773 ± 531
$D^+ \rightarrow K_S^0 \pi^+\pi^0 D^- \rightarrow K_S^0 \pi^-$	501 ± 625
$D^+ \rightarrow K_S^0 \pi^+\pi^0 D^- \rightarrow K_S^0 \pi^-\pi^0$	-197 ± 177
$D^+ \rightarrow K_S^0 \pi^+\pi^0 D^- \rightarrow K_S^0 \pi^-\pi^-\pi^+$	384 ± 745
$D^+ \rightarrow K_S^0 \pi^+\pi^0 D^- \rightarrow K^-K^+\pi^-$	110 ± 359
$D^+ \rightarrow K_S^0 \pi^+\pi^+\pi^- D^- \rightarrow K^+\pi^-\pi^-$	-227 ± 142
$D^+ \rightarrow K_S^0 \pi^+\pi^+\pi^- D^- \rightarrow K^+\pi^-\pi^-\pi^0$	47 ± 275
$D^+ \rightarrow K_S^0 \pi^+\pi^+\pi^- D^- \rightarrow K_S^0 \pi^-\pi^-$	-308 ± 295
$D^+ \rightarrow K_S^0 \pi^+\pi^+\pi^- D^- \rightarrow K_S^0 \pi^-\pi^0$	-22 ± 98
$D^+ \rightarrow K_S^0 \pi^+\pi^+\pi^- D^- \rightarrow K_S^0 \pi^-\pi^-\pi^+$	49 ± 356
$D^+ \rightarrow K_S^0 \pi^+\pi^+\pi^- D^- \rightarrow K^-K^+\pi^-$	-120 ± 196
$D^+ \rightarrow K^+K^-\pi^+ D^- \rightarrow K^+\pi^-\pi^-$	-38 ± 85
$D^+ \rightarrow K^+K^-\pi^+ D^- \rightarrow K^+\pi^-\pi^-\pi^0$	-89 ± 108
$D^+ \rightarrow K^+K^-\pi^+ D^- \rightarrow K_S^0 \pi^-$	16 ± 127
$D^+ \rightarrow K^+K^-\pi^+ D^- \rightarrow K_S^0 \pi^-\pi^0$	-51 ± 44
$D^+ \rightarrow K^+K^-\pi^+ D^- \rightarrow K_S^0 \pi^-\pi^-\pi^+$	186 ± 161
$D^+ \rightarrow K^+K^-\pi^+ D^- \rightarrow K^-K^+\pi^-$	-9 ± 87

9.2.1 CP Asymmetries

Although this analysis assumes equal rates for decays to charge-conjugate final states f and \bar{f} , the separately determined yields and efficiencies for charge-conjugate decays allow us to calculate CP asymmetries,

$$A_{CP}(f) \equiv \frac{N(f) - N(\bar{f})}{N(f) + N(\bar{f})},$$

for each mode f . $A_{CP}(f)$ is calculated from the background-subtracted, efficiency-corrected single tag yields for f and \bar{f} , using the information in Table ?? and the estimated backgrounds.

The calculation of the statistical uncertainty accounts for the (small) correlation between the extracted f and \bar{f} yields; they are correlated because they are determined in a simultaneous fit in which they share signal and background shape parameters. The correlation coefficients between f and \bar{f} yields are less than 0.2 (and positive) in all modes, and including them produces only small changes in the uncertainties.

Most systematic uncertainties cancel between f and \bar{f} , with the exception of charged pion and kaon tracking and particle ID. For these systematics, the relevant factor is the discrepancy between data and Monte Carlo of the *charge dependence* of the efficiencies. Separate K^+ , K^- , π^+ , and π^- tracking and PID efficiencies have been determined in CBX 2008-040 and CBX 05-43. We use these efficiencies to calculate, for each efficiency type, the charge asymmetry, $(\epsilon(+) - \epsilon(-))/(\epsilon(+) + \epsilon(-))$, in data and Monte Carlo. The difference between data and Monte Carlo is calculated, and the quadrature sum of the central value and uncertainty is taken as the systematic. The charge asymmetries, data-MC differences, and systematics are listed in Table ??.

The one exception to the above procedure is the kaon particle ID systematic for $D^0 \rightarrow K^-\pi^+$. This is the one mode in which the kaon always exceeds the RICH threshold of 700 MeV. As discussed in CBX 06-29B, the RICH is the primary source of the particle ID efficiency difference for K^+ and K^- , since kaons interact in the RICH radiator more often than elsewhere. The efficiencies measured in CBX 05-43 are an average over a momentum spectrum that lies mostly below 700 MeV. The difference between K^+ and K^- PID efficiencies above 700 MeV is of order 1%, corresponding to an asymmetry of 0.5%. We take this value of 0.5% as the kaon PID systematic for $D^0 \rightarrow K^-\pi^+$ only; it is approximately double the value used for the other modes. This has only a small effect, since the kaon tracking systematic still dominates the PID systematic.

To calculate the systematics for each decay mode, we use the following procedure:

- Pion and kaon systematics are assumed to be uncorrelated.
- When a decay mode has a positively and negatively charged particle of the same type (*e.g.* kaons in $D^+ \rightarrow K^-K^+\pi^+$), these particles are not assumed to cancel each other. The reason is that their momentum spectra may be different. For example, the K^- in $D^+ \rightarrow K^-K^+\pi^+$ and the K^+ in $D^- \rightarrow K^+K^-\pi^-$ may tend to exceed the RICH

Table 58: Efficiency asymmetries and systematics for CP asymmetries.

Efficiency	Data Asymmetry (%)	MC Asymmetry (%)	Data-MC Difference (%)	Systematic (%)
K tracking	0.42 ± 0.20	0.23 ± 0.04	0.18 ± 0.20	0.28
K PID	0.30 ± 0.15	0.12 ± 0.04	0.17 ± 0.15	0.23
π tracking	0.07 ± 0.12	0.04 ± 0.03	0.04 ± 0.12	0.12
π PID	-0.11 ± 0.04	0.02 ± 0.01	-0.13 ± 0.04	0.14

 Table 59: CP asymmetry for each decay mode, in percent.

Mode	CP Asymmetry (%)
$D^0 \rightarrow K^- \pi^+$	$0.3 \pm 0.3 \pm 0.6$
$D^0 \rightarrow K^- \pi^+ \pi^0$	$0.1 \pm 0.3 \pm 0.4$
$D^0 \rightarrow K^- \pi^+ \pi^+ \pi^-$	$0.2 \pm 0.3 \pm 0.4$
$D^+ \rightarrow K^- \pi^+ \pi^+$	$-0.3 \pm 0.2 \pm 0.4$
$D^+ \rightarrow K^- \pi^+ \pi^+ \pi^0$	$-0.3 \pm 0.6 \pm 0.4$
$D^+ \rightarrow K_S^0 \pi^+$	$-1.1 \pm 0.6 \pm 0.2$
$D^+ \rightarrow K_S^0 \pi^+ \pi^0$	$-0.1 \pm 0.7 \pm 0.2$
$D^+ \rightarrow K_S^0 \pi^+ \pi^+ \pi^-$	$0.0 \pm 1.2 \pm 0.3$
$D^+ \rightarrow K^+ K^- \pi^+$	$-0.1 \pm 0.9 \pm 0.4$

threshold more often than the other kaon in that decay, so their asymmetries would not completely cancel. In these cases, we take the uncertainty for that particle **once** – *i.e.* $D^+ \rightarrow K^- K^+ \pi^+$ has one kaon systematic and one pion systematic, rather than zero or two kaon systematics. The pions from K_S^0 's are not counted at all, since the momentum spectra of the π^+ and π^- are identical.

The asymmetries are shown in Table ???. The uncertainties are of order 1% in all modes, and no mode shows evidence of CP violation. We are insensitive to asymmetries at the level expected from the Standard Model, the largest of which are a few tenths of a percent in modes with a K_S^0 .

10 Conclusions

We have updated the hadronic branching fraction analysis to 818 pb^{-1} .

11 Figures

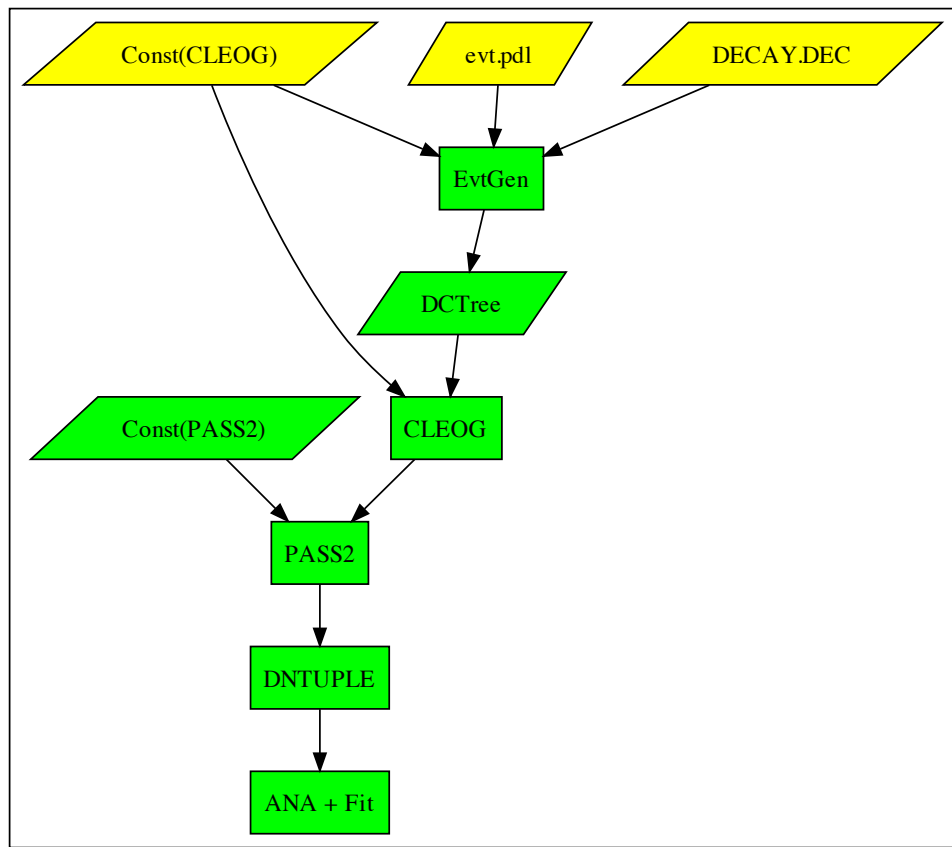


Figure 1: The process of tracing the MC difference. The “Yellow” process in the diagram means the sources contribute to the yield difference in MC.

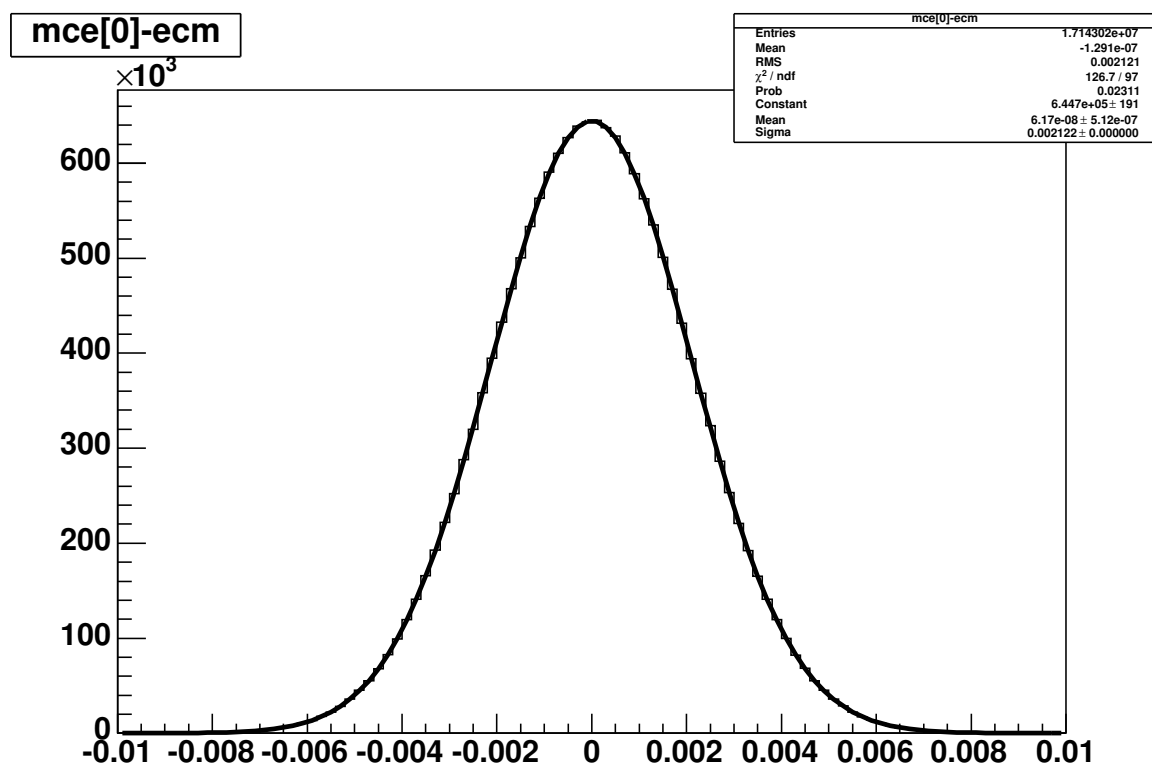


Figure 2: generic MC fit

Figure 3: Plots comparing track momentum spectra in data and MC for $D^0 \rightarrow K^- \pi^+ \pi^0$. These plots are used in determining the systematic uncertainty due to resonant substructure. The top left three plots show the MC truth (points) and fully-reconstructed (histograms) spectra in MC. The top right three plots show the effective efficiency as a function of the momentum of each daughter particle. The bottom left three plots compare the momentum distribution for the three D^0 decay products in data (points) and MC(histograms). The bottom right three plots show the same momentum spectra after correcting bin-by-bin for efficiency.

Figure 4: Plots comparing track momentum spectra in data and MC for $D^0 \rightarrow K^- \pi^+ \pi^+ \pi^-$. (π_1^+ is the higher-momentum pion and π_2^+ the lower.) These plots are used in determining the systematic uncertainty due to resonant substructure. The top left four plots show the MC truth (points) and fully-reconstructed (histograms) spectra in MC. The top right four plots show the effective efficiency as a function of the momentum of each daughter particle. The bottom left four plots compare the momentum distribution for the four D^0 decay products in data (points) and MC(histograms). The bottom right four plots show the same momentum spectra after correcting bin-by-bin for efficiency.

Figure 5: Plots comparing track momentum spectra in data and MC for $D^+ \rightarrow K^- \pi^+ \pi^+$. (π_1^+ is the higher-momentum pion and π_2^+ the lower.) These plots are used in determining the systematic uncertainty due to resonant substructure. The top left three plots show the MC truth (points) and fully-reconstructed (histograms) spectra in MC. The top right three plots show the effective efficiency as a function of the momentum of each daughter particle. The bottom left three plots compare the momentum distribution for the three D^+ decay products in data (points) and MC(histograms). The bottom right three plots show the same momentum spectra after correcting bin-by-bin for efficiency.

Figure 6: Plots comparing track momentum spectra in data and MC for $D^+ \rightarrow K^- \pi^+ \pi^+ \pi^0$. (π_1^+ is the higher-momentum pion and π_2^+ the lower.) These plots are used in determining the systematic uncertainty due to resonant substructure. The top left four plots show the MC truth (points) and fully-reconstructed (histograms) spectra in MC. The top right four plots show the effective efficiency as a function of the momentum of each daughter particle. The bottom left four plots compare the momentum distribution for the four D^+ decay products in data (points) and MC(histograms). The bottom right four plots show the same momentum spectra after correcting bin-by-bin for efficiency.

Figure 7: Plots comparing track momentum spectra in data and MC for $D^+ \rightarrow K_S^0 \pi^+ \pi^0$. These plots are used in determining the systematic uncertainty due to resonant substructure. The top left three plots show the MC truth (points) and fully-reconstructed (histograms) spectra in MC. The top right three plots show the effective efficiency as a function of the momentum of each daughter particle. The bottom left three plots compare the momentum distribution for the three D^+ decay products in data (points) and MC(histograms). The bottom right three plots show the same momentum spectra after correcting bin-by-bin for efficiency.

Figure 8: Plots comparing track momentum spectra in data and MC for $D^+ \rightarrow K_S^0 \pi^+ \pi^- \pi^+$. (π_1^+ is the higher-momentum pion and π_2^+ the lower.) These plots are used in determining the systematic uncertainty due to resonant substructure. The top left four plots show the MC truth (points) and fully-reconstructed (histograms) spectra in MC. The top right four plots show the effective efficiency as a function of the momentum of each daughter particle. The bottom left four plots compare the momentum distribution for the four D^+ decay products in data (points) and MC(histograms). The bottom right four plots show the same momentum spectra after correcting bin-by-bin for efficiency.

Figure 9: Plots comparing track momentum spectra in data and MC for $D^+ \rightarrow K^+ K^- \pi^+$. These plots are used in determining the systematic uncertainty due to resonant substructure. The top left three plots show the MC truth (points) and fully-reconstructed (histograms) spectra in MC. The top right three plots show the effective efficiency as a function of the momentum of each daughter particle. The bottom left three plots compare the momentum distribution for the three D^+ decay products in data (points) and MC(histograms). The bottom right three plots show the same momentum spectra after correcting bin-by-bin for efficiency.

Figure 10: Background-subtracted mass distributions for $K^- K^+$ (left) and $K^- \pi^+$ (right) in $D^+ \rightarrow K^+ K^- \pi^+$. Blue points are data and red points connected by lines are signal MC.

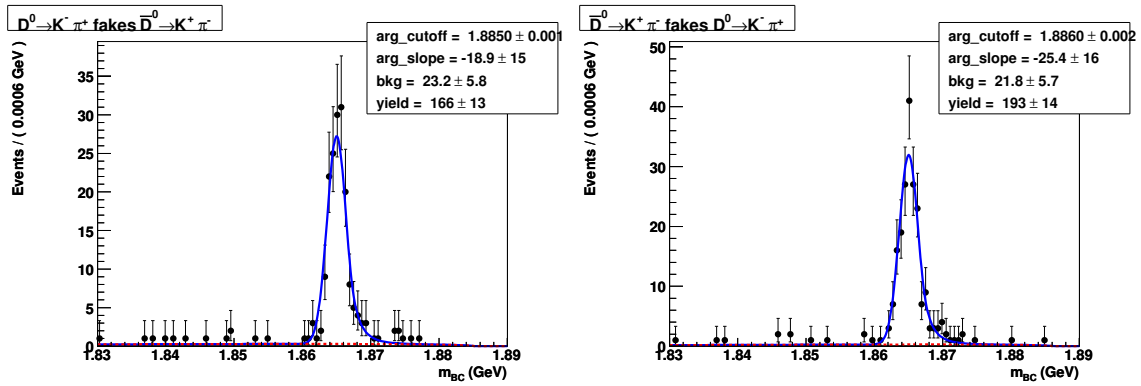


Figure 11: Single tag background extraction plots for the crossfeed modes.

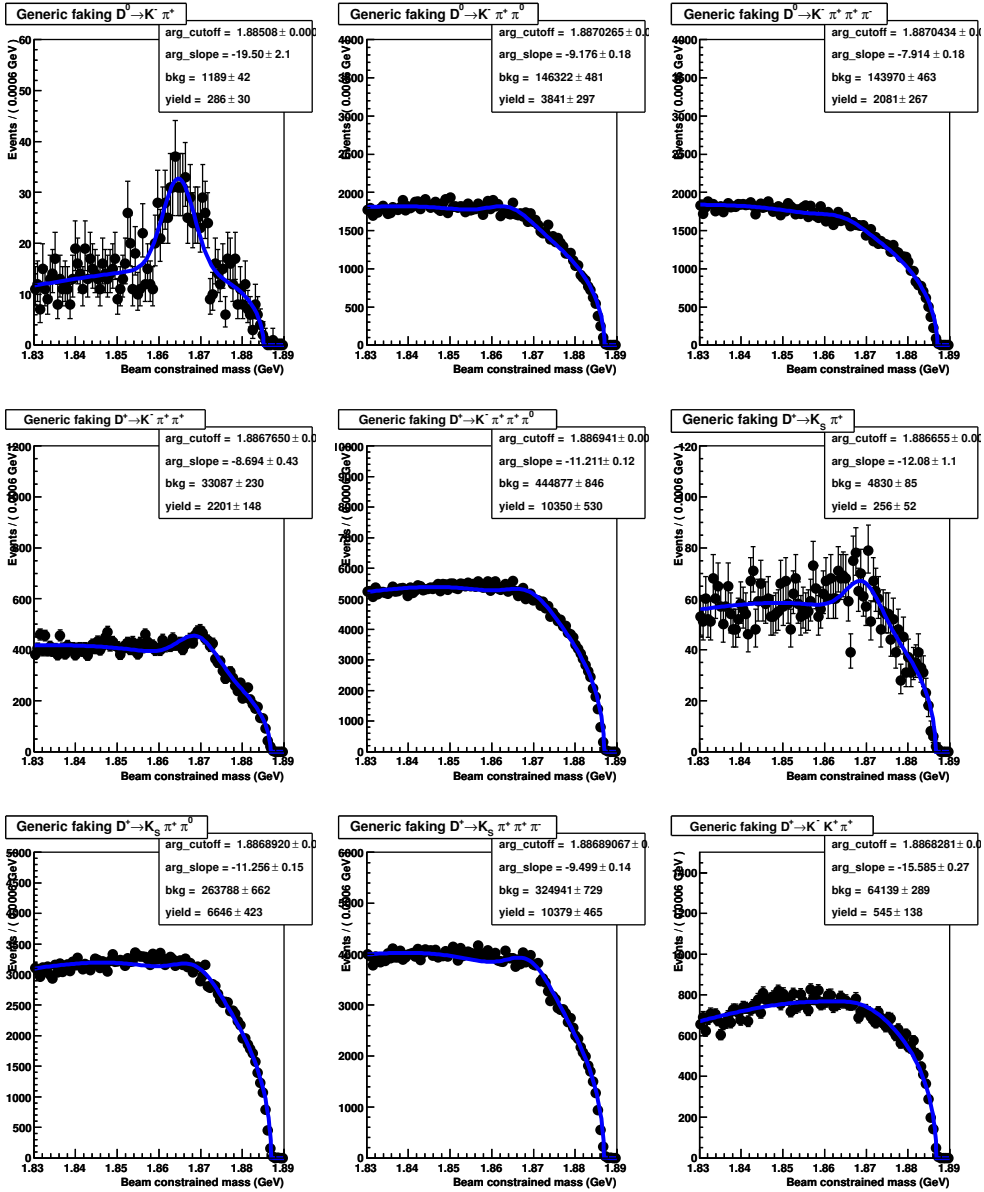


Figure 12: M_{BC} spectra of D candidates in generic Monte Carlo, once the background sources we account for are removed. The plots are fit to the sum of an Argus function and a Gaussian, constrained to the respective D masses and widths from the signal MC. There is no strong evidence of peaking background in most of the modes; the reported yields can be attributed to bad modeling of the non-peaking background.

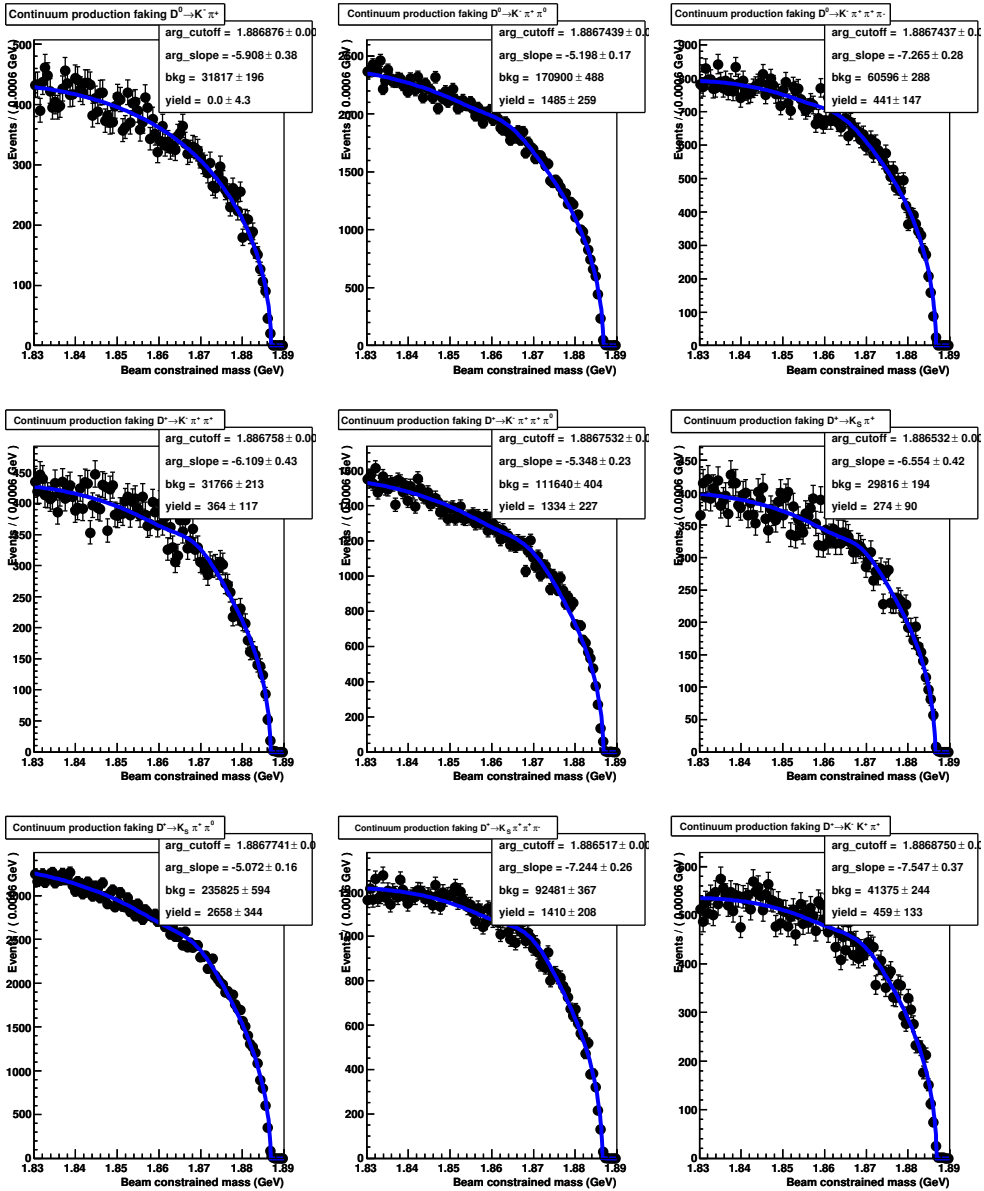


Figure 13: M_{BC} spectra of D candidates in continuum (non- $D\bar{D}$) Monte Carlo. The plots are fit to the sum of an Argus function and a Gaussian, constrained to the respective D masses and widths from the signal MC. There is no evidence of peaking background in any of the modes.

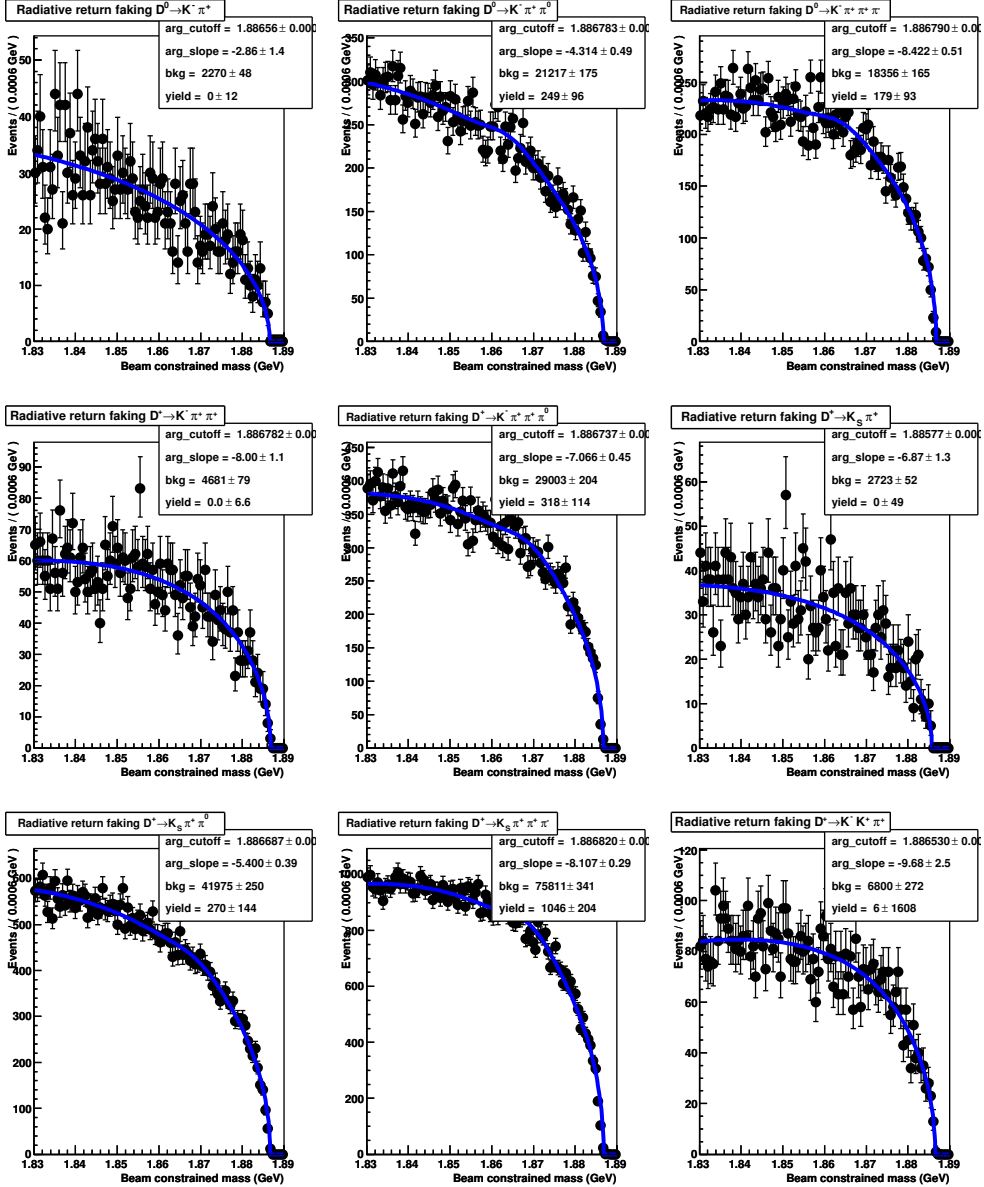


Figure 14: M_{BC} spectra of D candidates in radiative return Monte Carlo. The plots are fit to the sum of an Argus function and a Gaussian, constrained to the respective D masses and widths from the signal MC. There is no evidence of peaking background in any of the modes.

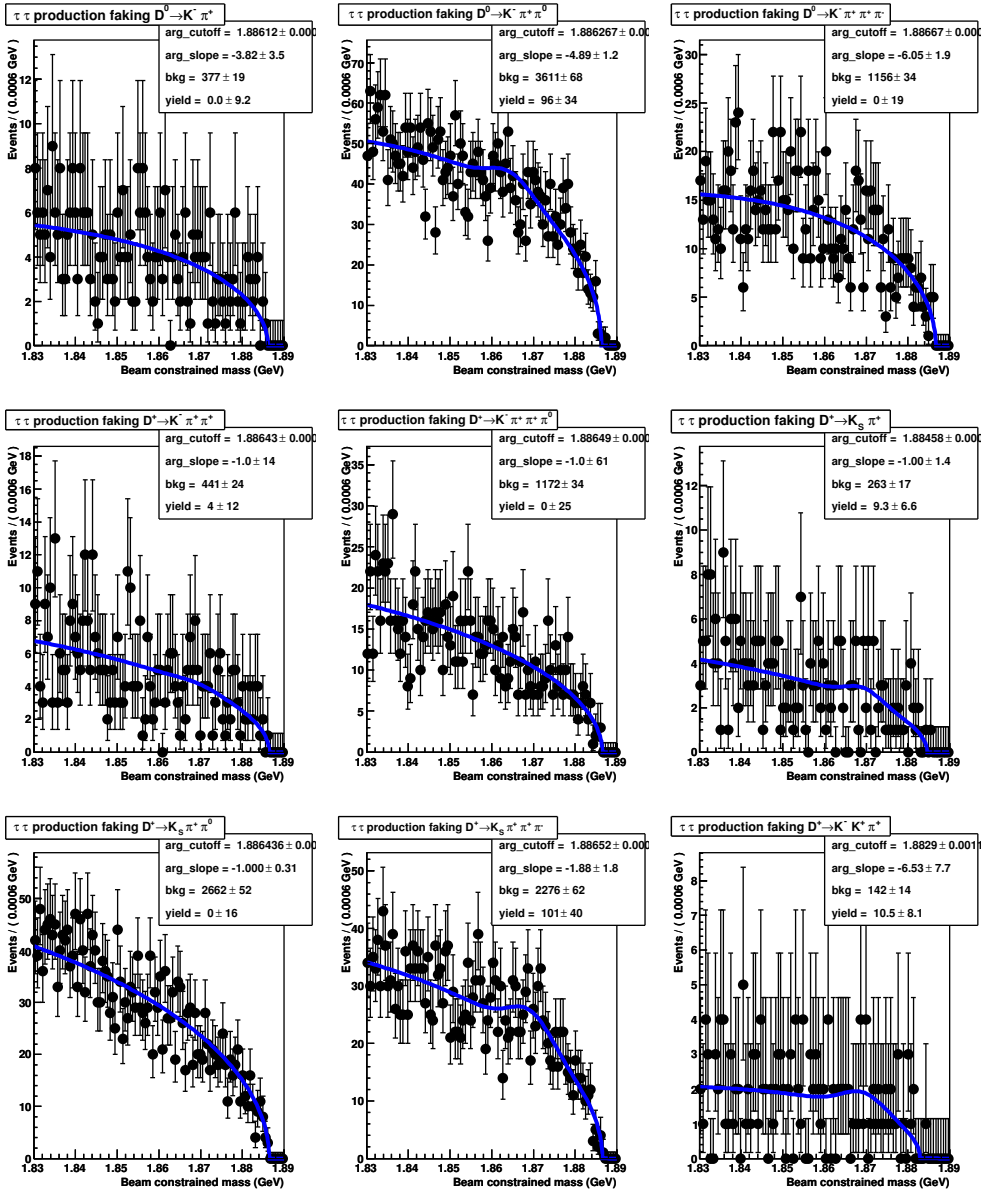


Figure 15: M_{BC} spectra of D candidates in τ -pair Monte Carlo. The plots are fit to the sum of an Argus function and a Gaussian, constrained to the respective D masses and widths from the signal MC. There is no evidence of peaking background in any of the modes.

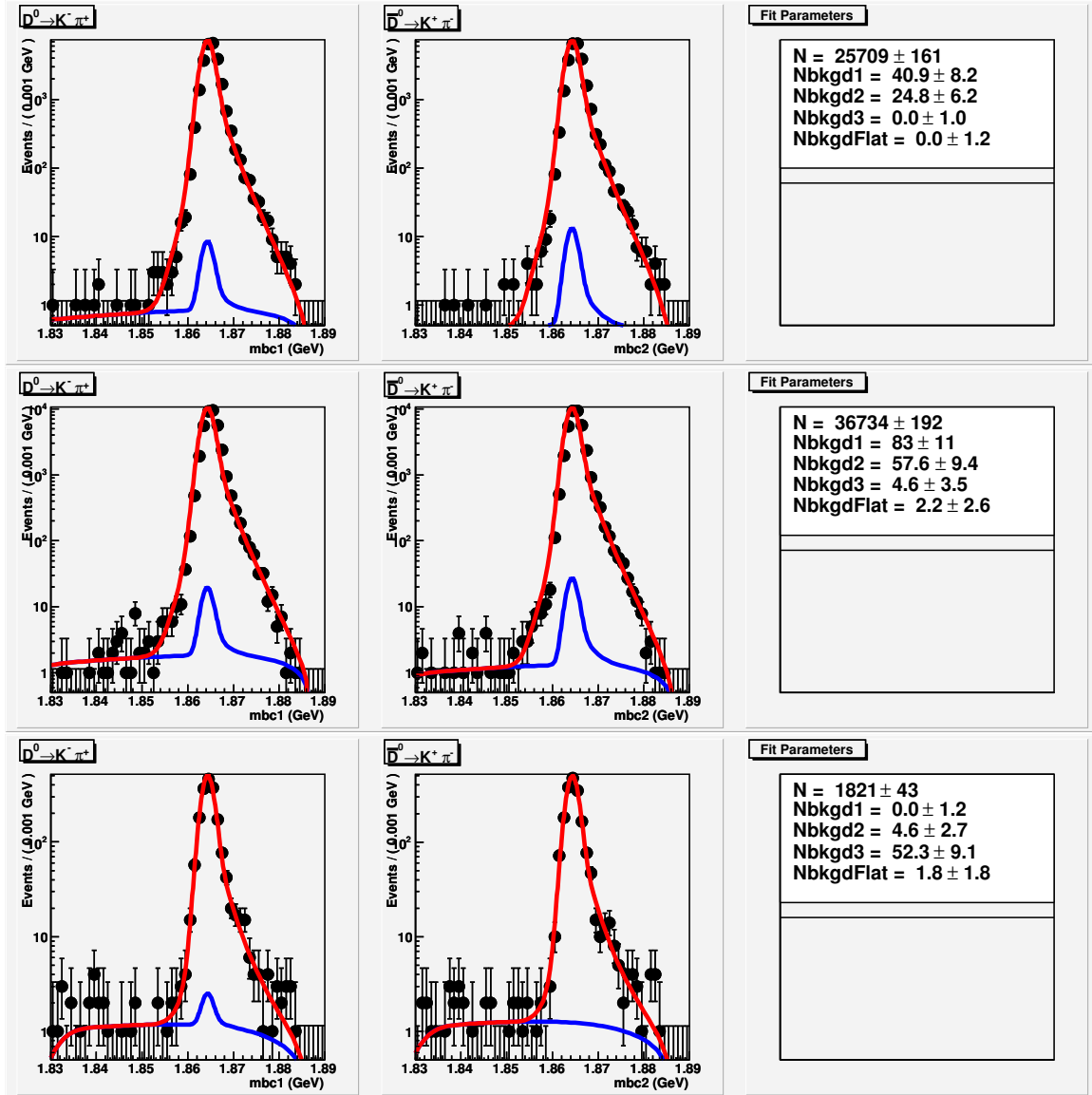


Figure 16: Fits for $K\pi$ v.s. $K\pi$ double tags. Top is signal Monte Carlo, middle is generic $D\bar{D}$ Monte Carlo and bottom is data.

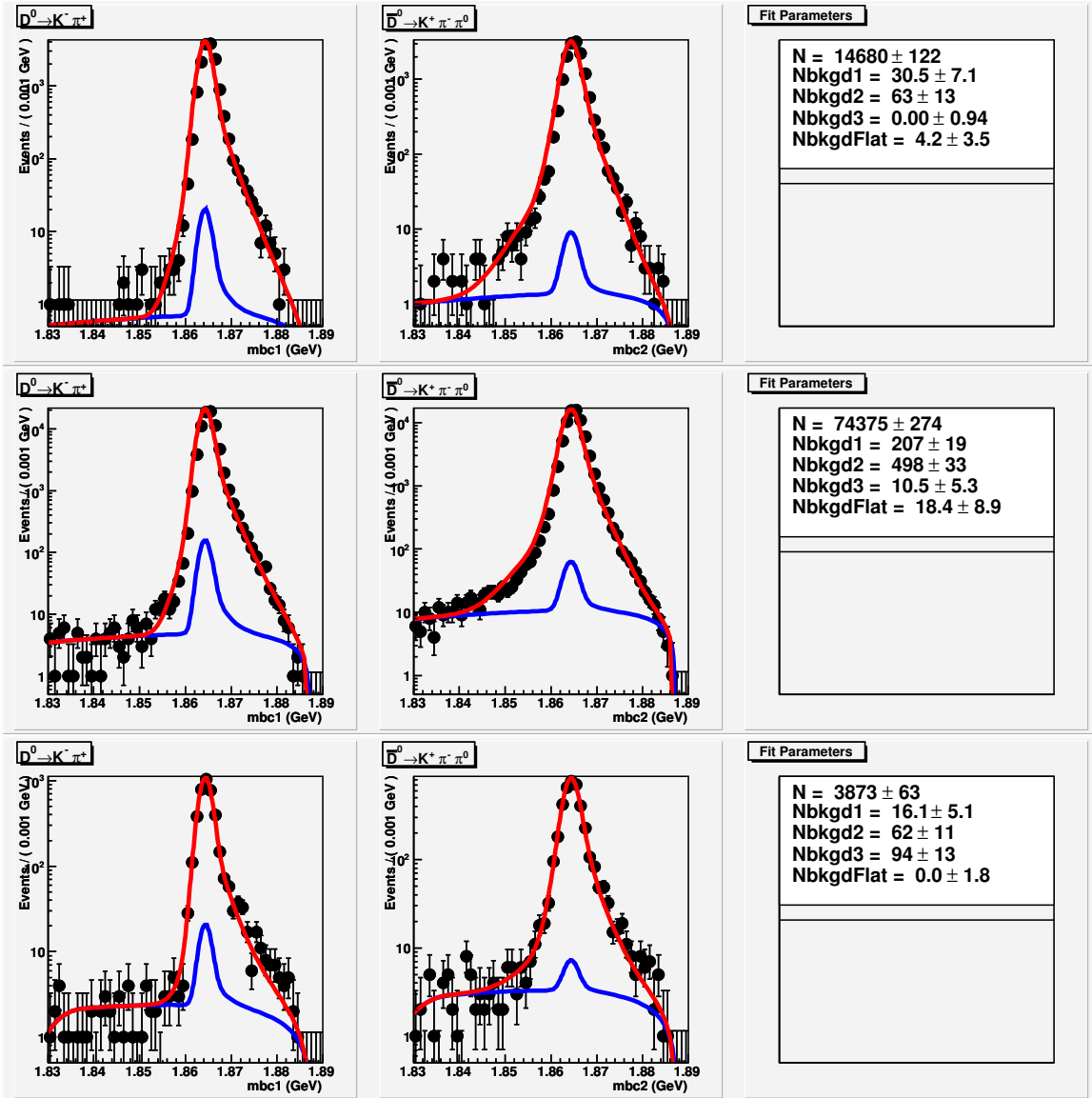


Figure 17: Fits for $K\pi$ v.s. $K\pi\pi^0$ double tags. Top is signal Monte Carlo, middle is generic $D\bar{D}$ Monte Carlo and bottom is data.

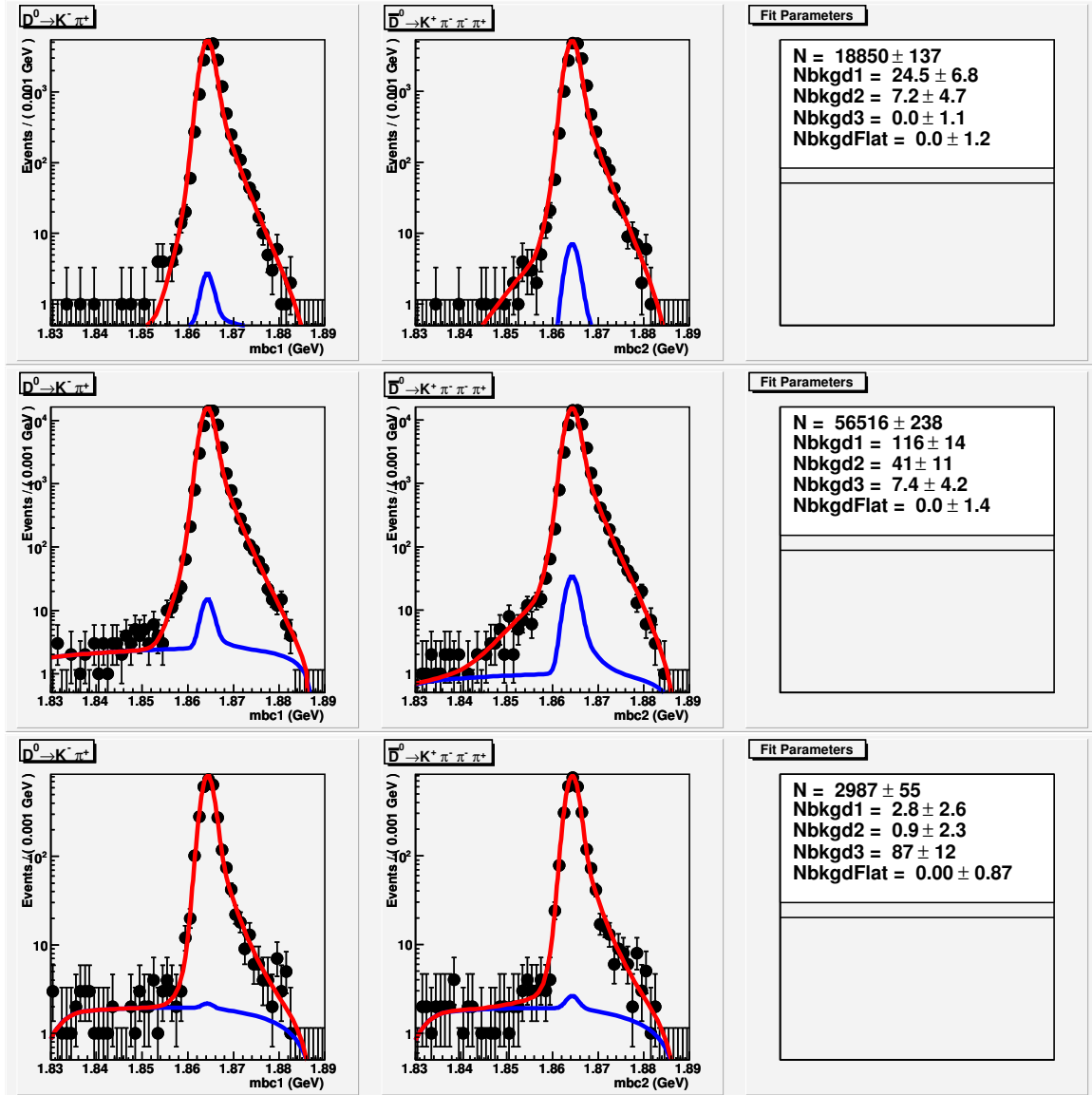


Figure 18: Fits for $K\pi$ v.s. $K\pi\pi\pi$ double tags. Top is signal Monte Carlo, middle is generic $D\bar{D}$ Monte Carlo and bottom is data.

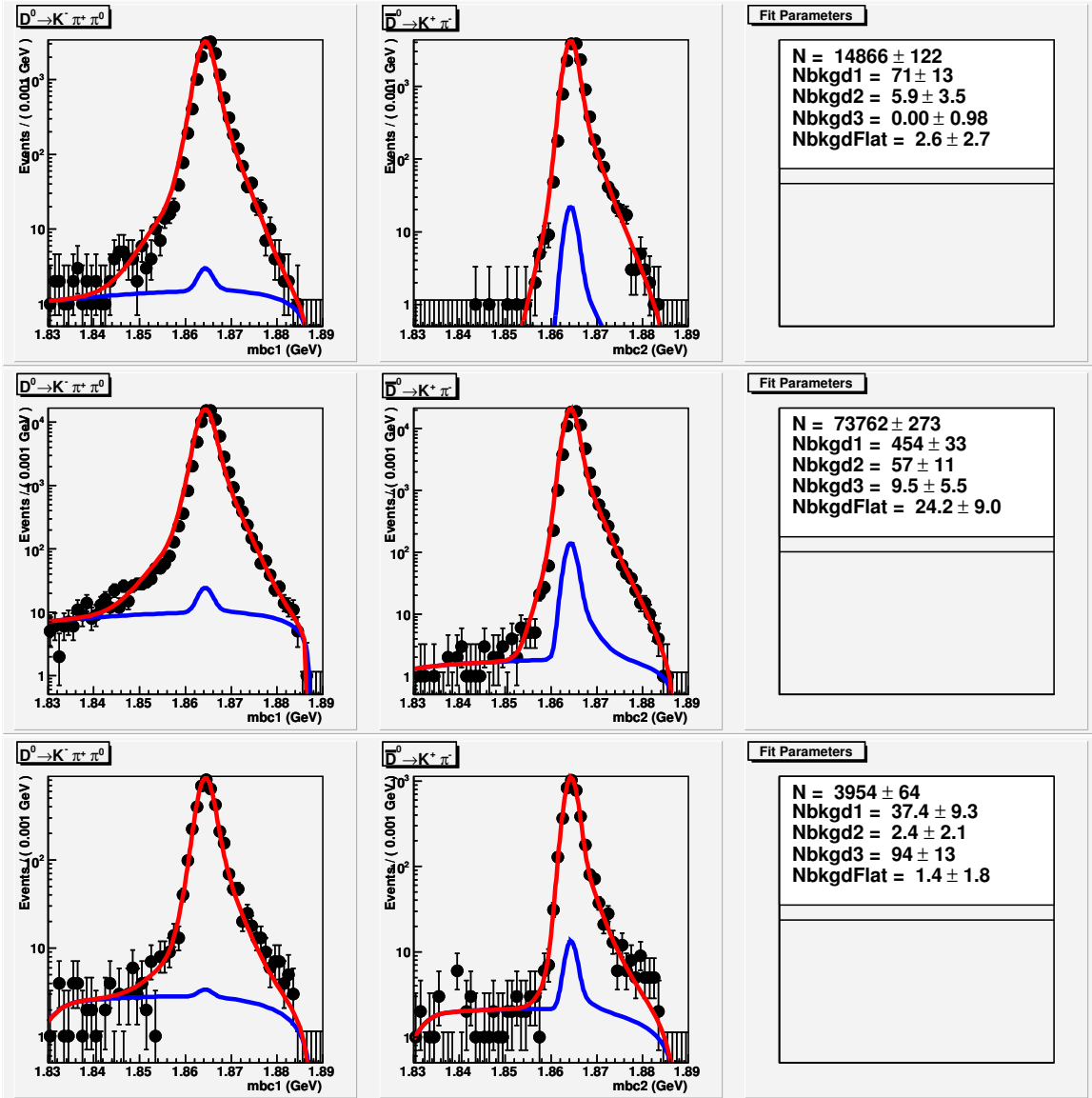


Figure 19: Fits for $K\pi\pi^0$ v.s. $K\pi$ double tags. Top is signal Monte Carlo, middle is generic $D\bar{D}$ Monte Carlo and bottom is data.

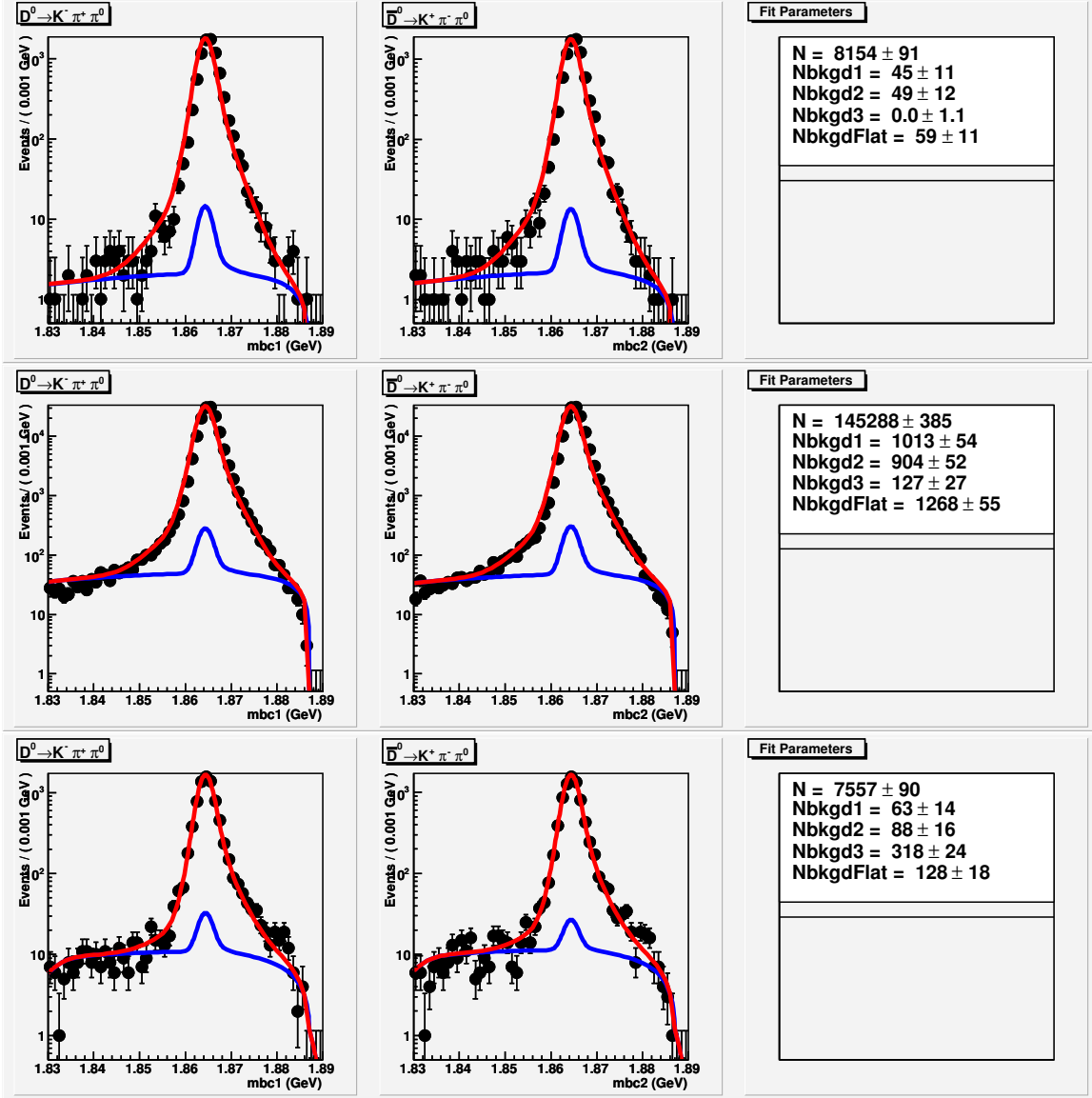


Figure 20: Fits for $K\pi\pi^0$ v.s. $K\pi\pi^0$ double tags. Top is signal Monte Carlo, middle is generic $D\bar{D}$ Monte Carlo and bottom is data.

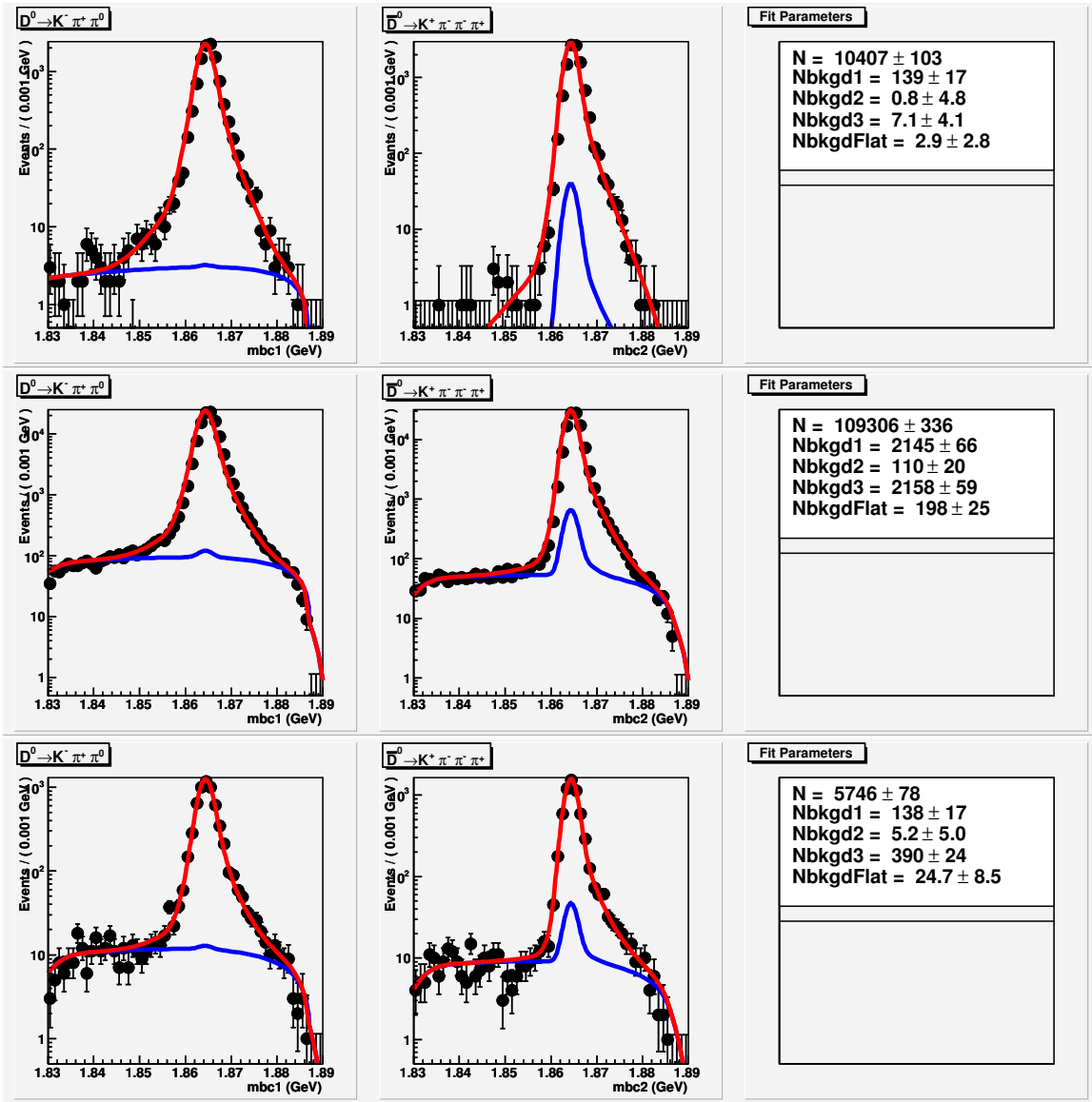


Figure 21: Fits for $K\pi\pi^0$ v.s. $K\pi\pi\pi$ double tags. Top is signal Monte Carlo, middle is generic $D\bar{D}$ Monte Carlo and bottom is data.

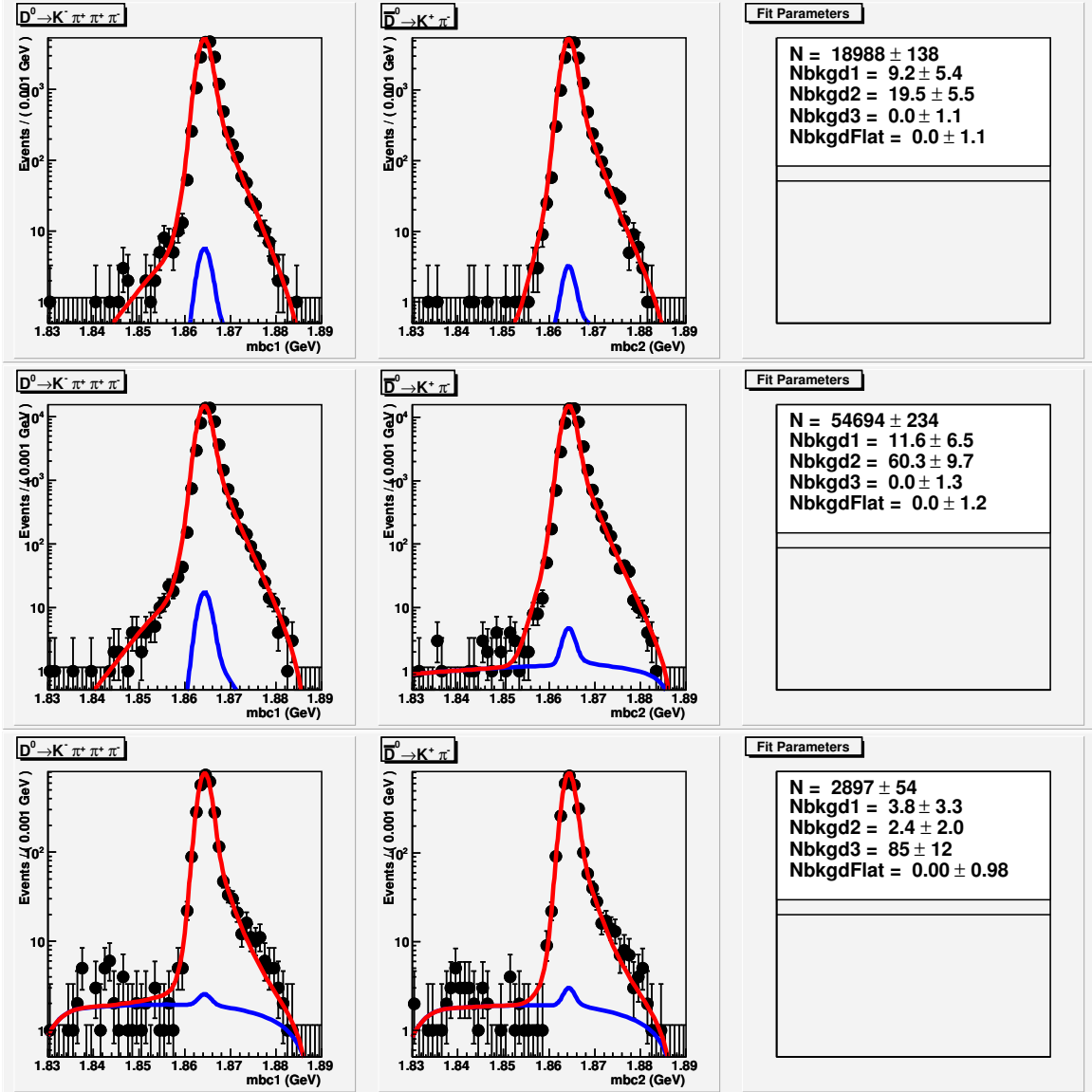


Figure 22: Fits for $K\pi\pi\pi$ v.s. $K\pi$ double tags. Top is signal Monte Carlo, middle is generic $D\bar{D}$ Monte Carlo and bottom is data.

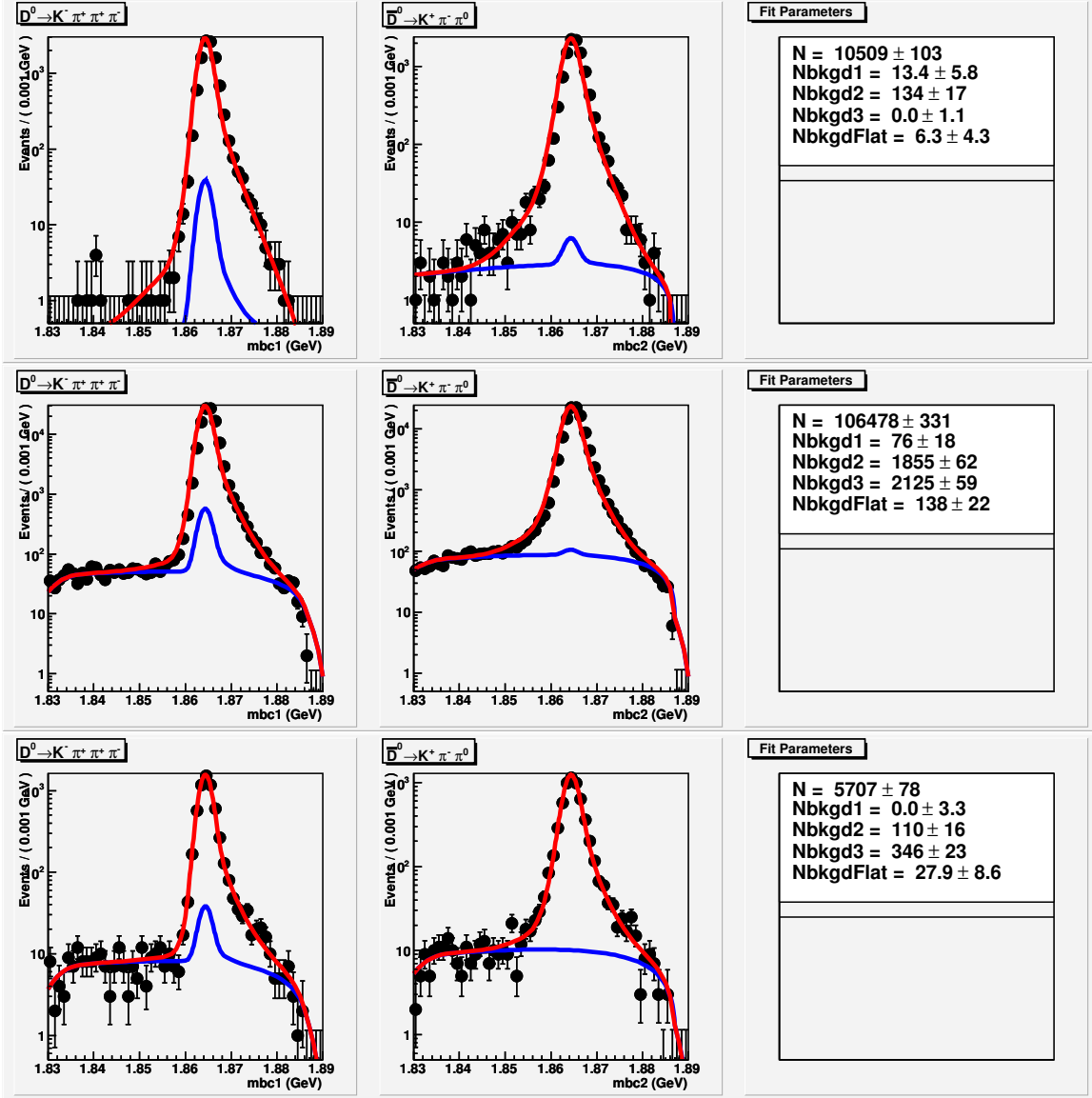


Figure 23: Fits for $K\pi\pi\pi$ v.s. $K\pi\pi^0$ double tags. Top is signal Monte Carlo, middle is generic $D\bar{D}$ Monte Carlo and bottom is data.

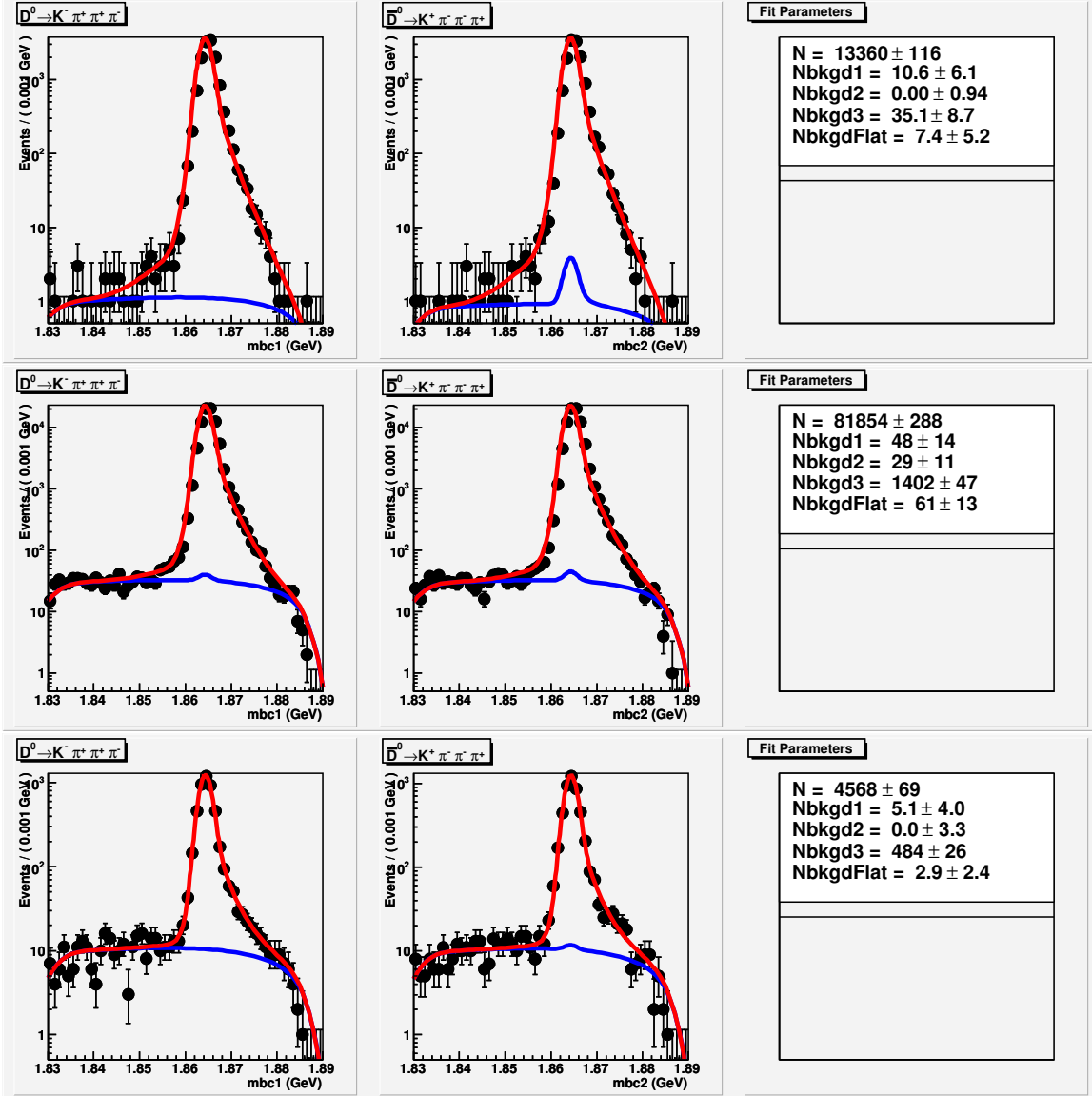


Figure 24: Fits for $K\pi\pi\pi$ v.s. $K\pi\pi\pi$ double tags. Top is signal Monte Carlo, middle is generic $D\bar{D}$ Monte Carlo and bottom is data.

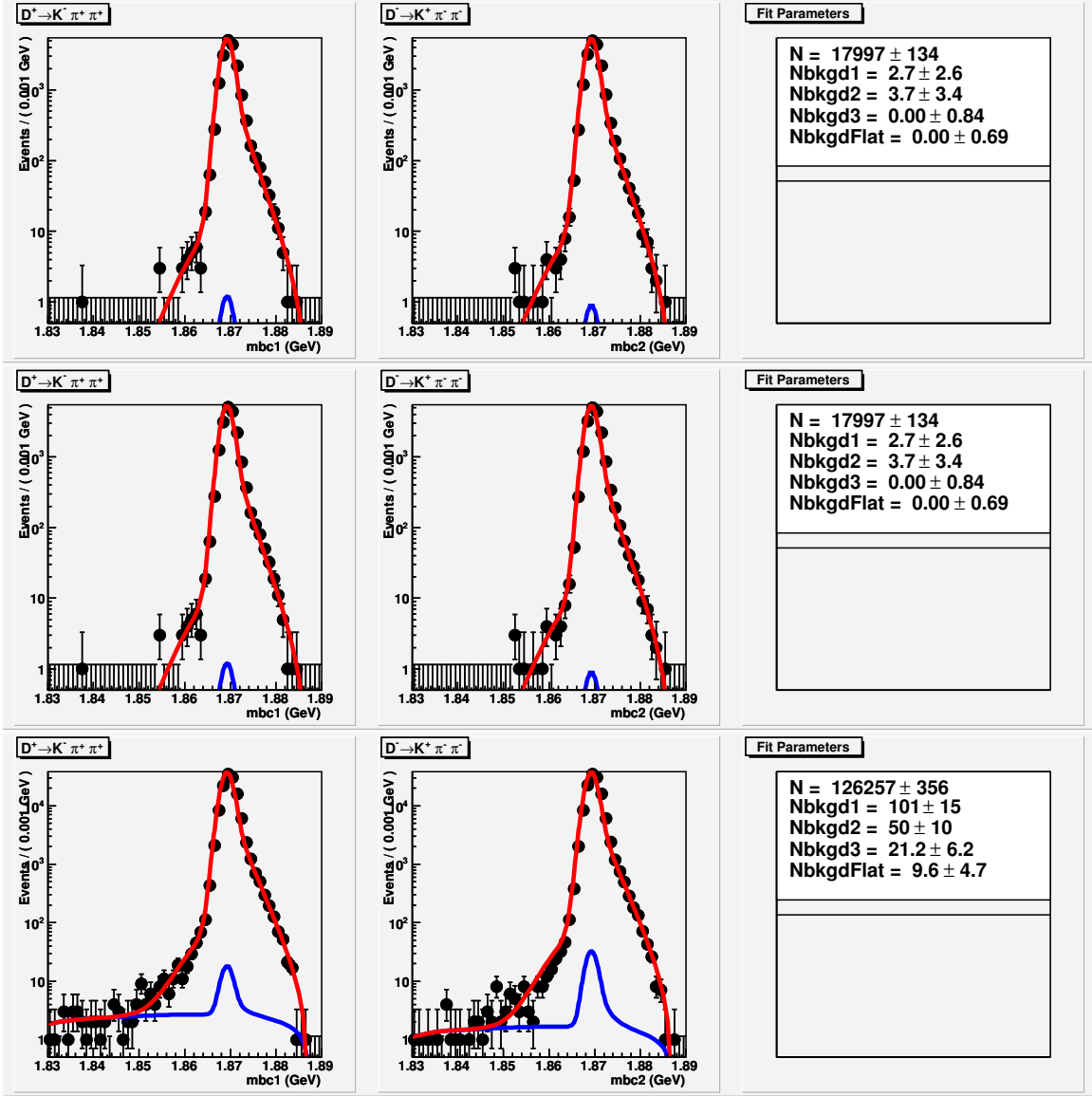


Figure 25: Fits for $K\pi\pi$ v.s. $K\pi\pi$ double tags. Top is signal Monte Carlo, middle is generic $D\bar{D}$ Monte Carlo and bottom is data.

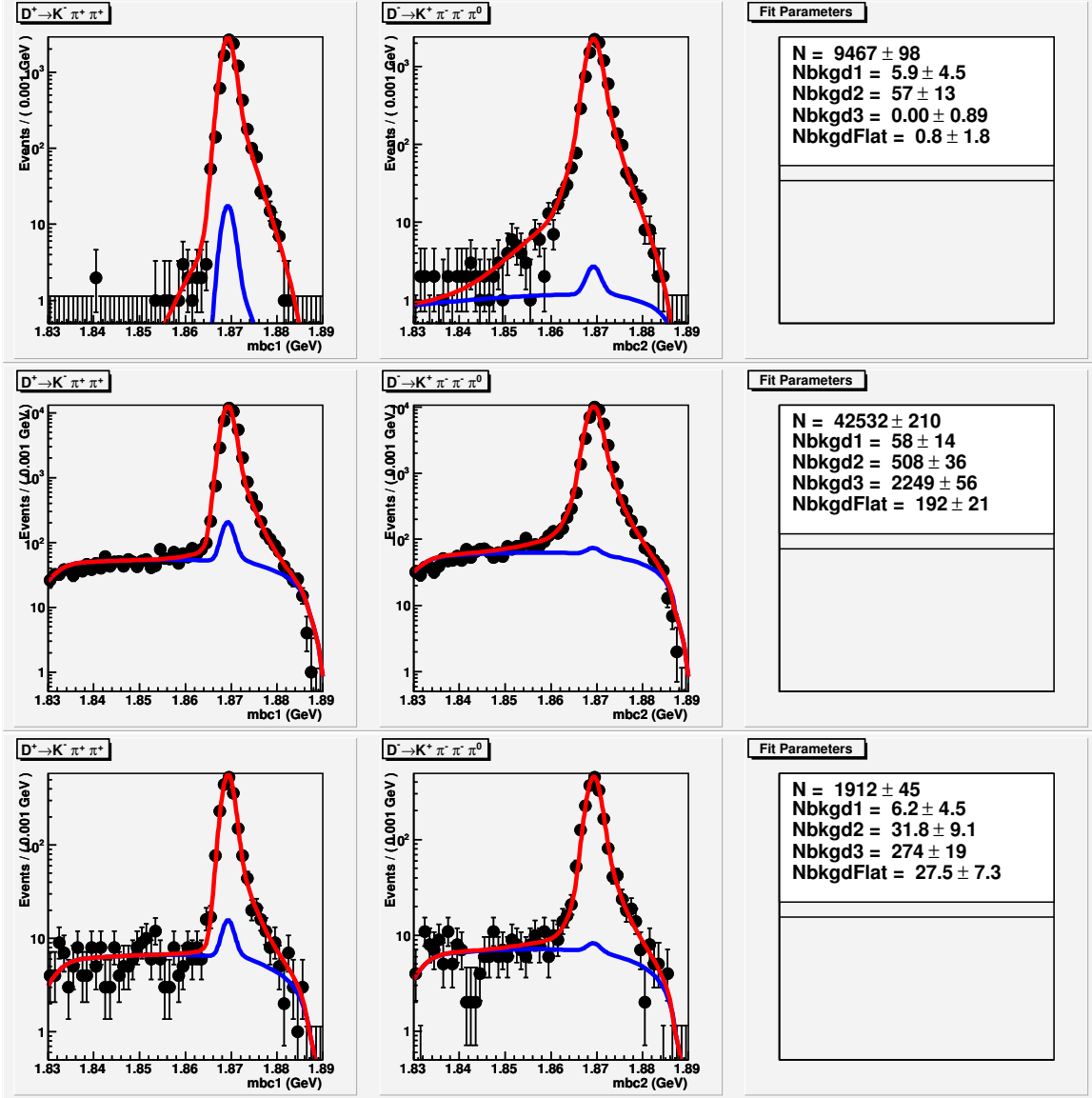


Figure 26: Fits for $K\pi\pi$ v.s. $K\pi\pi\pi^0$ double tags. Top is signal Monte Carlo, middle is generic $D\bar{D}$ Monte Carlo and bottom is data.

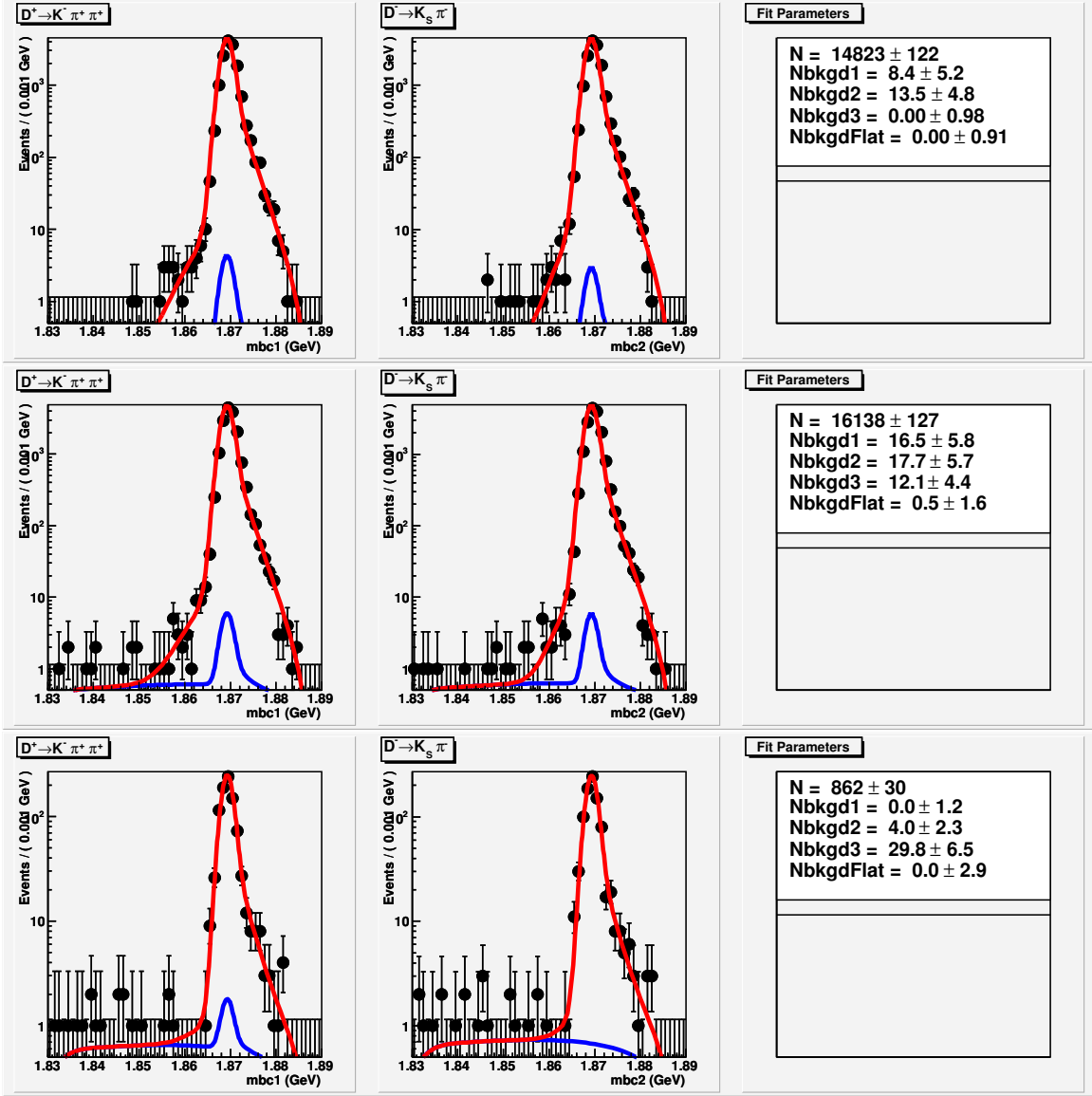


Figure 27: Fits for $K\pi\pi$ v.s. $K_S\pi$ double tags. Top is signal Monte Carlo, middle is generic $D\bar{D}$ Monte Carlo and bottom is data.

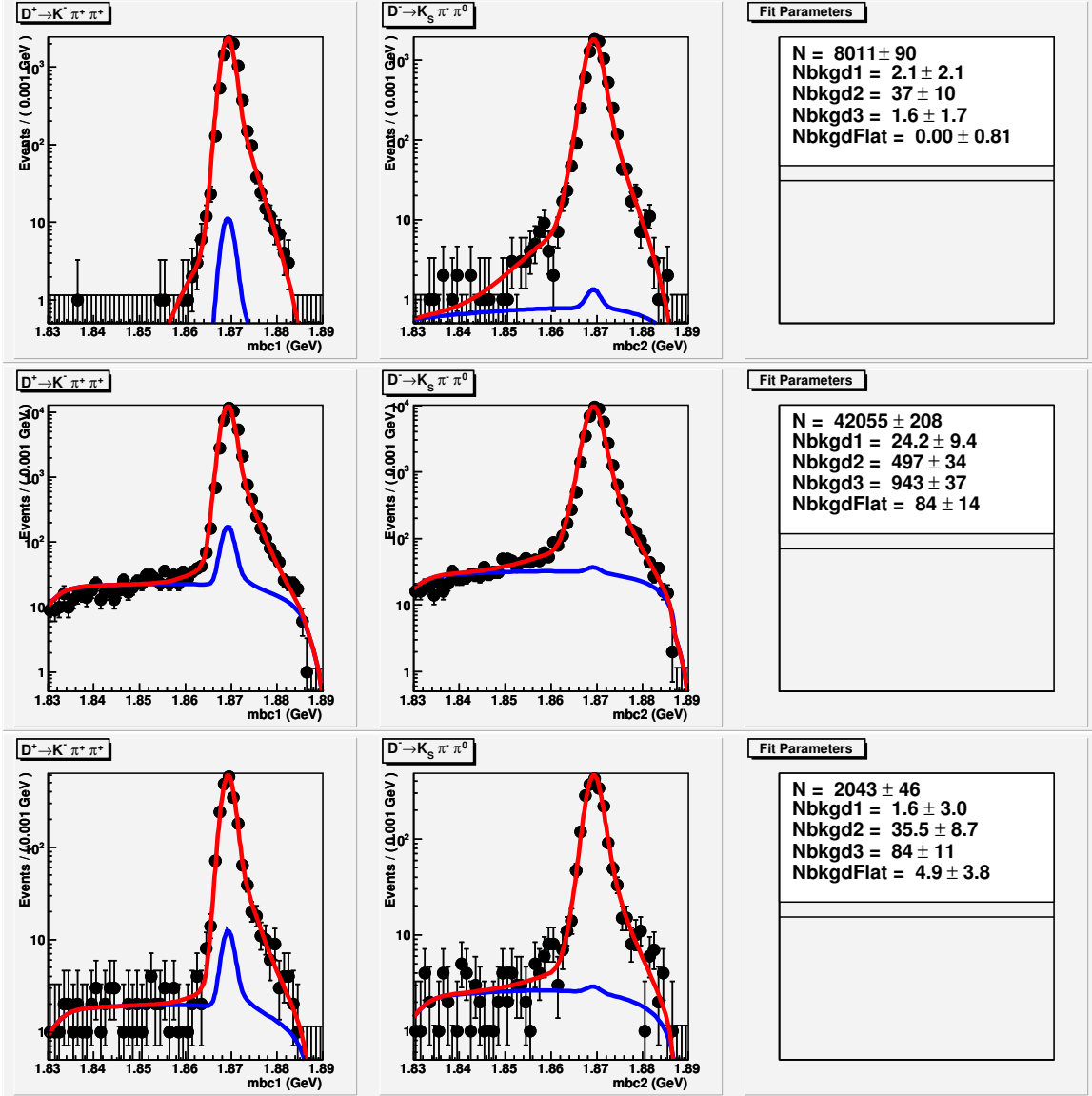


Figure 28: Fits for $K\pi\pi$ v.s. $K_S\pi\pi^0$ double tags. Top is signal Monte Carlo, middle is generic $D\bar{D}$ Monte Carlo and bottom is data.

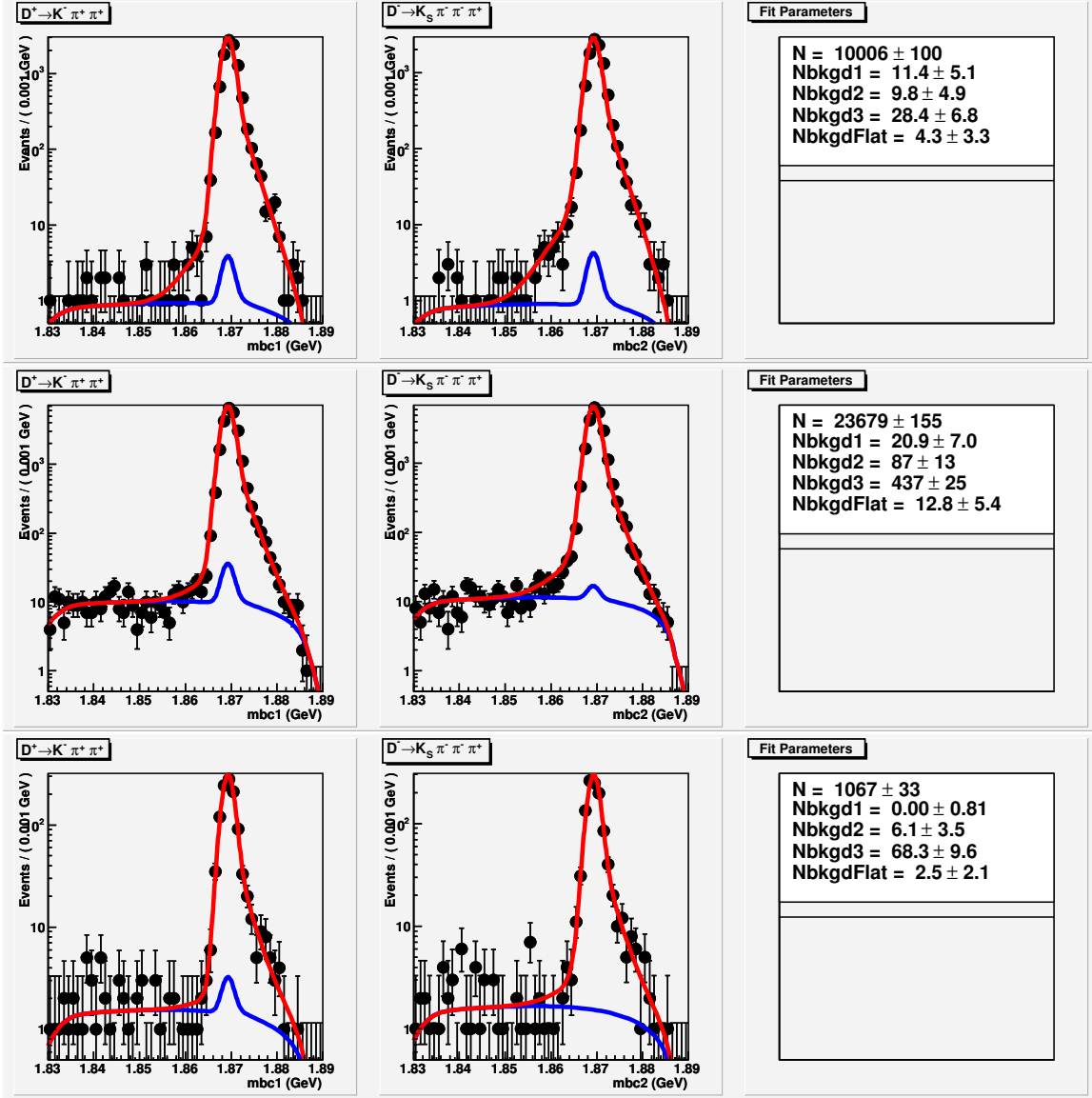


Figure 29: Fits for $K\pi\pi$ v.s. $K_S\pi\pi\pi$ double tags. Top is signal Monte Carlo, middle is generic $D\bar{D}$ Monte Carlo and bottom is data.

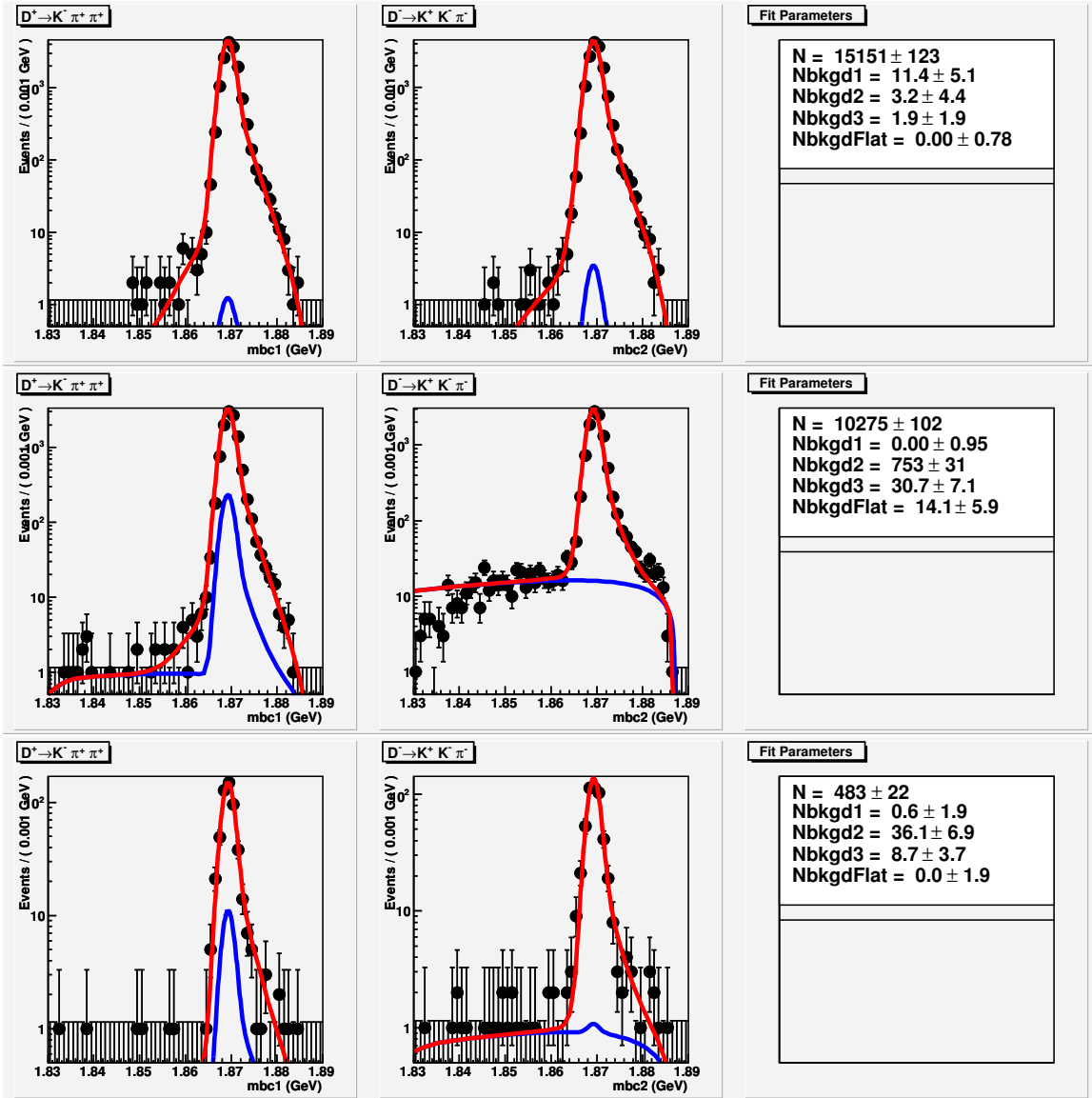


Figure 30: Fits for $K\pi\pi$ v.s. $KK\pi$ double tags. Top is signal Monte Carlo, middle is generic $D\bar{D}$ Monte Carlo and bottom is data.

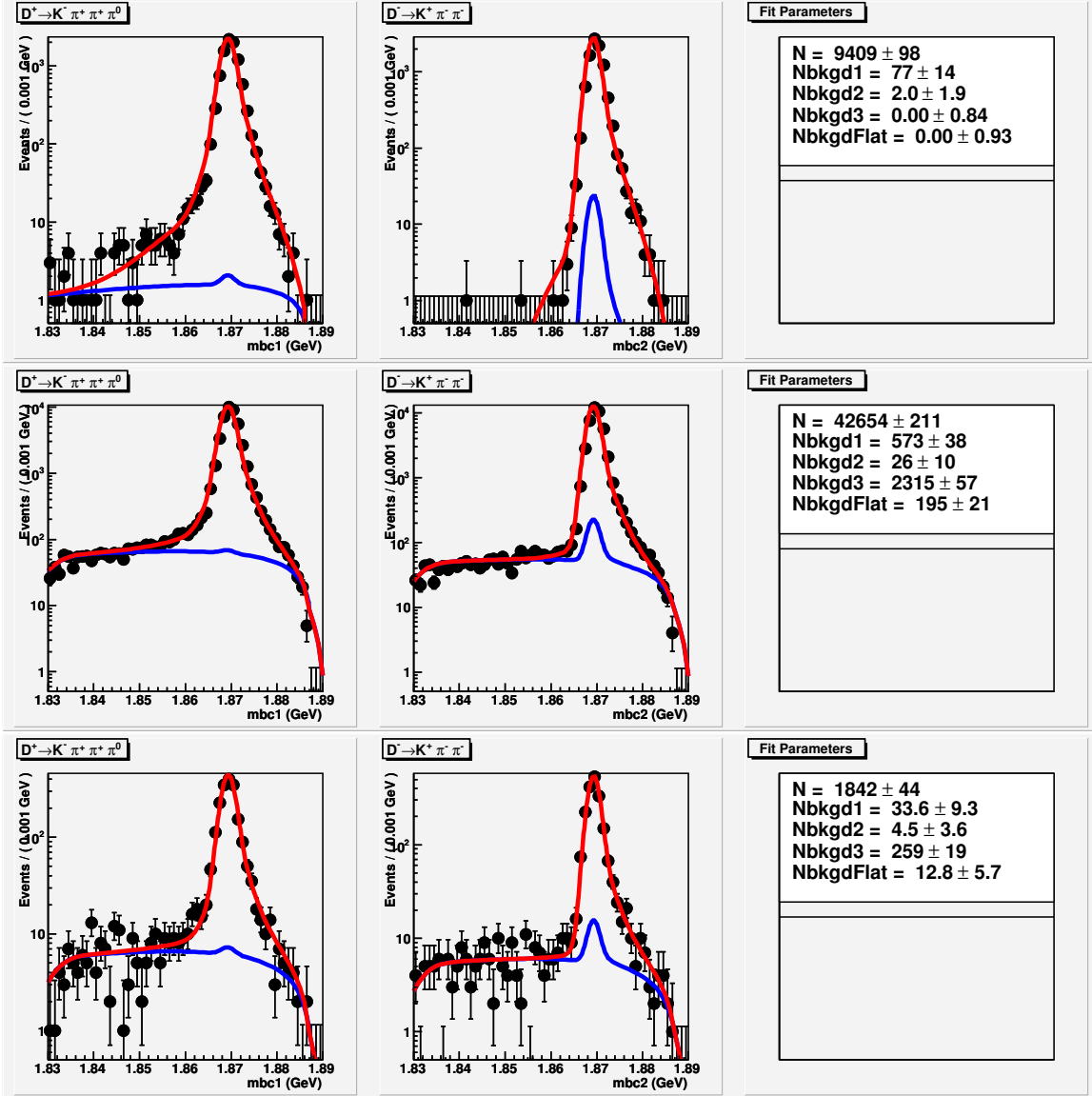


Figure 31: Fits for $K\pi\pi\pi^0$ v.s. $K\pi\pi$ double tags. Top is signal Monte Carlo, middle is generic $D\bar{D}$ Monte Carlo and bottom is data.

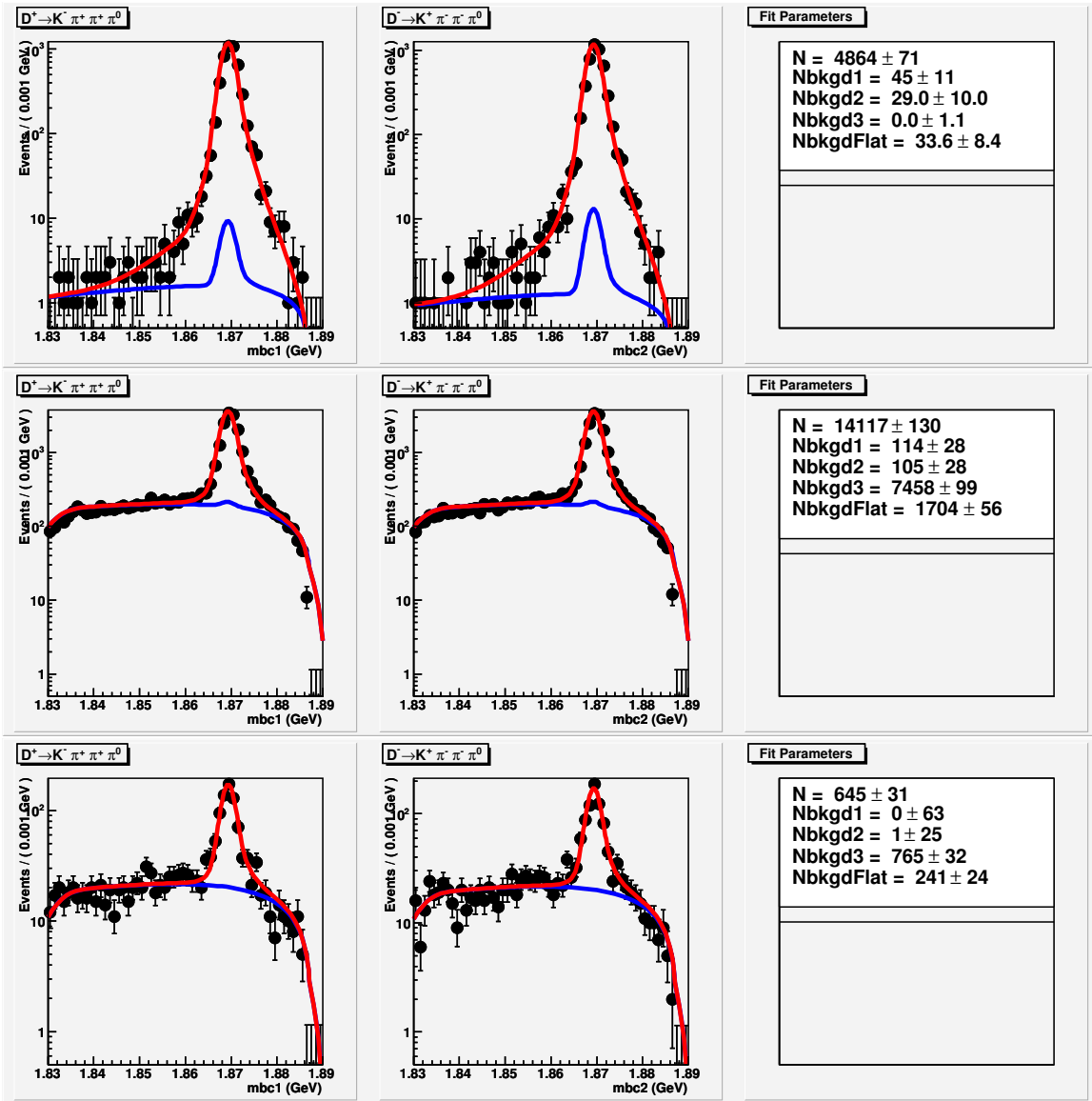


Figure 32: Fits for $K\pi\pi\pi^0$ v.s. $K\pi\pi\pi^0$ double tags. Top is signal Monte Carlo, middle is generic $D\bar{D}$ Monte Carlo and bottom is data.

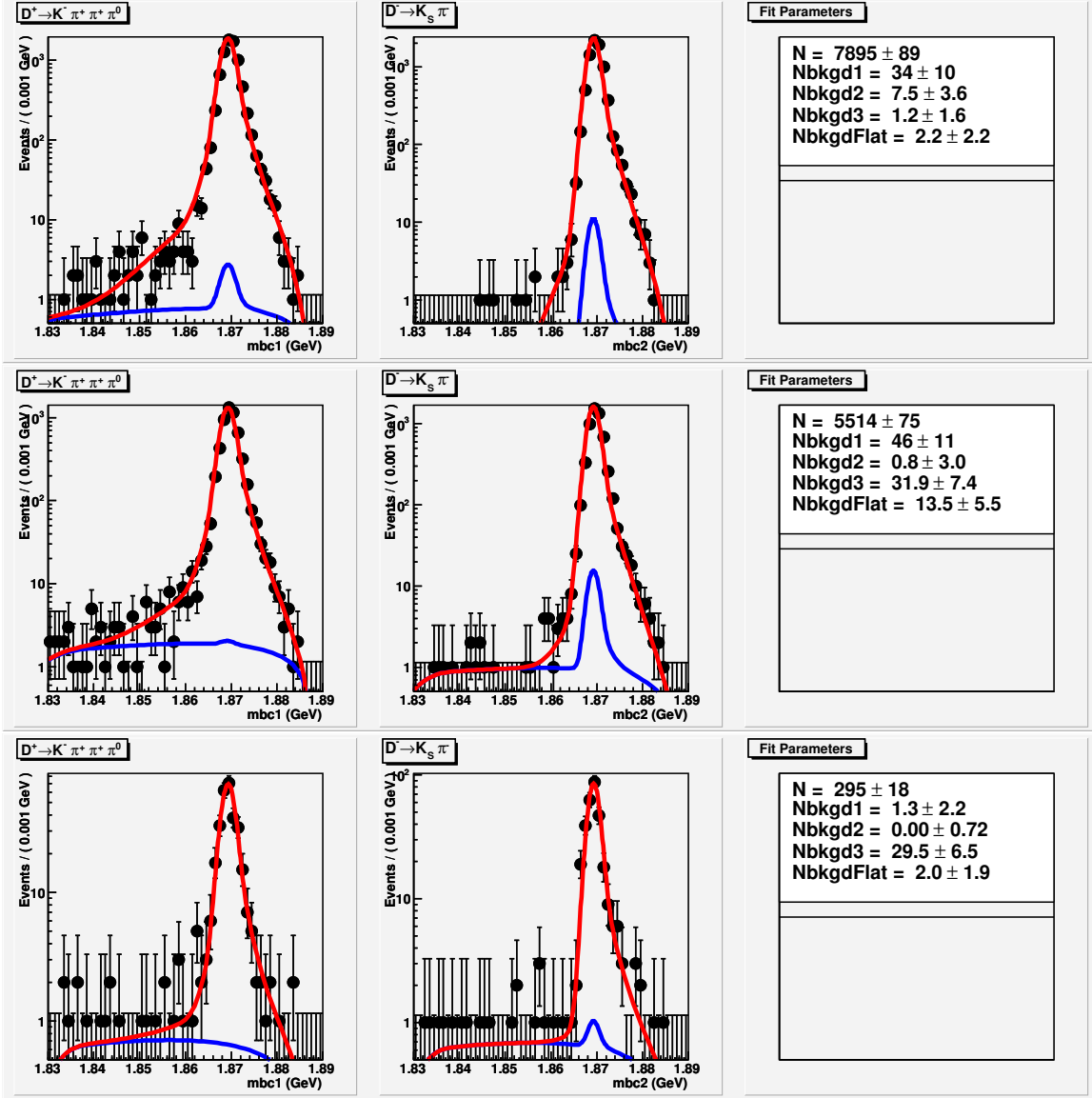


Figure 33: Fits for $K\pi\pi\pi^0$ v.s. $K_S\pi$ double tags. Top is signal Monte Carlo, middle is generic $D\bar{D}$ Monte Carlo and bottom is data.

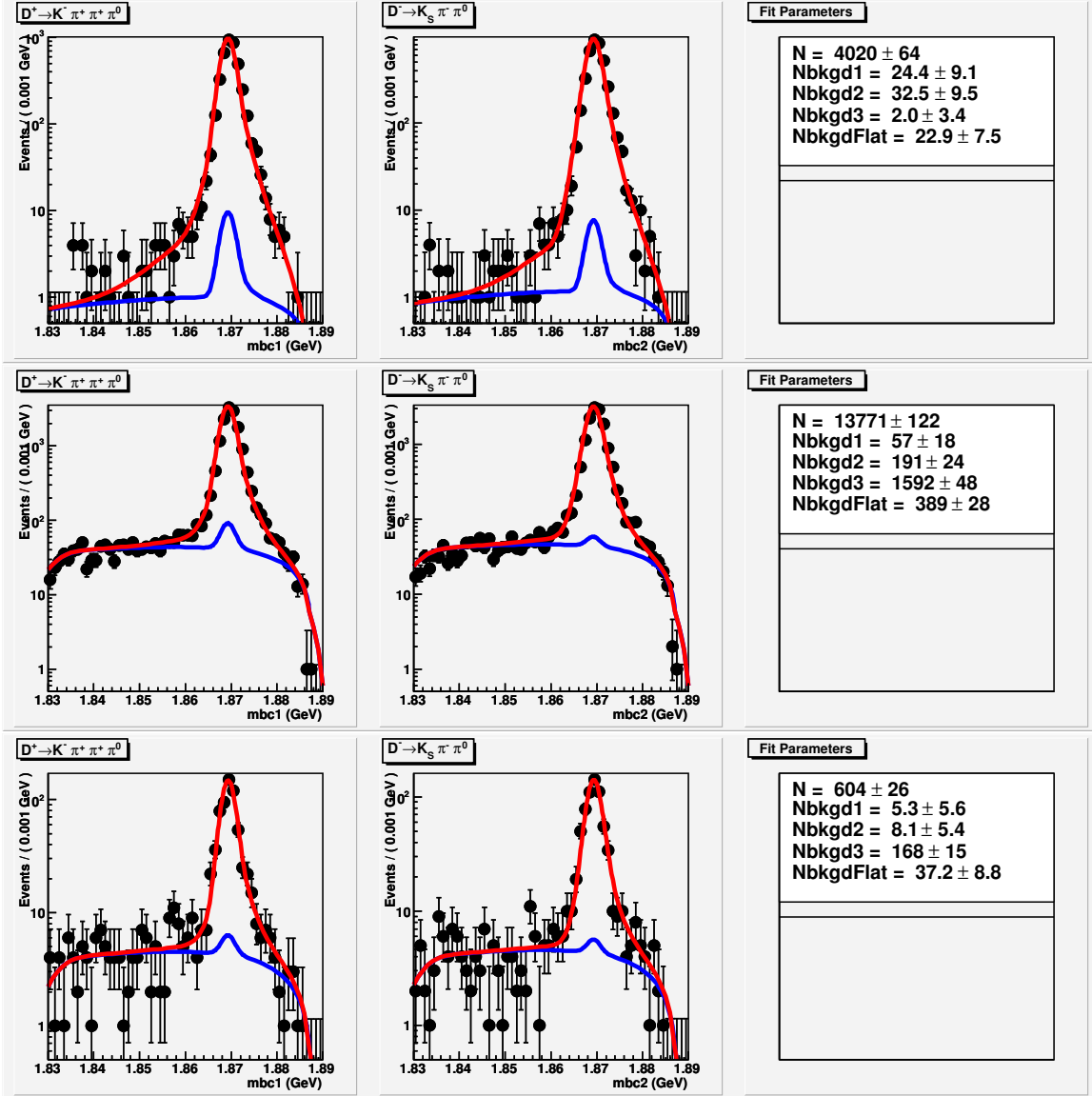


Figure 34: Fits for $K\pi\pi\pi^0$ v.s. $K_S\pi\pi^0$ double tags. Top is signal Monte Carlo, middle is generic $D\bar{D}$ Monte Carlo and bottom is data.

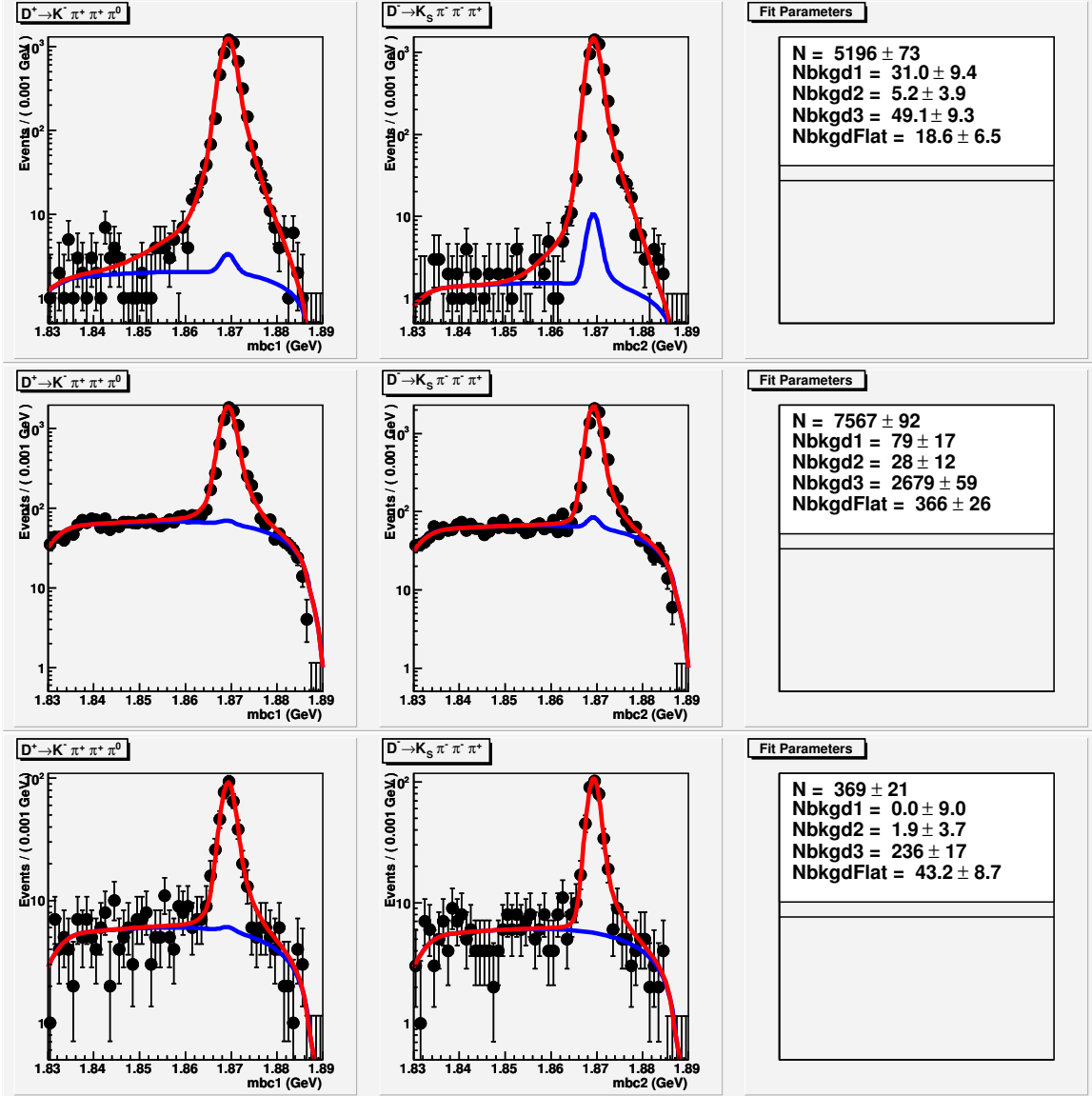


Figure 35: Fits for $K\pi\pi\pi^0$ v.s. $K_S\pi\pi\pi$ double tags. Top is signal Monte Carlo, middle is generic $D\bar{D}$ Monte Carlo and bottom is data.

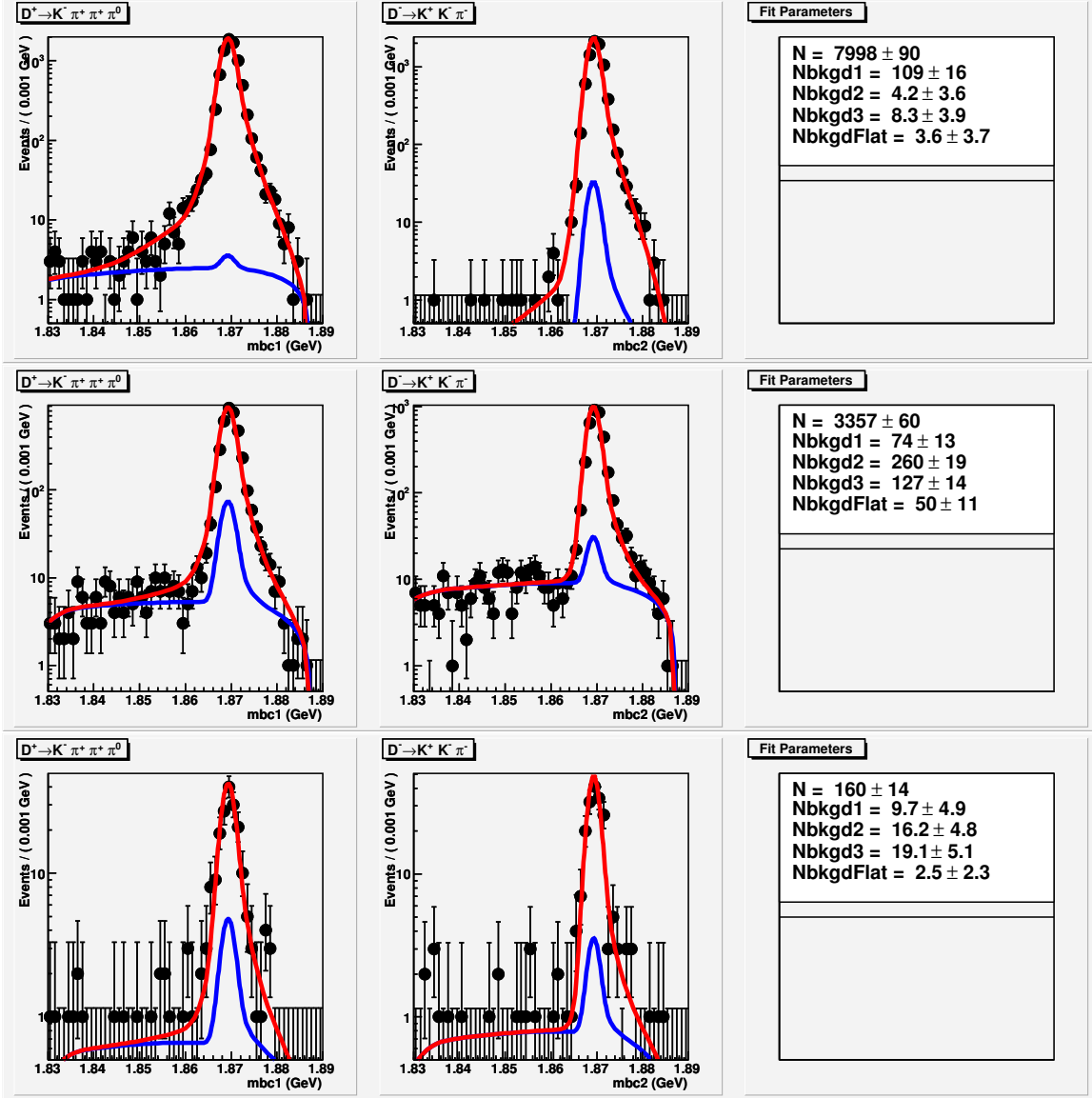


Figure 36: Fits for $K\pi\pi\pi^0$ v.s. $KK\pi$ double tags. Top is signal Monte Carlo, middle is generic $D\bar{D}$ Monte Carlo and bottom is data.

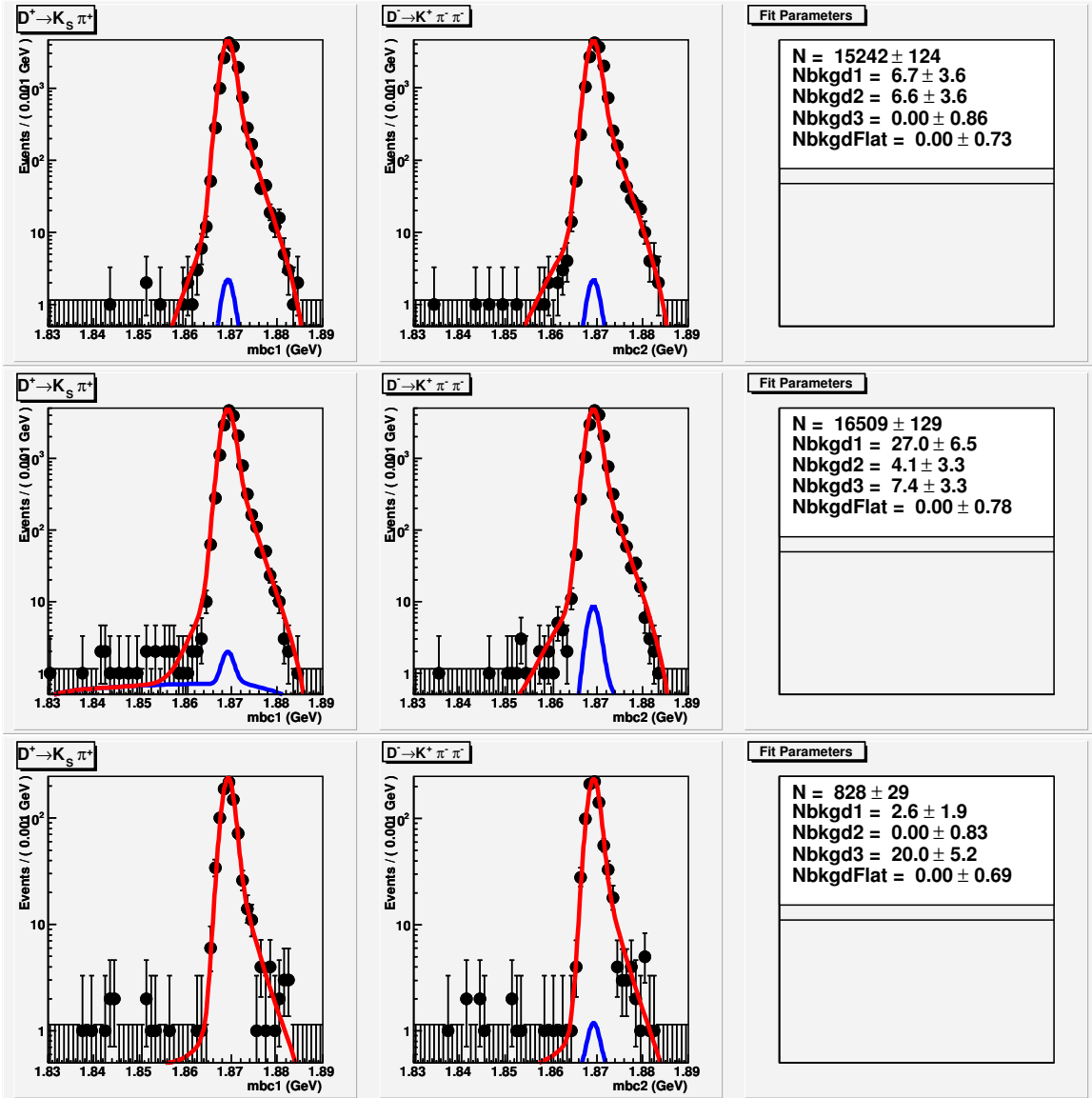


Figure 37: Fits for $K_S\pi$ v.s. $K\pi\pi$ double tags. Top is signal Monte Carlo, middle is generic $D\bar{D}$ Monte Carlo and bottom is data.

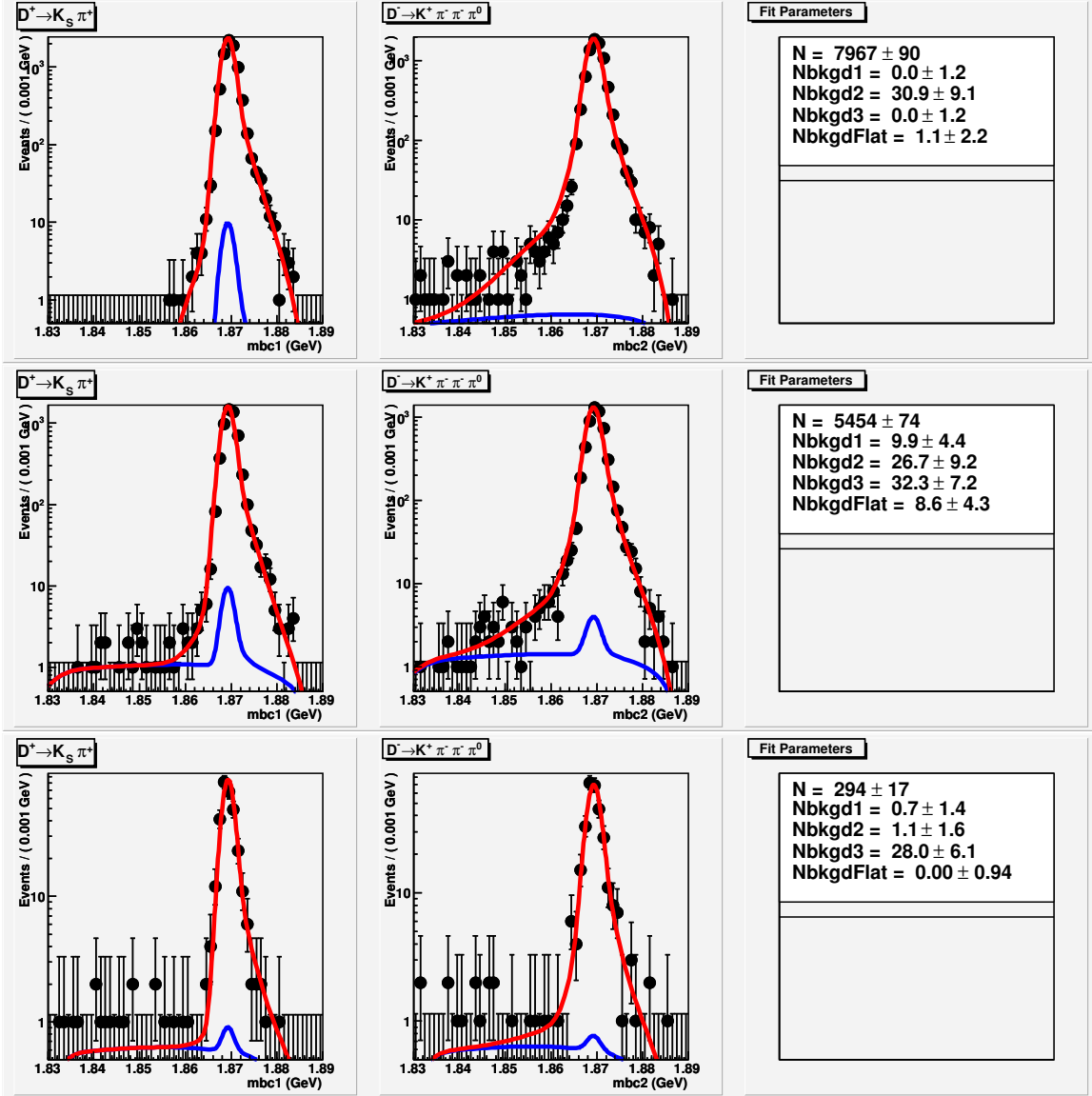


Figure 38: Fits for $K_S\pi$ v.s. $K\pi\pi^0$ double tags. Top is signal Monte Carlo, middle is generic $D\bar{D}$ Monte Carlo and bottom is data.

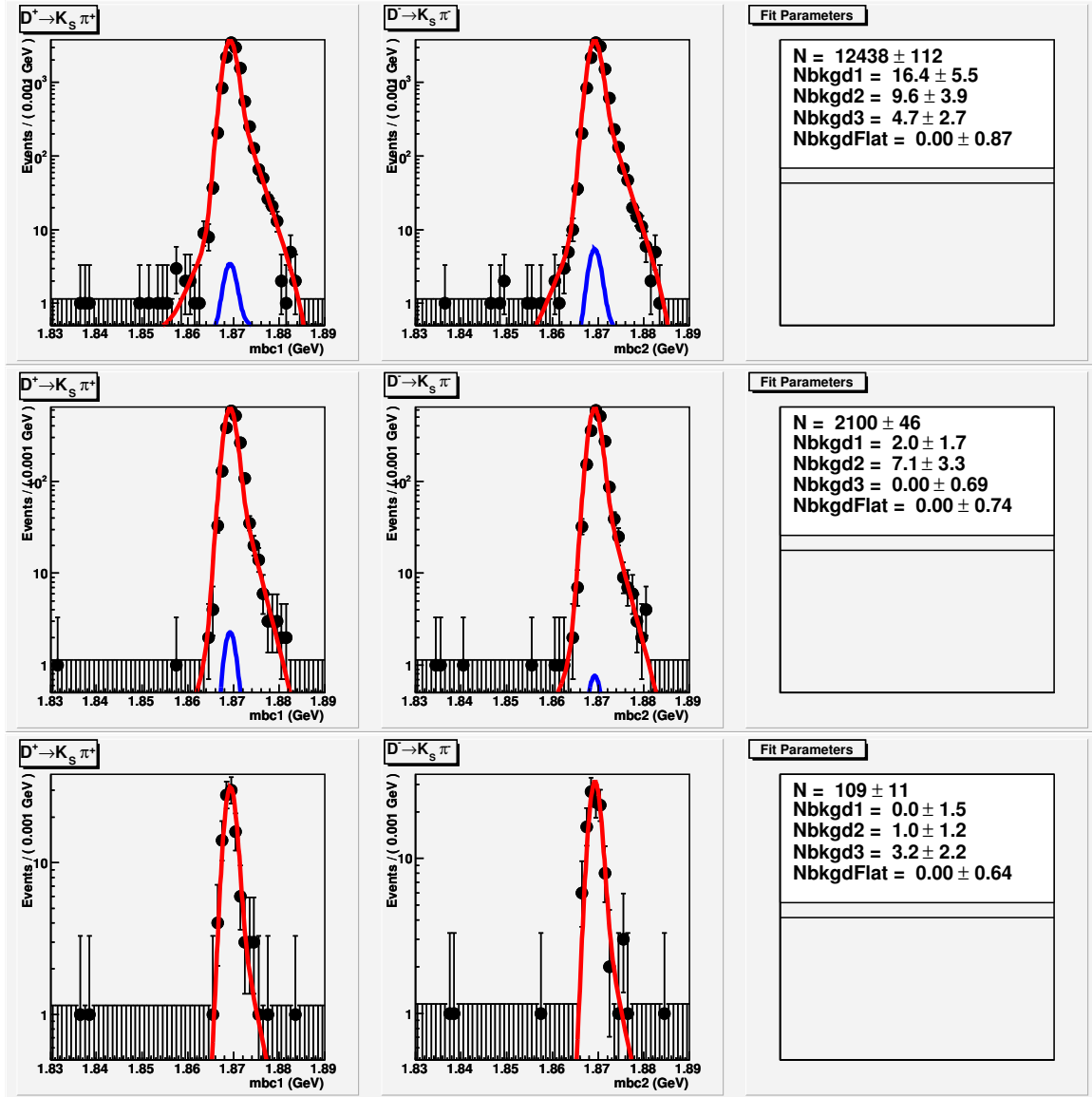


Figure 39: Fits for $K_S \pi$ v.s. $K_S \pi$ double tags. Top is signal Monte Carlo, middle is generic $D\bar{D}$ Monte Carlo and bottom is data.

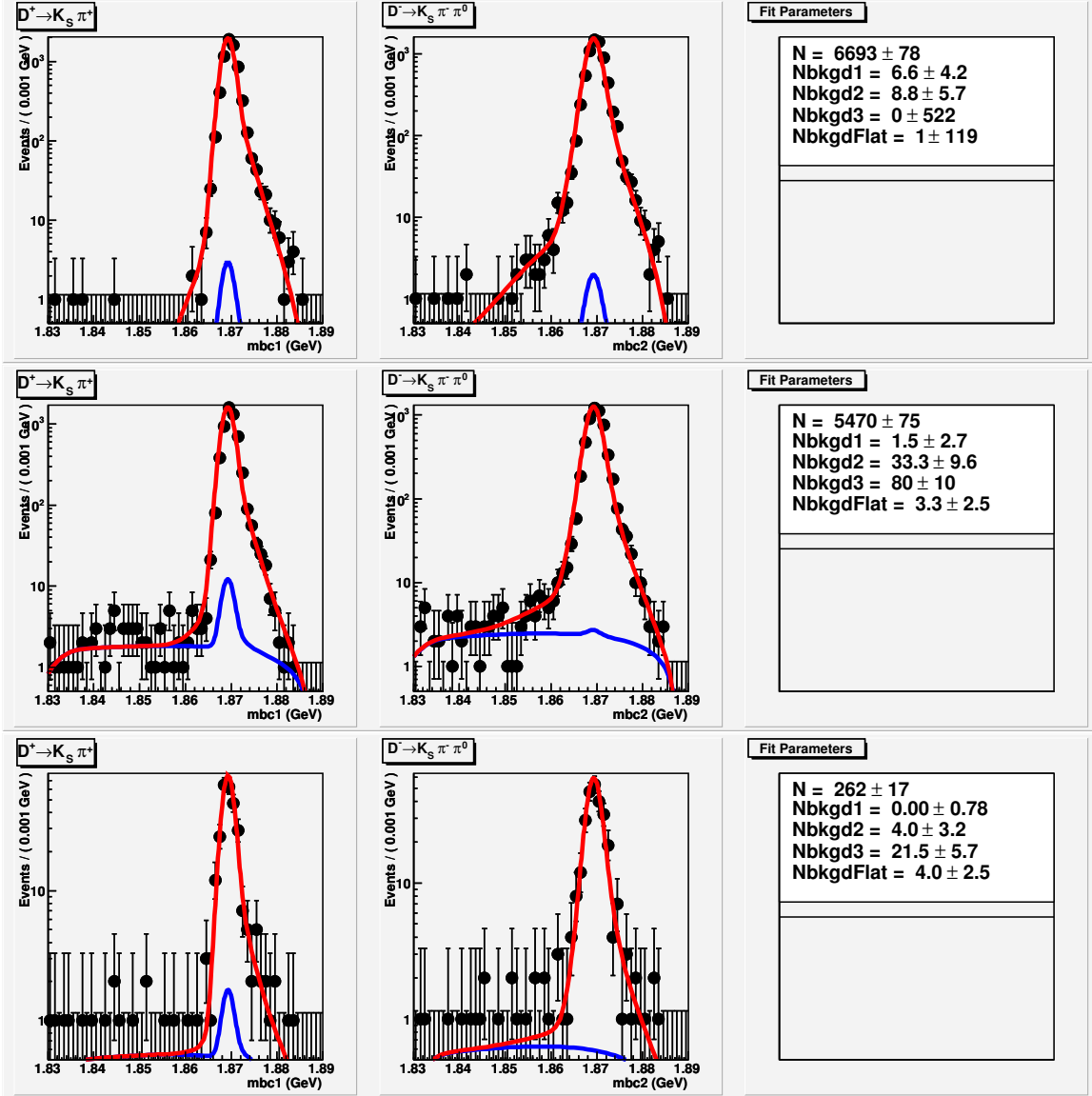


Figure 40: Fits for $K_S\pi$ v.s. $K_S\pi\pi^0$ double tags. Top is signal Monte Carlo, middle is generic $D\bar{D}$ Monte Carlo and bottom is data.

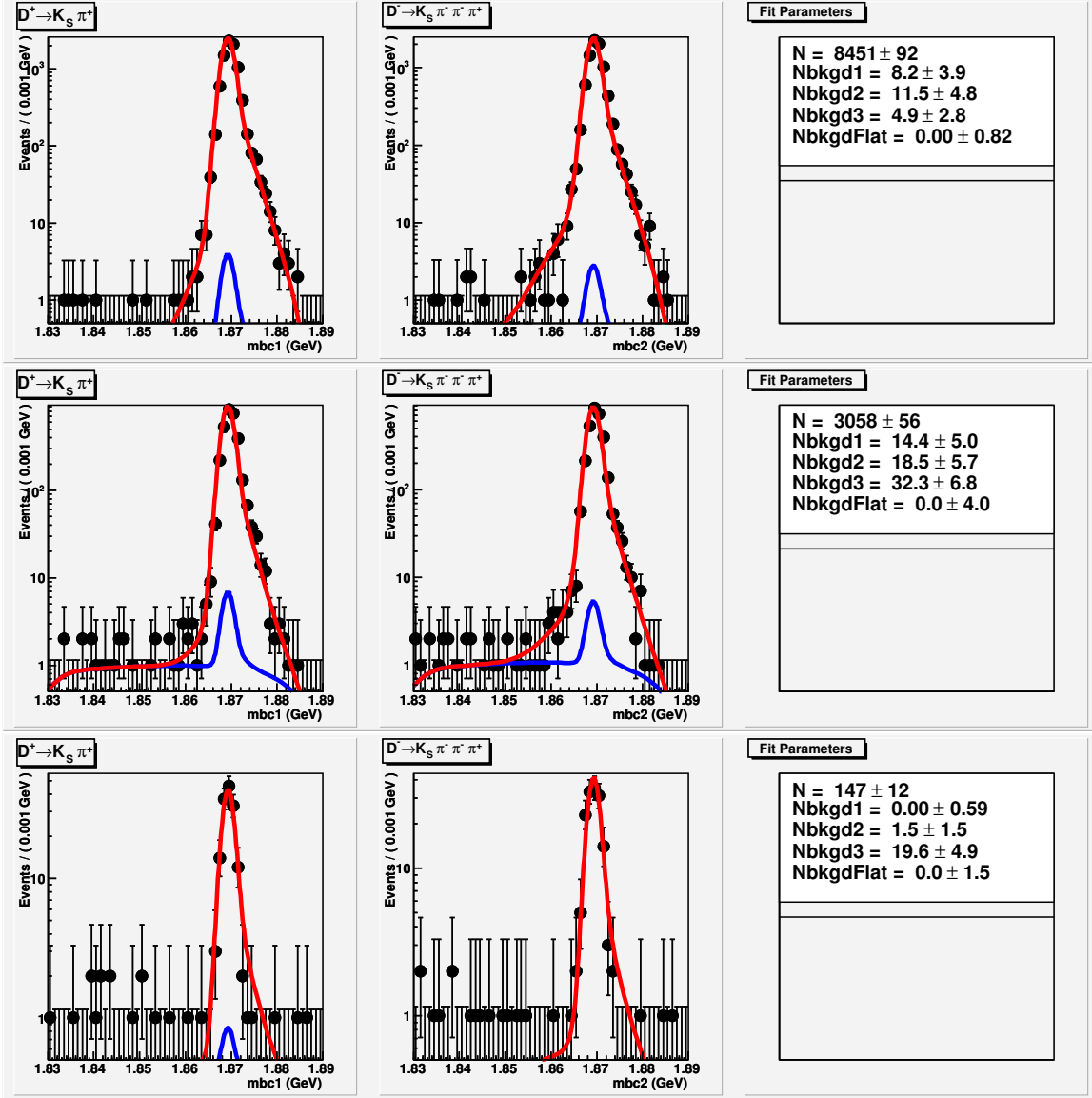


Figure 41: Fits for $K_S\pi$ v.s. $K_S\pi\pi\pi$ double tags. Top is signal Monte Carlo, middle is generic $D\bar{D}$ Monte Carlo and bottom is data.

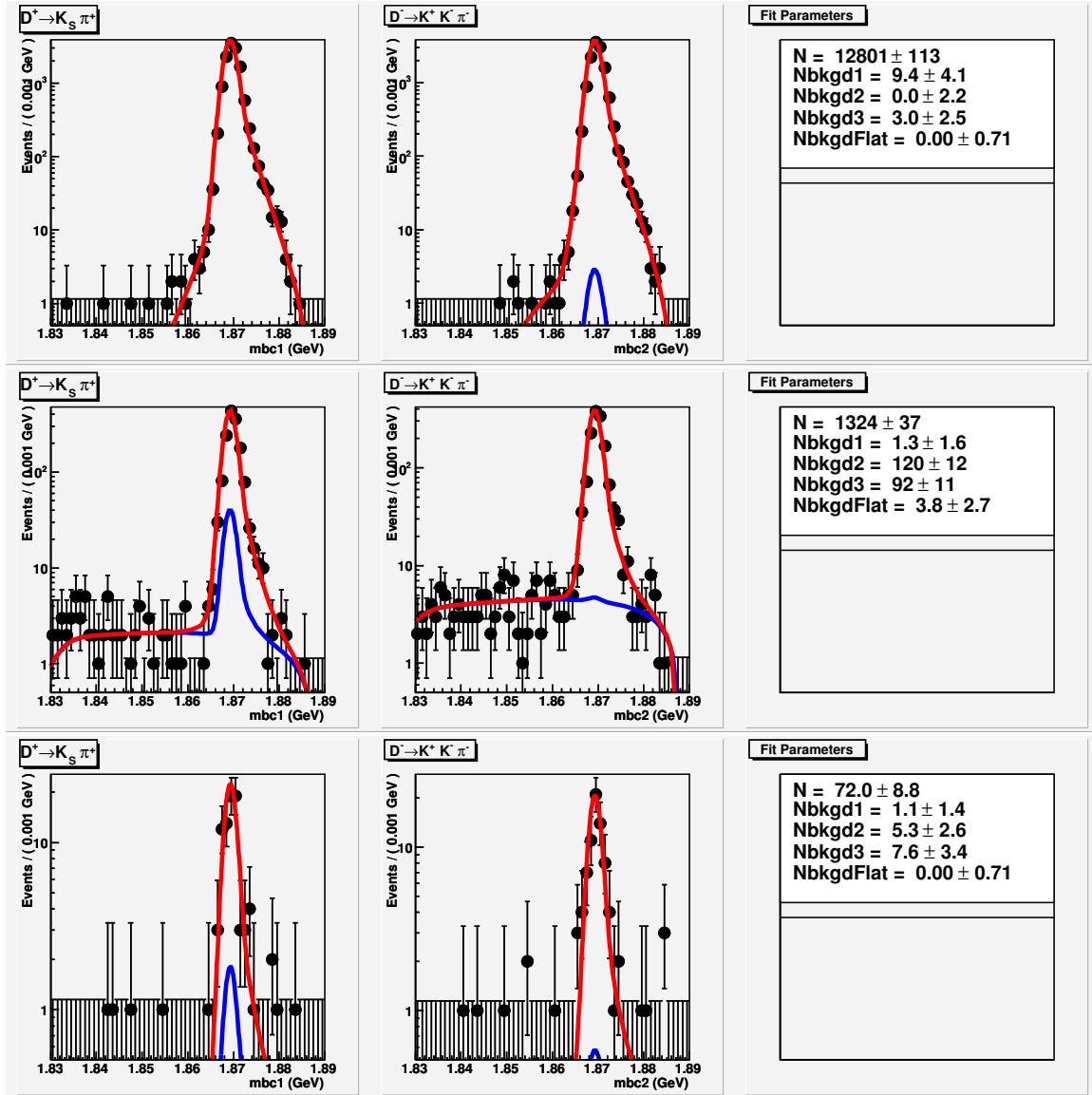


Figure 42: Fits for $K_S \pi$ v.s. $KK\pi$ double tags. Top is signal Monte Carlo, middle is generic $D\bar{D}$ Monte Carlo and bottom is data.

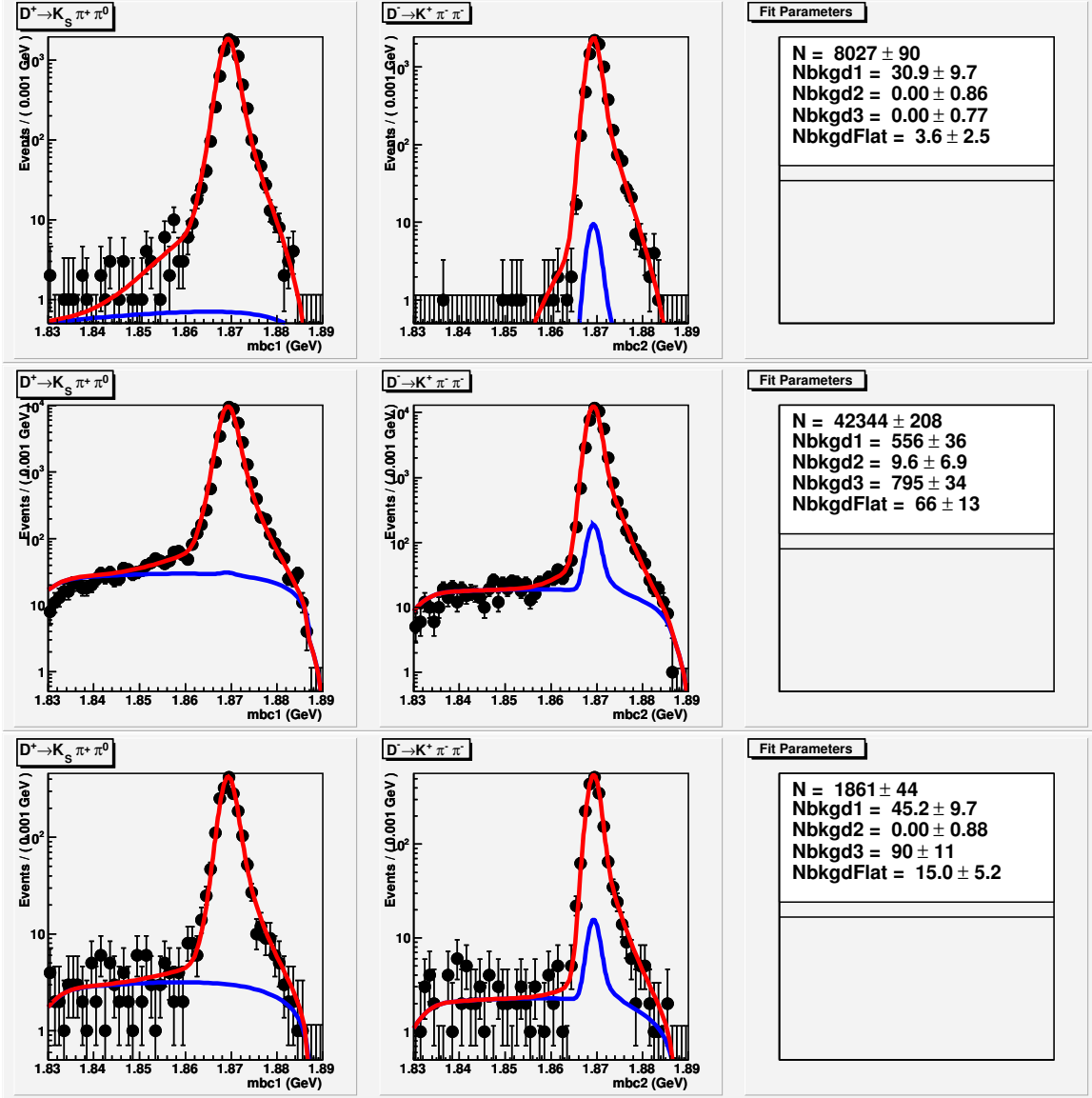


Figure 43: Fits for $K_S \pi\pi^0$ v.s. $K\pi\pi$ double tags. Top is signal Monte Carlo, middle is generic $D\bar{D}$ Monte Carlo and bottom is data.

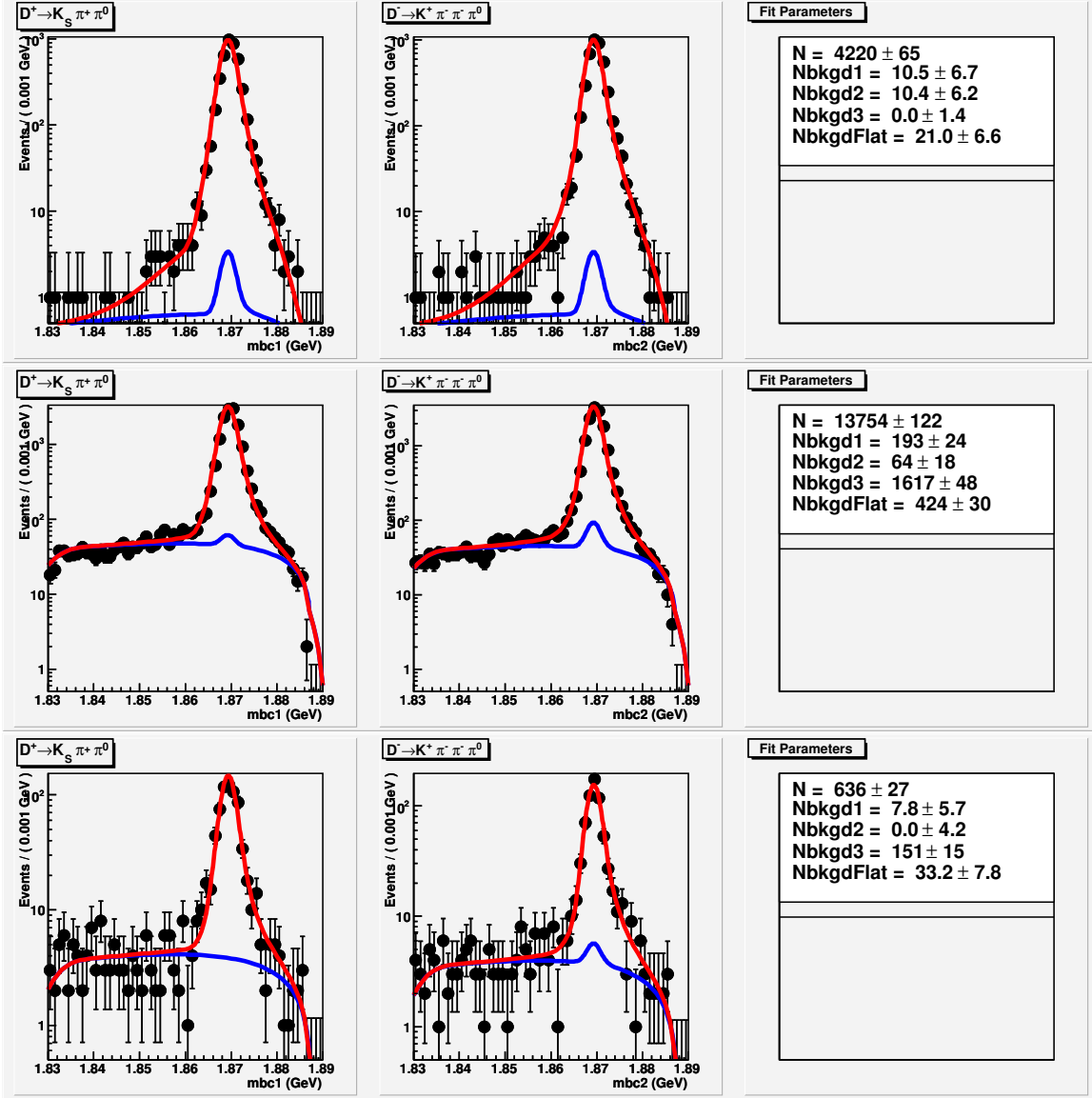


Figure 44: Fits for $K_S \pi\pi^0$ v.s. $K\pi\pi\pi^0$ double tags. Top is signal Monte Carlo, middle is generic $D\bar{D}$ Monte Carlo and bottom is data.

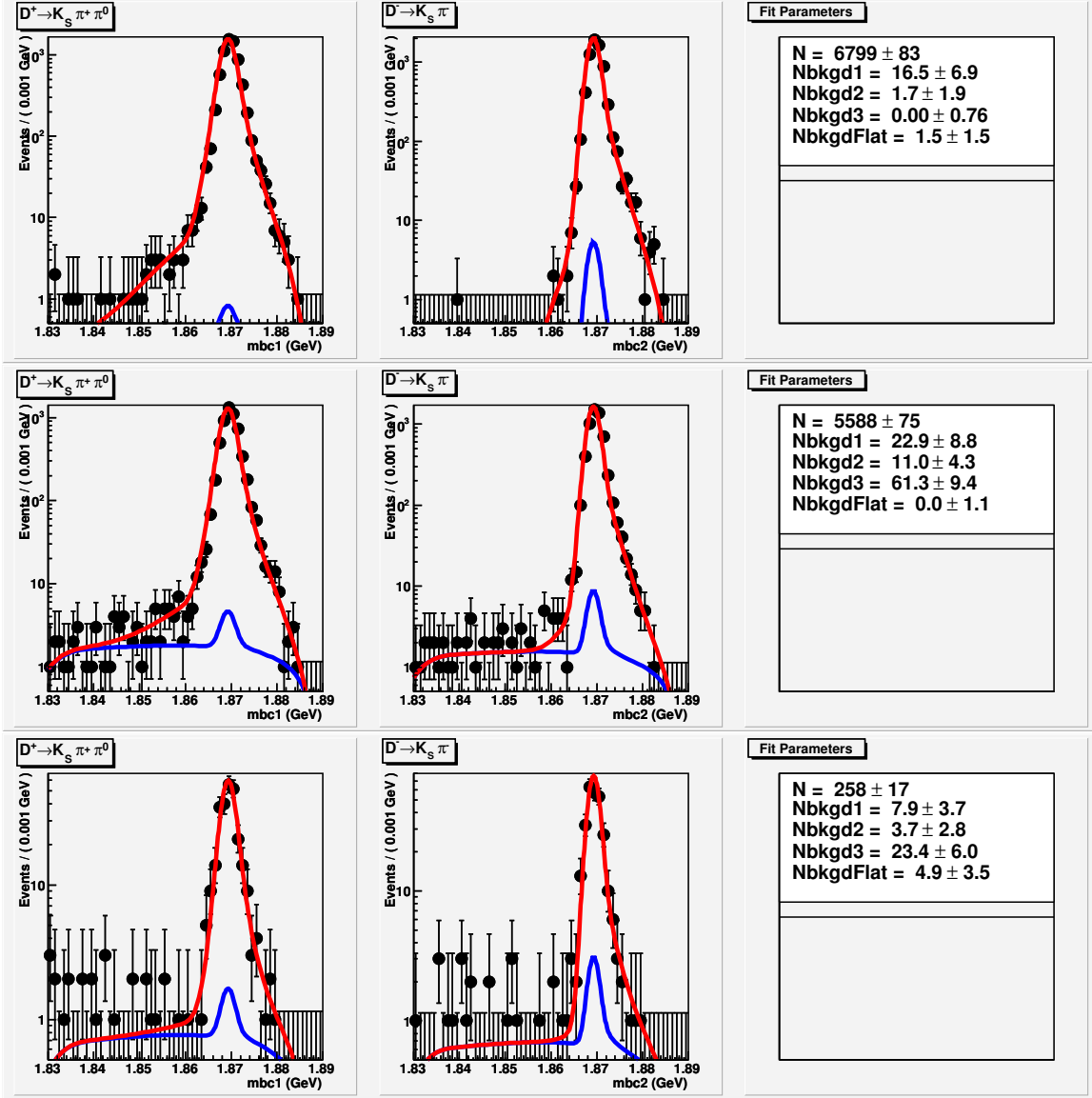


Figure 45: Fits for $K_S \pi\pi^0$ v.s. $K_S\pi$ double tags. Top is signal Monte Carlo, middle is generic $D\bar{D}$ Monte Carlo and bottom is data.

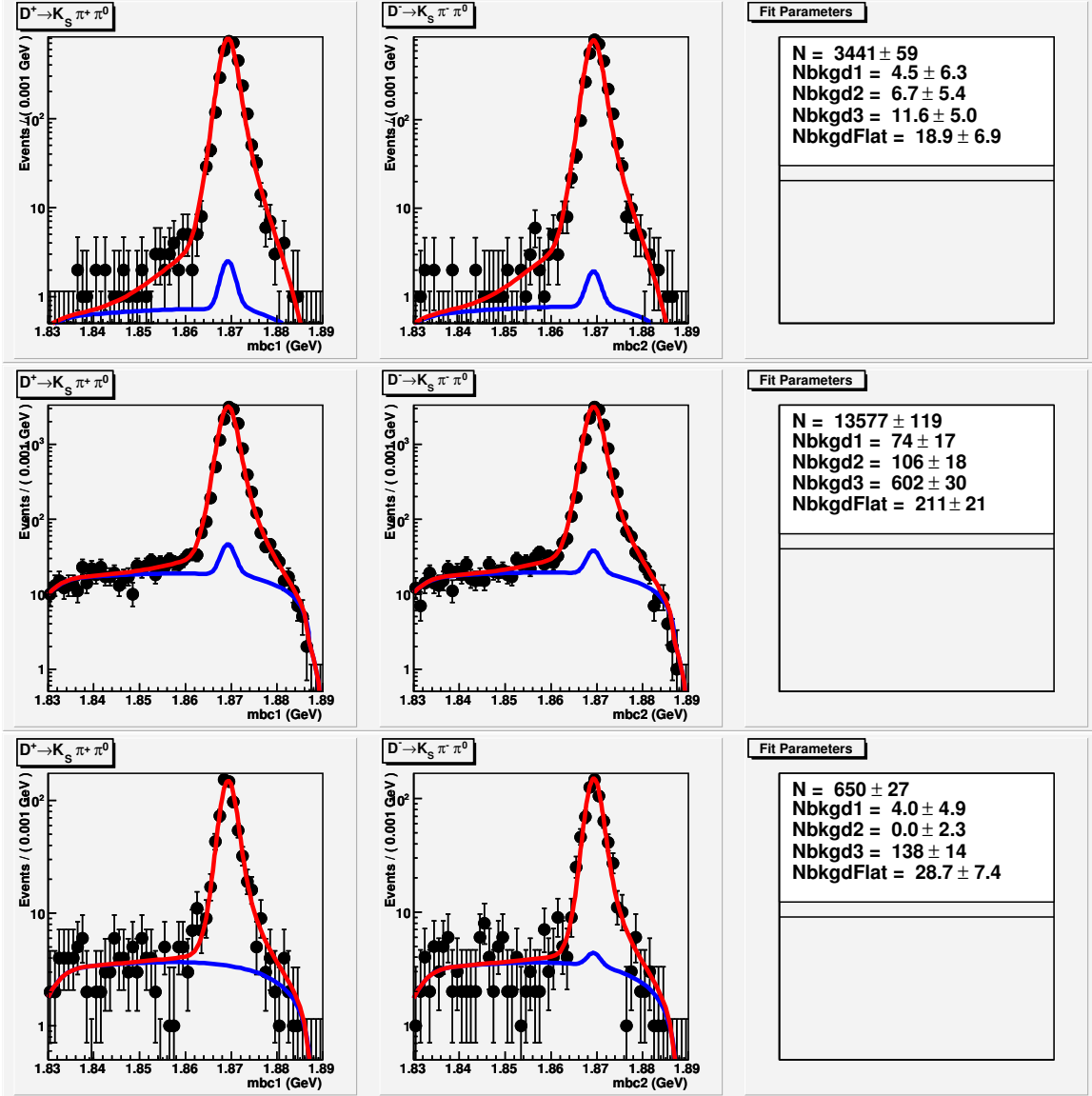


Figure 46: Fits for $K_S \pi^0$ v.s. $K_S \pi^0$ double tags. Top is signal Monte Carlo, middle is generic $D\bar{D}$ Monte Carlo and bottom is data.

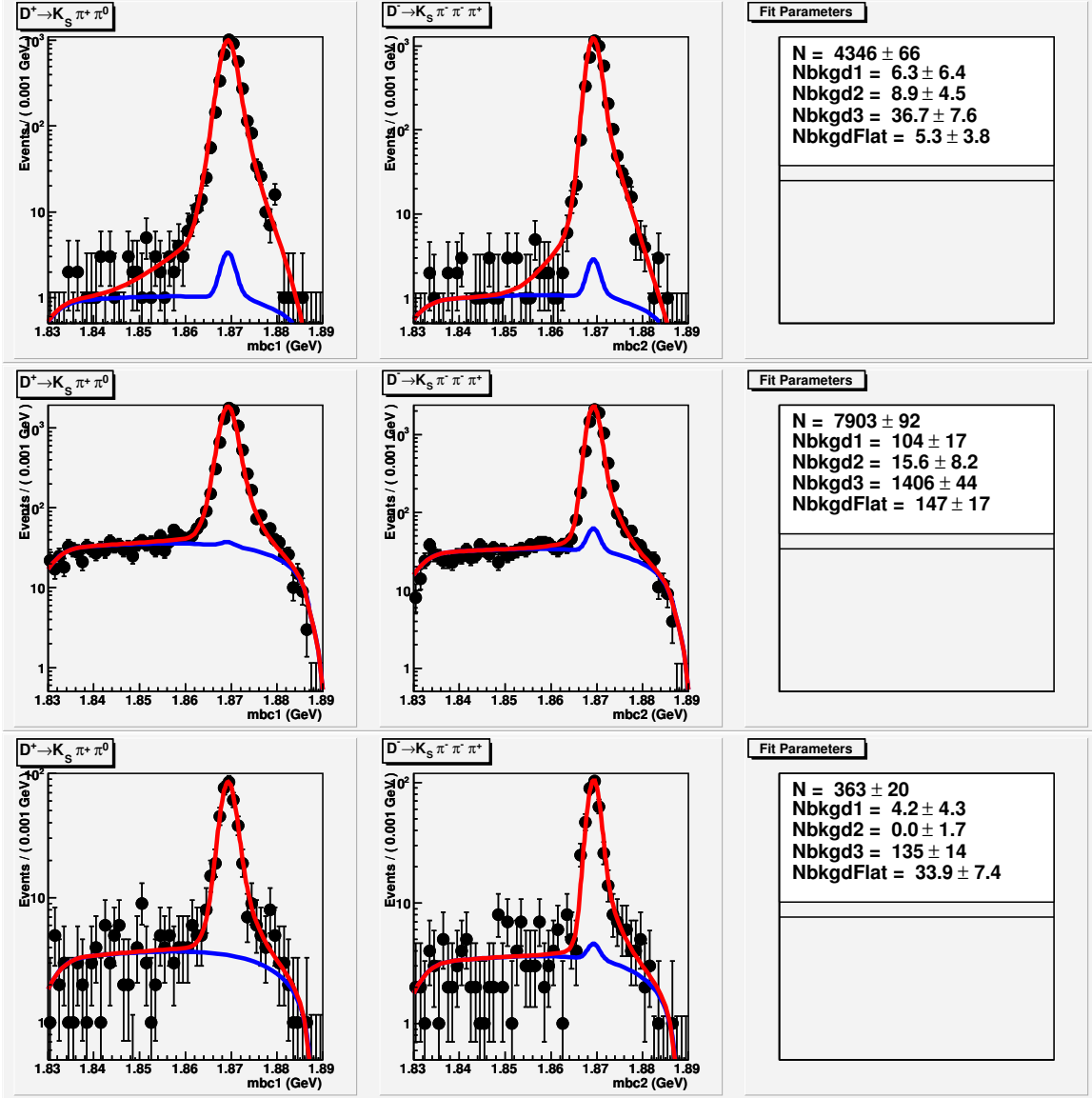


Figure 47: Fits for $K_S \pi\pi^0$ v.s. $K_S \pi\pi\pi$ double tags. Top is signal Monte Carlo, middle is generic $D\bar{D}$ Monte Carlo and bottom is data.

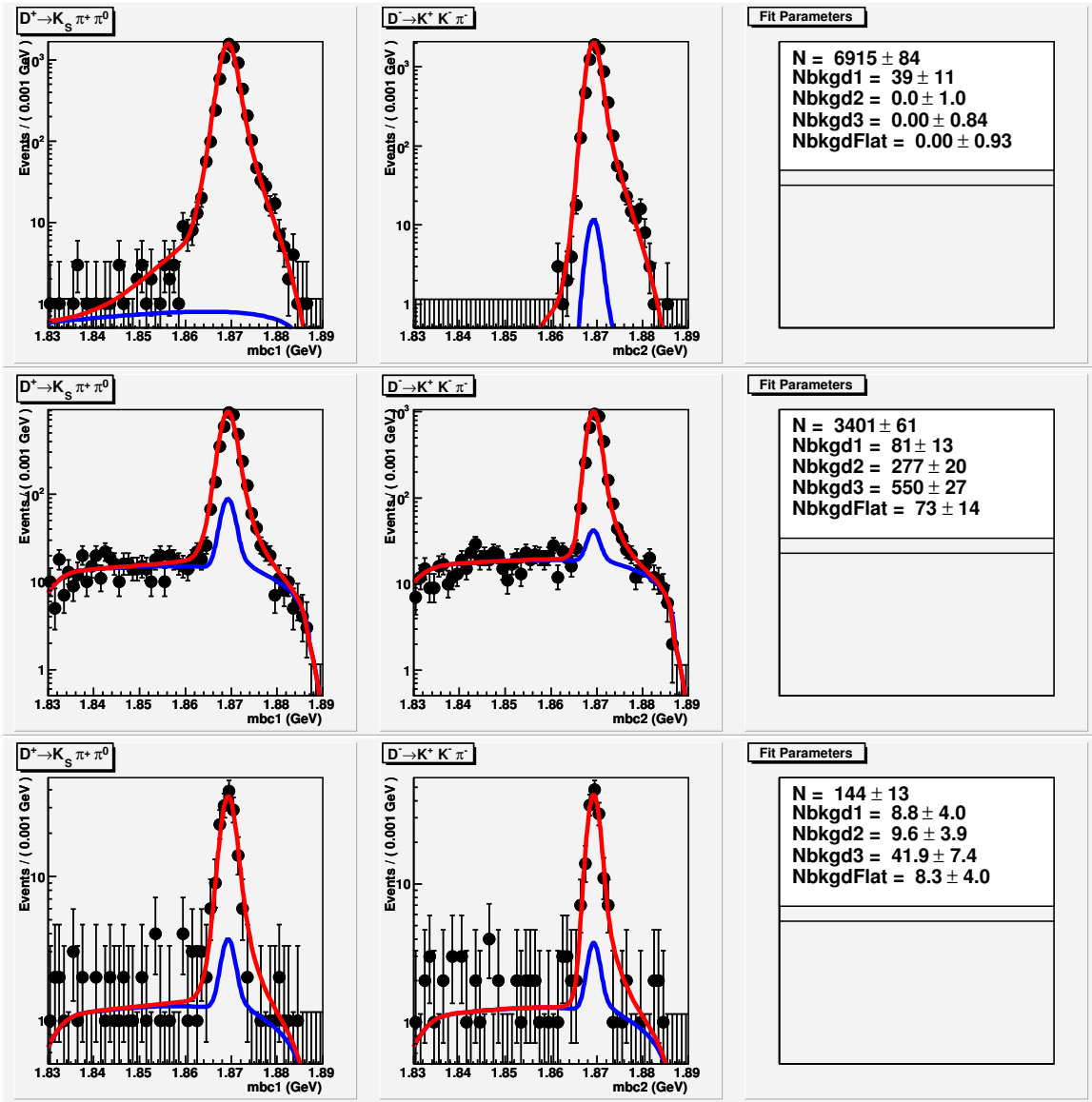


Figure 48: Fits for $K_S \pi\pi^0$ v.s. $KK\pi$ double tags. Top is signal Monte Carlo, middle is generic $D\bar{D}$ Monte Carlo and bottom is data.

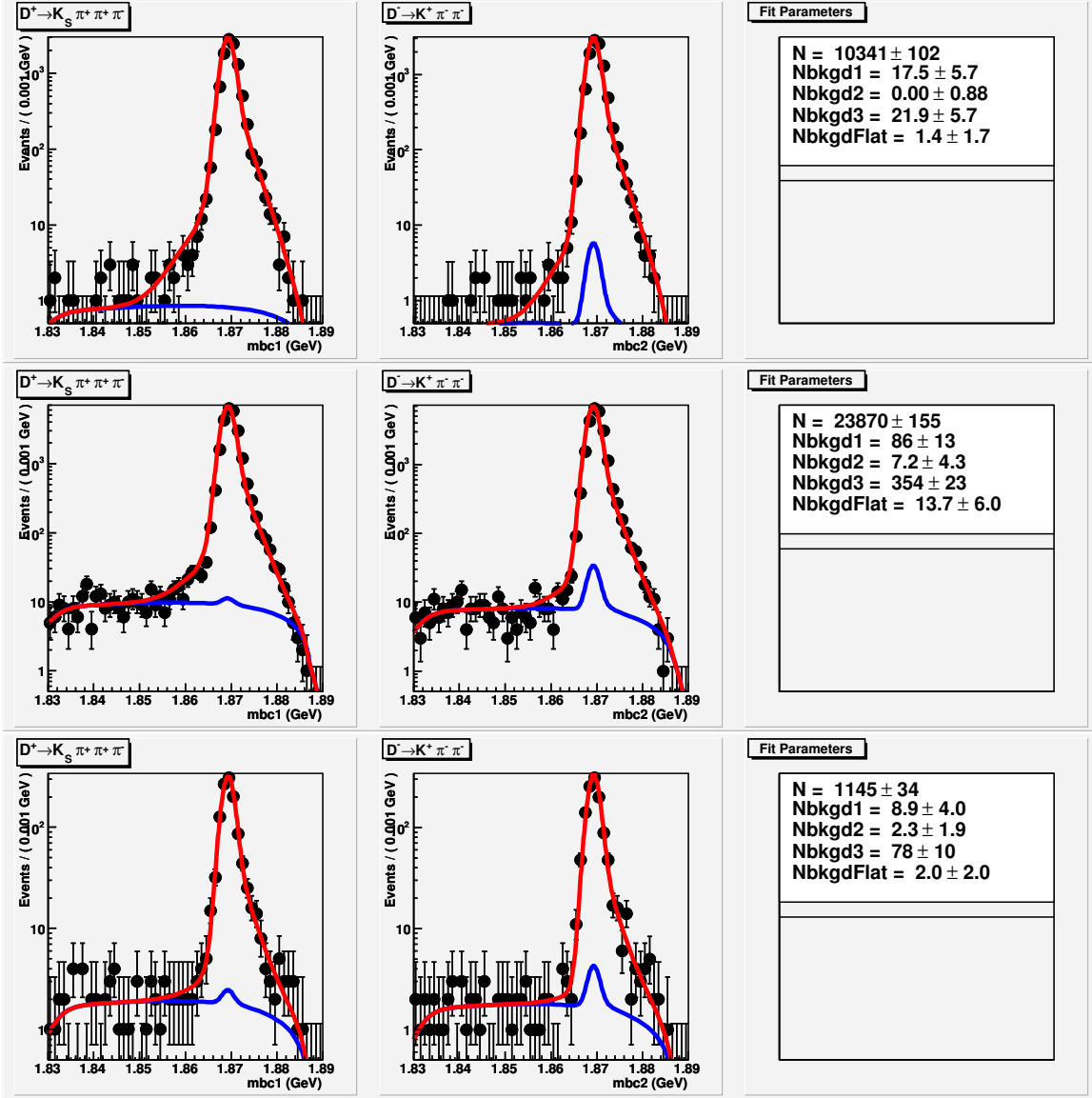


Figure 49: Fits for $K_S \pi\pi\pi$ v.s. $K\pi\pi$ double tags. Top is signal Monte Carlo, middle is generic $D\bar{D}$ Monte Carlo and bottom is data.

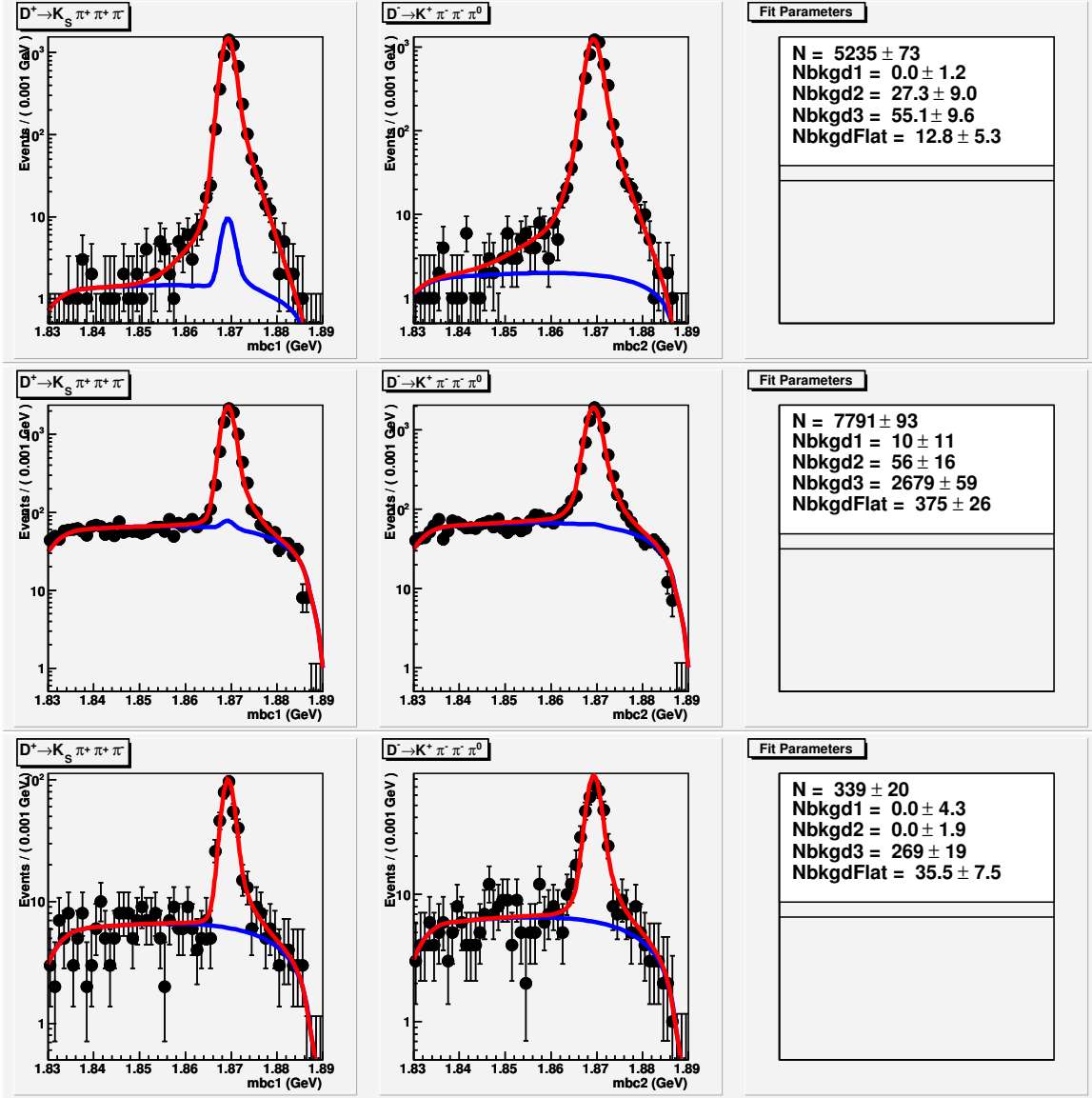


Figure 50: Fits for $K_S \pi\pi\pi$ v.s. $K\pi\pi\pi^0$ double tags. Top is signal Monte Carlo, middle is generic $D\bar{D}$ Monte Carlo and bottom is data.

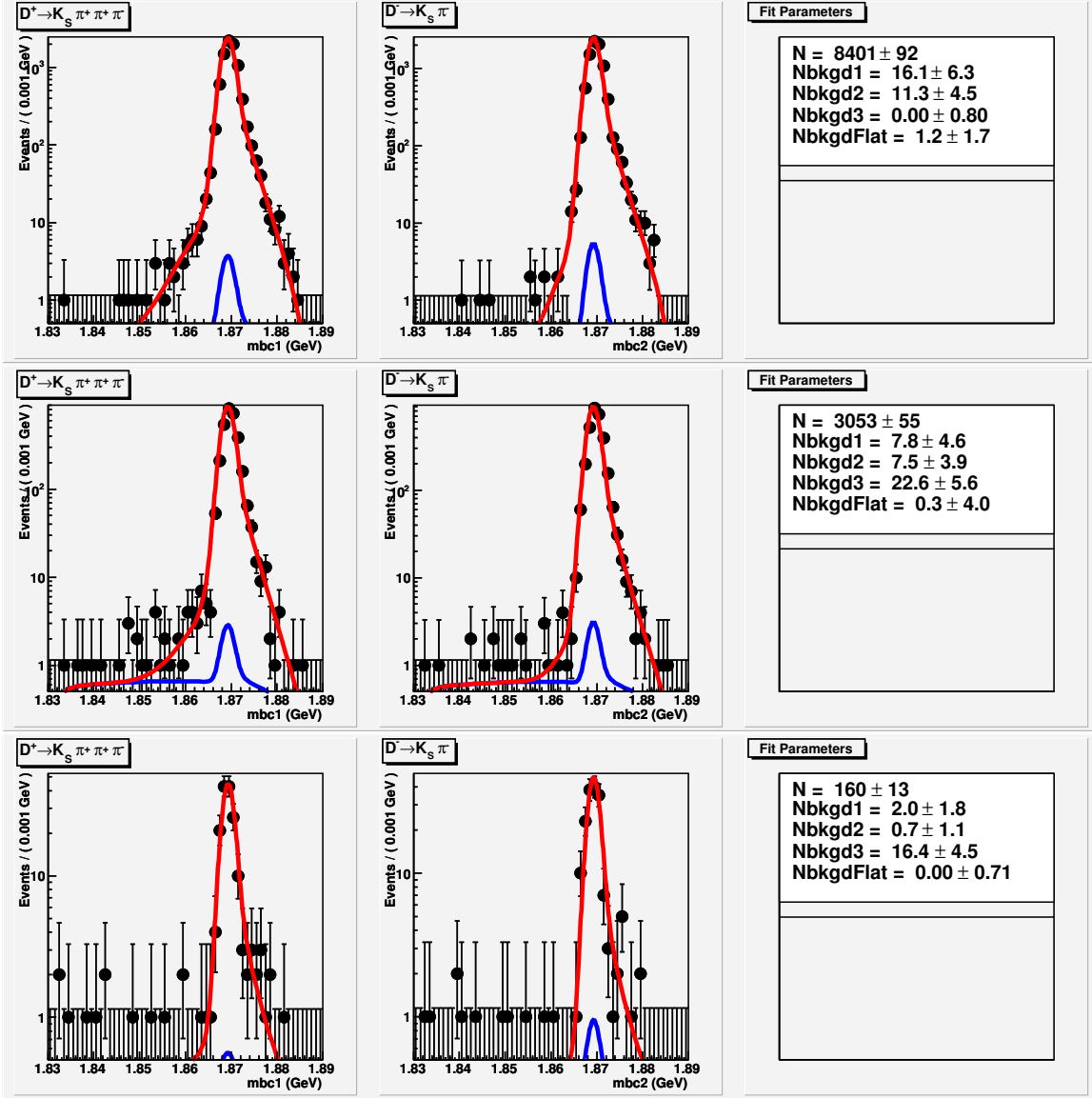


Figure 51: Fits for $K_S \pi \pi \pi$ v.s. $K_S \pi$ double tags. Top is signal Monte Carlo, middle is generic $D\bar{D}$ Monte Carlo and bottom is data.

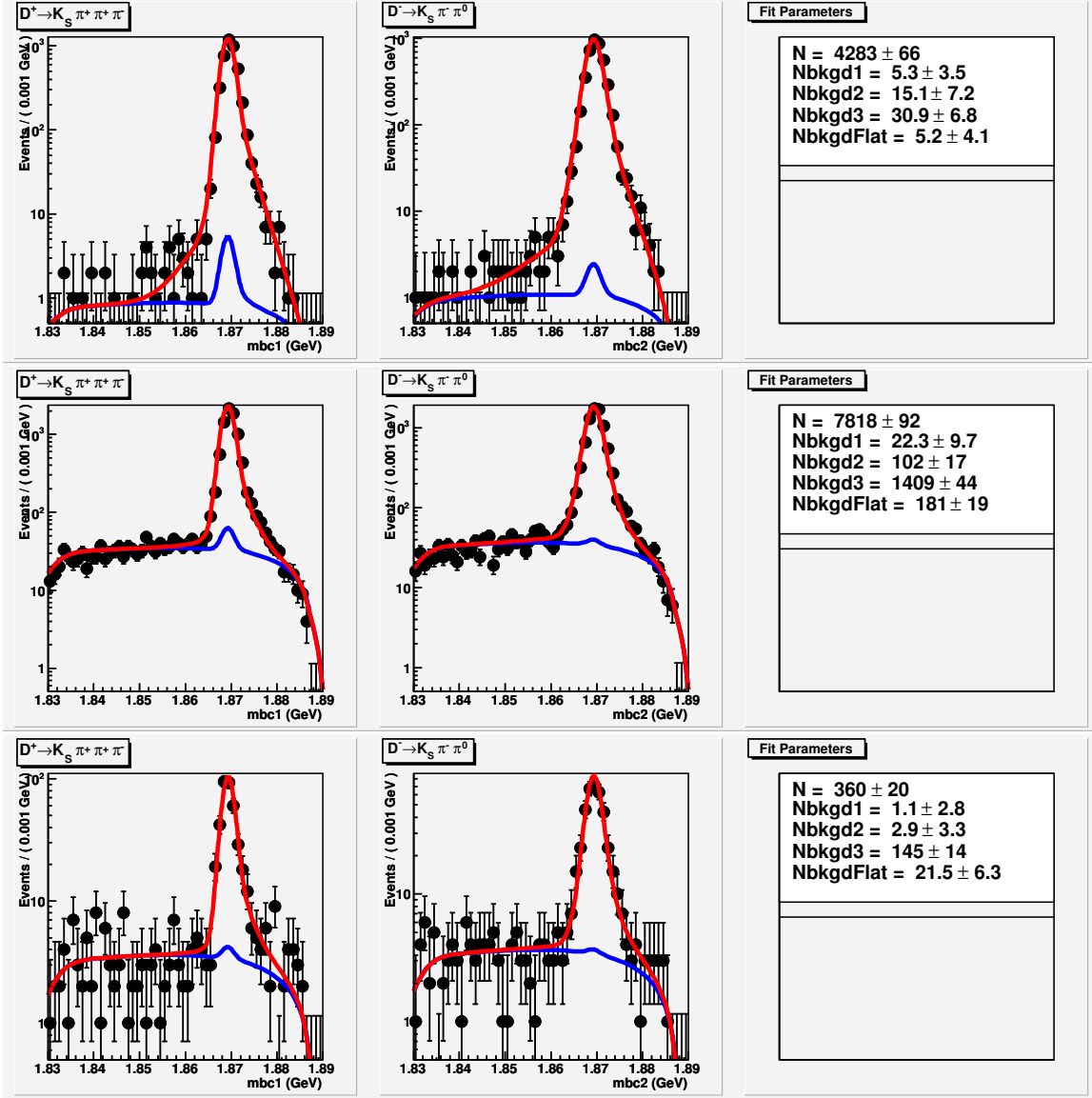


Figure 52: Fits for $K_S \pi\pi\pi$ v.s. $K_S \pi\pi^0$ double tags. Top is signal Monte Carlo, middle is generic $D\bar{D}$ Monte Carlo and bottom is data.

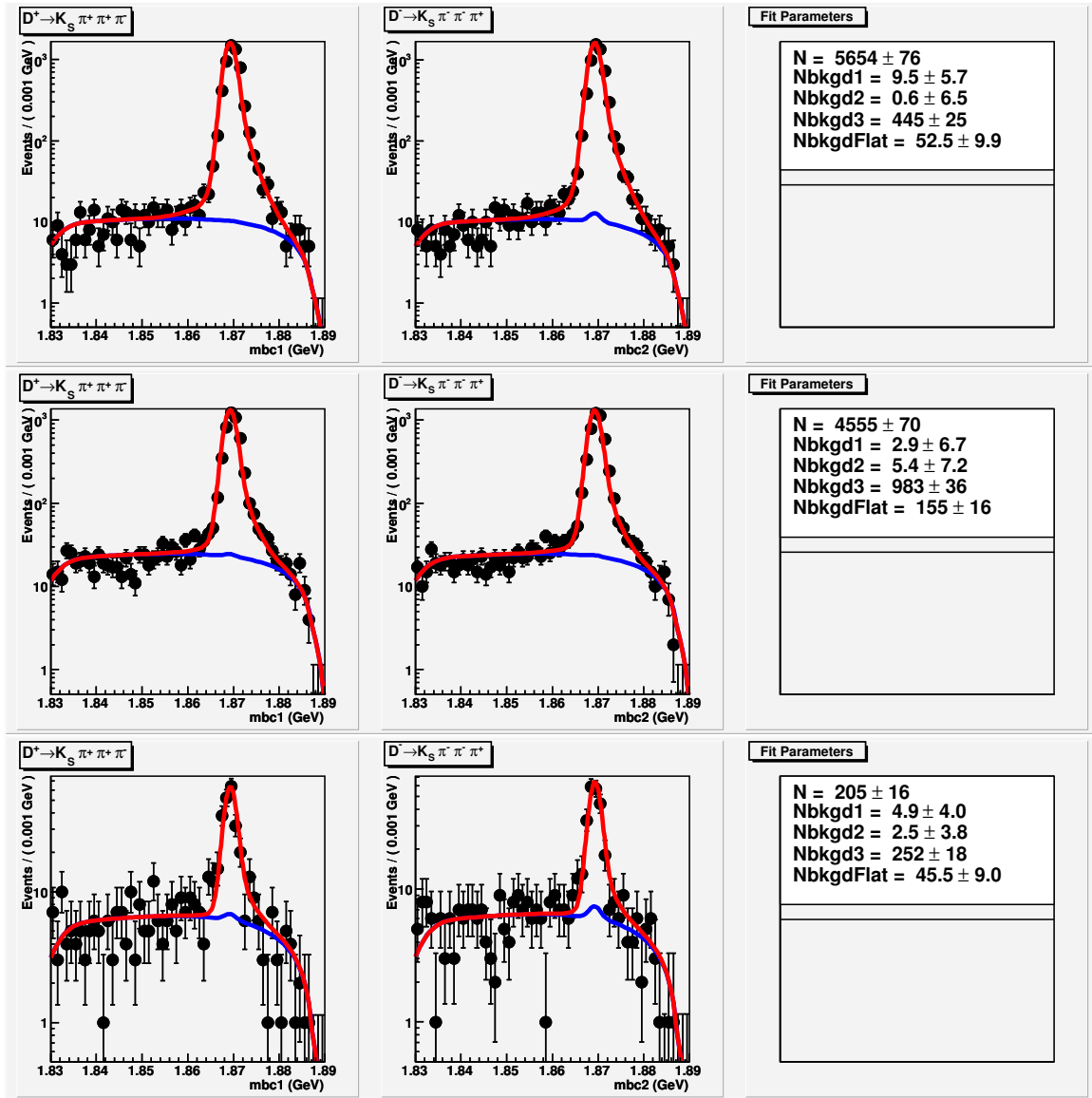


Figure 53: Fits for $K_S \pi\pi\pi$ v.s. $K_S \pi\pi\pi$ double tags. Top is signal Monte Carlo, middle is generic $D\bar{D}$ Monte Carlo and bottom is data.

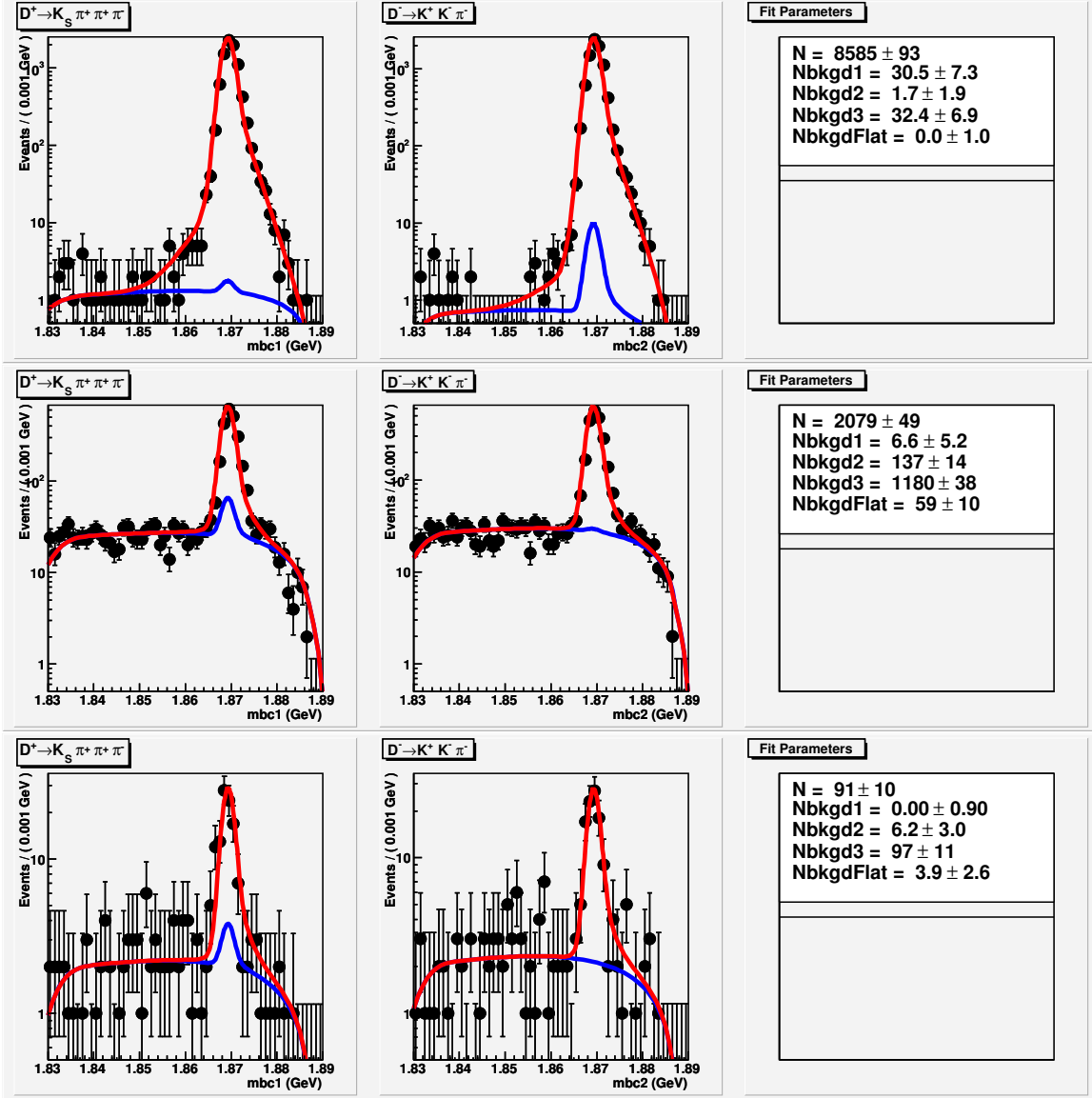


Figure 54: Fits for $K_S \pi\pi\pi$ v.s. $KK\pi$ double tags. Top is signal Monte Carlo, middle is generic $D\bar{D}$ Monte Carlo and bottom is data.

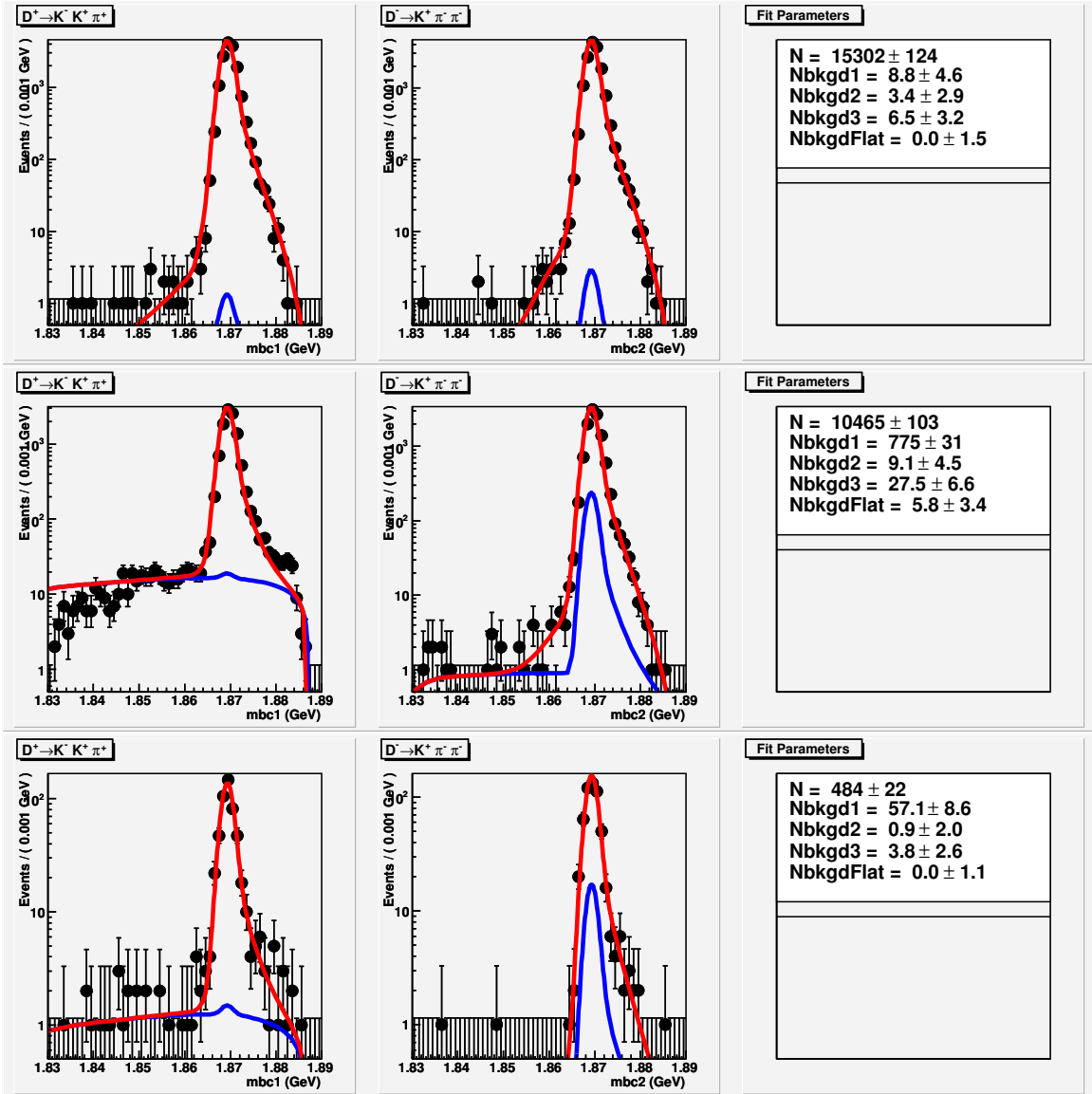


Figure 55: Fits for $KK\pi$ v.s. $K\pi\pi$ double tags. Top is signal Monte Carlo, middle is generic $D\bar{D}$ Monte Carlo and bottom is data.

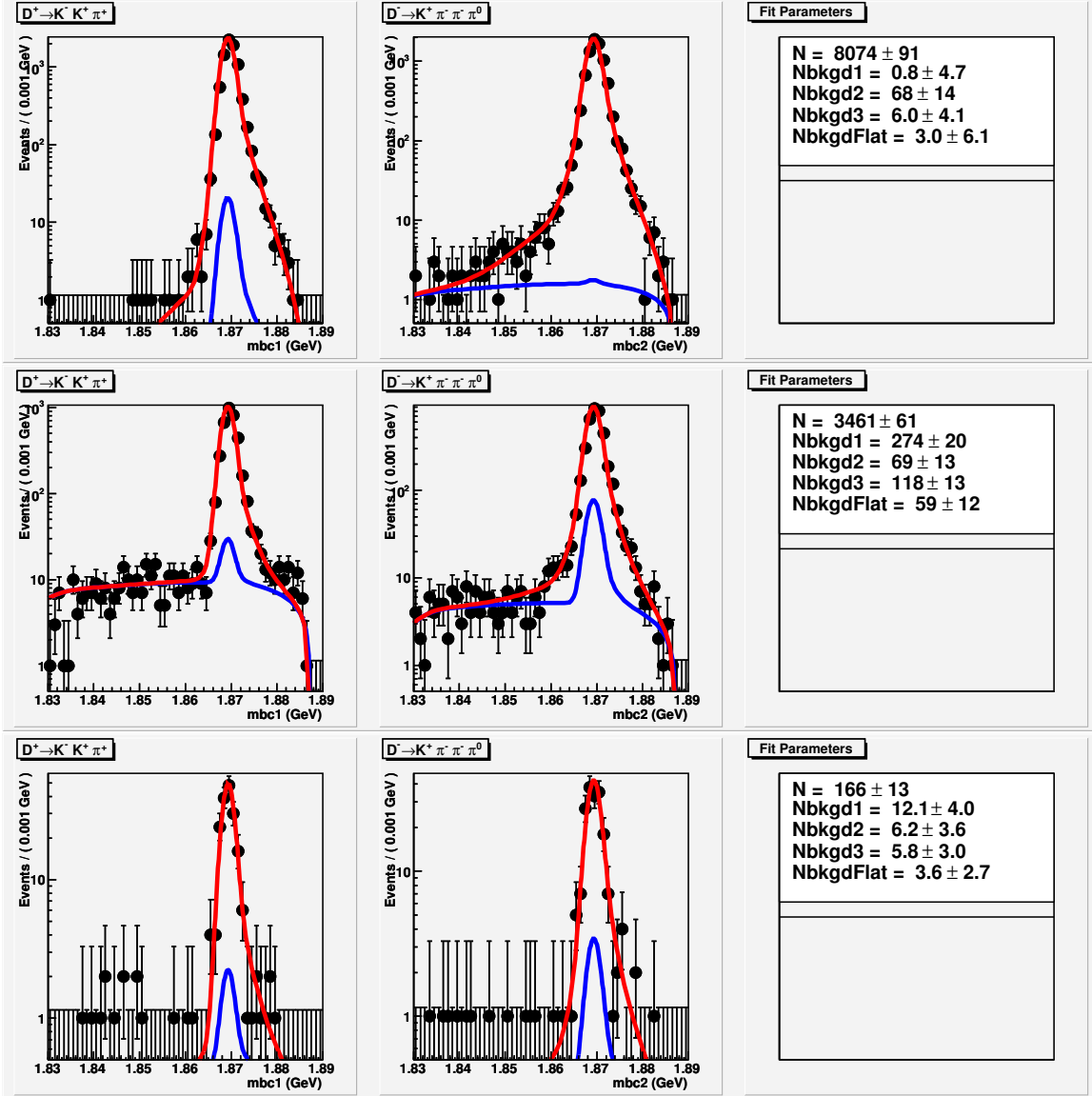


Figure 56: Fits for $KK\pi$ v.s. $K\pi\pi\pi^0$ double tags. Top is signal Monte Carlo, middle is generic $D\bar{D}$ Monte Carlo and bottom is data.

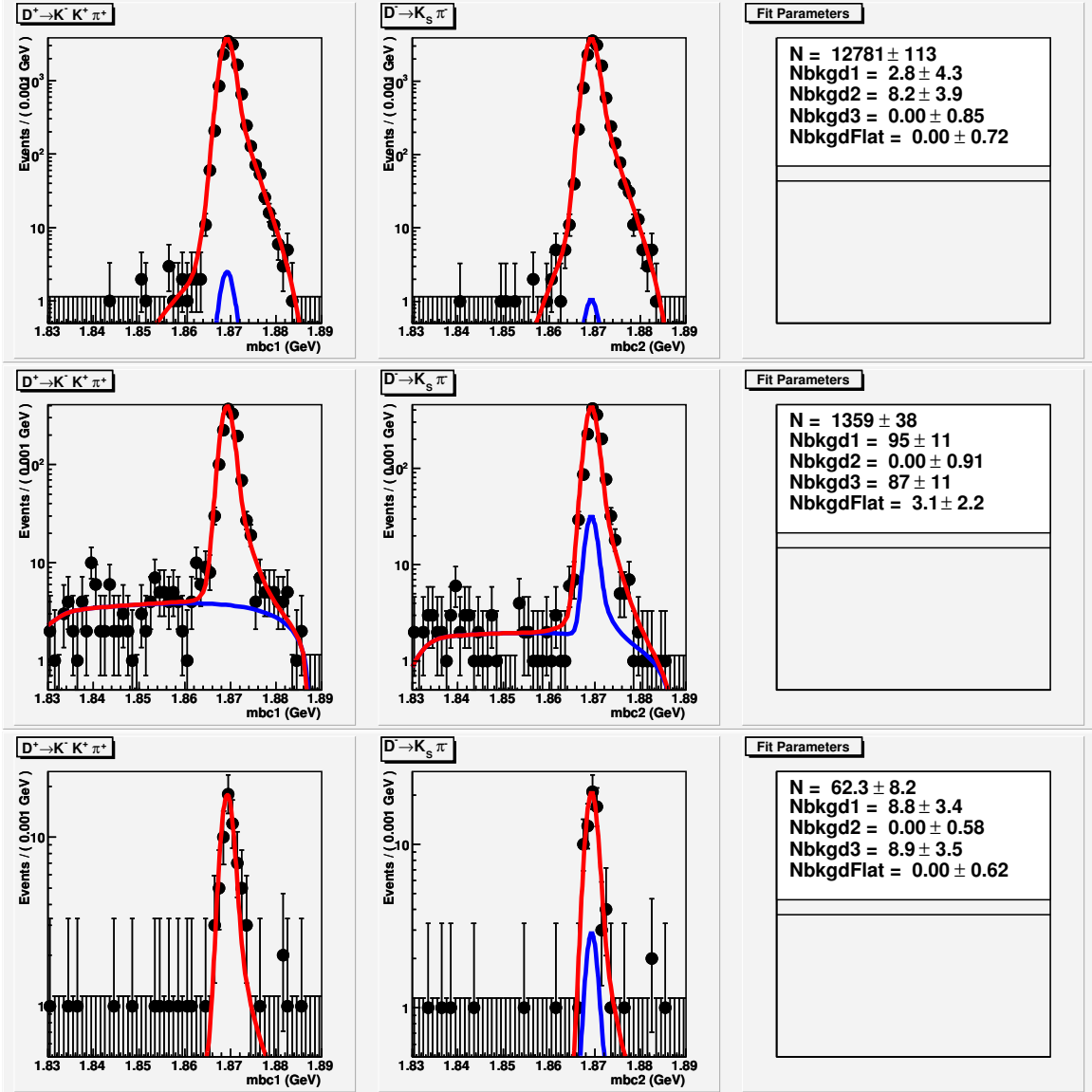


Figure 57: Fits for $KK\pi$ v.s. $K_S\pi$ double tags. Top is signal Monte Carlo, middle is generic $D\bar{D}$ Monte Carlo and bottom is data.

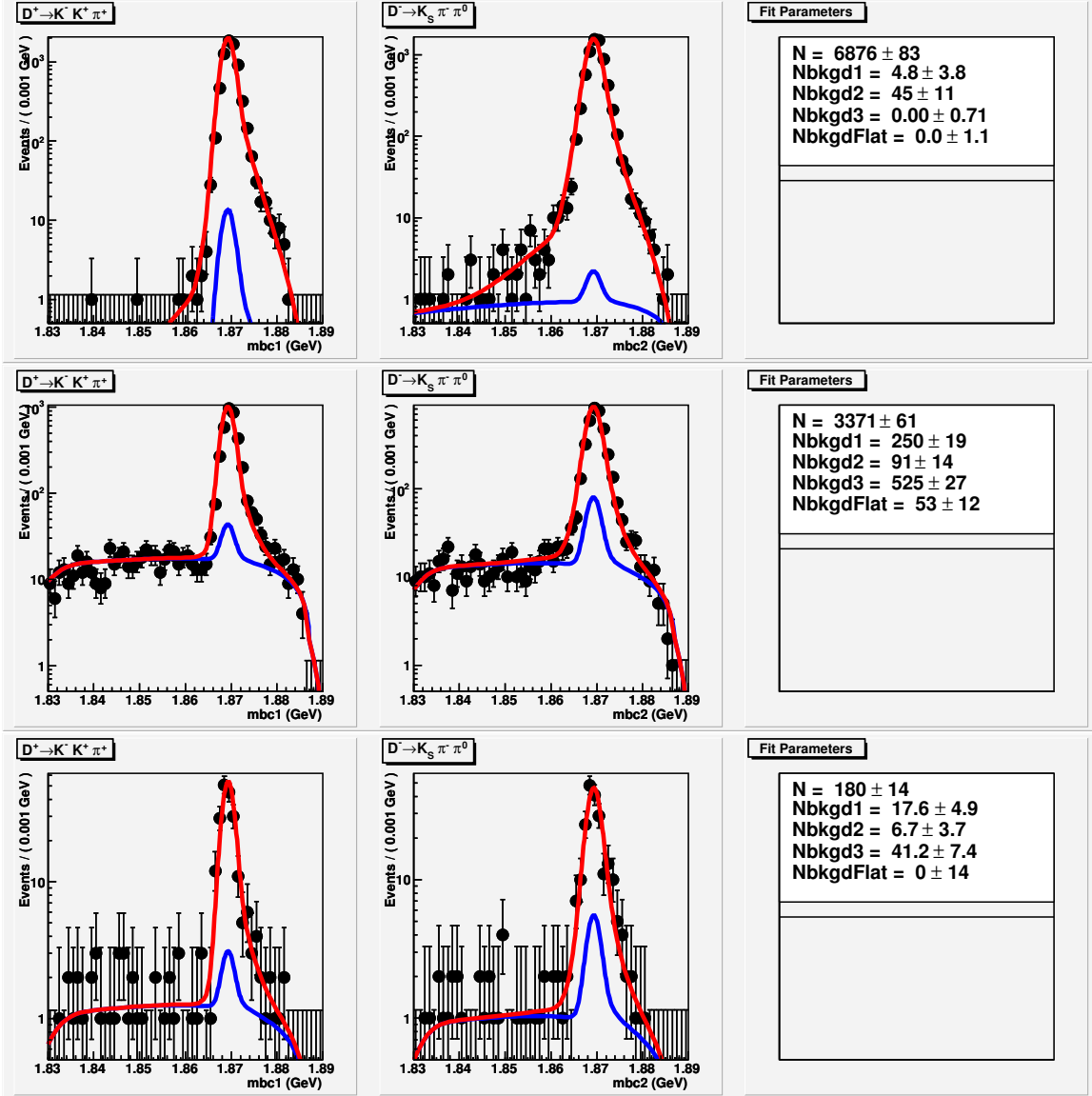


Figure 58: Fits for $KK\pi$ v.s. $K_S\pi\pi^0$ double tags. Top is signal Monte Carlo, middle is generic $D\bar{D}$ Monte Carlo and bottom is data.

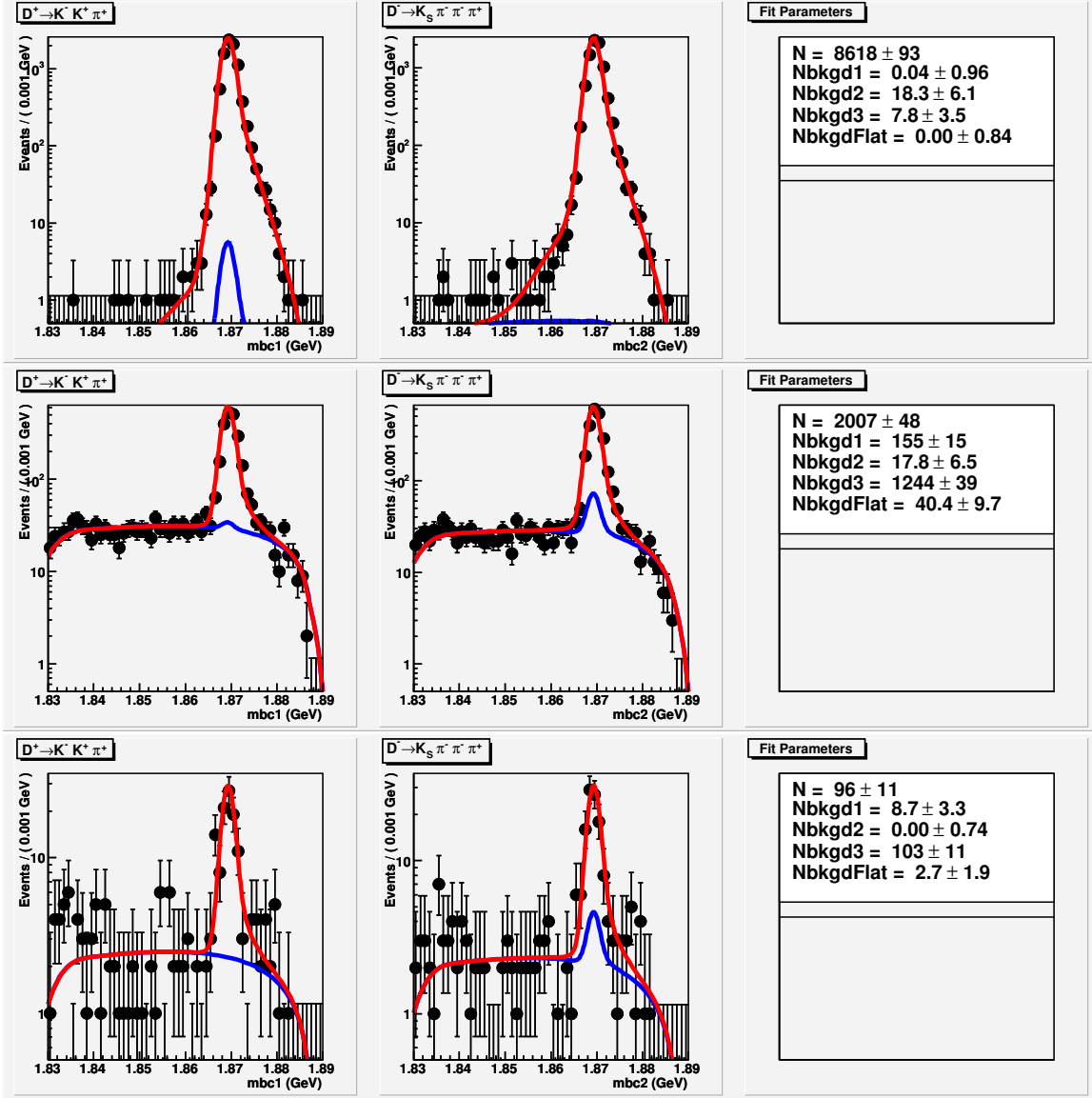


Figure 59: Fits for $KK\pi$ v.s. $K_S\pi\pi\pi$ double tags. Top is signal Monte Carlo, middle is generic $D\bar{D}$ Monte Carlo and bottom is data.

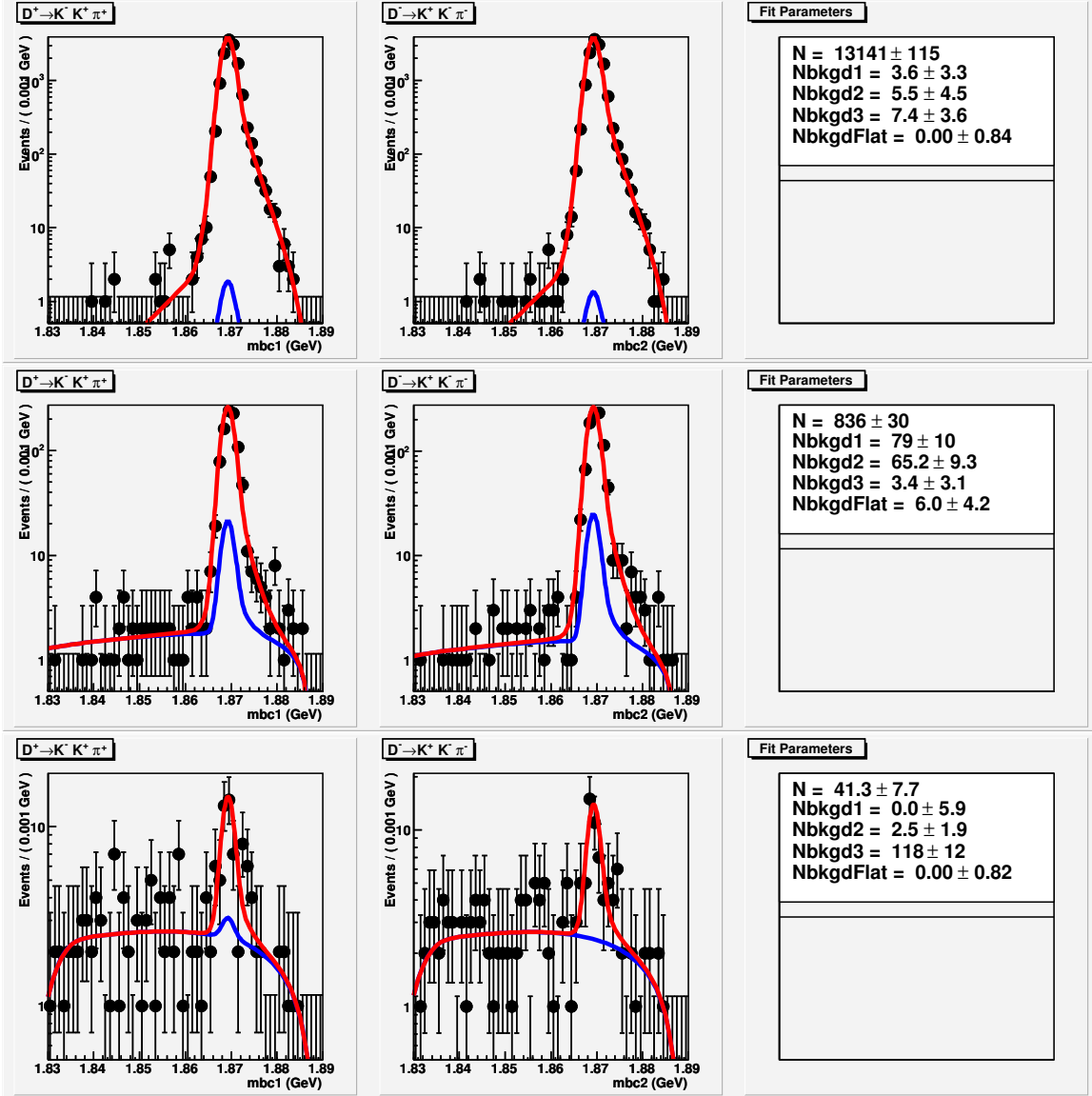


Figure 60: Fits for $KK\pi$ v.s. $KK\pi$ double tags. Top is signal Monte Carlo, middle is generic $D\bar{D}$ Monte Carlo and bottom is data.

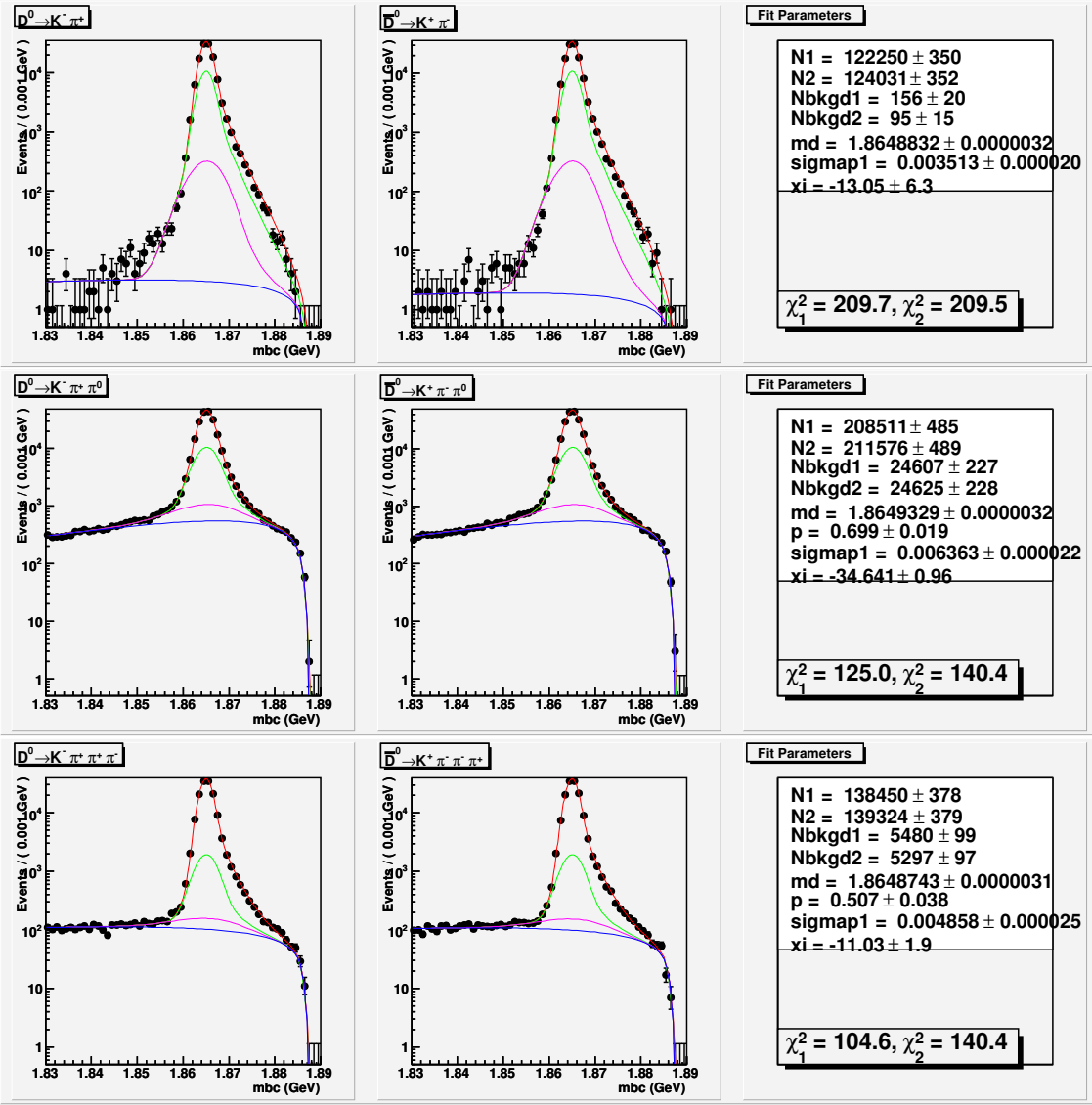


Figure 61: Single tag D^0 yields in signal MC. These plots show the beam constrained mass after choosing a candidate with minimum $|\Delta E|$.

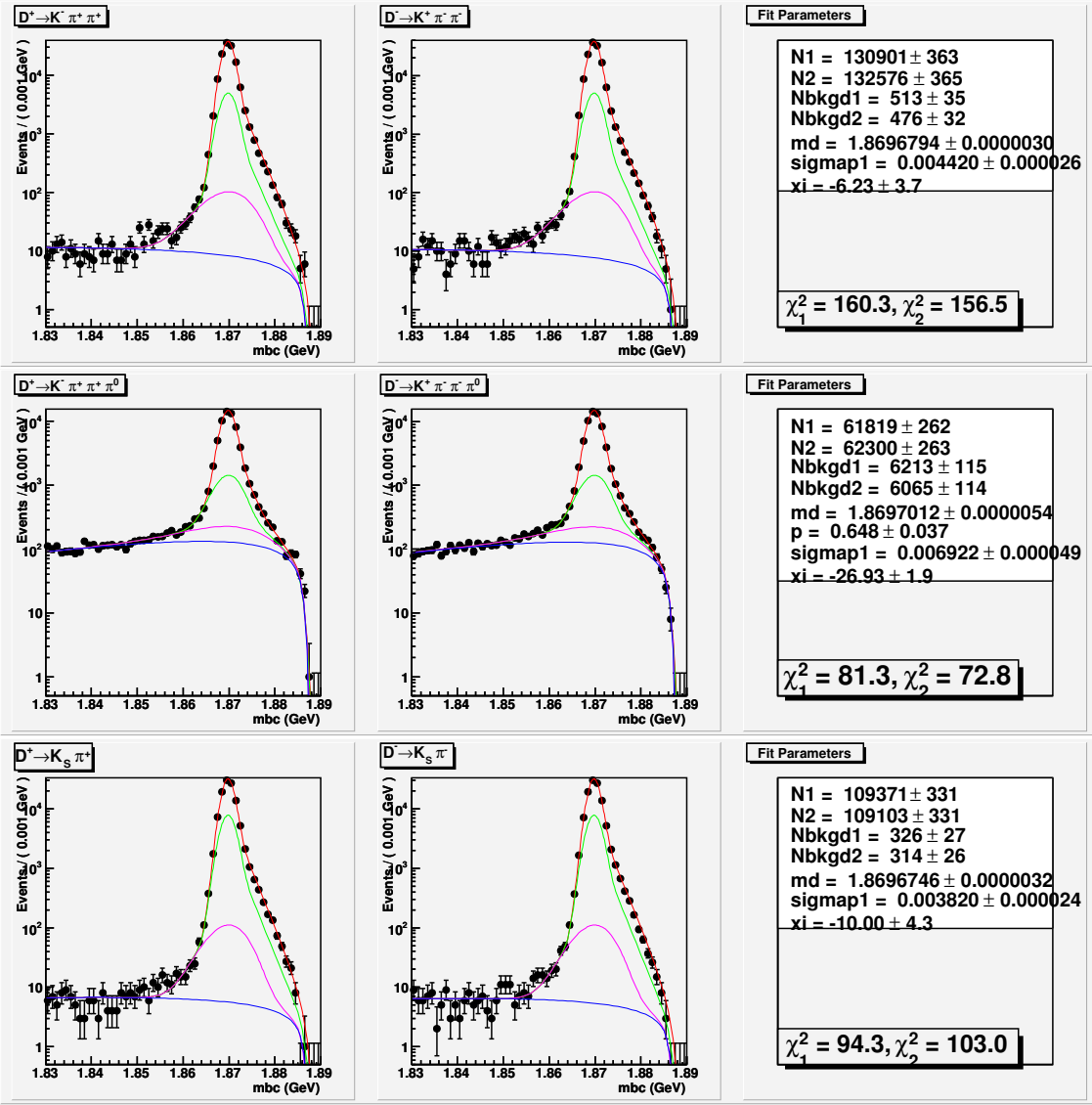


Figure 62: Single tag D^+ yields in signal MC. These plots show the beam constrained mass after choosing a candidate with minimum $|\Delta E|$.

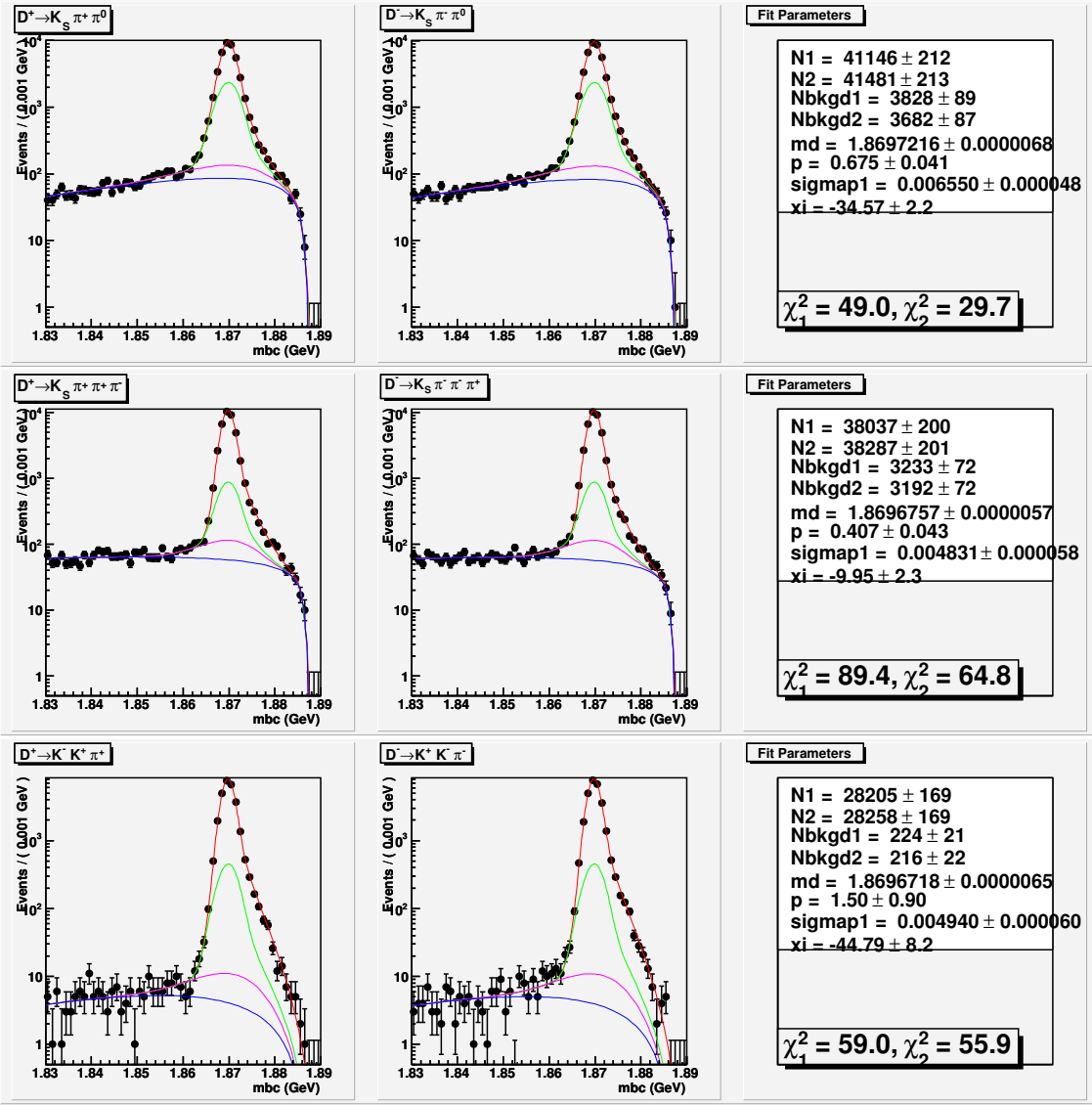


Figure 63: Single tag D^+ yields in signal MC. These plots show the beam constrained mass after choosing a candidate with minimum $|\Delta E|$.

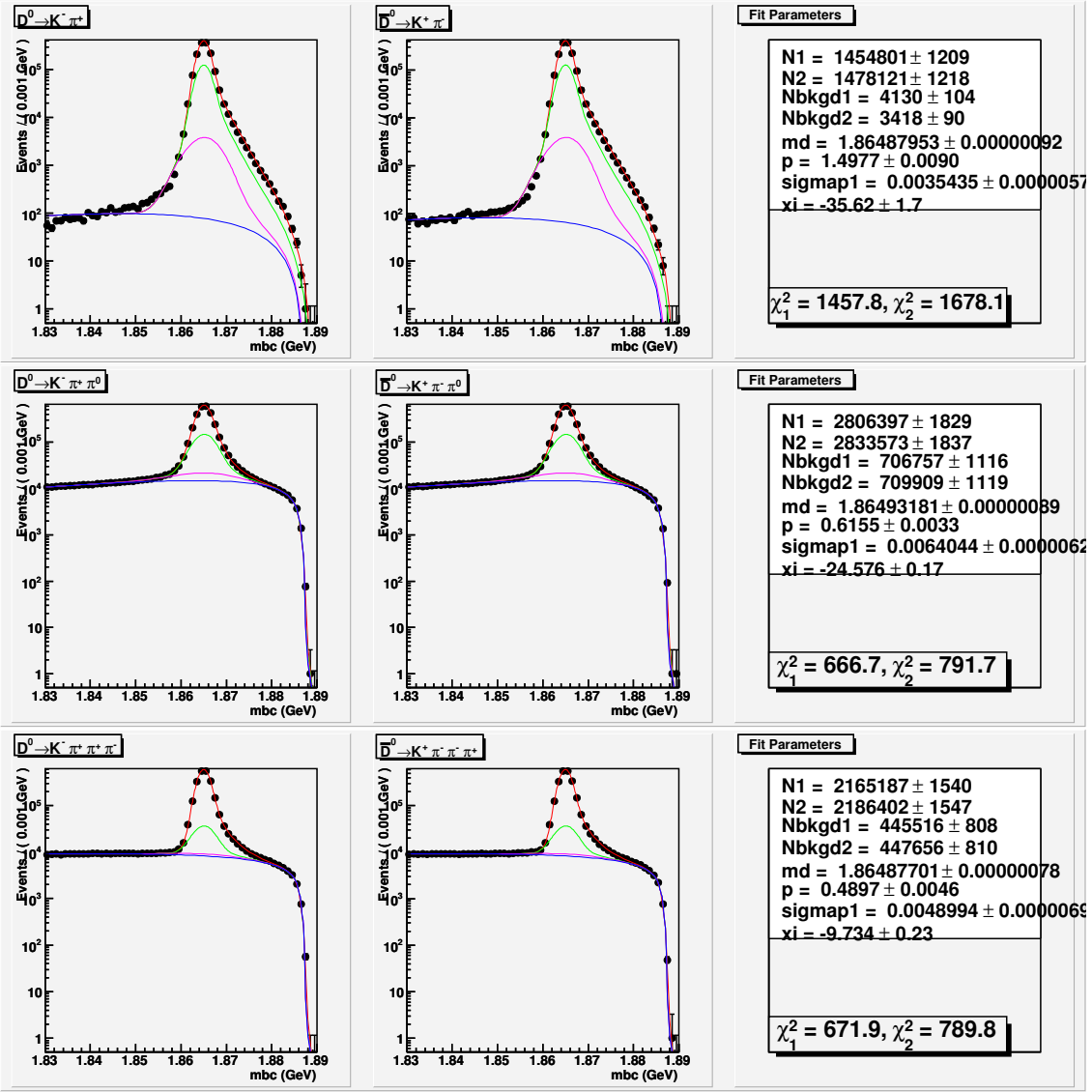


Figure 64: Single tag D^0 yields in generic MC. These plots show the beam constrained mass after choosing a candidate with minimum $|\Delta E|$.

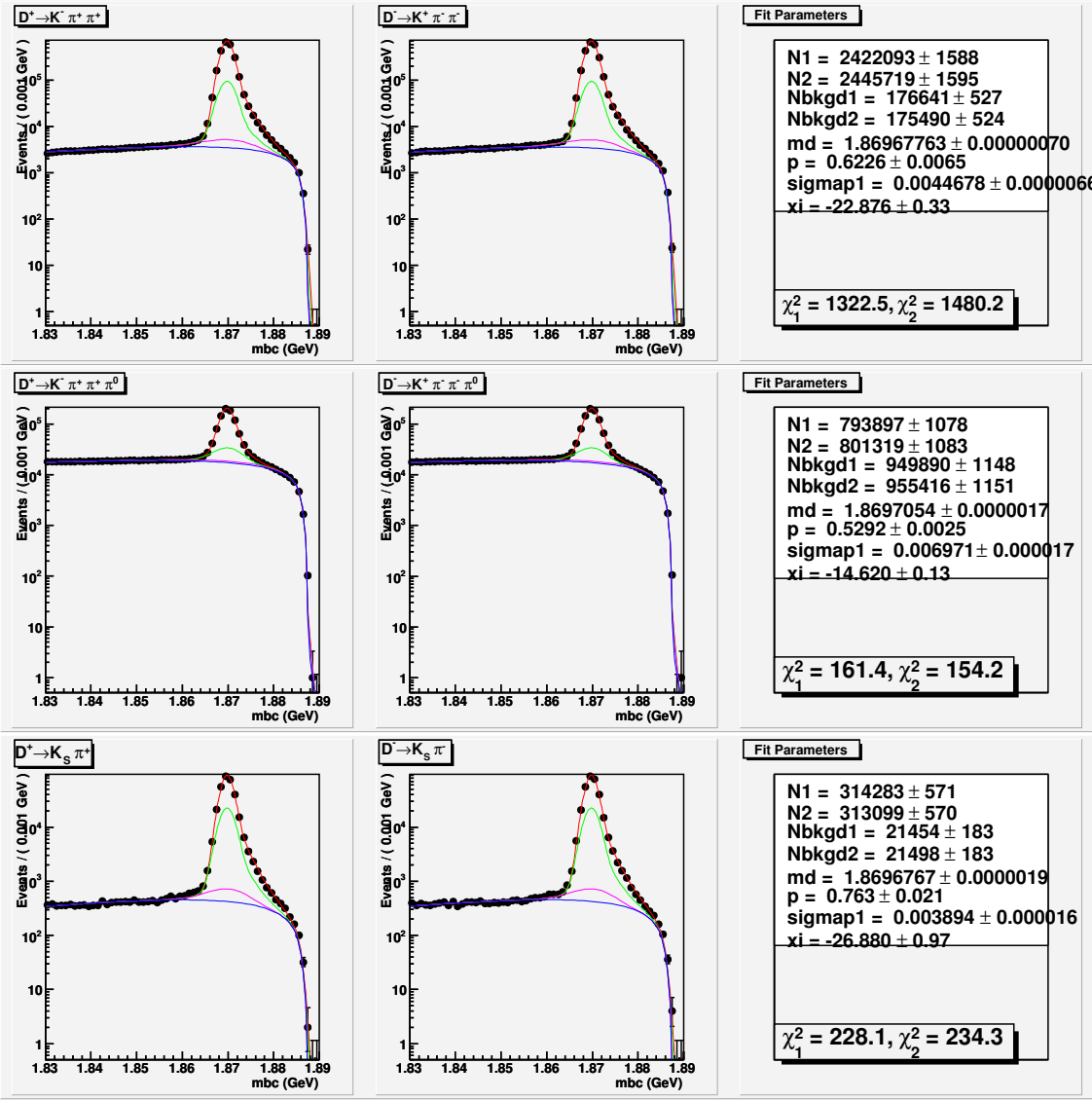


Figure 65: Single tag D^+ yields in generic MC. These plots show the beam constrained mass after choosing a candidate with minimum $|\Delta E|$.

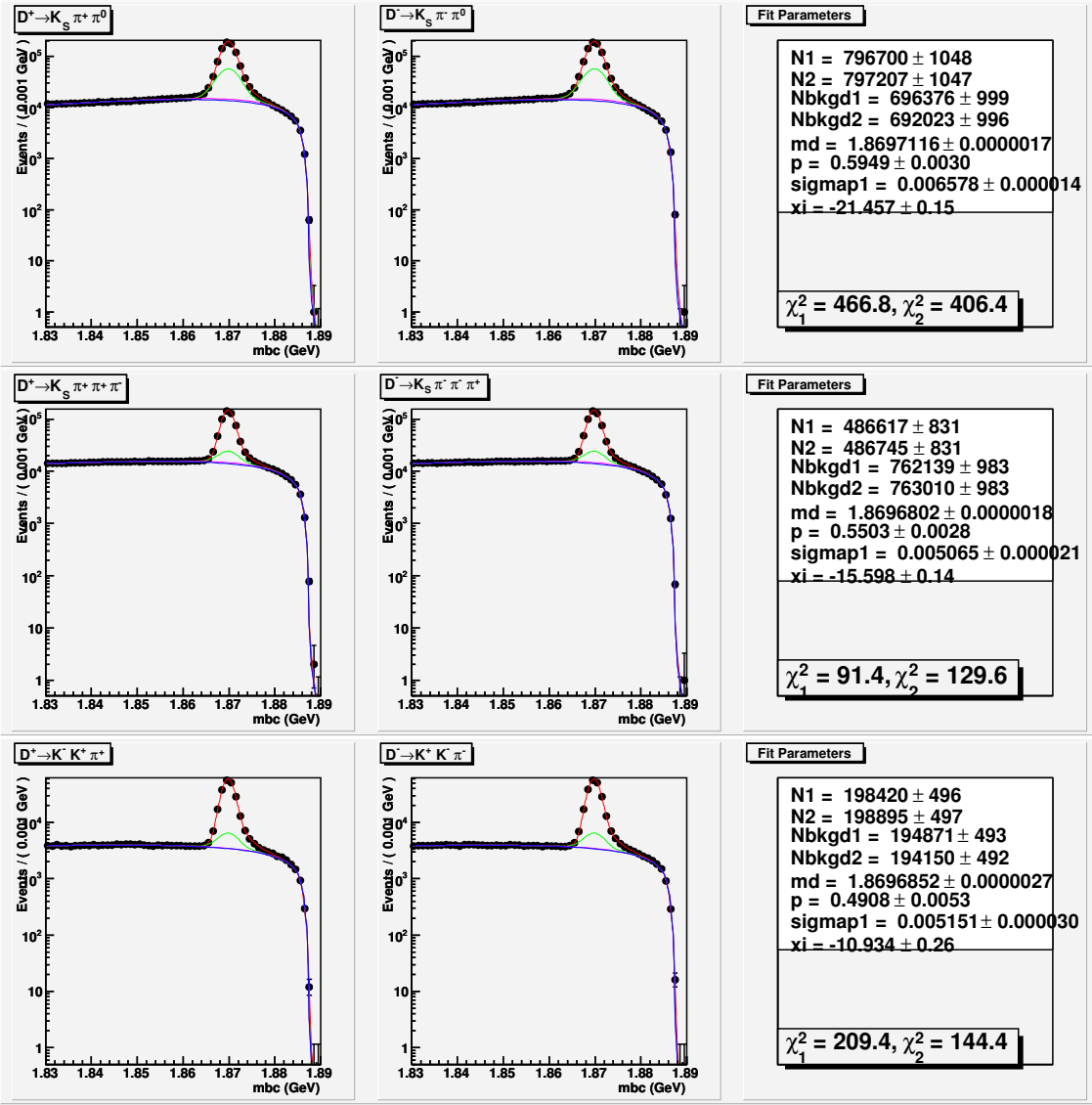


Figure 66: Single tag D^+ yields in generic MC. These plots show the beam constrained mass after choosing a candidate with minimum $|\Delta E|$.

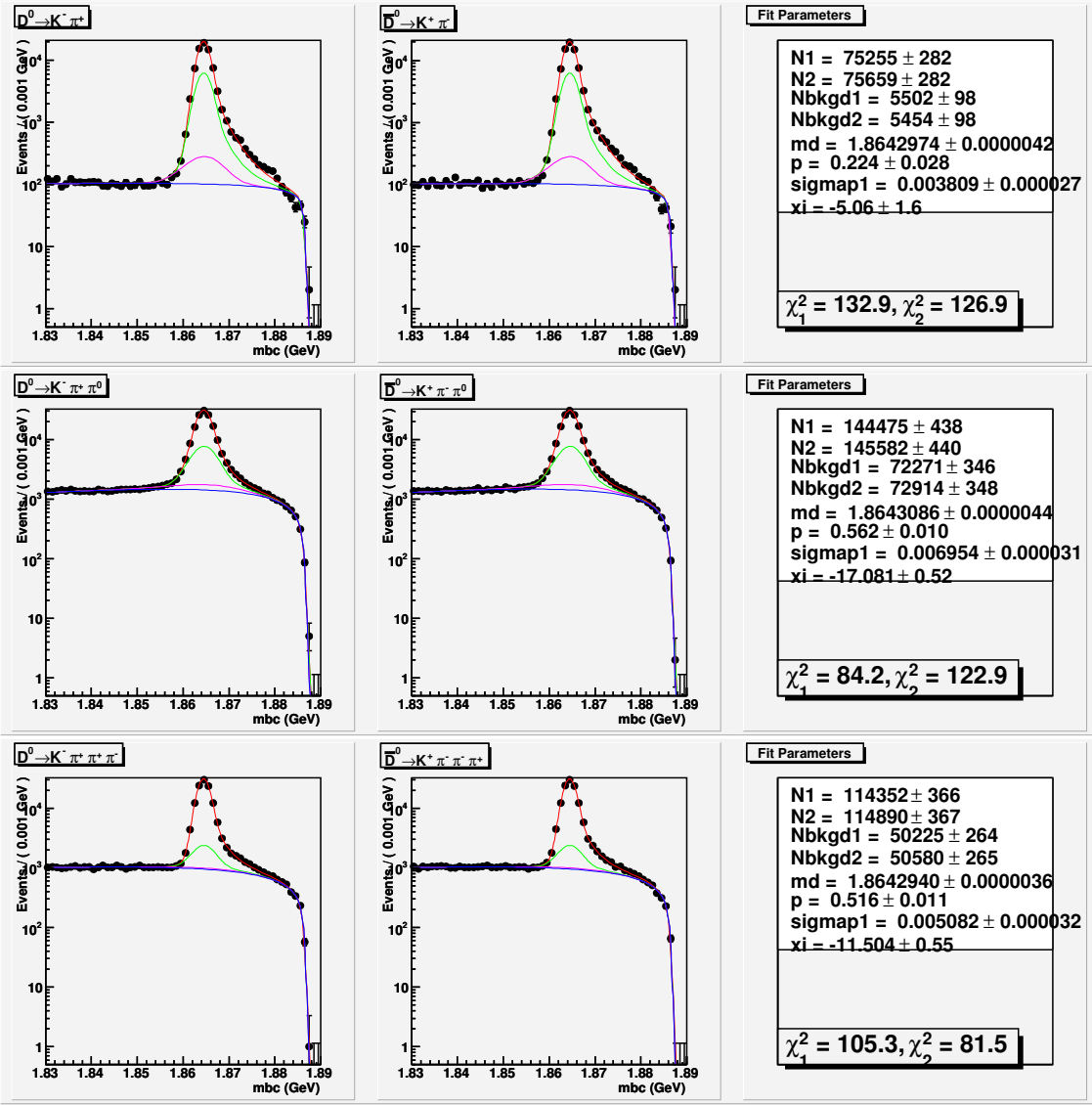


Figure 67: Single tag D^0 yields in data. These plots show the beam constrained mass after choosing a candidate with minimum $|\Delta E|$.

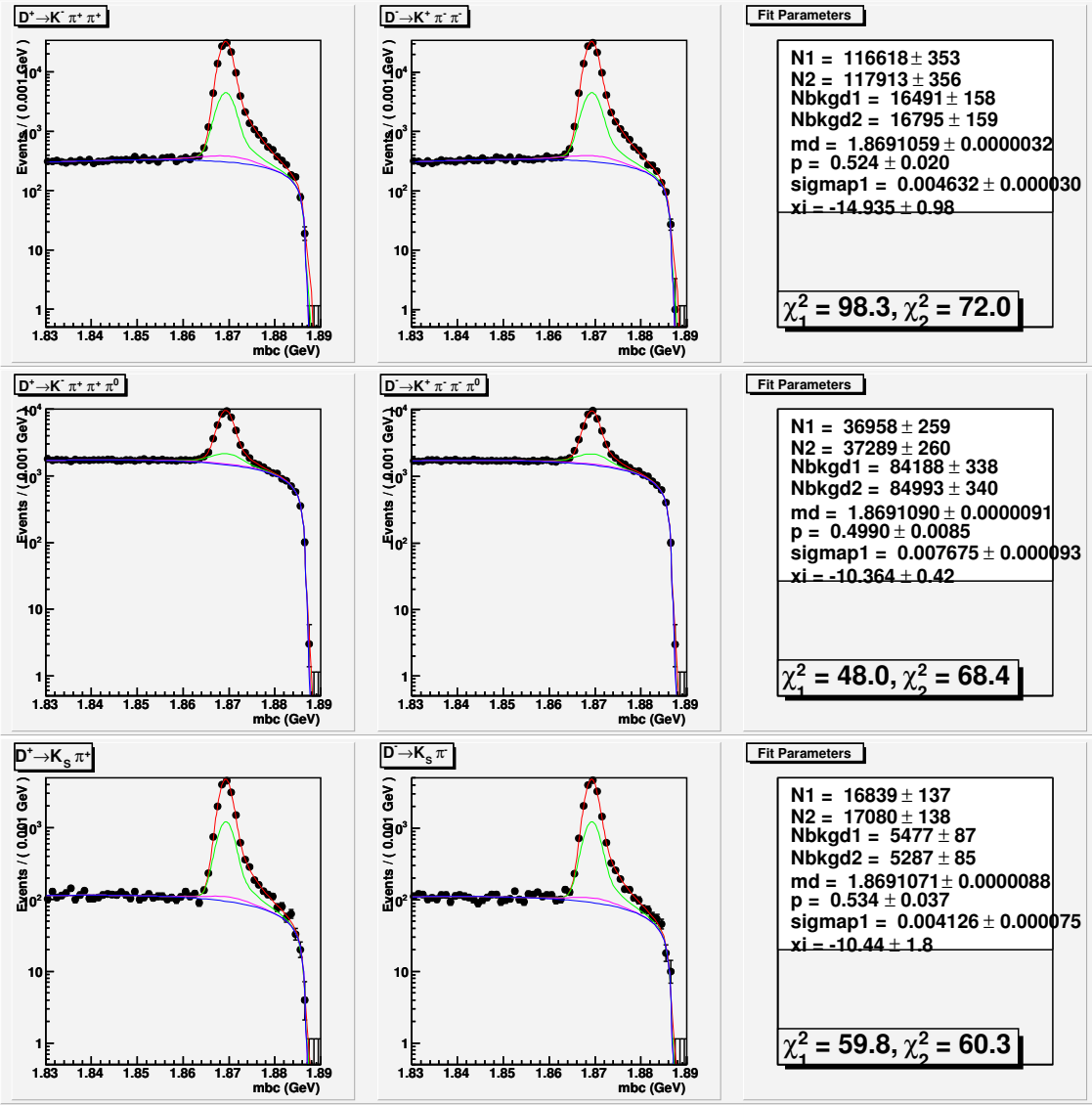


Figure 68: Single tag D^+ yields in data. These plots show the beam constrained mass after choosing a candidate with minimum $|\Delta E|$.

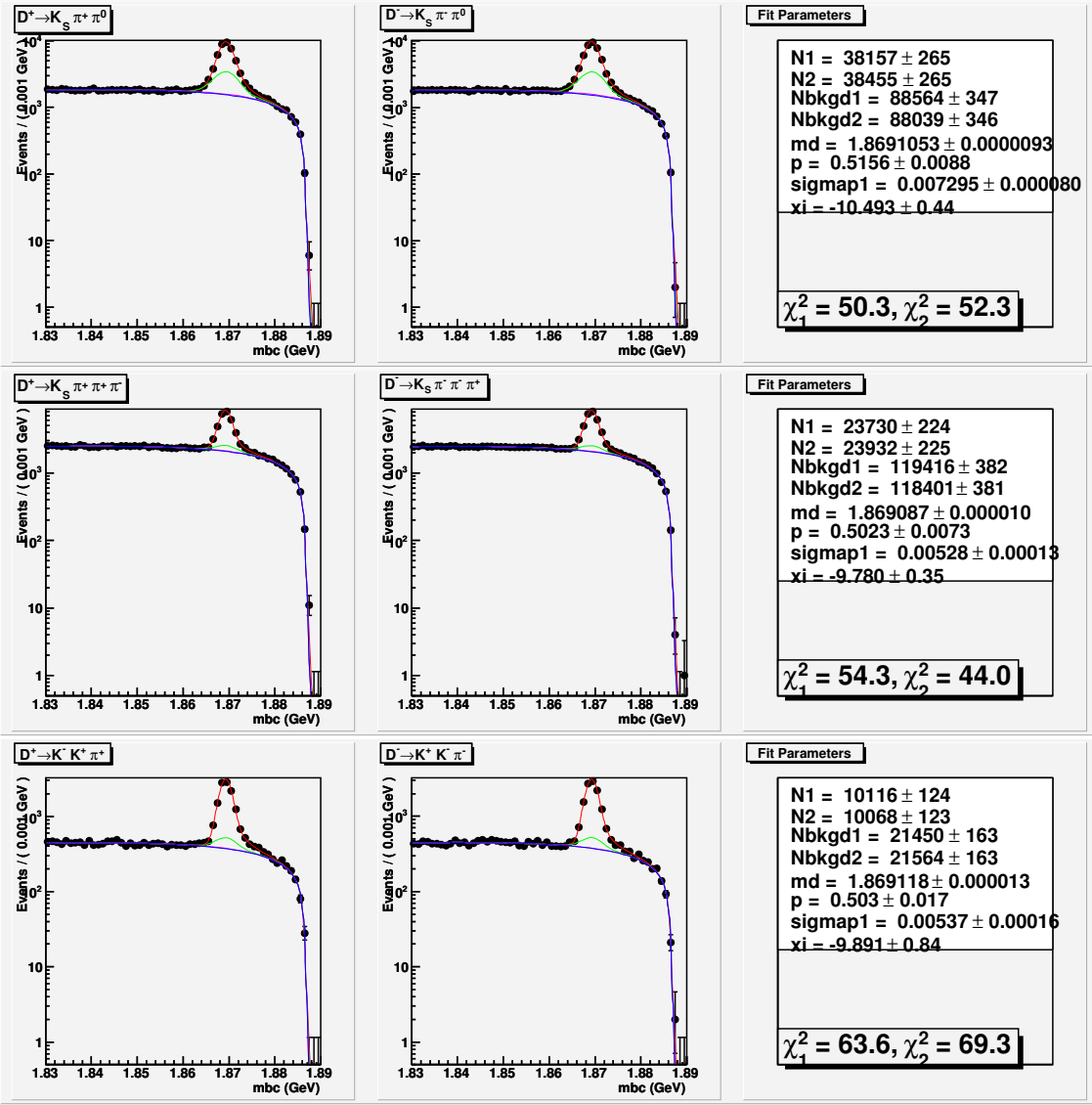


Figure 69: Single tag D^+ yields in data. These plots show the beam constrained mass after choosing a candidate with minimum $|\Delta E|$.

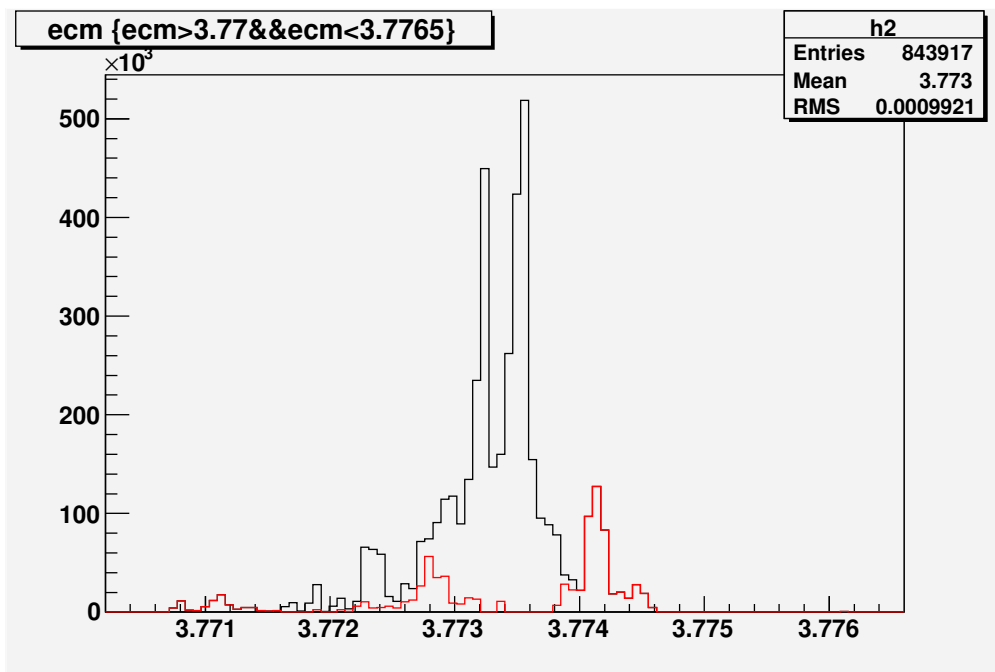


Figure 70: Distribution of \sqrt{s} in GeV for all $\psi(3770)$ runs, weighted by number of DTag candidates. The red histogram is the distribution for datasets 31–33.

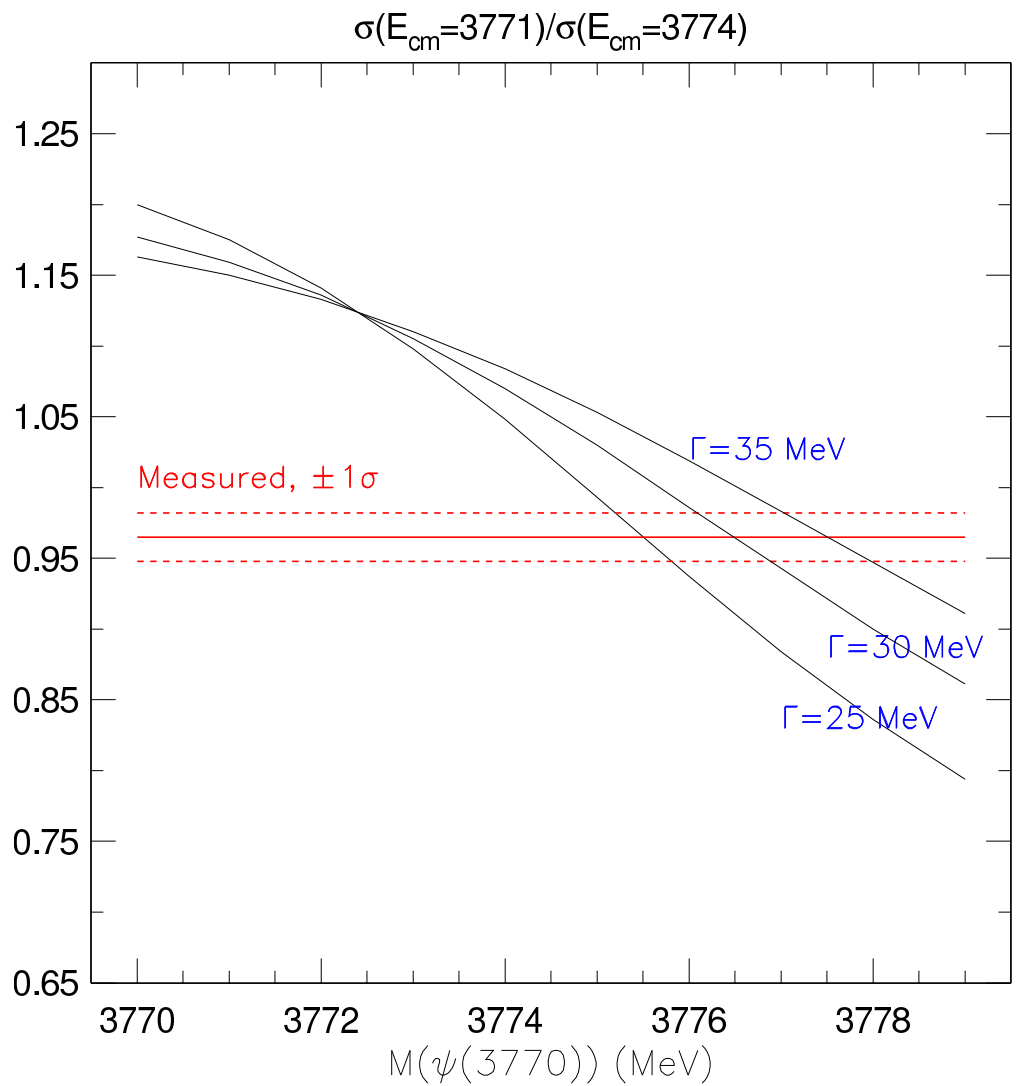


Figure 71: Predicted cross section ratio $\sigma(3771 \text{ MeV})/\sigma(3774 \text{ MeV})$ as a function of $M(\psi(3770))$ for various values of $\Gamma(\psi(3770))$, compared with the value measured in data.

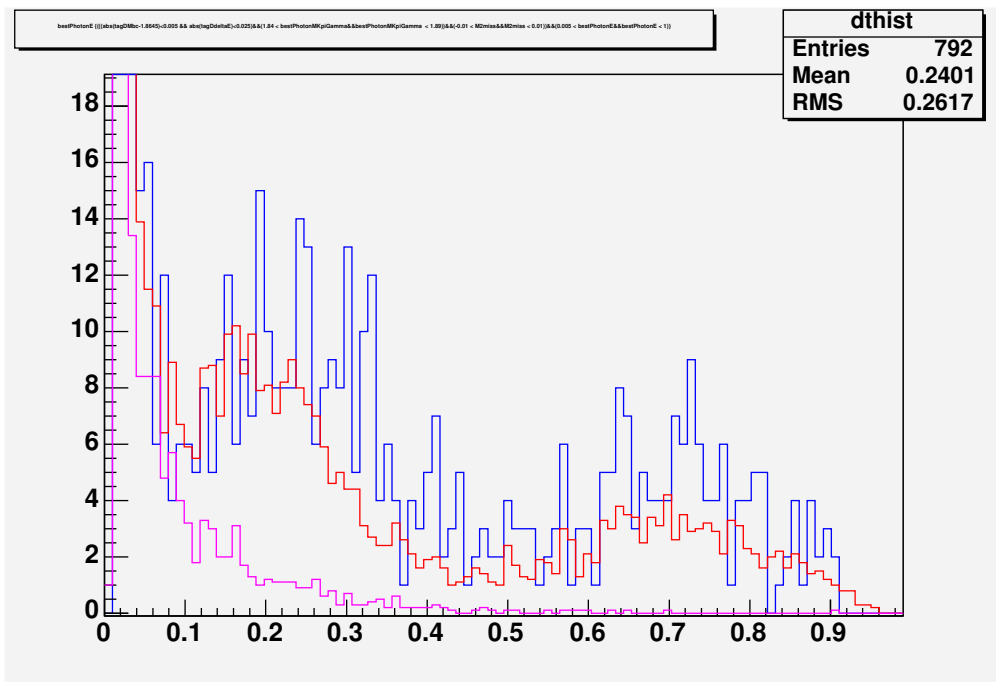


Figure 72: Energy (GeV) of the photon in $D^0 \rightarrow K^-\pi^+\gamma$ candidates. Data is shown in blue, scaled Monte Carlo in red, and truth-tagged $D^0 \rightarrow K^-\pi^+\gamma$ Monte Carlo events in purple. The signal region is relatively small in this plot – from 0.060 to about 0.120 GeV. In this plot we see that data and Monte Carlo are consistent, but many background events contaminate the signal. The bumps at higher photon energies come from $D^0 \rightarrow K^-\pi^+\pi^0$, and the low-energy peak (which goes off scale) comes from $D^0 \rightarrow K^-\pi^+$ events without FSR.

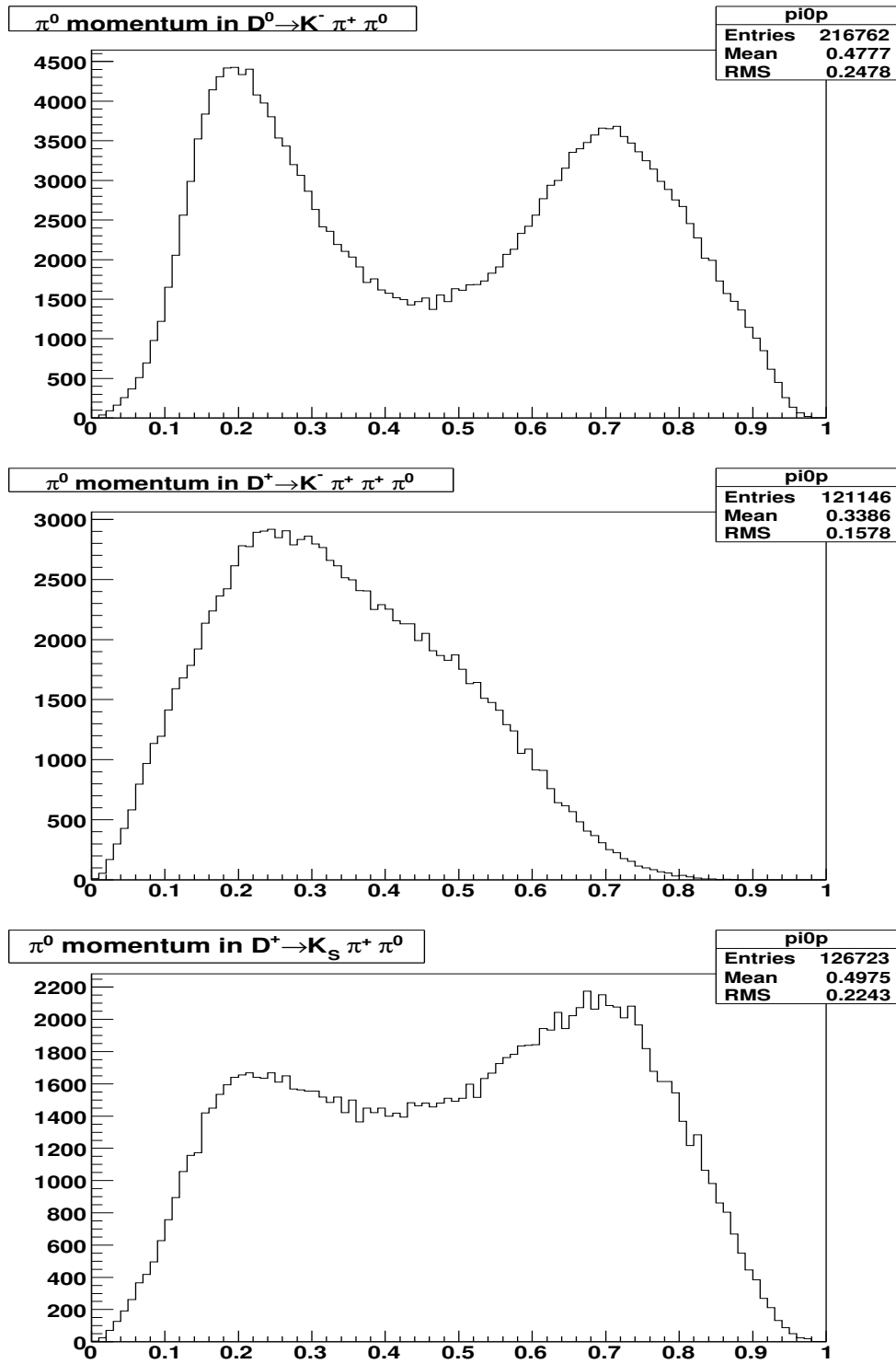


Figure 73: π^0 momentum in data for modes: $D^0 \rightarrow K^- \pi^+ \pi^0$, $D^+ \rightarrow K^- \pi^+ \pi^+ \pi^0$, and $D^+ \rightarrow K_S^0 \pi^+ \pi^0$.